



M.Sc. Bartłomiej Witkowski

**Investigation of the secondary organic aerosol (SOA) nucleation from α -
pinene ozonolysis**

Supervisor:

Dr hab. Tomasz Gierczak

Dedication

This thesis is dedicated to my loving wife, Anna, who has always put up with me for reasons not always obvious.

Acknowledgements

I would like to thank my supervisor, Dr hab. Tomasz Gierczak for support, guidance and providing wonderful opportunities for professional development.

I would like to thank Dr hab. Magdalena Biesaga for support, guidance and helping me to develop the skills needed to complete this thesis.

I would like to thank prof. dr hab. Jan Niedzielski for final proof-reading and language corrections.

I would like to thank Dr Ranajit K. Talukdar for guidance and helping me to develop the skills needed to complete this thesis.

I would like to thank Dr Ranajit K. Talukdar, Dr James B. Burholder and prof. A.R Ravishankara for their hospitality during my international training in NOAA, Boulder, CO.

I would like to thank the Structural Research Laboratory (SRL) at the Department of Chemistry of University of Warsaw for making LC/MS measurements possible. SRL has been established with financial support from European Regional Development Found in the Sectoral Operational Programme "Improvement of the Competitiveness of Enterprises, years 2004 –2005" project no: WPK_1/ 1.4.3./1/2004/72/72/165/2005/U. This work was also financed by 501/68-BW-172101 project. This work was supported by the European Science Foundation 2007/03-LCNANOP project co-operated with the Foundation for Polish Science MPD Programme co-financed by the EU European Regional Development Fund.

Fragments of the already published material were used under the license agreement number 3147151193702 between Bartłomiej M Witkowski and John Wiley and Sons, granting the author permission to use the whole published material for the purpose of writing this thesis.

Project operated within the Foundation for Polish Science MPD Programme MPD/2008/1 "International Scholarship Program for Graduate Studies in Faculty of Chemistry University of Warsaw" co-financed by the EU European Regional Development Fund. Economical support from the PhD grant number N~N204~116539 is gratefully acknowledged.



Abstract

Composition of the newly formed secondary organic aerosol (SOA) generated by ozonolysis of the cyclohexene (model precursor) and α -pinene was studied using liquid chromatography coupled to electrospray ionization tandem mass spectrometry (LC-ESI/MSⁿ). SOA was generated in the flow-tube reactor under standard conditions: 20°C and 1 atm. and the reaction time less than 1 min. In an attempt to resolve the current ambiguities, regarding the structure of the α -pinene SOA nucleating agents, analytical methods for analysis of α -acyloxyhydroperoxy aldehydes and high molecular weight (HMW) compounds containing carboxylic group were developed. Both groups of those compounds are currently considered as the potential nucleating agents. However, no analytical evidence proving the presence of α -acyloxyhydroperoxy aldehydes in the SOA samples have been presented. Also, very limited experimental data, indicating that the nucleating agents are acidic oligomers is currently available. The α -acyloxyhydroperoxy aldehydes were analyzed with LC-ESI/MSⁿ for the first time. Analysis of the tandem mass spectra of the α -acyloxyhydroperoxy aldehydes ammonia adducts was used to propose the general fragmentation mechanism, supported by the analysis of the isotopically labeled analogs. The proposed mechanism was used to predict the mass spectrum of the α -acyloxyhydroperoxy aldehydes that could not be synthesized. After analyzing the SOA samples, generated in the flow-tube reactor, it was concluded that α -acyloxyhydroperoxy aldehydes were not formed in significant quantities, and are unlikely to participate in the aerosol nucleation. Direct analytical evidence was found, arguing against the gas-phase nucleation and proving that acidic oligomers are formed in the early stages of SOA formation. Also, based on the acquired experimental data, it was concluded that the reactive uptake of carbonyl compounds is an important growth mechanism for the freshly formed SOA. For the first time, isotopically labeled analog of cyclohexene (cyclohexene-d10) was used to propose the structures for the up-to-date unknown oligomers. The acquired experimental data point out the need for revision of the current α -pinene SOA nucleation mechanism.

Abstrakt

Skład świeżo powstałego wtórnego aerozolu organicznego (*secondary organic aerosol*, SOA) został przeanalizowany za pomocą chromatografii cieczowej połączonej z tandemową spektrometrią mas z jonizacją przez elektrorozpylanie (LC-ESI/MSⁿ). SOA został wytworzony w reaktorze przepływowym w standardowych warunkach temperatury i ciśnienia: 20°C i 1 atm. a czas reakcji wynosił < 1 min. Aby rozstrzygnąć obecne niepewności dotyczące struktury załączków nukleacji SOA powstałego w wyniku ozonolizy α -pinenu, zostały opracowane metody analizy α -acyloksyhydroperoxy aldehydów oraz oligomerów zawierających grupę karboksylową. Obydwa typy związków są obecnie rozważane, jako potencjalne załączki nukleacji. Jednak, do tej pory nie zostały przedstawione żadne bezpośrednie dowody potwierdzające obecność α -acyloksyhydroperoxy aldehydów w próbkach SOA. Ponadto, tylko niewielka ilość danych wskazuje, iż załączkami nukleacji są kwasowe oligomery. α -Acyloksyhydroperoxy aldehydy po raz pierwszy zostały przeanalizowane za pomocą LC-ESI/MSⁿ. W wyniku analizy widm fragmentacyjnych został zaproponowany ogólny mechanizm fragmentacji adduktów amonowych α -acyloksyhydroperoxy aldehydów; mechanizm ten został potwierdzony za pomocą analizy izotopowo znaczonej analogów. Zaproponowany mechanizm fragmentacji został wykorzystany żeby przewidzieć widmo masowe α -acyloksyhydroperoxy aldehydów, które nie mogły być zsyntezowane. W próbkach SOA wytworzonych w reaktorze przepływowym, α -acyloksyhydroperoxy aldehydy nie zostały wykryte w znaczących ilościach i prawdopodobnie nie brały udziału w procesie nukleacji aerozolu. Otrzymane wyniki wskazują, iż nukleacja prawdopodobnie nie zachodzi w fazie gazowej. Jednocześnie, zostało udowodnione, że kwasowe oligomery są wytwarzane już na wczesnych etapach formowania SOA. Stwierdzono także, iż absorpcja związków karbonylowych w wyniku formowania się oligomerów jest ważnym mechanizmem wzrostu cząstek aerozolu na wczesnych etapach jego powstawania. Po raz pierwszy, izotopowo znaczony prekursor (cykloheksen-d10) został wykorzystany do zaproponowania struktur do tej pory nieznanymi oligomerów. Zidentyfikowane oligomery najprawdopodobniej powstały w wyniku reakcji związków karbonylowych. Wyniki przedstawione w tej pracy wskazują, iż obecnie zaproponowany mechanizm nukleacji powinien zostać zaktualizowany.

Table of contents

1. Introduction	9
1.1. Atmospheric aerosols – basic definitions historical outline.....	9
1.1.1. Size distribution, density and concentration.....	13
1.2. Global overview of aerosols properties.....	15
1.2.1. Sources.....	15
1.2.1.1. Primary aerosols.....	16
1.2.1.2. Secondary aerosols.....	16
1.2.2. Composition	17
1.2.3. Deposition mechanisms and lifetimes.....	18
1.2.3.1. Wet deposition.....	18
1.2.3.2. Dry deposition.....	19
1.2.4. Aerosols climate influence.....	19
1.2.4.1. Direct effects.....	20
1.2.4.2. Indirect and semi-direct effects.....	20
1.2.5. Health effects of atmospheric aerosols.....	21
1.2.5.1. Epidemiological studies.....	21
1.2.5.2. Toxicological studies.....	23
1.3. Secondary organic aerosols (SOA's)	24
1.3.1. Emission of biogenic secondary organic aerosols (BSOAs) precursors	26
1.3.2. Ozone in the atmosphere.....	28
1.3.3. Alkene ozonolysis.....	32
1.3.4. Liquid phase ozonolysis of the alkenes.....	38
1.4. SOA formation from the α -pinene ozone-initiated oxidation.....	41
1.4.1. α -pinene ozone-initiated oxidation mechanism.....	42
1.4.2. Laboratory studies of the α -pinene SOA formation.....	46
1.4.2.1. Smog chamber experiments.....	46
1.4.2.2. Flow – tube reactors.....	50
1.4.2.3. OH radicals scavengers.....	54
1.4.3. SOA composition analysis.....	56
1.4.3.1. Low – molecular weight (LMW) compounds	57
1.4.3.2. Oligomers and other high-molecular weight (HMW) compounds.....	59
1.4.3.3. Identification of the HMW α -pinene SOA components.....	65
1.4.3.3.1. Mass spectra interpretation and elemental formula assignment.....	65
1.4.3.3.2. The use of standard synthesis for the identification of the HMW α -pinene SOA components.....	69
1.4.3.4. Formation mechanisms of the high molecular weight (HMW) compounds formed during the SOA formation in the α -pinene/ozone system.....	71
1.4.3.4.1. Particle – phase reactions.....	71
1.4.3.4.2. Gas – phase reactions.....	74
1.4.4. Proposed nucleation precursors.....	76
2. Aim of this work	86
3. Experimental	88

3.1.	Reagents.....	88
3.2.	Apparatus.....	88
3.2.1.	Direct infusion electrospray tandem mass spectrometry (ESI-MSn).....	89
3.2.2.	Liquid chromatography coupled to the electrospray ionization tandem mass spectrometry (LC-ESI/MSn).....	89
3.2.2.1.	Carboxylic acids produced by gas-phase ozonolysis of cyclohexene.....	90
3.2.2.2.	α -Acyloxyhydroperoxy aldehydes synthesized using cyclohexene	90
3.2.2.3.	Carboxylic acids produced by gas-phase ozonolysis of α -pinene.....	90
3.2.2.4.	α -Acyloxyhydroperoxy aldehydes synthesized using α -pinene as the precursor...91	
3.2.3.	Elemental formula assigned for the synthesized α -acyloxyhydroperoxy aldehydes with high-resolution mass spectrometry (HR-MS).....	91
3.2.4.	α -pinene and cyclohexene quantification with GC/FID.....	92
3.3.	Standards synthesis.....	92
3.4.	Flow tube reactor.....	92
3.4.1.	Flow tube reactor experimental setup.....	93
3.4.2.	Conditions for the SOA generation	99
3.4.3.	SOA sampling.....	100
3.4.4.	Reactor cleaning.....	102
4.	Results and discussion.....	103
4.1.	Development of the SOA composition analysis method using liquid chromatography coupled to electrospray ionization tandem mass spectrometry (LC-ESI/MSn)	103
4.1.1.	Carboxylic acids analysis method	103
4.1.1.1.	Carboxylic acids obtained during cyclohexene ozonolysis.....	104
4.1.1.2.	Carboxylic acids obtained during α -pinene ozonolysis.....	112
4.1.2.	α -acyloxyhydroperoxy aldehydes analysis method.....	119
4.1.2.1.	Synthesis of the α -acyloxyhydroperoxy aldehydes standards.....	119
4.1.2.2.	Liquid phase ozonolysis solvent.....	121
4.1.2.3.	Evaluation of the ionization conditions.....	124
4.1.2.3.1.	Atmospheric pressure chemical ionization (APCI)	125
4.1.2.3.2.	Electrospray ionization (ESI)	125
4.1.2.4.	Confirmation of the elemental formulas of α -acyloxyhydroperoxy aldehydes with HR-MS.....	126
4.1.2.5.	Investigation of the fragmentation mechanism.....	127
4.1.2.6.	Isotope study	140
4.1.2.7.	Analysis of the ammonium cationized α -acyloxyhydroperoxy aldehydes synthesized using α -pinene.....	148
4.1.2.8.	Optimization of the MS/MS conditions and predicted MRM (pMRM) method.....	151
4.2.	SOA formation in the flow – tube reactor.....	156
4.2.1.	Flow conditions calculations.....	157
4.2.2.	Box model calculations.....	158
4.2.3.	Precursors concentrations monitoring.....	161
4.2.4.	OH radicals scavengers.....	163
4.3.	Analysis of SOA samples generated in the flow tube reactor.....	164
4.3.1.	SOA produced from ozonolysis of the model compound – cyclohexene.....	165

4.3.1.1.	Carboxylic acids identification.....	165
4.3.1.1.1.	Isotope study.....	171
4.3.1.2.	Investigation of α -acyloxyhydroperoxy aldehydes formation.....	174
4.3.1.3.	Formation of other high-molecular weight SOA components.....	180
4.3.1.3.1.	Isotope study and identification of the HMW compounds.....	184
4.3.1.4.	Relative humidity influence on the composition of SOA resulted from cyclohexene ozonolysis.....	191
4.3.1.4.1.	Carboxylic acids.....	191
4.3.1.4.2.	α -acyloxyhydroperoxy aldehydes.....	193
4.3.1.4.3.	Other high-molecular weight SOA components.....	193
4.3.2.	SOA produced from α -pinene ozonolysis	194
4.3.2.1.	Carboxylic acids identification.....	194
4.3.2.2.	Investigation of α -acyloxyhydroperoxy aldehydes formation.....	203
4.3.2.3.	Formation of other high-molecular weight SOA components.....	208
4.3.2.4.	Relative humidity influence on SOA composition.....	216
4.3.2.4.1.	Carboxylic acids.....	216
4.3.2.4.2.	α -Acyloxyhydroperoxy aldehydes.....	217
4.3.2.4.3.	Other high-molecular weight SOA components.....	218
5.	Summary and conclusions.....	219
6.	List of abbreviations.....	222
	Conferences, publications and abroad internships.....	225
	References.....	226

1. Introduction

This introduction is divided into four sections; in section 1.1 basic definitions related to the atmospheric particles are given. The most prominent historical events, related to the origin of scientific interest in the atmospheric aerosols and air pollution in general are also outlined. Subsequently, the currently used measures of the aerosols size distribution and concentrations are presented in section 1.1.1.

In the second part of the introduction (section 1.2.), brief global overview of atmospheric aerosols is presented, including sources (section 1.2.1), composition (section 1.2.2.), deposition mechanisms (section 1.2.3), as well as climate (section 1.2.4.) and health effects (section 1.2.5.).

The third section of the introduction describes the secondary organic aerosols (SOAs) formation by alkene ozonolysis in the gas-phase; section 1.3. SOA formation by α -pinene ozone-initiated oxidation in the gas-phase is discussed in section 1.4.

1.1. Atmospheric aerosols – basic definitions and historical outline

Aerosol is a relatively stable suspension of very fine, solid or liquid particles in the gas phase. In this definition, the term aerosol applies to both the gas and the suspended particles. However, in the majority of the published literature, the term aerosol is most often associated only with the suspended particles. In this introduction the terms aerosol, atmospheric particles and particulate matter (PM) are used interchangeably. A number of common terms, associated with the atmospheric aerosols, are listed in Table 1.1. Please note that definitions given in Table 1.1 are not strictly scientific.

Table 1.1 Common terms associated with the atmospheric particles*

Term	Definition	Size range (μm)
Aerosol	Fine particles dispersed in gas	0.002 – 100
Bioaerosol	Fine, biogenic particles dispersed in gas, e.g. fungal spores and pollens	1 – 100
Cloud	A visible agglomeration of mainly water droplets or ice crystals	\approx 10

Dust	Solid, irregular particles, produced via mechanical processing (crushing, grinding) of various materials	1 - 100
Fume	Solid particles produced by condensation of vapors or gaseous precursors oxidation	< 0.5
Haze	Aerosol that obscures visibility	< 0.5
Mist/Fog	Spherical particles, usually condensed water or ice, the term fog commonly applies to clearly visible aerosol	1 - 200
Smog	The term smog originates from the combination of terms smoke and fog, used to describe aerosol – polluted air	1 - 2
Smoke	Particles produced as a result of incomplete combustion	≥ 0.01
Soot	Particles, mainly consisting of elemental carbon, also produced as a result of incomplete combustion	0.03-0.15

*adapted from ref. ¹ – pages 3-6, and ref. ² Table 2.18, page 56

As listed in Table 1.1, diameters of the aerosol particles fall in the range from about 0.002 μm to more than a 100 μm. ¹⁻³ Since a significant fraction of the particles encountered in the atmosphere are not spherical, the diameters listed in this section are aerodynamic diameters, not the geometric diameters. The definition of aerosol aerodynamic diameter is given in section 1.1.1.

The aerosol size range is not strictly defined, with the lower size limit corresponding to a cluster of molecules; fine mineral dust can be given as example of the particles with diameters from the upper size limit. ^{1,2} A number of commonly encountered aerosols, together with their corresponding size ranges, are listed in Fig. 1.1.

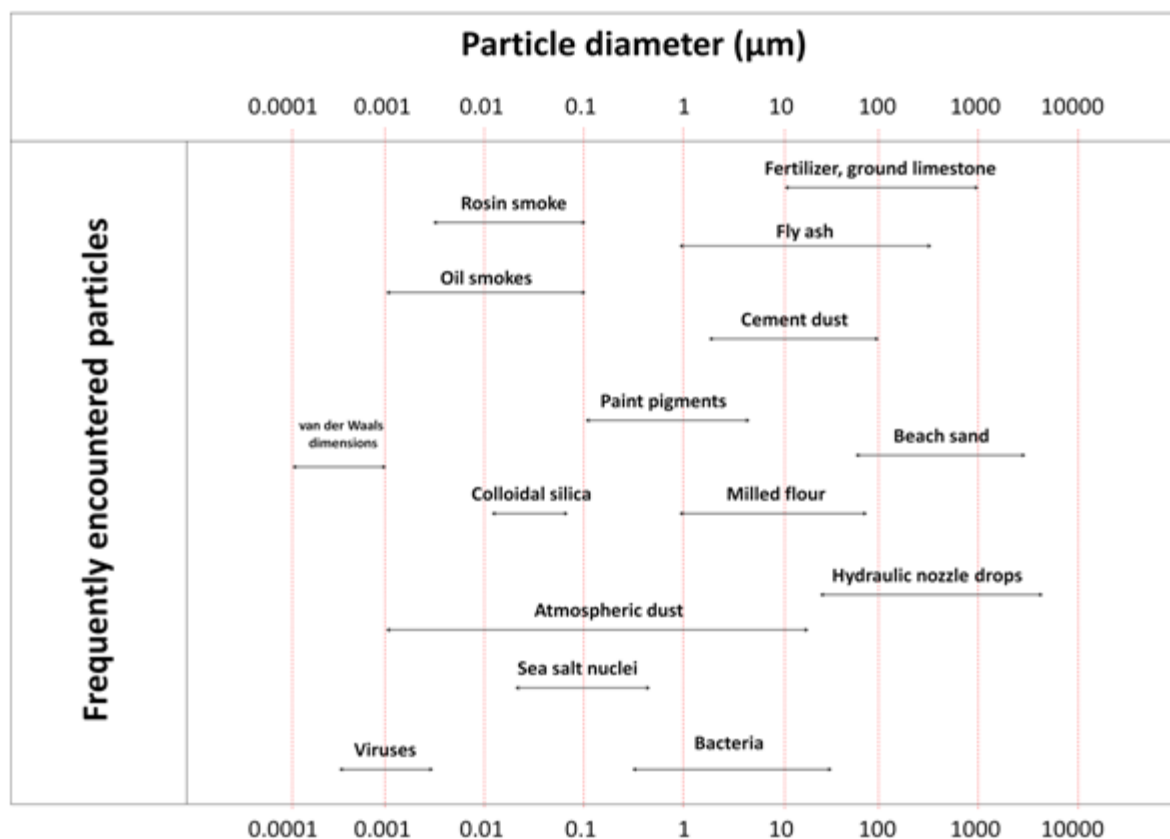


Figure 1.1 Sizes of the commonly encountered particles (adapted from ref. ³, Figure 9.1. page 350 and ref. ², Figure 1.6. page 9)

As shown in Fig. 1.1, size distribution of the commonly encountered particles is very broad, ranging from sub-micrometer particles to coarse, visible particles like e.g. fine sand. Diameters of particles most relevant to the atmospheric chemistry and physics are within the range from 0.002 to about 10 μm . ¹ Most common forms of expressing the particles size distribution and concentration are described in section 1.1.1.

Aerosol particles remain in the atmosphere for a fixed period of time and are eventually deposited onto the Earth surface as described in section 1.2.3. The stability of the aerosols ranges from a few seconds – very large particles – up to a year. ^{2,3}

As listed in Table 1.1, atmospheric aerosols particles can contain wide range of organic or inorganic materials. They can also be directly introduced into the atmosphere (e.g. dust particles) or formed in the gas phase from a variety of volatile precursors. Sources and composition of the atmospheric aerosols are described in sections 1.2.1 and 1.2.2, respectively.

Air pollution problem has been recognized and documented since the early 19th century, and earlier.^{1,4,5} Table 1.2 lists the most famous historical air pollution events, resulting, in most cases, in a considerable number of excess deaths. Excess deaths reflect the abnormal mortality, compared to the number of expected deaths, calculated using the previous year's mortality data. Although these events were not caused by aerosol air pollution alone, it is important to notice that black carbon (BC) particles (soot) were concluded to be present in extremely high concentrations during London, Meuse Valley and Donara Valley events.

Table 1.2 Dates and locations of the historical, air pollution events

Date	Location	Description	Reference
17 th century	Westminster	Queen Elizabeth I forbids coal burning near the palace	4
1661	London	John Evelyn suggests moving the factories away from London due to high smoke emissions	1,4
1930	Meuse Valley Belgium	63 excess deaths due to the use of coal in domestic heaters	1,4
1948	Donora Valley, US	20 excess deaths due to the use of coal in domestic heaters	1,4
1952	London	Approx. 4000 excess deaths caused by air pollution	1,5,6
1962	London	Approx. 700 excess deaths caused by air pollution	1

London smog on December 1952 was a famous air pollution event, frequently listed as the most prominent example of negative influence of PM inhalation and gaseous air pollutants on human health. The so called great smog lasted for four days and it is believed to cause approx. 4000 excess deaths due to extremely high concentrations of black smoke and SO₂. Health effects of atmospheric aerosols are further described in section 1.2.5.

Severe smog episodes were observed in the middle of 19th century over Los Angeles. The Los Angeles smog significantly differs from London smog by both composition and origin.¹ It was concluded that clearly visible haze over Los Angeles area was a result of tropospheric ozone interaction with a variety of volatile organic compounds (VOCs), resulting in the atmospheric aerosol formation. Similar to London smog, pollution over Los Angeles also consisted of a variety of trace gases, mainly NO_x, O₃ and VOC's. The mechanism of aerosol formation due to ozone –

initiated oxidation of unsaturated compounds, namely α -pinene is described in section 1.4. Ozone was produced over Los Angeles area as a result of sunlight interaction with traffic related pollution, containing large amounts of nitrogen oxides (NO_x). Similar phenomena were observed in a number of cities across the globe, near the end of the 20th century; for example in Athens, regions adjacent to Sydney, Mexico City and Tokyo to name a few. ^{1,4}

As a consequence of the extensive air pollution, observed over highly urbanized areas, air quality legislation was introduced in a number of countries. In response to the London events from December 1952, a Clean Air Act was passed by the UK Parliament in 1956. The Clean Air Act from 1956 significantly reduced the number of excess deaths, following the London smog event in 1962, leading to approx. 700 as opposed to 4000 excess deaths during the previous event – see Table 1.2. Later, in 1987 World Health Organization (WHO) introduced the Air Quality Guidelines for Europe, establishing standards for both SO_2 and black smoke concentrations. ⁶

1.1.1. Size distribution, density and concentration

In order to describe the physical properties of the aerosols, several important definitions need to be presented. Size is the most important PM property, all crucial aerosol properties are size - dependent. ^{1,2} As already discussed in section 1.1., aerosols encountered in the atmosphere are often non-spherical. Therefore, effective diameters are used to approximate the sizes of non-spherical particles and the most popular one is aerodynamic diameter. Aerosol aerodynamic diameter is defined as the diameter of unit density sphere (1 g/cm^3) having the same terminal falling velocity as the particle of interest. ¹⁻³ Therefore, aerodynamic diameter for non-spherical particles describes their dry deposition efficiency. ⁷

Particle size distribution can be presented by plotting the number of particles (ΔN) against the diameter interval (ΔD) in either linear or logarithmic scales. Frequently, a plot of $\Delta N/\text{Log}\Delta D$ as a function of ΔD or $\Delta \log D$ is used. Particle distribution data are usually not continuous, and are expressed as a particle number in a given diameter interval. Such data representation was concluded to be the most convenient and representative. ^{1,2} A typical plot of particles size distribution, $\Delta N/\Delta \log D$ against ΔD is shown in Fig. 1.2. Please note that the plot shown in Fig. 1.2 does not represent any actual experimental data.

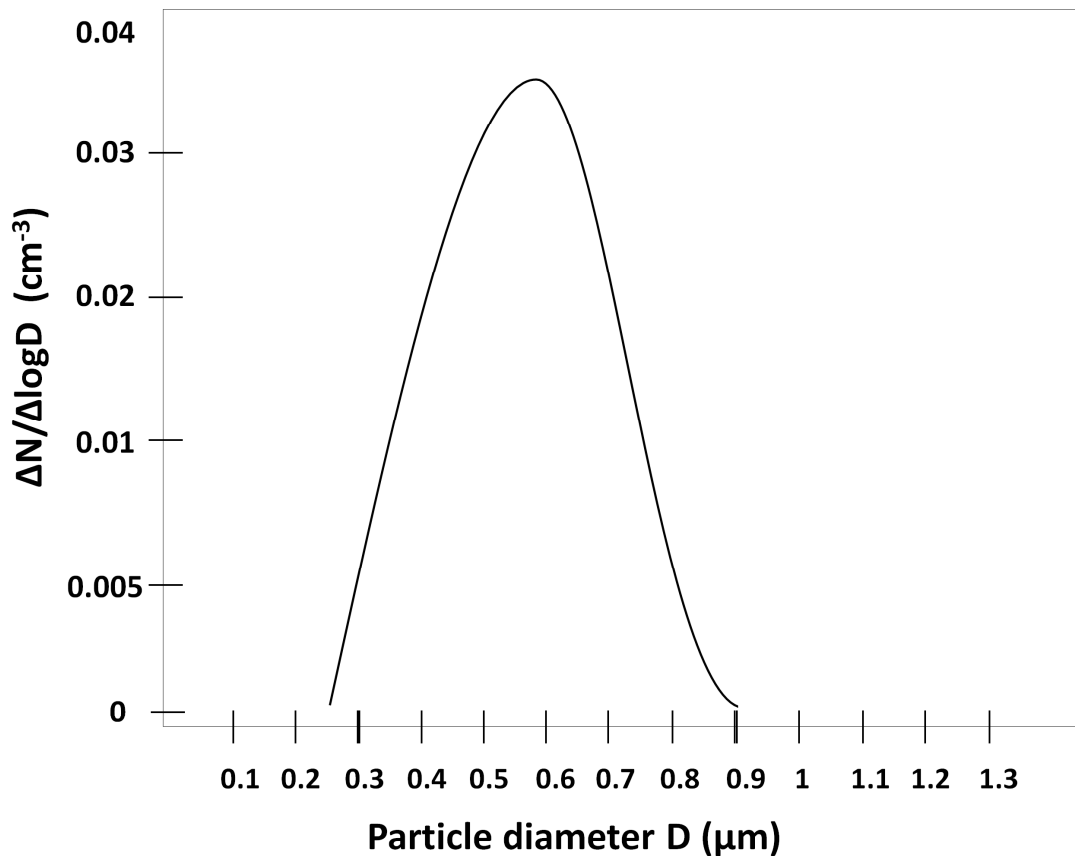


Figure 1.2 Typical plot of the particle size distribution

The data shown in Fig. 1.2 should be interpreted as follows: by integrating area under the curve, a number of particles falling in a given size range can be calculated. Other properties can be illustrated in the same manner, such as particles volume, surface or velocity.^{1,2,8}

When sizes of atmospheric particles are considered, distinction between specific groups of particles is very often made. Particles having a diameter less than 2.5 μm ($\text{PM}_{2.5}$) are referred to as fine, whereas particles having a diameter greater than 2.5 μm are called coarse. This distinction was concluded to be a fundamental one, taking into account different origins, atmospheric processing and removal mechanisms for fine and coarse particles.^{1,3} Ultrafine particles (UFP's) is a subcategory of fine particles ($\text{PM}_{2.5}$), having a diameter less than 0.01 μm .^{1,3} Particles having a diameter less than 10 μm (PM_{10}) is another frequently monitored aerosol fraction; standards for PM_{10} are also included in the air quality legislation.³ The PM_{10} and $\text{PM}_{2.5}$ distinction is due to different penetration of human respiratory track by the particles having different diameters (see

Section 1.2.5). It is also important to emphasize, that PM_{10} should not be confused with coarse particles. PM_{10} is a subfraction of coarse particles, just like UFP's are the subfraction of $PM_{2.5}$. Even so, a number of studies defines coarse fraction as particles having diameters between 2.5 and 10 μm .⁹

There are several common conventions used to describe the aerosol concentration, the most common one is mass concentration. Aerosol mass concentration provides particles mass in a volume of gas, and is often expressed in $\mu g/m^3$. The aerosol mass concentration in $\mu g/m^3$ is also commonly used in air quality legislation. Another popular measure of aerosol concentration is the number of particles (N) per volume of gas, given in N/ml.²

Particle density differs from the bulk density of the aerosol – particles plus the bath gas, since it describes the density of particles only. Particles density also differs from the parent material, due to non-uniform structures of the particles, like cracks and void spaces.¹

1.2. Global overview of aerosols properties

This part of the introduction presents an overview of the atmospheric particles properties on a global scale. In Section 1.2.1, anthropogenic and biogenic PM sources are described, for both primary (Section 1.2.1.1.) and secondary (Section 1.2.1.2.) aerosols. Afterwards, bulk, global aerosol composition is presented, based on the currently published measurements of aerosol optical depth and modeling studies – Section 1.2.2. Two critically important aerosols – related topics, climate and human health influence are described in Section 1.2.4 and Section 1.2.5, respectively. Influence of the atmospheric aerosols on global climate, by both direct (Section 1.2.4.1.) and indirect (Section 1.2.4.2.) effects are outlined. Aerosols health effects are described based on the currently published epidemiological (Section 1.2.5.1.) and toxicological (Section 1.2.5.2.) investigations.

1.2.1. Sources

As outlined in Section 1.1., aerosols can be introduced into the atmosphere from a number of different sources. Significant portion of the atmospheric particle originates from the natural sources. However, increased industrialization over highly urbanized areas, is the cause of constantly-growing contribution of the anthropogenic aerosols to the yearly, global aerosol flux.

^{2,3,10-13} Particles can be either directly introduced into the atmosphere (primary aerosols) or formed from a variety of precursors (secondary aerosols). Formation of secondary organic aerosol by ozone – initiated oxidation of α -pinene is described in section 1.4.

1.2.1.1. Primary aerosols

The main components of natural, primary aerosols are mineral dust and sea salt. It is currently estimated that 75% of the global dust emission can be ascribed to the natural sources.¹⁴ The remainder of the mineral dust emission is due to the agricultural activity.^{14,15} Current and past estimations of the global dust emissions were summarized by Zender et al.¹⁶ Sea salt aerosol, sometimes referred to as a sea spray is emitted into the atmosphere due to wind activity over oceans and breaking of the ocean waves.^{9,17} Volcanic dust is also believed to be an important constituent of the primary, aerosol.¹⁸ However, contribution of the volcanic dust to the total biogenic, primary aerosols emission is estimated to be about two orders of magnitude less than mineral dust and sea salt aerosols, similar to particles emitted into the atmosphere due to forest fires.^{2,3} Primary biological aerosols consist mainly of bacteria, fungal spores, pollens, and viruses.^{2,7,19}

Primary anthropogenic aerosols sources are fossil fuels combustion and industrial processes.^{3,9} Significant source of the anthropogenic particles, besides the agricultural processes is also burning of wood fuel. Primary particles introduced into the atmosphere due to human activities include BC, industrial dust and organic aerosols (organic carbon; OC).

1.2.1.2. Secondary aerosols

Secondary aerosols are formed directly in the atmosphere due to processing of volatile precursors, leading to the formation of products that can subsequently undergo gas-particle partitioning. Processes leading to the new particles formation include condensation, nucleation as well as a variety of chemical reactions.²⁰ Atmospheric trace gases such as SO₂, dimethyl sulfide (DMS), ammonia (NH₃) and nitrates are the major precursors of the secondary aerosols. SO₂ is emitted into the atmosphere mainly due to fossil fuels burning and industrial processes,⁹ but also from natural sources.³ These atmospheric trace gases (SO₂ and NO_x) are transformed into the

corresponding inorganic acids. The inorganic acids can subsequently react with NH_3 , to yield ammonium salts, and form particles. Secondary organic aerosols are also formed by condensation of low-volatile products, produced by oxidation of VOCs. Oxidants that are known to react with a variety of precursors to form aerosols, include O_3 , atomic oxygen and radicals: Cl, OH and NO_3 .^{21,22} Such conversion produces numerous organic compounds, many of which have been identified in the previously published studies – see Hallquist et al.²⁰ and references cited therein. Detailed description of the secondary organic aerosol (SOA) formation during ozone - initiated oxidation of α -pinene is given in Section 1.4.1. Structures of the high-molecular weight (HMW) components, tentatively identified in the currently published studies of α -pinene SOA are described in Section 1.4.3.

1.2.2. Composition

Composition of the atmospheric particles is not constant, since it varies in time, depending on the type of particles and their atmospheric processing (aging). Aerosol composition is dependent on source and type of the aerosol, precursor, oxidant (for secondary aerosols) and formation conditions. Since e.g. SOAs are known to contain numerous organic compounds, only brief overview of the global, bulk aerosols compositions will be presented here. Bulk aerosol composition varies significantly, dependent on the sampling site. As already discussed in Section 1.2.1, the bulk aerosol components are: sulphates, nitrates, sea salt, mineral dust, OC and BC from both biomass burning and fossil fuels burning. Pöschl¹⁰ in his recent review outlined the bulk aerosols concentration collected in the urban and remote mountain region. The data, based on the $\text{PM}_{2.5}$ composition analysis from a number of studies, shows a large composition variation between urban and mountain-region aerosols. Indeed, comparison of the data from the recent compilation of the aerosol optical depth measurements,²³ complemented by modeling estimates of the particles composition²⁴ illustrates that either component listed above can be a dominating one, depending on the sampling site. It is important to note that there are still significant uncertainties about global aerosol composition, e.g. global SOA emission may have been underestimated in some modeling studies.²⁰

1.2.3. Deposition mechanisms and lifetimes

As already discussed in section 1.1, aerosols are eventually removed from the atmosphere and deposited onto the Earth's surface. Relative lifetimes of the atmospheric particles vary significantly, and are strongly dependent on a number of variables, including particles size, density and chemical composition as well as local weather conditions (see below).^{12,25} The lifetimes of atmospheric particles varies from days to weeks, as opposed to e.g. various trace gases encountered in the atmosphere, whose lifetime varies from a few seconds up to a century.^{3,10} Particles, as well as gaseous pollutants are removed from the atmosphere in the presence or absence of precipitation. These two mechanisms are termed wet and dry deposition. It is currently estimated that the wet deposition is the main removal pathways of the atmospheric aerosols.¹⁰ However, the main deposition pathway is very strongly dependent on a number of local factors (see section 1.2.3.1.). Therefore, local removal pathways sometimes differ significantly from the global tendencies.¹ For example, Matsuda et al.²⁶ investigated deposition pathways of BC (soot) particles in Thailand tropical forest and concluded that dry deposition for these particles was much more important than the wet deposition.

1.2.3.1. Wet deposition

Removal of the particles by any form of precipitation is defined as wet deposition. Particles can be scavenged by rain, snow, fogs and clouds and delivered onto Earth's surface. It is important to underline, that deposition classification refers only to the transportation mechanism.¹ For example, deposition of the organic aerosols by rainfall onto the desert surface is still termed wet deposition. Efficiency of the removal mechanism depends on a number of factors. When the particle is deposited via wet deposition, it must first come in contact with water or ice particles. Whether or not this occurs, strongly depends on the amount of precipitation in the region. If the solubility of particles under consideration is sufficiently high, it can be scavenged by water or ice particles. In turn, the solubility of the specific particles and whether they are scavenged by ice or snow depends on pH of the precipitation, size and number of water droplets present etc.¹ Before the precipitation reaches the Earth's surface, scavenged aerosol can undergo a number of chemical transformations. Frequently, scavenged particles are again released, by e.g. evaporating

rain droplets.³ Naturally, wet deposition is very important sink of the aerosols acting as a cloud condensation nuclei (CCN) and ice nuclei (IN) – see Section 1.2.4.

1.2.3.2. Dry deposition

Gravitational setting of the aerosol particles, as well as adhesion and diffusion onto the Earth's surface is termed dry deposition. Dry deposition is defined as any form of aerosols removal from the atmosphere that does not involve water droplets or ice crystals, as opposed to wet deposition.^{3,10} Dry deposition is strongly dependent on the type of the surface. Particles can be deposited directly on to the soil, as well as on the plants surface and buildings; chemical nature of both the surface and the identity of deposited particles governs the dry deposition efficiency. Generally, it is assumed that gravitational setting and sedimentation is the predominant removal mechanism for particles having diameters larger than 10 μm .⁷ As already discussed in Section 1.1.1, aerodynamic diameter defines the efficiency of particles deposition, in the absence of precipitation. Similar to wet deposition, particle size, density and shape^{3,27} can determine whether or not the dry removal occurs. Speed and direction of wind near the surface itself was also concluded to be a very important factor, governing the efficiency of particles dry removal. Again, the nature of the surface itself does not affect the removal mechanism classification. As already discussed, dry deposition of atmospheric PM is believed to be less important than wet deposition.

1.2.4. Aerosols influence on the climate

Aerosols, as the natural components of the atmosphere, have significant impact on the Earth's radiation balance and climate. However, as discussed in Section 1.2.1, since the preindustrial era, anthropogenic sources of the atmospheric PM have an ever-growing contribution to the global aerosol budget. Aerosols are believed to cool the Earth's atmosphere, as opposed to greenhouse gases (GHGs).¹³ The net effect of GHGs and aerosols is measured by their radiative forcing, given in watts per meter squared ($\text{W}\cdot\text{m}^{-2}$). Greenhouse effect is caused by trapping the part of the outgoing Earth's infrared (IR) radiation by GHG's and reflecting some part of it back onto the surface, thus causing the planet's temperature to rise. Positive value of the GHGs radiative forcing indicates that their warming effect has increased since the preindustrial era. The increase of GHGs radiative forcing is currently estimated to be about $2.4 \text{ W}\cdot\text{m}^{-2}$.¹³ It is

estimated that the cooling effect produced by anthropogenic particles compensate, to some extent, atmosphere warming caused by anthropogenic emission of the GHG.^{13,28,29} Aerosols influence the Earth's radiation budget by absorbing and scattering solar radiation (direct effects) and by altering clouds properties (indirect effects). The aerosols negative radiative forcing is estimated to be from -2.5 to -0.5 $W \cdot m^{-2}$, with the largest contribution from the direct effects.^{24,28,30-32} Those two mechanisms will be briefly described in Sections 1.2.4.1. and 1.2.4.2.

1.2.4.1. Direct effects

Aerosols directly influence the radiation budget by absorption and scattering of the incoming solar radiation. As the aerosol particles size becomes close to the wavelength of the incoming solar radiation, scattering can occur, and thus the amount of radiation reaching the surface is decreased. While scattering is a portion of the incoming solar radiation reflected back into space, leading to the cooling effect, absorption is a component of the semi direct effect (see section 1.2.4.2.).³ Scattering and absorption efficiency is dependent on the size and the number of aerosol particles and also on their chemical composition.^{13,28} In addition to reflecting a part of incoming solar radiation back into space, aerosols can also reflect part of the radiation back onto the surface. The absorbing and scattering efficiency is described by the single scattering albedo (SSA).^{13,32} SSA is defined as the ratio of scattering to the sum of scattering and adsorption. As already discussed, direct effects have the largest contribution to the observed aerosol net cooling effect.^{13,33}

1.2.4.2. Indirect and semi-direct effects

The most important indirect effect is aerosol interactions with clouds. In the atmosphere, clouds are formed on the preexisting seed particles, as opposed to homogenous nucleation of water vapor. Aerosols can act as both CCN and ice nuclei IN. The potential of specific particles to act as the CCN depends largely on their size and hygroscopicity.^{7,34} The increase in the atmospheric particles concentration due to human activities, resulted in enhanced concentration in CCN and IN. Higher number of CCN and IN, leads in turn to the formation of smaller and more numerous cloud droplets; such clouds reflect the solar radiation more efficiently. This is the major indirect effect, also termed cloud albedo or Twomey effect.^{28,29,33} As already discussed, cloud

warming due to more efficient absorption of solar radiation, leads to their evaporation, thus allowing more radiation to reach the surface. This is called a semi direct effect, since it is a consequence of the aerosol absorption properties, but also affects the clouds. In general, indirect effects are considered to be less important on a global scale, than direct radiative forcing.

1.2.5. Health effects of atmospheric aerosols

Adverse PM human health effects have been investigated by both epidemiological and toxicological studies. Both short and long term effects of the PM exposure on human health have been reported. Particle size determines how deeply particles penetrate the respiratory system.^{8,35,36} Smaller particles can travel deeper into the human respiratory track, and most frequently cause more severe health problems. As already discussed in section 1.1, for the purpose of air quality control, PM_{2.5} and PM₁₀, are the two routinely monitored aerosol fractions⁸. Ultrafine particles are believed to be particularly toxic fraction of the PM_{2.5}.^{4,6,10,35,37,38}

Currently, it is estimated that increase of PM₁₀ concentration by 10 µg m⁻³ results in mortality risk increase between 0.1 and 1% for all-cause mortality, as well as for cause-specific studies, including cardiovascular and respiratory conditions^{4,6,8,35,39}. Smaller particles are believed to be significantly more toxic, which is reflected by the increased health risks and the premature death risk increase associated with the elevated PM_{2.5} concentration. Increase in PM_{2.5} concentration by 10 µg m⁻³ was reported to increase all-cause mortality by approx. 4%^{4,8} and by 8% increase in lung cancer mortality.⁵ Consequently, a decrease of 10 µg m⁻³ in PM_{2.5} concentration was estimated to increase the mean life expectancy by 0.61 ± 0.20 years in 51 US metropolitan areas.^{8,40} Brook et. al.³⁹ in their review summarized a number of studies investigating relative mortality risk due to PM_{2.5} and PM₁₀ exposure published since 2004. It is also important to notice that apparently there is no threshold concentration below which health effects of PM exposure are no longer observable.^{5,8}

1.2.5.1. Epidemiological studies

A number of end-points have been used to analyze association between PM pollution and adverse human health effects, and all-cause mortality was most commonly studied. Additionally, in a number of studies specific health risks and cause-specific mortality were also included in the

reported evaluations. Cause - specific studies investigated correlations between PM exposure and variables like neurotoxic effects, cardiovascular and respiratory disorders, asthma, hospital admissions as well as work and school absences. Several studies reported positive correlations between increased mortality and concentrations of PM₁₀ as well as PM_{2.5}, for both short and long term exposures. In the study by Dockery et. al,⁴¹ it was concluded that inhalation of PM resulted in excess mortality in six United States cities. In a follow-up study Laden et. al.⁴² reported that air quality improvement i.e. reduction of PM_{2.5} concentration resulted in reduced mortality risk, for all-cause mortality as well as cardiovascular and lung cancer mortality. Similar correlation between PM₁₀ as well as total suspended particles (TSP) concentration and increased all-cause mortality were observed in Utah Valley⁴³ and in a number of US cities, including Los Angeles,⁴⁴ Steubenville in Ohio⁴⁵ and Detroit.⁴⁶ Concentration of total PM and SO₂ were also found to be positively correlated with increased mortality in Philadelphia, as reported by Schwartz and Dockery.⁴⁷ Also, it was concluded the exposure to PM_{2.5} and EC particles inhibited development of children's lungs between 10 and 18 years old.⁴⁸ Xu et al.⁴⁹ reported a strong correlation between the decrease of pulmonary function of adults and air pollution by PM and SO₂, produced mainly due to the extensive use of household coal heaters. Elevated concentrations of PM₁₀ were also found to cause respiratory distress in Utah, Salt – Lake city and Cache Valleys.⁵⁰ Inhalation of diesel exhaust particles was reported to be related to enhancement in certain allergic responses and asthma symptoms.⁵¹⁻⁵³ Pope et al.⁵⁴ described positive association between fine PM exposure, i.a. PM_{2.5} and all-cause, cardiopulmonary and lung-cancer mortality, studying the data for 500000 adults in the US. A detailed list of variables investigated in cause – specific studies, together with a number of papers published for each variable, for both short and long – term investigations can be found in a recent review by Ruckel et al.⁵

Majority of published studies reported positive correlations between all-cause mortality as well as case-specific mortality and PM exposure for general population.⁸ However, an exposure to PM pollution was proven to affect human health on all stages of life.⁵ Therefore, several studies included variables like age; such as already discussed investigations by Gauderman et al.⁴⁸ and Xu et al.⁴⁹ studied negative effects on children and adults health, respectively. A review of studies investigating association between PM exposure and respiratory symptoms in children was

published by Wards and Ayres.⁵⁵ Adverse human health effects of PM pollution were studied for both short and long-term exposures.^{4,5,8} Long term studies investigated the effects of PM inhalation over several years,⁴² while short-term studies usually cover the time-scales from a few days to several months, like for instance, the study by Wards and Ayres.⁵⁵

1.2.5.2. Toxicological studies

A number of studies proposed specific aerosols components to be responsible for the adverse PM health effects. Exposure to the bulk inorganic aerosols components, such as sulphates and nitrates was concluded to be only slightly correlated with the negative aerosol health effects.^{8,56,57} Transition metals are often associated with the cell damage by PM due to the redox activity.^{4,8,37} In their review Chen and Lippmann⁵⁸ identified a number of transition metals, associated with the aerosols adverse health effects, mainly Ni, V, Pb and Zn.⁸

Polycyclic aromatic hydrocarbons (PAHs) are compounds that, alongside transition metals like As and Ni,⁸ are often associated with the cancerogenic potential of the ambient PM, especially PM_{2.5}.^{4,59} PAHs were also concluded to have mutagenic properties. PAHs are produced mainly due to incomplete combustion processes and road traffic.⁴ Particles produced as a result of combustion processes are also believed to have free radicals permanently bounded to their matrix.⁴

It was proposed, that due to the larger surface area, UFP retain toxic substances more efficiently, in comparison to particles with larger diameters.^{4,8,38} Very small diameter results in even deeper penetration of the human respiratory system by UFP; also, these particles are capable of transition into the bloodstream. Ultrafine particles were also proven to generate free radicals, and thus leading to the lung damage and DNA mutation, oxidative stress and inflammation.^{4,37} However it is important to underline, that aerosols toxicity should not be associated only with their chemical composition. Rather, the observed health effects were concluded to be combination of detected trace components and particles sizes, which in turn determines their biological processing, as discussed above. Indeed, MacNee and Donaldson³⁷ demonstrated that UF BC particles generate oxidative stress in a different manner than transition - metals mediated mechanism.

1.3. Secondary organic aerosols (SOAs)

SOA is formed when the volatile precursors are transformed into low-volatile products by various atmospheric processes and form particles via gas-particle partitioning. Ozone as well as NO_3 , OH and Cl radicals are the major oxidants in the troposphere.^{20,60} The formation pathways of the NO_3 , OH and Cl radicals in the atmosphere are well known,^{1,21,60} and will not be described here. Emissions and relative importance of the BVOC are outlined in Section 1.3.1, followed by the tropospheric ozone formation mechanism, described in section 1.3.2. General alkene ozonolysis mechanism is presented in Section 1.3.3.

Since α -pinene and ozone reaction is described in detail in the subsequent section (1.4), only general VOC oxidation mechanism will be presented here. Atmospheric degradation of BVOCs begins with the formation of the alkyl or substituted alkyl radicals.^{20,21,60} For the BVOCs, the radicals can be formed via two possible mechanisms: addition of O_3 , NO_3 or OH radicals to the carbon-carbon double bond or by H atom abstraction from C-H or, less commonly, from O-H bond.²¹ General mechanism of BVOC's oxidation in the atmosphere is shown in Fig. 1.3.

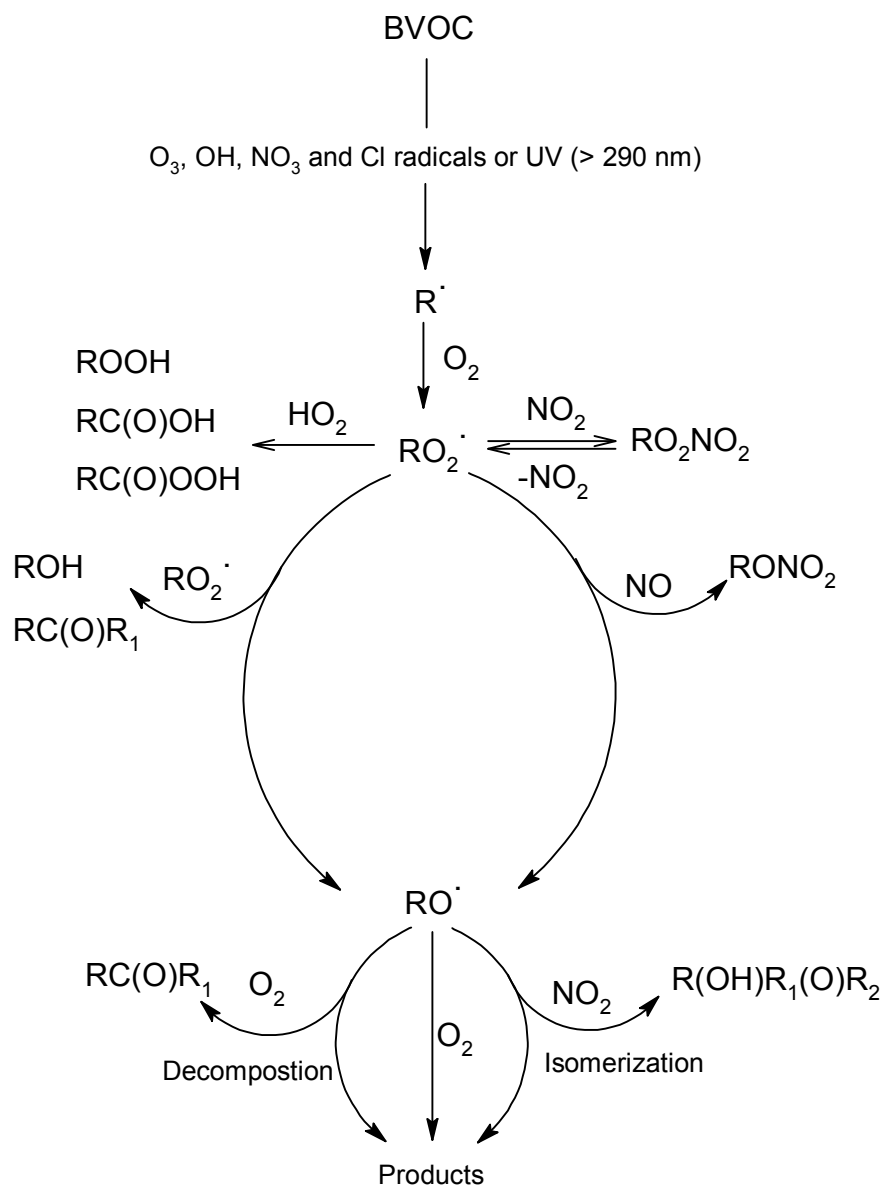


Figure 1.3 General mechanism of BVOC's oxidation in the atmosphere

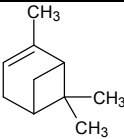
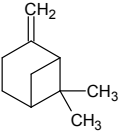
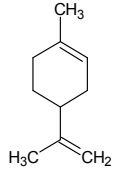
As shown in Fig. 1.3, alkyl radicals, formed by BVOC reaction with oxidants and/or UV photolysis subsequently react with atmospheric oxygen, to form organic peroxy (RO₂) radicals. ^{20,21,60} RO₂ radicals can react with HO₂ radicals to form hydroperoxides, carboxylic acids and peroxy acids. Reversible reaction with NO and NO₂ leads to the formation of nitrates and peroxy nitrates, respectively. The second key intermediates in the atmospheric processing of BVOCs are alkoxy

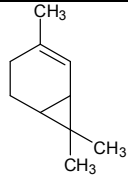
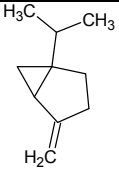
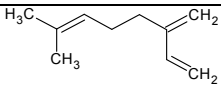
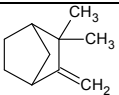
radicals (RO). Alkoxy radicals can decompose to form carbonyl compounds or isomerize to form hydroxycarbonyls and other products.

1.3.1. Emission of biogenic secondary organic aerosols (BSOAs) precursors

A variety of BVOCs have been recognized as the important SOAs precursors. The most important SOA precursors are alkanes, alkenes and aromatic hydrocarbons.⁶¹ Oxygenated VOCs were also concluded to be important SOA precursors, such as aldehydes, ketones, aliphatic alcohols, esters and alkyl nitrates.^{21,60} It is estimated that biogenic VOCs emission accounts for more than 90 % of the total non-methane organic compounds emission.^{60,62} 1150 Tg of BVOCs are emitted to the atmosphere every year from vegetation and around 100 Tg/year from the anthropogenic sources.⁶¹ Isoprene and monoterpenes are the most abundant natural volatile organic compounds. It is estimated that isoprene accounts for 30 – 44 % of the global BVOCs emission.^{21,61,62} Monoterpenes account for 10 % of the yearly BVOCs flux,^{21,60,63} with the α -pinene, β -pinene and limonene being the most abundant in the ambient atmosphere - see Table 1.3.^{20,21,62-66} Compounds in Table 1.3 are listed in the order: from the most studied BSOA precursor to the precursor that received the least interest in the current literature.

Table 1.3 Names and structures of the unsaturated, biogenic monoterpenes studied as the BSOAs precursors

Name	Structure
α -pinene	
β -pinene	
Limonene	

Δ^3 -Carene	
Sabinene	
Myrcene	
Camphene	

As listed in Table 1.3 α -pinene, β -pinene and limonene are the most extensively studied precursors of the BSOA. Other, less abundant monoterpenes, such as Δ^3 -carene, sabinene, myrcene and camphene have received considerably less attention, due to lower atmospheric concentration of these compounds.

Isoprene, α and β -pinene are generated due to plants vegetation and are synthesized from the common precursors: dimethylallyl pyrophosphate (DMAPP) and isomer isopentenyl pyrophosphate (IPP).^{63,67} The precursor of monoterpenes, geranyl pyrophosphate, is synthesized via condensation of DMAPP and IPP.

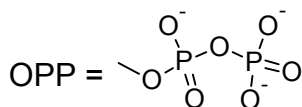
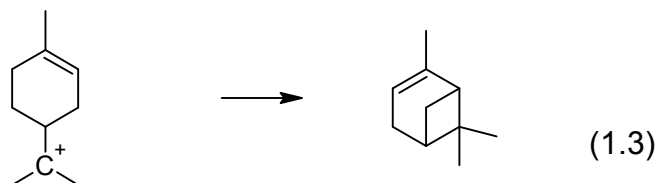
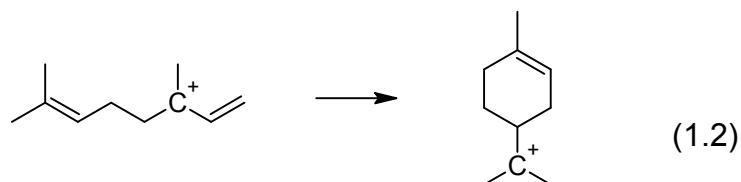
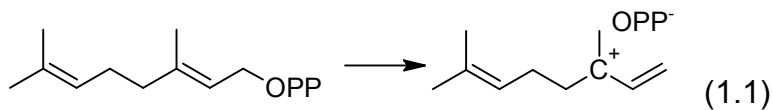


Figure 1.4 Biosynthesis of α -pinene

As shown in Fig. 1.4, the first step of the biosynthesis of α and β -pinene is the dissociation of geranyl pyrophosphate – reaction 1.1. Subsequently, enzymatic cyclizations of the geranyl pyrophosphate (reaction 1.2) lead to the formation of α or β -pinene – reaction 1.3.^{63,67}

1.3.2. Ozone in the atmosphere

Ozone is an important trace constituent of the Earth's atmosphere, found mainly in the stratosphere. Region of the stratosphere with the highest ozone concentration is called ozone layer. About 90% of the atmospheric ozone can be found in the stratosphere.

Stratospheric ozone production/decomposition cycle involves a series of photochemical reactions, originally proposed in 1930's by Sir Sydney Chapman, and thus referred to as the Chapman cycle: reactions - 1.4 – 1.7 in Fig. 1.5.⁶⁸

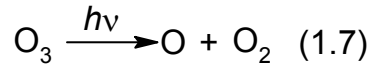
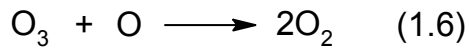
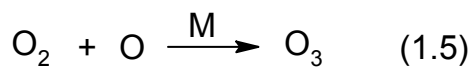
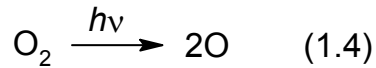


Figure 1.5 Chapman cycle reactions

The UV absorption by the ozone molecule leads to the formation of two oxygen atoms (reaction 1.4). Atomic oxygen subsequently reacts with oxygen molecule to produce ozone via reactions 1.5. In reaction 1.5, M symbolizes a third body, required for the stabilization of high – energy byproduct of the atomic oxygen addition to the oxygen molecule.⁶⁹ In this reaction, excess energy is released as heat. If the ozone molecule is encountered by the atomic oxygen, it can recombine to form two oxygen molecules – reaction 1.6. Ozone can dissociate to form energetically excited oxygen molecule and atomic oxygen. Excess energy, after the UV absorption in the reaction 1.7 is also released as heat, thus both reactions 1.5 and 1.7 are responsible for the increase of temperature in the stratosphere.

Ozone layer causes the increase of temperature in the stratosphere, as compared to the troposphere. Troposphere is mainly heated by the surface thermal radiation, and the temperature in this layer decrease with the increasing altitude. However, in the stratosphere the excess energy of the UV radiation absorbed by the ozone, is emitted as heat, therefore rising the temperature as the altitude increases.

Ozone absorbs UV radiation with the wavelengths shorter than 290 nm. It is well known, that increased amount of the UV-B radiation (280–315 nm) significantly impacts both climate and all living species (including humans). Depletion of the ozone layer, and thus increase in the amount of the UV-B radiation reaching the planet’s surface was concluded to be associated with various adverse human health effects, including skin cancer, as well as conditions like age-related macular degeneration and ocular melanoma. Exposure to UV radiation was also concluded to suppress

some aspects of the immune system.^{70,71} It is important to note that increased exposure to UV-B radiation also promotes the production of vitamin D, thus counteracting to some extent the remainder of negative health effects.⁷¹

Depletion of the ozone layer was also concluded to have significant impact on the climate and plants, including alterations in the biological cycles, aquatic ecosystems, Earth's radiation balance and hydrological cycle.^{70,72} Ozone is also the third most important greenhouse gas.

Therefore, preserving the protective ozone layer is critical for the life on Earth. It is important to underline, that while the regulations of the Montreal Protocol are essential for protection of the ozone layer, it will take several decades to repair the damage caused by Halons after 1980.⁷²

The importance of the ozone layer was recognized in Vienna Protocol (1985). Although Vienna Protocol was ratified by 196 countries, it did not contain any legally binding regulations regarding the production and emission of the substances with high ozone depletion potentials (ODP's). Such regulations were included in the Montreal Protocol (1997), which is currently ratified by 197 countries, including all members of the United Nations and European Union.⁷³ The Montreal Protocol contains legally binding regulations, effective from 1st of January 1989, regarding reduction in emissions of the substances with high ODPs. Briefly, the protocol regulations contain reduction schedules for the halogenated hydrocarbons emission, responsible for the rapid sink of the protective ozone layer.⁷⁴ All halogenated hydrocarbons were concluded to significantly decrease the stratospheric ozone concentration, with the exception of hydrofluorocarbons (HFCs).⁷⁵⁻⁷⁷

Tropospheric ozone is produced mainly via photolysis of the gaseous air pollutants. It is important to underline, that small concentration of the natural, background ozone is also present near the surface. However, tropospheric ozone production is known to be significantly enhanced due to atmospheric processing of the anthropogenic pollutants.

The major precursor of ozone in the troposphere is NO₂. NO₂ is photolysed by solar UV radiation to form O₃, as shown in Fig. 1.6. Initially, photodissociation of the NO₂ molecule leads to

the formation of the NO molecule and ground state atomic oxygen – reaction 1.8. Afterwards, atomic oxygen reacts with the oxygen molecule, (reaction 1.9).^{69,78,79}

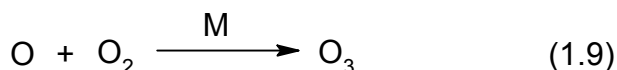
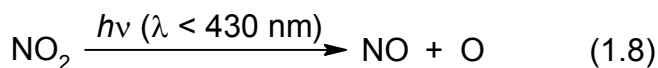


Figure 1.6 Photolysis of NO₂ and formation of tropospheric ozone

It is well known that NO_x emission is mainly associated with the human activity, such as road traffic, and industrial fuel combustion. NO is oxidized to NO₂ via series of photochemical reactions in the presence of VOCs and sunlight- Fig. 1.7.^{69,78,79}

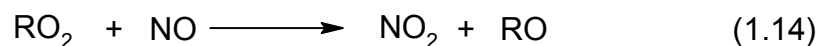
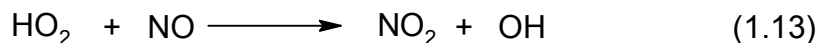
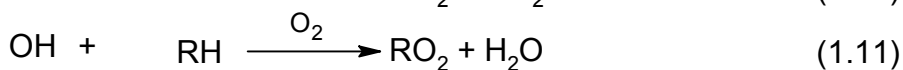
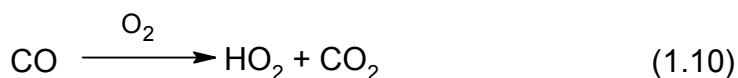


Figure 1.7 Production of the NO₂ in the presence of VOCs

As shown in Fig. 1.7, both RO₂ and HO₂ radicals rapidly oxidize NO to NO₂ – reactions 1.13 and 1.14.^{69,78,79} HO₂ radicals can be generated by reaction of OH with CO.⁷⁹ If the small alcohol molecule reacts with OH, it can also generate HO₂ via the reaction of alkoxy radical (RO) radical with O₂.⁶⁹ After oxidation of NO to NO₂, OH radical is regenerated, this propagates the chain – reaction 1.13. The major chain termination step is reaction 1.15, oxidation of NO₂ to HNO₃

– a major component of acidic rain.⁶⁹ Since the air pollution is the cause of the elevated NO_x concentration, ozone is the component of the urban smog.

The remaining 10% of ozone is found in the troposphere and it is considered to be a harmful contaminant, negatively affecting both human health and plants. High concentrations of the ground – level ozone are known to have negative impact on the vegetation such as crop yields, biomass accumulation and forest growth.⁷⁹⁻⁸² Since the elevated ozone concentration, can reduce the forest growth rate, it can also significantly impact the removal of the CO₂ from the atmosphere, and in this way strongly influence the carbon cycle.⁸³

Human exposure to the elevated ozone concentrations is known to be associated with health effects such as skin cancer, allergic responses and increased mortality.^{84,85} Thus, the human health effects of the ground level ozone significantly differ from those of the stratospheric ozone, with the latter one composing the protective ozone layer.

As already discussed in Section 1.3, ozone is one of the major tropospheric oxidants. Ozone reaction with the natural, unsaturated compounds is known to produce SOA. In section 1.3.3, general alkene ozonolysis mechanism is described.

1.3.3. Alkene ozonolysis

Ozone is one of the main thropospheric oxidant of the BVOCs. The reaction of alkenes with ozone is also known to produce SOA. Large quantities of the biogenic alkenes are emitted to the atmosphere from natural sources, such as plant vegetation, as outlined in Section 1.3.1. Therefore, detailed knowledge of the atmospherically relevant alkene ozonolysis mechanism is essential. In this section, general alkene ozonolysis mechanism is described. Subsequently, overview of the previously published data on the ozonolysis reactions in the liquid phase is presented in Section 1.3.4, focusing primarily on the standards synthesis for SOA composition analysis. α -Pinene ozonolysis mechanism is presented in Section 1.4.1.

Currently accepted alkene ozonolysis mechanism was originally proposed by Rudolf Criegee,⁸⁶ hence the by-products of this reaction are referred to as excited Criegee intermediate (ECI) and stabilized Criegee intermediate (SCI) – see below.

Ozone addition across the carbon-carbon double bond initially leads to the formation of an unstable primary ozonide, as shown in Fig. 1.8, reaction 1.16.

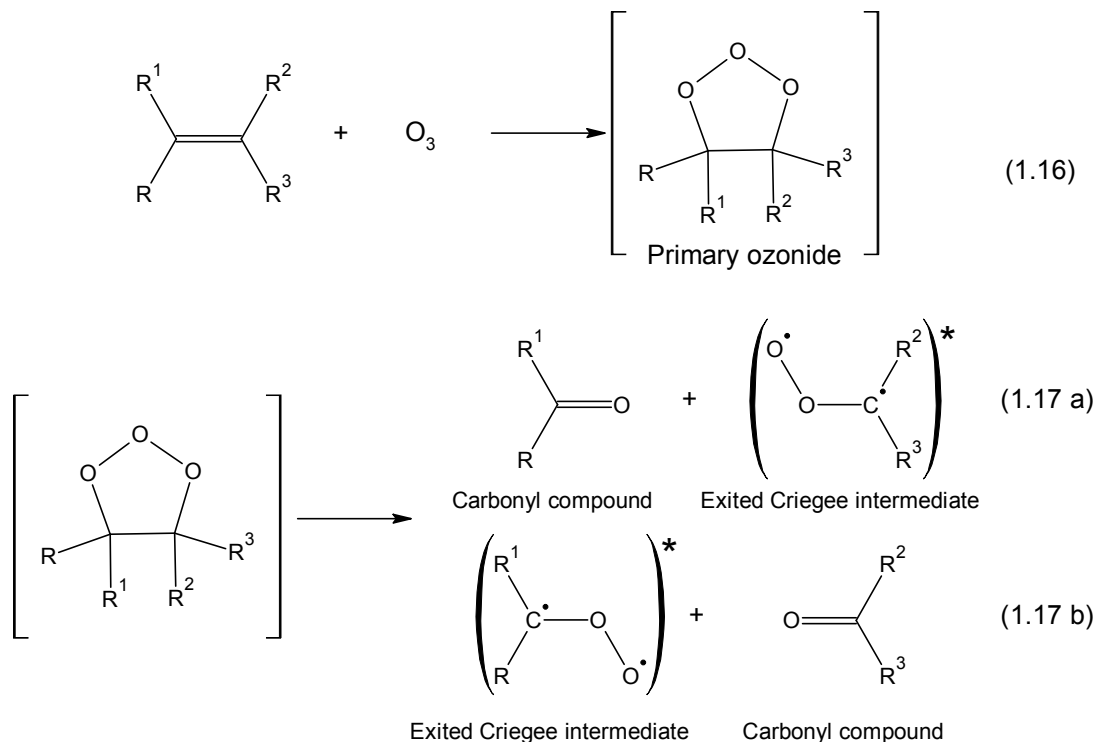


Figure 1.8 Formation of primary ozonide and its decomposition yielding carbonyl compound and excited Criegee intermediate (ECI)

As stated in the Criegee paper,⁸⁶ primary ozonides are unstable and rapidly decompose to yield ECIs and carbonyl compounds, reactions 1.17a and 1.17b. ECIs are also termed Criegee biradicals or Criegee zwitterions or carbonyl oxides. In Fig. 1.8, ECIs have been denoted as biradicals, however, denoting those intermediates as zwitterions with positively charged carbon atom and negatively charged oxygen atom, is also accepted. Indeed, the zwitterion notation is most often used when describing the liquid-phase ozonolysis reaction,^{1,87} while the biradical notation is used when describing reactions in the gas phase.^{1,88} In some publications, neither zwitterion nor radical notation is used, like for instance in Tobias and Ziemann papers.⁸⁹⁻⁹¹ The writing convention is not strictly defined, with all notation used interchangeably. This may be due to ambiguous nature of the ECIs, since, as stated by Finlayson-Pitts and Pitts Jr,¹ the intermediates

have either more radical or zwitterionic character. Decomposition of non-symmetric alkene can yield two possible carbonyl compound and ECIs. It is important to note that carbon-carbon double bond cleavage by ozone addition leads to the formation of two molecules only in case of linear and exocyclic alkenes. For instance ozonolysis of exocyclic terpene, β -pinene, will result in the formation of two molecules.⁹² However, in case of endocyclic alkenes, like cyclohexene and α -pinene, the carbon-carbon double bond cleavage results in ring opening and the resulting products contains both ECI and carbonyl group.

For the symmetrical alkenes (cyclic and linear), reactions 1.17a and 1.17b will lead to the formation of the identical products. However, when non-symmetrical alkene is considered, a more substituted ECI is more likely to be formed. According to the previously published studies, the formation of a more substituted ECI is only moderately favored, with both possible biradicals formed with comparable yields. The formation ratio for the two ECIs for α -pinene is 6:4, favoring the methyl substituted biradical.⁹³ Finlayson-Pitts and Pitts Jr¹ have summarized the data from a number of studies.^{17,18,94-97} According to the presented data, it can be concluded that more alkyl substituents enhance the formation yield for a given ECI. Formation yields of 0.65 (substituted) and 0.35 (not substituted) were reported for the alkene containing two non-hydrogen substituents on one side of the carbon-carbon double bond and no substituents on another.

After the formation, the ECIs are known to undergo several transformations. The subsequent reactions of ECI's strongly depend on whether the reaction is conducted in the gas or liquid phase and on whether the large quantities of scavengers are present.

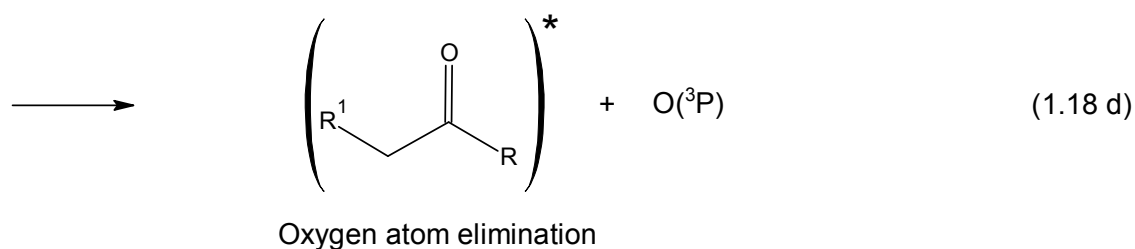
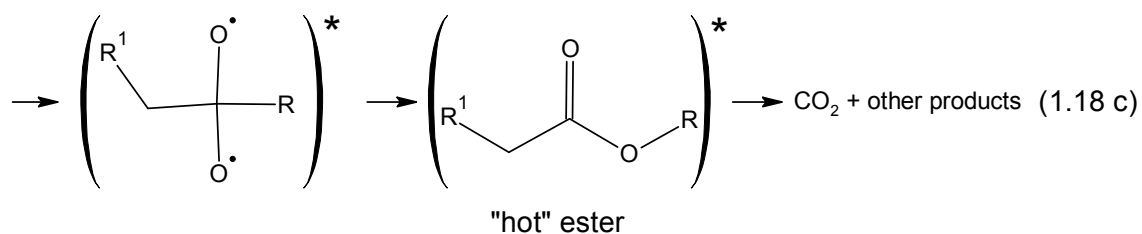
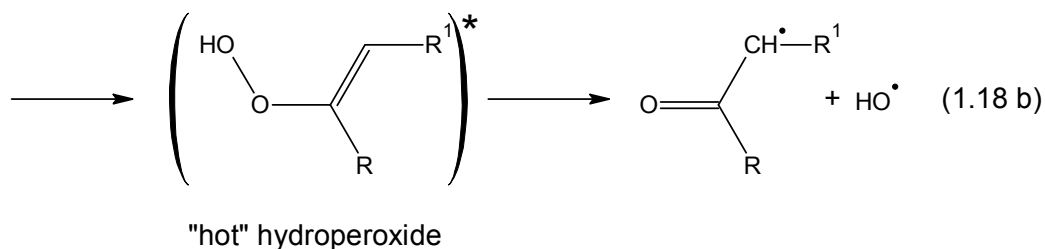
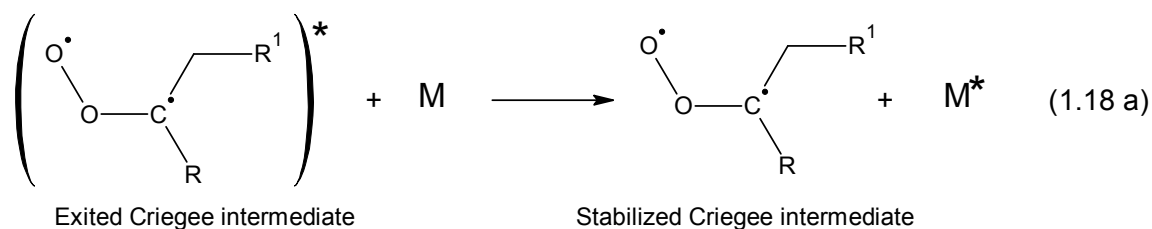


Figure 1.9 Possible reaction pathways of Exited Criegee intermediate

In the gas phase, a portion of formed ECIs can be stabilized by losing excess energy via collisions with bath gases, to yield SCI – reaction 1.18a in Fig. 1.9. Stabilization yields differ for different alkenes, and generally fall into the range from 0.10 to 0.47 at 298 K and 1 atm in air.^{1,98,99} Since it occurs via collisions with gas molecules, the stabilization is strongly pressure dependent, and significantly reduced at lower pressures.^{88,100} SCIs can subsequently react with other molecules, including H₂O,¹⁰¹ SO₂,¹⁰¹ NO₃, and CO as well as organic compounds. SCI reactions with carboxylic acids (1.19c), alcohols (1.19b) and carbonyl compounds (1.19 d) are shown in Fig. 1.10.

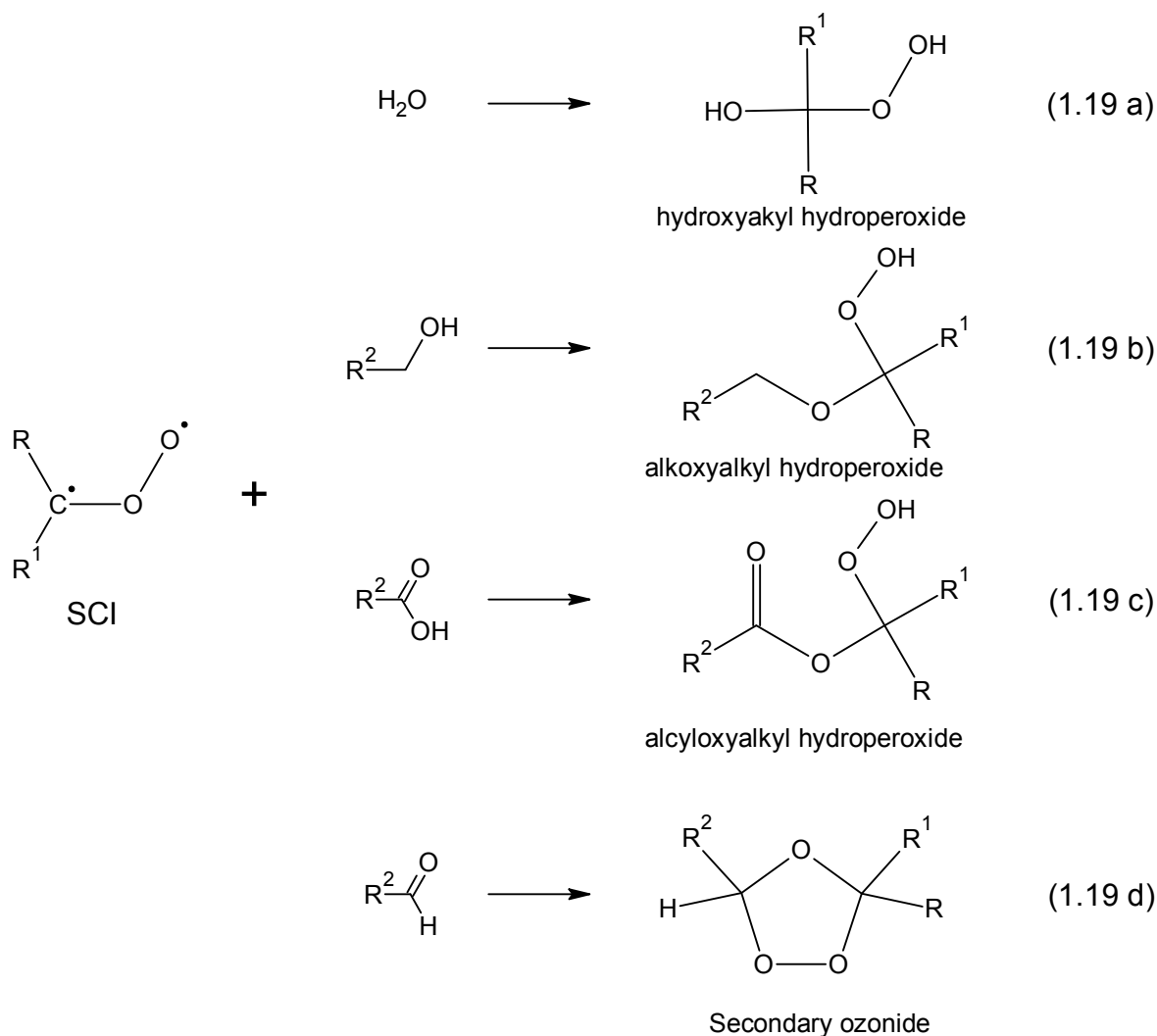


Figure 1.10 Reactions of SCI with water, alcohols, carboxylic acids and aldehydes

SCI reactions with water, alcohols, carboxylic acids and aldehydes lead to the formation of hydroxyalkyl, alkoxyalkyl, acyloxyalkyl hydroperoxides and secondary ozonides, respectively. SCI can also react with the organic scavengers and water, in the gas phase⁹¹ as well as in the liquid phase. Some of the reactions, shown in Fig. 1.10, are believed to produce a fraction of oligomers, recently detected in SOA samples, as discussed in Section 1.4.3.4.2., as well as participate in the new particles formation, as described in Section 1.4.4. Rate coefficients of the reactions shown in Fig. 1.10 in the gas-phase were reported, relative to water, and are listed in Table 1.4.

Table 1.4 SCI gas-phase reaction rate coefficients with alcohols, carboxylic acids and aldehydes relative to water

SCI scavenger	Reaction rate coefficient, relative to H ₂ O	Reference
R-OH	22 – 50	91
R ₁ (O)H	100 – 2700	91,93,102
RCOOH	6700 – 17000	91,93,103

As listed in Table 1.4, water is the least effective SCI scavenger. However, since water is present in the atmosphere in significantly larger quantities than the organic scavengers, it is considered to be the most important SCI scavenger under ambient conditions.²⁰ The reactivity for the rest of SCI scavengers increases from alcohols to carboxylic acids. As concluded by Tobias and Ziemann,⁹¹ the carboxylic acids are most reactive, since the reaction with SCI involves O-H bond breaking in the scavenger molecule. Indeed, the relative rate coefficients, reported in Table 1.4, were found to increase with decreasing $\Delta G_{\text{acidity}}$, for the gas-phase dissociation of the neutral scavenger molecule into H⁺ and the corresponding anion. Thus, a given scavenger reacts faster, if the bond dissociation is more energetically favored.

Aside stabilization, fraction of ECIs formed in the gas-phase undergoes isomerization to form a high-energy hydroperoxide – reaction 1.18b. Afterwards, the “hot” hydroperoxide undergoes O-OH bond dissociation for produce the OH radical and the corresponding alkoxy radical. This channel is considered very important, since such decomposition introduce OH radicals to the atmosphere. As summarized by Finlayson-Pitts and Pitts Jr,¹ the yields of OH radical in the ozonolysis reaction for a number of alkenes varies in the range from 0.01 to 0.9.^{1,18,104} For α -pinene, the OH radicals yield is believed to be about 0.85.^{1,105} Since reaction of OH radicals with α -pinene^{101,105} is about 6 orders of magnitude faster than reaction with ozone,^{98,99,101,105} such high OH yield creates an important feedback loop in the α -pinene/ozone system. In order to suppress the precursor consumption by highly reactive OH radicals, in a number of laboratory ozonolysis studies, large excess of OH radical scavengers is often added to the system – refer to Section 1.4.2.3 for more detailed discussion.

Another important ECI reaction pathway is reaction 1.18c shown in Fig. 1.9, involving rearrangement to a “hot” ester, and subsequent decomposition with CO₂ elimination and/or formation of other products.¹⁰⁶ Formation of specific products depends on the precursor under study, with simple precursors yielding simple hydrocarbons, in addition to CO₂.^{18,104,106}

Reaction 1.18d shown in Fig. 1.9 is the third possible ECI decomposition pathway, and it is considered minor under atmospheric conditions.^{1,106} Yields of the oxygen atom elimination from the CI were reported to be less than 0.05.⁹⁹

1.3.4. Liquid phase ozonolysis of the alkenes

In this section, the liquid phase alkene ozonolysis is discussed. However it is not a complete review of the alkene-ozone liquid phase chemistry. A brief overview of the liquid phase ozonolysis is given, focusing on atmospheric chemistry – related investigations. The aim of the presented studies was mainly the standard synthesis for the subsequent SOA composition analysis or the ozonolysis product study of the atmospherically relevant alkenes. Based on the studies summarized in Table 1.5, synthesis method used in this work, for a number of α -acyloxyhydroperoxy aldehydes was developed. Standards were prepared by liquid – phase ozonolysis of cyclohexene in the presence of different carboxylic acids – see section 3.3.¹⁰⁷ Two α -acyloxyhydroperoxy aldehydes were also prepared using α -pinene as the precursor and, *cis*-pinonic acid as well as pinic acid as the SCI scavengers. The α -acyloxyhydroperoxy aldehydes are currently considered as important intermediated in the SOA nucleation, formed by gas-phase ozonolysis of alkenes, such as α -pinene – see Section 1.4.4. Analysis of the synthesized compounds is described in Section 4.1.2.

Liquid phase ozonolysis of alkenes was previously utilized to investigate alkene ozonolysis products, as well as to synthesize compounds shown in Fig. 1.10. In the liquid phase, the ozonolysis mechanism is significantly different from the gas-phase mechanism. ECI stabilization yield is much higher in the liquid than in the gas-phase. For example, the α -acyloxyhydroperoxy aldehydes formed during liquid–phase ozonolysis of alkenes were reported to be produced in nearly quantitative yields, proving that almost all of the produced ECIs were stabilized.⁶⁴ Stabilization (reaction 1.18a shown in Fig. 1.9) is therefore the dominant pathway for the ECI formed during alkene liquid-phase ozonolysis.

Liquid phase ozonolysis can be conducted in participating and non-participating solvents. Generally, solvents that cannot act as SCI scavenger, and thus had no impact on the products distribution, are considered non-participating. Examples of such solvents include ACN,^{107,108} CCl₄,¹⁰⁹ CH₂Cl₂¹⁰⁸ and alkanes^{91,107,109-111} as listed in Table 1.5. Participating solvents include H₂O, aldehydes, alcohols and other compounds that can act as the SCI scavengers, aside from been used as the reaction medium. Participating solvents significantly affect the products distribution, since they are usually present in large excess as compared to the precursor. Reactions of the SCI with water, alcohols, carboxylic acids and aldehydes are shown in Fig. 1.10.

Due to “solvent cage” effect,¹ the resulting SCI and aldehyde remain in close proximity and can subsequently react to form secondary ozonide, reaction 1.19d in Fig. 1.10. Of course, non-participating solvent has to be used to promote SCI reaction with aldehyde. This method was utilized by Tobias et al.¹¹⁰ to synthesize secondary ozonide by 1-tetradecene ozonolysis in hexane. For a number of endocyclic alkenes, it was concluded that self-reaction of the SCIs leads to the formation of intramolecular secondary ozonides.¹¹¹ Ozonolysis of cholesterol in hexane or CCl₄ lead to the similar conclusions, resulting in the formation of dimer hydroperoxides and secondary ozonides.¹⁰⁹ Similar dimer peroxides were generated as a result of verbenone ozonolysis in non-participating ACN and CH₂Cl₂.¹⁰⁸

Products distribution can be also controlled by adding the SCI scavenger, most often in large excess, to the reaction mixture. Frequently, a given scavenger can also act as the reaction medium – participating solvents discussed above. Docherty et al,¹¹² Murai et al,¹¹³ Ziemann⁸⁹ as well as Tobias and Ziemann^{114,115} utilized this approach to prepare a series of α -methoxyalkyl hydroperoxides, using simple alcohols as reaction solvents. Methanol and water were also used as participating solvents in cholesterol ozonolysis, leading to the association of the formed SCI with the solvent molecules.¹¹⁶

Alkene ozonolysis in the presence of carboxylic acids resulted in the formation of acyloxyalkyl hydroperoxides.^{91,107,114} Carboxylic acids are usually not used as the participating solvents. Similarly as in the formation of the intramolecular secondary ozonides, non-participating solvent is preferable to avoid competing reactions. This approach was used by Tobias and Ziemann⁹¹ for the synthesis of α -hydroperoxytridecyl heptanoate from the terminal alkene: 1-tetradecene

and heptanoic acid in cyclohexane. Tobias and Ziemann ¹¹⁴ also used formic, acetic, heptanoic and nonanoic acids as the SCI scavengers, to synthesize a series of α -acyloxyalkyl hydroperoxides from 1-tetradecene. In the study discussed above acetone was used as a solvent.

Table 1.5 Liquid phase alkenes ozonolysis

Alkenes	Solvents	SCI scavengers	Products	Reference
1-octene, 1-nonene, 2-methyl-1-octene, 1-decene, 1-dodecene, and 1-tetradecene	Methanol		α -Methoxyalkyl hydroperoxides	¹¹²
1-octene	Ethanol		1-Ethoxy-n-heptyl Hydroperoxide	¹¹³
Cyclohexene, cycloheptene, cyclooctene, and cyclodecene	Methanol or 1-propanol		Alkoxyhydroperoxy Aldehydes	⁸⁹
Verbenone	Methylene chloride or acetonitrile	SCI (self reaction)	Dimer peroxides	¹⁰⁸
Cholesterol	Water/THF or MeOH/ methylene chloride	MeOH, Water	Hydroxy, hydroperoxy bishemiacetals and other	¹¹⁶
	Hexane or carbon tetrachloride	None (self reactions)	Dimeric secondary ozonides and hydroperoxides	¹⁰⁹
1-Tetradecene	Hexane	Tridecanal (self reaction)	Secondary ozonide	¹¹⁰
	Cyclohexane	Heptanoic acid	α -Hydroperoxytridecyl heptanoate	⁹¹
	2-propanol		α -Methoxyalkyl hydroperoxides	¹¹⁵
	2-Propanol, methanol, acetone, cyclohexane	2-propanol, MeOH, Formic, acetic, heptanoic and nonanoic acids	α -Methoxyalkyl hydroperoxides α -Acyloxyalkyl hydroperoxides	¹¹⁴
Limonene, 3-carene, 4-carene and possibly isolimonene	Pentane	None (self reaction)	Intramolecular secondary ozonides	¹¹¹

Cyclohexene, α -pinene	Acetonitrile or cyclohexane	C ₅ -C ₁₀ linear carboxylic acids, C ₄ -C ₈ linear dicarboxylic acids, 4-Oxopentanoic acid 5-Oxohexanoic acid, cis-pinonic acid and pinic acid	α -Acyloxyhydroperoxy aldehydes	107
-------------------------------	-----------------------------	---	--	-----

1.4. SOA formation from the α -pinene ozone-initiated oxidation

As described in Section 1.3.2, ozone is one of the major atmospheric oxidants. α -Pinene is the most abundant monoterpenes emitted from the natural sources, as already discussed in Section 1.4.1. Therefore, SOA formation from the α -pinene initiated oxidations is of great atmospheric importance.

In Section 1.4.1, SOA formation mechanism in the α -pinene/ozone system is described. Afterwards, overview of the laboratory studies of SOA formation from α -pinene ozonolysis is presented – Section 1.4.2. The presented review includes description of the smog chamber studies – Section 1.4.2.1. – and the flow tube reactor experiments – Section 1.4.2.2, as well as discussion about the use of the OH radicals scavengers – Section 1.4.2.3. Afterwards, instrumental techniques used for the α -pinene/ozone SOA composition analysis are described in Section 1.4.3.

At this point it is important to present the currently accepted classification criterion for a given compound as a LMW or HMW α -pinene SOA component. Generally, it is accepted that LMW α -pinene SOA components masses are centered roughly around 150 – 180 Da. Examples of such compounds are presented in section 1.4.1. On the other hand, association products of these stable molecules, as well as reaction of LMW compounds with SCI are considered HMW α -pinene SOA components. The masses of HMW dimers are centered around 350 - 380 Da, as far as α -pinene SOA composition is considered.

Initially, identification of the LMW α -pinene SOA components in the studies published earlier is discussed in Section 1.4.3.1. Afterwards, the analysis methods of the HMW SOA fraction are described. Analysis methods of HMW SOA components are discussed in Section 1.4.3.2 and Section 1.4.3.3.

Afterwards, proposed formation pathways of the detected HMW compounds are described in Section 1.4.3.4, including condensed – phase reactions and gas – phase reactions, Sections 1.4.3.4.1. and 1.4.3.4.2, respectively.

Previously proposed nucleation mechanisms of the SOA formed in the α -pinene/ozone system are summarized in Section 1.4.4.

1.4.1. α -pinene ozone-initiated oxidation mechanism

General alkene ozonolysis mechanism is described in section 1.3.3. In this section, ozone-initiated α -pinene oxidation mechanism will be presented. Since detailed evaluation of the α -pinene oxidation by ozone and OH radicals is beyond the scope of this introduction, only brief summary of the currently accepted and proposed formation pathways of the stable products are shown in Fig. 1.11 and Fig. 1.12. Incorporation of the oxygen atoms into the α -pinene structure results in the formation of low-volatile products, subsequently partitioning between the gas and particle-phase, according to the currently accepted model. A number of by-products, as well as addition, rearrangement and elimination reactions were omitted in Fig.1.11 and Fig. 1.12 for clarity. For example, water addition to the SCI leads to the formation of the α -hydroxyalkyl hydroperoxides. SCI can rearrangement to form a hot hydroperoxide, as already described in Section 1.3.3; the subsequent reactions of the high-energy hydroperoxide involve elimination of the OH radicals as well as reactions with NO and RO₂ radicals.

Please note that only products detected in the particles phase are included in the summary; however, the majority of the α -pinene ozonolysis products partition between gas and particle phase.

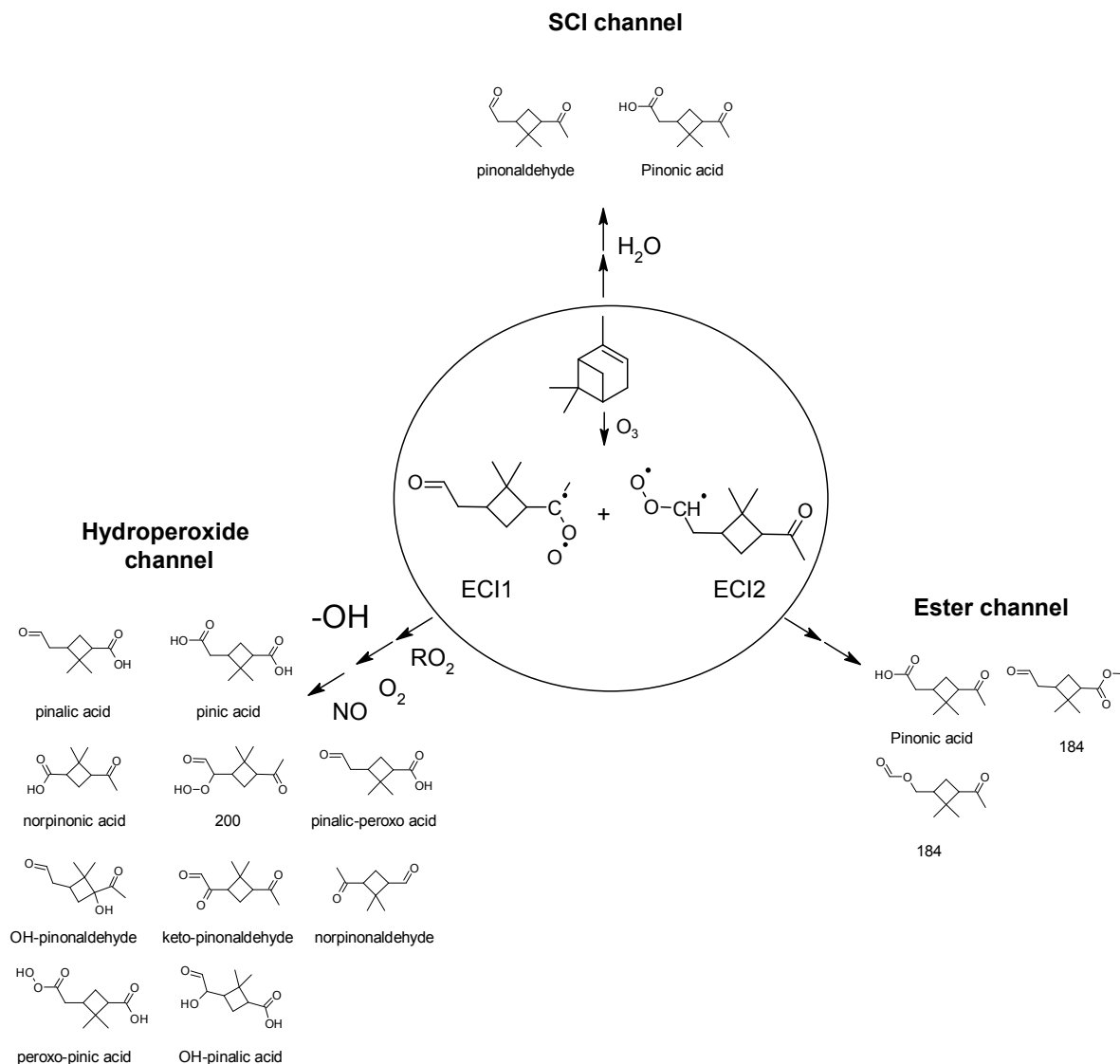


Figure 1.11 Formation channels of some stable LMW products from α -pinene reaction with ozone

For α -pinene, two ECIs can be formed as a result of the ozone addition to the carbon-carbon double bond, as shown in Fig. 1.11. The formation ratio for two ECIs was reported to be about 6:4, favoring the methyl substituted biradical with the stabilization yields of about 0.15 for both ECIs.^{93,117} As already discussed in Section 1.3.3, there are three possible channels for the ECI decomposition. OH radicals are formed via hydroperoxide channel, and the reported yields of the OH radicals formation from the α -pinene ozonolysis are in the range from 0.70 to 0.85.^{21,93,117-119} Such high OH radicals yield warrants the description of the SOA formation in the α -pinene/ozone system as ozone – initiated oxidation rather than ozonolysis. Since the OH radicals reacts with α -

pinene much faster than ozone,¹⁰¹ in order to study “pure” ozonolysis, in a number of laboratory studies, large excess of the OH radicals scavengers are often added to the system. The use of the OH radical scavengers in the laboratory studies of SOA formation in the α -pinene/ozone system is discussed in section 1.4.2.3.

As shown in Fig. 1.11, few products were proposed to be formed via SCI and ester channel, with the majority of the stable compounds produced via hydroperoxide channel. The most important product, proposed to be formed via ester channel is pinonic acid.¹²⁰⁻¹²³ Alongside pinonic acid, other compounds with MW 184 were also proposed to be formed via this channel.¹²² Pinonaldehyde as well as cis-pinonic acid are believed to be produced after SCI reaction with water, via SCI channel.^{93,122,124,125} The rest of ozonolysis products shown in Fig. 1.11 are produced via hydroperoxide channel, via series of reactions with various radical species and stable molecules. Products shown in Fig. 1.11 were included in the mechanism presented by Ma et al.¹²⁰ and Winterhalter et al.¹²²

When no scavengers are present, which is the case in the ambient atmosphere, reaction of OH radicals with α -pinene is important oxidation pathway, and thus should also be described in this section, in order to present complete overview of the ozone – initiated α -pinene SOA formation. OH addition to the carbon-carbon double bond results in the formation of the two possible radical: by-products I and II shown in Fig. 1.12.^{117,122} The OH – α -pinene adducts I and II can subsequently isomerize, resulting in the formation of new carbon-carbon double bond – adduct III shown in Fig. 1.12^{117,122,126} or react with O₂ to produce alkylhydroxylperoxy radicals.^{117,122} The isomerization product (III) also reacts with O₂ to yield alkylhydroxylperoxy radical. Addition by-product III can yield stable compounds such as acetone and compound with MW 126, as shown in Fig. 1.12. Also, 8-hydroxy-menthen-6-one, a stable product of the radical III reaction with O₂, can be further oxidized by yield highly oxygenated product with MW 200.

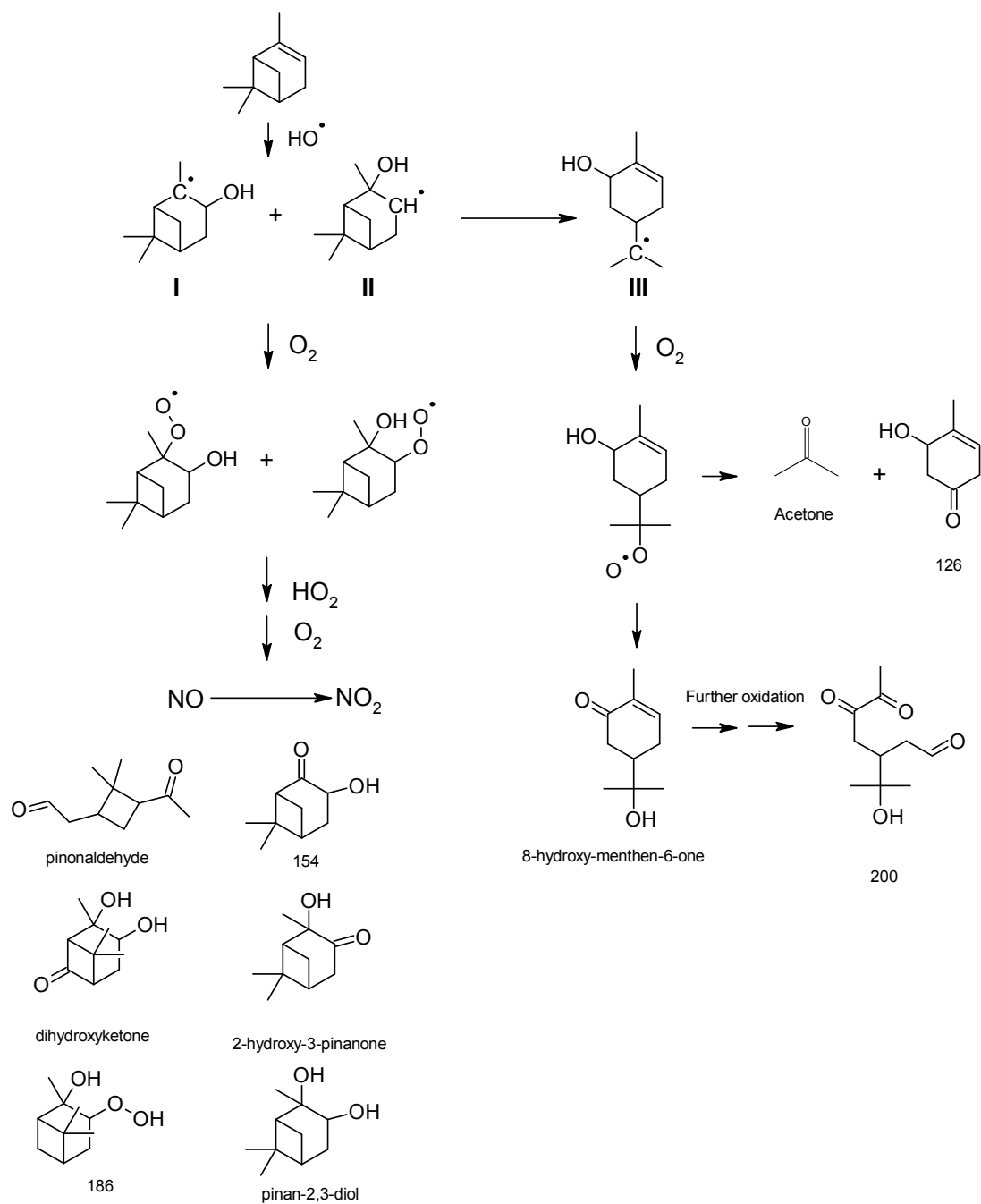


Figure 1.12 Formation channels of the stable LMW products from α -pinene reaction with OH radicals

As shown in Fig. 1.11, pinonaldehyde is produced via reaction of SCI with water, however, this compound is also a main products of the α -pinene oxidation by OH radicals.^{93,117,122,127,128}

1.4.2. Laboratory studies of α -pinene SOA formation

In this section, the laboratory methods for α -pinene SOA generation are described. Laboratory SOA generation experiments are conducted in order to mimic, to some extent, the ambient aerosol formation conditions. Most frequently, laboratory studies focus on investigating a small portion of the processes, leading to the formation of SOA in the atmosphere. Those studies are usually limited to one oxidant and one precursor, in order to get insights into specific reaction(s). Afterwards, results of such investigation are often extrapolated to the atmospheric conditions in order to estimate the SOA forming – potential of specific mixtures of oxidant and precursor under study.

In this section, laboratory studies of α -pinene reaction with ozone are summarized, focusing on SOA composition analysis, since such analysis was also the main objective of this thesis. SOA composition analysis methods are discussed separately in Section 1.4.3.

Generally, two types of laboratory SOA formation studies can be found in the current literature; smog chamber studies and flow – reactors experiments. Studies investigating SOA produced as a result of α -pinene ozone-initiated oxidation are summarized in Section 1.4.2.1. (smog – chamber experiments) and Section 1.4.2.2. (flow – tube reactors experiments).

1.4.2.1. Smog chamber experiments

SOA generation experiments in smog – chambers are most often aimed for using low reactants concentrations, close to those encountered in the ambient atmosphere and therefore have large volumes ranging from 1 m³ to 200 m³, as listed in Table 1.6.

Table 1.6 Summary of the smog – chamber α -pinene SOA generation conditions

α -pinene concentration	RH (%)	OH scavenger	Ozone concentration	Chamber size	Residence time	Aerosol composition analysis	Reference
44 ppb	Not specified	2-propanol 88 ppb	176 ppb	50 m ³	After complete α -pinene consumption	GC/MS	¹²⁹
3.7 ppm	Not specified	None/cyclohexane 1860 ppmv	1.5 ppm	0.5 m ³	After 95% of ozone reacted	GC/MS	¹³⁰
0.96 ppm	18-40	none	Not specified, initial NO _x 0.45 ppmv	190 m ³	15 h	GC/MS	^{117,131}
330 – 510 ppb	0 – 80	None/cyclohexane 3.5 ppmv	190 – 508 ppb	0.002 and 0.5 m ³	1.45 and 66 min	Online APCI/MS	¹³²
15 ppb	50 <	none	100 ppb	600 m ³	> 1h	none	¹³³
300 – 500 ppb	4 – 40	none	300 – 500 ppb	0.012 and 0.5 m ³	Not specified	Online APCI/MS ⁿ	¹³⁴
700 ppb	10 <	none	560 ppb	Dual 0.5 m ³	55 min	none	¹³⁵
100 ppb	0 – 50	none	135 ppb	Dual 200 m ³	Not specified	LC-ESI/MS LC-APCI/MS	¹²²
12 – 135 ppb	55	cyclohexane	24 – 270 ppb	Dual 28 m ³	5 – 7 h	ESI/MS LC-ESI/MS ⁿ	^{136,137}
100 ppb	40 – 50	none	70 ppb	9 m ³	2.5 h	CE-ESI/MS	¹³⁸
3.4 ppm	28 – 30	none	0.8 ppm	0.5 m ³	1 h	MALDI, ESI-MS, Desorption CI and ESI-FTICRMS	¹³⁹
4.5 ppm	0.5 – 50	Cyclohexane, 1-propanol, formaldehyde	2.7 ppm	7 m ³	After all of the ozone reacted	Online TDPBMS	¹²⁵

		320 – 490 ppm					
300 ppb	24 – 27	none	700 ppb	2 m ³	1.5 h	GC/MS	¹⁴⁰
200 ppb	2 <	none	240 ppb	27 m ³	7.5 h	ESI- FTICRMS	¹⁴¹
200 ppb	1 <	none	1 ppm	0.5 m ³	19 min	LC-ESI/MS ⁿ	¹⁴²
12 ppb	1 <	None/CO	209.3 ppb	200 m ³	2 – 3 h	ESI/MS LC-ESI/MS ⁿ	¹⁴³
0.7 ppm	4 <	Hexane 20 – 100 ppmv	250 ppb	9 m ³	Not specified	ESI-FTICRMS	¹⁴⁴
6.1 ppm	5	none	150 - 200 ppb	0.5 m ³	45 min	ESI-MS/MS and ESI- FTICRMS	¹⁴⁵
252 – 254 ppb	1 <	none	1300 – 1400 ppb	4.2 m ³	3.5 h	LC-ESI/MS ⁿ	¹⁴⁶
100 ppb	1 <	none	116 - 100 ppb	25 m ³	Not specified	HPLC- ESI/TOF-MS	¹⁴⁷
5 - 20 ppb	1 <	none	50 - 100 ppb	10 m ³	5 h	Online CIMS (NO ₃ ⁻)	¹⁴⁸
280 - 350 ppb	0.7 – 3.5	2-butanol	450 – 600 ppb	5.5 m ³	5 ± 0.5 h	GC/MS	¹⁴⁹

Complete list of abbreviations is provided in section 6.

The smog chambers are made from Teflon,^{117,125,129,133,135,136,139,141,144,147,149} glass^{130,132,134,142} or stainless steel.¹⁴⁶ These three materials are most frequently selected for constructing the inner part of the reaction vessel, since the reactor material should be chemically inert, in order to avoid interactions with the reactants.

The smog chamber itself is the reactor vessel in which the VOC of interest reacts with the selected oxidant. The reaction vessel is, of course, the central part of the installation. However, in order to draw any meaningful conclusion from the acquired experimental data, all of the smog chambers, listed in Table 1.6 are equipped with the large number of analytical instruments, for monitoring the critical reaction parameters, as well as for aerosol sampling.

Concentrations of the reactants used in the chamber experiments described in the literature are listed in Table 1.6. α -Pinene concentrations used in these experiments ranged from

few ppbs^{122,129,132,136-138,143,148} to a few ppms,^{125,130,139,144,145} in case of a few studies listed in Table 1.6. Large volume of the chamber allows using small concentrations of the reactants, closer to those encountered in the ambient atmosphere. Large reaction vessel volumes are necessary when using low reactants concentration, since sufficient amount of aerosol and consequently ozonolysis products need to be present due to limited sensitivity of the analytical instruments. Relative humidity (RH) was also included in Table 1.6, since it is an important parameter for the smog-chamber investigations of SOA formation as a result of α -pinene ozonolysis. Water is very important SCI scavenger, when alkene ozonolysis under atmospheric conditions is considered, as already discussed in Section 1.3.3.

Ozone concentration is usually kept in the similar range as the concentration of the precursor,^{134,141,147} with a number of studies using excess of the α -pinene^{125,130,135,139,144,145} or ozone.^{129,140,142,143,146,148,149} OH radicals scavenger, if used in a given experiment, is also listed in Table 1.6. Briefly, when OH radicals are produced with high yields during the α -pinene ozonolysis, as already discussed in Section 1.4.1, the large excess of the scavenger is added to suppress the alkene consumption by the generated radicals.^{125,129,130,132,136,137,143,144,149} The use of different OH radicals scavengers is discussed in Section 1.4.2.3.

Time scale of the smog-chamber experiments are also listed in Table 1.6. The main aim of the smog chamber experiments is to study SOA formation and composition in a large time scales, therefore reaction times listed in Table 1.6 vary from 20 min^{132,142,145} to a few hours.^{117,131,133,136-141,143,146,148,149} These long time scales allow studying the SOA aging and time evolution of aerosol. Studies of SOA formation on much shorter time scales are performed in the flow-tube reactors, as discussed in Section 1.4.2.2.

In the majority of the smog-chamber studies, ozone is added directly to α -pinene in the presence or absence of the OH radicals scavengers. However, in a number of studies reactions involving ozone generation from NO_x mixtures were also employed, in order to mimic the photosmog formation in the ambient atmosphere.¹¹⁷ Such reactions are usually performed exclusively in the smog-chambers, since due to low amounts of the reactants used and long time-

scale of the ozone generation reaction from NO_x these experiments are unsuitable for the flow-reactors.

After SOA generation, its analysis can be performed either online,^{125,132,134,148} or offline.^{117,122,129-131,136-147,149} The latter is performed after SOA collection. When online analysis is utilized, particles are focused into a narrow stream, usually with aerodynamic lenses, and directed to the analytical instrument.^{125,132,134,148} For the offline analysis, filter sampling is utilized most frequently;^{117,122,130,131,136-139,141-147,149} sampling with the impinger¹²⁹ was also used. When filter sampling is performed, the chamber is evacuated, and air with particles is forced to pass through the filter and/or denuder,^{117,131,138,142,146} for retaining the particulate and gaseous reaction products.

Analytical technique, used for SOA composition analysis in the specific experiment is also listed in Table 1.6. It is important to underline, that SOA composition analysis is not always the main object of the given investigation.^{133,135} In a number of studies, very valuable conclusions were presented, without identifying the compounds, composing the aerosol particles. However, since the main aim of the experiments performed in this work was investigating the SOA composition, only the analytical techniques, used for composition analysis were included in Table 1.6. Again, it is important to note that the analytical instruments, connected to the smog-chamber in the specific experiment were not limited to those listed in Table 1.6. The instrumental methods, used for SOA composition analysis include offline and online methods, as well as chromatographic techniques. α -Pinene SOA composition analysis methods are described in Section 1.4.3.

1.4.2.2. Flow – tube reactors

Flow – tube reactors, as opposed to smog chambers, are used for studying the SOA formation on a short time scale. Most frequently, such studies are performed to provide insights into SOA formation mechanism and/or to measure reaction rate coefficients of ozone with aerosol precursors e.g. α -pinene, for the investigations listed in Table 1.7. The most significant difference between the experiments performed in the smog-chambers and flow-tube reactors is time scale of the reaction. Since flow-tubes are used to investigate the SOA properties on the early stages of aerosol formation, the times scales of the reaction range from less than a second to a couple of

minutes. Similarly to the smog-chambers, flow reactors experimental setup allows to monitor all of the critical reaction parameters, as well as to sample the particles and gaseous products, if offline composition analysis is performed.¹⁵⁰ Filter sampling is the most frequently used SOA collection method for offline analysis, along with the collection of gaseous reaction products with denuder.^{150,151} SOA sampling on an impactor (plate) was also used; sampling method described by Heaton et al.¹⁵² required the use of aerodynamic lenses to focus the generated particles on a very narrow spot on the collection plate. Afterwards, collected particles are extracted and subjected to the composition analysis by various analytical techniques, as described in Section 1.4.3. Reactants concentrations used in the given flow-tube experiment are listed in Table 1.7. The reactants concentrations used in the flow-tube α -pinene SOA formation experiments are much higher than those, used in the smog-chamber experiments. The much smaller volumes of the flow-tube reactors, as compared to the smog-chamber experiments require using higher reactants concentrations, to produce sufficient SOA, since, as already discussed in Section 1.4.2.1, the analytical techniques used for aerosol analysis have limited sensitivity. As listed in Table 1.7, in the majority of experiments performed in the flow-tube reactors, reactants concentrations are in the ppm range, from a few ppm to about 200 ppm.

Lengths and diameters of the flow-tube reactors, described in the literature are also listed in Table 1.7. As already discussed, flow-tubes usually have much smaller volumes than smog-chambers, since those most frequently consist of approx. 1-3 m glass tube with the ID's from 2 to 10 cm. Reaction time is controlled by the reactants residence time in the reactor, which in turn depends on the total volumetric flow through the reactor, reactor length and ID.

The parameter describing the flow conditions inside the reactor is the Reynolds number.¹⁵³ When gas flow in a round pipe is considered, Reynolds number value depends on dimensions of the tube, volumetric flow of gas and air kinematic viscosity. The equation is provided in section 4.2.1, where Reynolds number calculations are presented, for the flow-tube reactor used in this work. The air kinematic viscosity is of course constant, under standard conditions. The tube dimensions and flow rate, however, can be considered user adjustable parameters, since the size of the tube is selected during the reactor construction, and the flow rate is adjusted during the

experimental run. In order to calculate the reactants mean residence time in the flow – tube reactor, the reaction has to be performed under laminar flow conditions. If the reaction was performed under turbulent flow conditions, it would be very difficult to draw any meaningful conclusion, especially when kinetic studies are considered.¹⁵⁴

In a pipe reactor, the flow can be considered laminar when Reynolds number, calculated for a given set of experimental conditions, is less than 2100, while values larger than 4000 indicate the fully developed turbulent flow.¹⁵³ If the Reynolds number is in the intermediate region, the flow conditions are expected to randomly change between the laminar and turbulent regimes, thus preventing to obtain reproducible results.¹⁵³

Reynolds numbers are listed for each of the flow-tube reactors experiments summarized in Table 1.7. If the authors did not report the Reynolds number for their system, the values listed in Table 1.7 were calculated using the equation from Section 4.2.1. As listed in Table 1.7, for all of the summarized studies, Reynolds number values are well below the threshold value of 2100, thus proving that the reactions were performed under laminar flow conditions.

Table 1.7 Summary of the flow – tube reactors experiments for studying SOA formation in the α -pinene/ozone system

α -Pinene concentration	RH (%)	OH scavenger	Ozone concentration	Flow tube length and ID	Reaction time	Aerosol composition analysis	Reynolds number	Ref.
5.5 – 22 ppm	3	none	0.5 ppm	1 m x 2.5 cm	0.6 s	GC/MS	281	¹⁵⁰
11 – 136 ppm	5 <	none	1 ppm	1.25 m x 2.22 cm	3 - 22 s	Online PIAMS	150	¹⁵⁵
1.86 ppm	5 <	CO	0.19 ppm	1 m x 10 cm	0.5 – 5 min	none	20 - 50	¹⁵⁴
Not specified	5 <	Hexane	2 – 3 ppm	1.2 m x 9 cm	Not specified	LC-ESI/MS ⁿ	Inssufficient data was provided to calculate the	¹⁵¹

							number	
155-200	16 – 52	none	0.57 – 0.88 ppm	1 m x 2.5 cm	12 s	FTIR	123 - 140	¹³⁵
40 ppm	5 <	none	500 ppb	1.25 m x 2.22 cm	23 s	Online NAMS ESI-FTICR-MS	150	¹⁵²
20 ppb	1 – 85	none/2- butanol	1 ppm	1.4 m x 4.6 cm	270 s	none	25	¹⁵⁶
0.74 – 8 ppm	2 <	none	0.04 – 0.4 ppm	1 m x 10 cm	17 – 48 s	none	107	¹⁵⁷

Complete list of abbreviations is provided in Section 6.

Flow tube reactors, described in the investigations, summarized in Table 1.7 usually share a number of design features, such as the glass tubes acting as a reaction vessel and relatively small volumes, as compared to the smog-chambers, described in Section 1.4.2.1. If the experiment requires changing the reactants residence time inside the flow – tube, sliding injectors (plungers) are often used.^{154,156,157} The most obvious way to change the reaction time in the flow-tube would be to alter the flow rate of a carrier gas. However, it is not convenient changing the reaction time in such a manner, due to the risk of pressure rise inside the reactor or developing a turbulent flow. Also, once the total flow is changed, all reactants concentrations would change, due to different dilutions e.g. for ozone introduced from the separate line, most frequently from the ozone generator. Ozone generators are usually calibrated for operating under specific flow conditions, and changing the flow would require recalibration under new flow conditions. The same conclusion can be made for all other chemical species introduced to the flow reactor. Therefore, the use of movable plungers (injector) is convenient, since the reaction time can be adjusted without altering the reaction conditions and enables to avoid troublesome recalibration. It is also convenient to use the movable injectors, if reaction time needs to be shortened, while avoiding too high flow of a carrier gas. In many flow-tube experimental setups, employing the movable injectors, the ozone was introduced via the plunger. α -Pinene, diluted with the carrier gas was introduced directly to the reactor, and came in contact with the ozone upon reaching the plunger tip.^{154,156,157}

In a number of studies, when reactants residence time is only controlled by the flow rate of the carrier gas, mixing plates are often employed, in order to ensure sufficient reactants mixing after entering the reactor.^{135,150} When movable plungers are used, their design is usually more complex than a narrow tube, sliding inside the reactor. This is because, aside from acting as a sliding ozone injector, a second function of a movable plunger is mixing of the reactants, after initiating the reaction. This is not always the case, like for the experimental setup, described by Jonsson et al,¹⁵⁶ when injection was performed by a movable, narrow glass – tube, connected directly to the ozone generator and installed in the middle of the flow-tube reactor. The movable mixing plunger, described by Duncianu et al.¹⁵⁴ contained small glass beads, to ensure sufficient mixing of alkenes and ozone. Simpler design of a mixing plunger was described by Bernard et al,¹⁵⁷ where the mixing plunger was constructed from a three, parallel plates, with openings on each side of a plunger, forcing the gas to circulate inside the injector, and thus ensuring sufficient mixing of the reactants. The detailed design of the flow – tube reactor used in this work is presented in Section 3.4.1.

1.4.2.3. OH radicals scavengers

A number OH radicals scavengers were utilized in investigations of α -pinene SOA formation performed in smog-chamber experiments,^{125,129,130,132,136,137,143,144,149} as well as in flow-tube reactors studies.^{151,154,156} The aim of the OH radicals scavengers, is to reduce the secondary reactions between α -pinene and OH radicals during ozonolysis. As already discussed in Section 1.4.1, OH radicals are produced with very high yields (approx. 0.7 - 0.85^{21,93,117-119}) during the α -pinene ozonolysis reaction. The reaction rate coefficient of OH radicals with α -pinene is estimated to be about $5 \times 10^{-11} \text{ cm}^3 \text{ molecule}^{-1} \text{ s}^{-1}$.^{101,158} Reaction rate coefficient of α -pinene with ozone is $8 \times 10^{-17} \text{ cm}^3 \text{ molecule}^{-1} \text{ s}^{-1}$ (see section 3.8.1), which is about 6 orders of magnitude lower as compared to the reaction with OH radicals. This creates a very important feedback loop in the α -pinene/ozone reaction system,¹⁵⁷ and significantly affects the products distribution.

The most straightforward method of minimizing the OH reaction with the parent alkene, e.g. in the case of α -pinene ozonolysis, is to add a large excess of the other reactant, to scavenge the generated OH radicals. Naturally, such scavenger needs to be reactive towards OH and

unreactive towards ozone, as well as sufficiently volatile to be introduced in the required concentrations. Ideally, the scavenger needs to react with OH while not yielding any products that could alter the ozonolysis reaction mechanism, and thus lead to the incorrect conclusions regarding the ozonolysis mechanism. There are several sufficiently volatile compounds, highly reactive towards OH and at the same time unreactive towards ozone. The compounds previously used as the OH radicals scavengers in the laboratory studies of α -pinene ozone initiated SOA formation are listed in Table 1.8.

Table 1.8 OH radicals scavenger used in some of the studies, summarized in Table 1.6 and Table 1.7

OH scavenger	Reaction rate coefficient with OH ($\text{cm}^3 \text{ molecule}^{-1} \text{ s}^{-1}$)	Reference
Cyclohexane	7×10^{-12}	125,130,132,136,137
CO	$(1.5 - 2) \times 10^{-13}$	154
2-butanol	8.5×10^{-12}	129,149,156
hexane	5.5×10^{-12}	144,151
formaldehyde	1×10^{-11}	125
1-propanol	5.5×10^{-12}	125

Reaction rate coefficients listed in Table 1.8 were summarized in the NIST kinetic database.¹⁰¹ As listed in Table 1.8, reaction rate coefficients of OH with all listed scavengers are significantly smaller than that of OH radicals with α -pinene. Consequently, a large excess of all the scavengers listed in Table 1.8, as compared to α -pinene need to be introduced into the reaction system. Indeed, as summarized in Table 1.6 and Table 1.7, very high concentrations of the OH radical's scavengers were present in the reaction mixtures.

However, as discussed above, the ideal scavenger should not alter the ozonolysis reaction mechanism, and consequently, the ozonolysis reaction products distribution. The addition of excess scavenger is required when the focus of a given study is exclusively on the investigation of the ozonolysis mechanism.¹²⁰ However, if the results of the laboratory investigation are to be extrapolated for the ambient conditions, careful evaluation of the possible alterations from the OH radical's scavengers is essential.

In the paper by Lee and Kamens, ¹⁵⁰ it was suggested that scavengers, such as cyclohexane and 2-butanol, can produce carbonyl compounds and alcohols when reacting with OH radicals. Subsequently, these compounds can act as the SCI scavengers and thus alter the reaction mechanism. Also, it is important to underline, that scavengers such as alcohols, ^{125,129,149,156} and formaldehyde ¹²⁵ can also, by themselves, act as SCI scavengers, as it was discussed in Section 1.3.3 and Section 1.3.4; especially when present in large quantities, as compared to the unsaturated precursor. Ma et al. ¹²⁰ in their investigation concluded, that the presence of the OH radicals scavengers, such as cyclohexane and methanol, alter the ratio of the RO₂ to HO₂ radicals in the system, and thus influence the major products yields. Similar conclusions were presented in the modeling study by Jenkin, ¹⁵⁹ when it was concluded, that the large excess of cyclohexane and 2-butanol altered the yields of the major LMW products.

Jonsson et al. ¹⁶⁰ investigated the effects of the OH radicals scavengers on SOA formation. It was concluded, that SOA formation was affected by both OH radical's scavenger type and concentration. Similarly to other studies, it was argued that the observed effects on SOA formation can be explained by the alteration of the RO₂ and HO₂ radicals concentrations by the OH scavengers. Jonsson et al. ¹⁶⁰ also summarized the results of other studies, where similar conclusions were presented.

1.4.3. SOA composition analysis

Analysis of SOA's composition, including aerosol produced in the α -pinene/ozone system, is carried by a variety of analytical techniques. These techniques were summarized in a number of recent reviews, ^{20,161-163} therefore, a complete summary will not be presented here. The review presented in this section will focus only on the most popular analytical techniques, used for α -pinene SOA composition analysis.

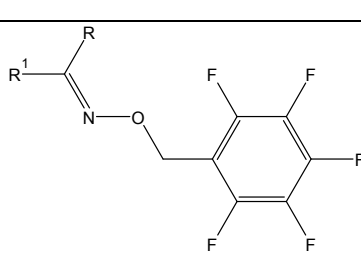
Initially, methods for the analysis for the LMW and HMW α -pinene SOA components are summarized in Sections 1.4.3.1 and 1.4.3.2. Afterwards, identification methods and proposed formation pathways for the detected HMW α -pinene SOA components are discussed in Section 1.4.3.3 and Section 1.4.3.4.

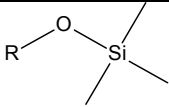
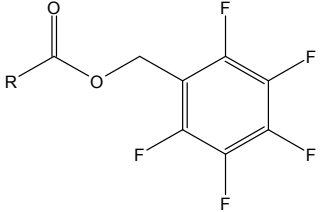
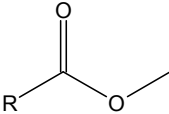
1.4.3.1. Low – molecular weight (LMW) compounds

Earlier studies of SOA composition were very often carried out with the capillary gas chromatography coupled to mass spectrometry (GC/MS).^{93,117,129-131,140,149,150,163-166} It is well known that OAs, including SOAs contain extremely high number of different organic compounds.¹⁶⁷ Even if only SOA composition from just a single organic precursor is considered, like α -pinene, the resulting mixture of organic compounds is very complex, requiring analytical methods with high separation power. Capillary GC/MS appears to be very well suited for analyzing such complex organic compounds mixtures, due to very high resolution, sensitivity and ability to provide molecular identification of the compounds of interest.^{20,161-163}

However, GC/MS also has certain drawbacks which were proven to prevent analyzing and identifying the HMW portion of SOA mass. In order to be analyzed by GC, the compounds of interest should be volatile and relatively non-polar. The variety of the LWM α -pinene ozone-initiated oxidation products, as presented in Section 1.4.1, are highly oxygenated compounds, with the functional groups like carbonyl ($\text{RC}(=\text{O})\text{R}'$), carboxylic ($-\text{C}(=\text{O})\text{OH}$), hydroperoxide ($-\text{OOH}$) and alcohol ($-\text{OH}$). Therefore, to enhance the volatility and reduce polarity of these compounds, various derivatization procedures were used.

Table 1.9 Derivatization methods used for analysis of the oxygenated α -pinene SOA compounds, used prior to GC/MS analysis

Derivatization method	Derivative	Functional group derivatized	Reference
O-(2,3,4,5,6-pentafluorobenzyl) hydroxylamine (PFBHA)		Carbonyls	93,131,164,165

silylation reagent N,O-bis(trimethylsilyl)- trifluoroacetamide (BSTFA)		Carboxylic acids, alcohols	149,164-166
Pentafluorobenzyl bromide (PFBBr)		Carboxylic acids	93,131,150
BF ₃ /MeOH		Carboxylic acids	130,131

Methods, listed in Table 1.9 transform the non-volatile, polar SOA components into their corresponding, volatile and less polar derivatives, and thus making them amenable for the GC/MS analysis. Beside been complex and time consuming, derivatization procedures are also known to produce artifacts that can alter the original products distribution in the studied SOA sample.

It was also proven that HMW SOA components are not amenable to be analyzed by GC/MS.^{110,114,115} The HMW SOA components are usually extremely non-volatile and thermally labile. They can be decomposed during the derivatization step or by high temperature in the GC injector. Even if the HMW compounds were able to be separated by GC, the electron impact (EI) ionization, used in the vast majority of the GC/MS system, would result in extensive fragmentation of these compounds, since it is characteristic for this type of ionization method.¹⁶² The EI mass spectra for the vast majority of the organic compounds is complex,¹⁶⁸ due to high number of mass peaks. For more complex compounds, such as HMW SOA components (see section 1.4.3.3) data interpretation is much more challenging, than for simple monomers.

This is the most significant drawback of the GC/MS analysis, since it is currently well known that HMW components consist of a significant fraction of SOA, including α -pinene SOA.^{20,136,169} Thus, data obtained from SOA composition solely by GC/MS analysis is not reliable, since the HMW

fraction would not be quantified. Therefore, different techniques have to be used for the complete analysis of the SOA composition, especially for analysis of oligomers and other HMW compounds.

1.4.3.2. Oligomers and other high-molecular weight (HMW) compounds

Complete list of abbreviations used in this section is provided in Section 6.

A number of recent studies have demonstrated that soft ionization method like ESI and APCI are especially suitable for analysis of the HMW SOA components.^{20,161,162} ESI^{122,136-139,141-147,151,152} and APCI^{132,134} are capable of preserving the molecular integrity of the analyzed compounds. When analyzing polar compounds with LC/MS, derivatization is not required since typical LC/MS analysis conditions were proven to be very well suited for analyzing polar and non – volatile HMW compounds. Direct analyses of the liquid samples by ESI or APCI also minimize the risk of the analytes decomposition, as compared to the GC/MS analysis using EI. It is also very important to underline, that the LMW compounds, mostly analyzed by GC/MS, can also be analyzed by ESI and APCI without the time consuming and complex derivatization procedures. Recent studies, utilizing ESI and APCI for analysis of α -pinene SOA samples are summarized in Table 1.10.

Table 1.10 Detection of different compound classes in SOA samples with ESI and APCI

Ionization method	Ions detected	Reference
ESI	M+Na ⁺	136,139,141,143,145,152,169
	M+K ⁺	139
	M+H ⁺	145,169
	M-H ⁻	136,138,142-147,152,169-171
APCI	M-H ⁻	134,172

	M+H ⁺	122,132
--	------------------	---------

Electrospray can operate in both positive and negative ionization modes, when the detection of cations and anions is performed, respectively. The preferable ionization mode depends on the analyte structures, and the presence of the positive and negative ionization sites, such as e.g. functionalities containing basic nitrogen and carboxylic group. When the detection of positively charged ions is performed, the spectrum is usually more complex, due to the higher number of possible adduct ions, like for instance metal cluster ions - see Table 1.10. Of course, detection of the protonated, pseudo-molecular ions is preferable. Adducts with the eluent additives can be also formed in the negative ionization mode, like for instance $M+HCOO^-$.¹⁷³ In both positive and negative ionization mode, non-covalently bonded analyte clusters can also be formed.

Since the use of ESI is becoming very popular as the ionization method of choice for the analysis of the HMW SOA components, a more detailed description of this ionization method is presented in this section. The mechanism of ESI is shown in Fig. 1.13.

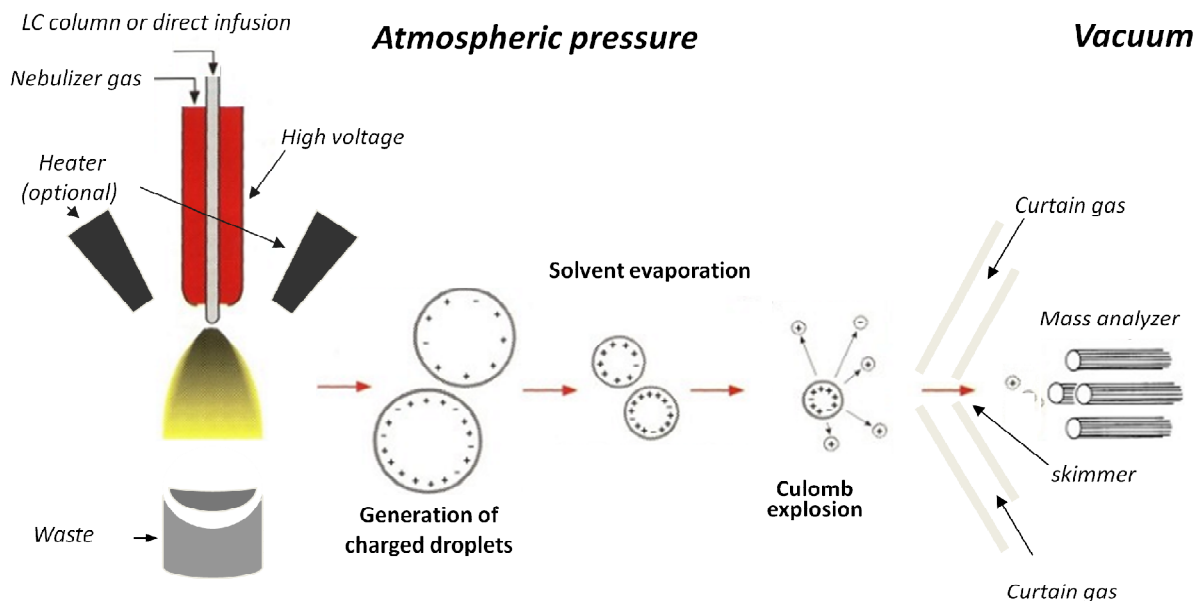


Figure 1.13 Mechanism of ionization using electrospray ion source

As shown in Fig. 1.13, when liquid sample is ionized with ESI, initially liquid is forced through a narrow capillary, with high voltage (2 – 5 kV, dependent on the polarity) applied. Also, nebulizer gas flows around the capillary, to assist the spray formation and solvent evaporation; the latter one can be also enhanced by heating the spray. Applying a high voltage results in the formation of the Taylor cone (not shown in Fig. 1.13) at the tip of the capillary and the charged droplets generation.¹⁷³ Afterwards, the droplets volumes reduce, and at some point, when the repulsion of the ions inside the droplets overcomes the surface tension, a set of smaller charged droplets is formed. It is repeated, until the ions are formed in the gas-phase. Subsequently, ions are transferred from the ion source (atmospheric pressure) into the mass analyzer (vacuum).

This ionization mechanism has several important consequences for the mass spectrum appearance, and also for subsequent data interpretation. ESI is considered one of the “softest” ionization methods. If the ionization conditions are adjusted correctly, there is little to none in-source fragmentation. As a result, ESI is very well suited for determining the molecular mass of the compound of interest. If a mass resolution of the analyzer is sufficiently high (TOF or FTICRMS), elemental formula for the compounds of interest can be calculated (see section 1.4.3.3.1).

Also, tandem mass analyzers are used in the current, state-of-the art mass spectrometers, utilizing ESI. Additional information about the compounds of interest can be obtained using tandem mass spectrometers. Such data subsequently provides very valuable structural information, even for the unknown compounds, which is especially important when SOA samples are analyzed. Of course, this approach also possesses certain limitations, as discussed in Section 1.4.3.1.1. However, it is important to underline that the structural information acquired using tandem mass spectrometer cannot be obtained with the simpler apparatus equipped with single mass analyzer. Obtaining the fragmentation spectra (MS^2 and MS^3 scans) of the selected precursor ion using triple quadrupole mass spectrometer is described below.

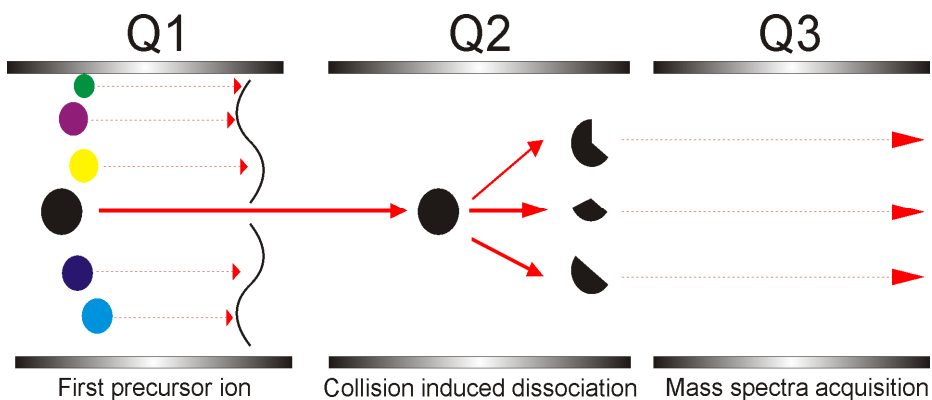


Figure 1.14 Operation schematic of a tandem mass spectrometer

In the tandem mass spectrometer, such as the triple quadrupole spectrometer shown in Fig. 1.14, the precursor ion is selected in the first mass analyzer (Q1) and introduced into the collision cell (Q2). Here, the collision induced dissociation (CID) takes place – MS^2 scan. In the collision cell, the ion is subjected to fragmentation by collision with the neutral gas molecules (most often N_2) and obtained fragments are analyzed by the third quadrupole (Q3). Similar analysis can be performed in the mass analyzers equipped with the quadrupole followed by linear ion trap (LIT). The degree of fragmentation can be controlled by adjusting the specific parameters, and the resulting fragmentation spectrum can provide structural information about the analyzed compounds. Multiple reactions monitoring (MRM) mode is a specific variant of the MS^2 scan, used mostly for quantitative analysis. In the MRM mode, fragmentation conditions for each pair of ions (parent ion/fragmentation ion) are optimized for the maximum sensitivity. MRM mode coupled with the LC analysis significantly enhances the sensitivity and nearly eliminates the background noise, as compared to the total ion current (TIC) mode. Another mode of operation of the triple quadrupole mass spectrometer is the MS^3 mode, in which the fragmentation spectrum of one of the fragment ion is obtained, by causing the fragmentation in both Q2 (collision gas) and Q3 (excitation energy). MS^2 and MS^3 modes are especially useful in studying the fragmentation pathways of the compounds of interests, providing structural information. Such approach, often coupled with the elemental formula assignment is utilized very frequently in studies investigating the structures of the HMW SOA components, as described in Section 1.4.3.3.1.

ESI, as well as all other ionization techniques, also has a number of drawbacks. The very little in-source fragmentation can be regarded as an advantage or disadvantage, depending on the aim of analysis and compounds of interest. This can be overcome by the use of tandem mass analyzers, equipped with the collision cell, which enables the operator to adjust the degree of fragmentation of a selected precursor ion. Another drawback is the ability to directly detect only the molecules containing labile hydrogens in their structures, like carboxylic acids or amines.¹⁷³ Therefore, ESI is unable to directly detect hydrocarbons or even carbonyls and alcohols. This second limitation can be, to a certain degree, avoided by detecting adduct ions of the compounds of interest, usually with metal cations, as will be described below.

Another limitation of ESI is the formation of the non-covalently bonded analytes cluster ions.^{141,145,170} Formation of the non-covalently bonded clusters of the simpler molecules has to be taken into account, especially when analysis of the HMW components of SOA is performed in the direct infusion mode. Formation of such clusters can be, to a certain degree, avoided by proper calibration of the ion source or separation of the sample components by LC prior to the introduction into the ion source. The advantages of the LC/MS analysis over the analysis performed in the direct infusion mode are discussed in Section 4.3.1.3.

As listed in Table 1.10, when HMW α -pinene SOA components are considered, ions that are most often detected are sodium adducts – $M+Na^+$, potassium adducts were also utilized. Protonated ions were detected in two studies, which strongly indicate that HMW SOA components usually do not have ionization site, enabling the formation of protonated or deprotonated ions. A large number of studies used ESI operating in the negative ionization mode to study SOA composition. The use of ESI in the negative ionization mode is convenient, since a large number of SOA components contains carboxylic group, and thus can be readily detected as anions. Also, there are less adduct ions in the negative ESI and compared to the positive polarization, however, as already discussed above, adduct formation can be an issue in both ionization modes.

The APCI ionization mechanism is significantly different from ionization in ESI, even though both ion sources operate under atmospheric pressure. In APCI, similar to the ESI, the liquid sample is pumped through a narrow capillary, and solution is vaporized by applying high temperature.

Afterwards, the sample is sprayed to the corona discharge needle. APCI ionization mechanism is similar to the mechanism in chemical ionization (CI), in such a way, that the analyte is ionized by gas-phase charge-transfer reactions of the compound of interest molecules with charged molecules of eluent and bath gas. Some of the reactions, involved in positive APCI ionization, are shown in Fig. 1.15.¹⁷³

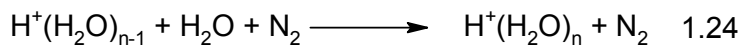
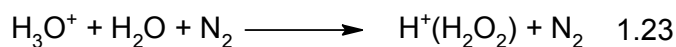
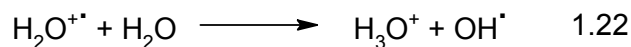
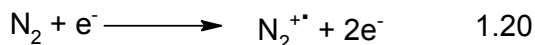


Figure 1.15 Ionization process in APCI

As shown in Fig. 1.15, reactions 1.20 – 1.24 involve the formation of the gas bath gas and solvent ions, initiated by the electrons emitted from the corona-discharge needle. Afterwards, analyte (A) can be ionized by charge transfer reaction 1.25 or proton transfer reaction 1.26.

APCI is significantly less popular ionization method, used mostly in online investigations,^{132,134} although it is also suitable for analyzing the liquid samples, either by direct infusion, or by connecting the ion source to LC.¹²² Due to the APCI ionization mechanism, this technique is less suited for the detection of large, polar compounds. In case of α -pinene SOA samples, it can be concluded that only analytes with molecular masses < 200 Da can be detected. The HMW compounds most likely decompose in the ion source.¹³² However, it should be noted that in the study by Hoffman et al.¹⁷² it was possible to ionize stable HMW compounds using APCI.

Due to the “softer” ionization conditions in APCI than in, for instance EI, there is also relatively little in-source fragmentation. However, since the sample spray is not generated by applying high voltage to the capillary, but by vaporizing the sample with high temperature, thermal decomposition is still an issue. Also, gas-phase reactions involved in the ionization process can result in fragmentation/decomposition of the more labile analytes even though this process leads to the formation of ions with significantly lower amounts of excess energy, as compared to EI. However, APCI is capable of directly ionizing such compounds as carbonyl or alcohols, and thus was used as the ionization method complementary to ESI,¹²² which in turn cannot ionize some molecules.

1.4.3.3. Identification of the HMW α -pinene SOA components

In this section, identification methods of the HMW SOA components are summarized. Due to the lack of the appropriate standards, the structures and therefore formations pathways of the HMW SOA components can be only tentatively identified, although very significant progress was made in recent years. Structures of the HMW compounds, proposed as a potential nucleation precursors of SOA generated in the α -pinene/ozone system are discussed separately in Section 1.4.4. The most widely utilized approach is based on the elemental formula assignment by high resolution (HR) - MS and/or tandem mass spectra interpretation, discussed in Section 1.4.3.3.1. The more problematic but also more reliable approach of identifying the HMW SOA components, involving synthesis of the actual standards for the compounds of interest is discussed in Section 1.4.3.3.2.

1.4.3.3.1. Mass spectra interpretation and elemental formula assignment

Mass spectra interpretation frequently supported by the elemental formula assignment is most often utilized approach used for the identification of HMW SOA components. Studies utilizing either one of both of the methodologies, are listed in Table 1.11

Table 1.11 Methods of HMW α -pinene SOA components identification

Identification method	Reference
Interpretation of the fragmentation spectrum	136-139,142,145,147,151,170,172
Elemental formula assignment	139,141,144,145,152,170

Structures proposed in the currently published studies are based on either the elemental formula assignment by high resolution (HR) - MS and/or tandem mass spectra interpretation. An example of such investigation, picturing both advantages and disadvantages of this approach will now be presented, based on the results described by Hall et al.¹⁴⁵ In the discussed study, state of the art FTICRMS was used to provide extremely high mass resolution, enabling to assign the elemental composition for over a 1000 of mass peaks. This, of course, provided very valuable data about the SOA elemental composition. However, as stated by the Hall et al,¹⁴⁵ due to the number of monomers and possible association mechanisms of these monomers it was impossible to propose the structures for a majority of the detected compound. In fact, for the peak with m/z 375.214 Da, there were 18 equally probable structures. Even when fragmentation spectrum was acquired, the authors concluded that, in most cases, it did not provide the sufficient data to reduce the number of possible structures. It is very important to underline, that authors recognized the problem of the number of possible structures, by conducting extensive monomer investigation, and thoroughly examining the possible association mechanisms. Such careful evaluation is necessary to recognize the complexity of the problem, so that possible structures of the compound under consideration are not proposed, based on limited structural information available.

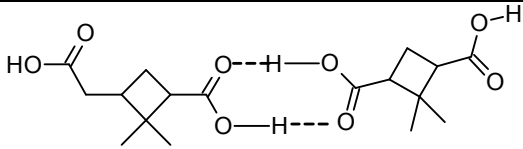
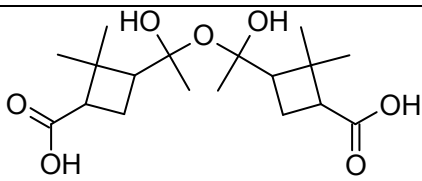
For a number of mass peaks, however, it was concluded that based on the acquired data, the observed mass peaks can be explained only by one or two (or both) possible structures of compounds with a given elemental composition and MW. It was concluded that neutral losses of a certain masses indicate the presence of certain functionalities, which is a widely used approach.

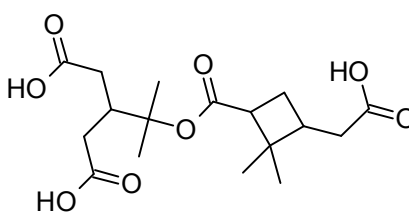
However, as stated by the Hall et al, ¹⁴⁵ evidence for certain oligomers formation was less compelling. Experimental evidence was presented, supporting all of the formation mechanisms, ^{125,135-139,141-143,145-147,152,174} discussed in Section 1.4.3.4. However, as also stated by the Hall et al, ¹⁴⁵ the presented results should not be considered definitive, unless these were supported by the analysis of the actual standards. Similar conclusion can also be applied to all of the other studies, utilizing HR-MS together with the tandem mass spectra analysis to propose the structures and formation pathways of the detected HMW SOA components.

Also, studies like the investigation presented by Hall et al. ¹⁴⁵ are often performed directly introducing the sample into the ion source in MS, and thus the limitation to be considered is the ion-source formation of adducts, very characteristic when ESI is used – see section 1.4.3.2. In the Hall et al. ¹⁴⁵ study special attention was paid to avoid in-source adducts formation. It was also concluded that the ion-source artifacts formation cannot be avoided in the negative ionization mode, thus only the data from positive ionization mode was analyzed.

To underline advantages as well as limitations of the analytical approach presented in this section the change in the structure understanding of the extensively studied HMW α -pinene SOA component, a compound with MW 358 Da is presented in Table 1.12

Table 1.12 Structures of the compound with MW 358 Da proposed between 1998 and 2013

Proposed structure	Year published	Reference
	1998	172
	2004	137

	2010	175
	2010	174
	2012	146
	2013	147

As listed in Table 1.12, this compound has been detected in number of studies and thus extensively analyzed. For the first time, a presence of the compound with MW 358 Da was reported in the chamber study of α -pinene ozone – initiated SOA formation by Hoffman et al.¹⁷² At that time, it was proposed this compound was a stable adduct of pinic and norpinic acid. That adduct was concluded to be very stable, even under the LC analysis conditions. The discussed study was published 15 years ago, thus it may be argued that these results should not be compared with the currently available data. However, analytical tools used by Hoffman et al. did not differ from those used in the studies published in 2013 (LC coupled to the MSⁿ), as well as in a number of other investigations, summarized in Table 1.10 (section 1.4.3.2). The main objective of the summary, presented in Table 1.12, is to show, that the same data can be interpreted differently, providing a reasonable justification of the fragmentation spectrum obtained for a given mass peak. Fragmentation spectrum reported by Hoffman et al. 15 years ago agrees perfectly with the spectra reported in more recent studies. Gao et al.¹³⁷ also investigated the structure of the compound with MW 358 Da, again obtaining the same fragment ions as those reported in a more recent investigations. In a number of recent studies, after extensive investigation of the MSⁿ spectra, the compound with MW 358 Da was established to consist of diaterpenylic acid and cis-pinic acids.¹⁷⁵ This structure is currently accepted as a correct one.

The fact that the proposed structure of the compound with MW 358 Da changed significantly since the detection of this compound in 1998, illustrates the speculative nature of the results obtained by elemental formula assignment and/or interpretation of the fragmentation spectrum. The obtained fragment ions can be explained by a number of structures. Especially when simple bond cleavage is considered as the only possible fragmentation mechanism which

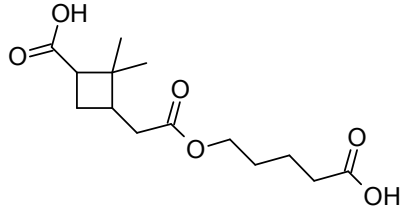
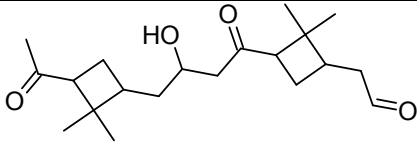
was, for some reason, accepted practice in all of the studies summarized in Table 1.11. Also, it should be noted that the structure of the compound with MW 358 Da was finally resolved, since it was consistently detected in a number of studies. This compound is now considered a very important α -pinene SOA tracer.¹⁷⁵

However, for a large portion of the HMW compounds detected in SOA samples, such extensive investigations were not conducted. As already discussed above, the structures of detected HMW compounds are often tentatively proposed, to explain their masses and elemental formulas. Tandem mass spectrometry provides information about structures of the compounds of interest. Structures presented in the studies summarized in this section, should be therefore, to a certain degree, considered uncertain. While providing very valuable data, such methodology is only capable of reducing the number of possible structures for the compounds under consideration.²⁰ Of course, a significant advantage of this approach is that all of the detected compounds can be analyzed in this manner, as opposed to the approach involving standard synthesis, discussed in the following section.

1.4.3.3.2. The use of standard synthesis for the identification of the HMW α -pinene SOA components

Analysis of the actual standards has proven to be necessary for unambiguous identification of SOA components.^{139,142,176-178} Synthesizing the actual standards for the compounds of interest basically eliminates the need of time consuming data analysis. Results of standard analysis need to be compared with those, obtained from the actual sample. Using this approach, unambiguous identification of SOA components is possible, as opposed to the approach, presented in section 1.4.3.3.1. Studies, utilizing standard synthesis for the unambiguous identification of the HMW SOA components, are listed in Table 1.13.

Table 1.13 Synthesized standards of the α -pinene SOA HMW components

Standard synthesized	Reference
	142
	139

As shown in Table 1.13, very few studies, utilizing the actual standards synthesis can be found in the literature. Beside frequently complex synthesis procedure, the lack of standards, even for LMW ozonolysis products and/or OH-initiated oxidation products of α -pinene is a main issue. Tolocka et al.¹³⁹ synthesized aldol condensation product of two pinonaldehyde molecules and subsequently detected this aldol product in the actual SOA sample. In a number of studies, surrogate precursors like cyclohexene was used,¹⁷⁶ or experiments were preformed, using the mixture of α -pinene and cyclohexene.¹⁴² The use of cyclohexene is frequent, since due to the simpler structure, a larger number of its ozonolysis products can be purchased. Mixed studies provide more mechanistic than structural information, since the certain mechanism of the oligomer formation (e.g. esterification) can be justified.¹⁴² For the “pure” α -pinene/ozone system, few standards for the LWM products were also synthesized, since even for the simple compounds standards are frequently not available.¹⁷⁷

For example, synthesizing all of the 18 possible structures of the compound corresponding to the ion m/z 375.214 Da, discussed in the previous section (1.4.3.3.1) would required a tremendous amount of time and effort, even assuming that all the monomers are available for synthesis, which

is rarely the case. Even if synthesis of the 18 possible structures was conducted, it would only lead to resolving the structure of one compound, out of the approx. 1000 assigned elemental compositions,¹⁴⁵ therefore providing little to none insights into the formation processes of the bulk of HMW α -pinene SOA components. The most popular analytical techniques used for SOA composition analysis, such as ESI/MSⁿ and LC-ESI/MSⁿ (see section 1.4.3.2), are well suited for unambiguous identification of a known compounds in the complex, unknown matrices. However, since the availability of the standards is very limited, approach described in this section is often impractical or impossible to be used for analysis of a majority of SOA samples.

It is, of course, possible, that the compound with the same mass, similar fragmentation and the same retention time as the synthesized standard is a different chemical individual, with nearly identical properties as the reference compound. However, the possibility of such scenario is significantly lower than the incorrect identification using the methodology described in section 1.4.3.3.2, when no standards are available. Still, lack of commercially available standards drastically limits the use of the methodology outlined in this section.

1.4.3.4. Formation mechanisms of the high molecular weight (HMW) compounds formed during the SOA formation in the α -pinene/ozone system

Two formation pathways of the α -pinene SOA HMW components were proposed, based on the data summarized in Section 1.4.3.3. The first set of reactions possibly leading to the observed HMW compounds involve particle – phase reactions for coupling of the stable, first generation products – Section 1.4.3.4.1. Proposed gas – phase reactions also involve the association of the stable molecules. However, more frequently, reactions of radical intermediates with the stable oxidation products in the gas phase are proposed as the dominant pathway of HMW compounds formation – Section 1.4.3.4.1. Please note that no distinction is made between studies where experimental results were presented, supporting the proposed oligomer formation and studies where authors only hypothesized the formation of a given compound. Identification methods of the specific classes of the HMW SOA components are discussed separately in Section 1.4.3.3.

1.4.3.4.1. Particle – phase reactions

It was suggested (see Table 1.14) that, primary products could act as the building blocks to form oligomers, mostly by the acid – catalyzed, particle - phase reactions. These reactions were proposed as possible association pathways of the LMW SOA components, and are summarized in Table 1.14^{20,92,125,135-142,179} A number of the reactions, summarized in Table 1.14 can be catalyzed by either acid or base, however, in case of SOA particles acid catalysis is believed to be dominant.^{20,179,180} It is important to underline, that usually there is more than one possible coupling mechanism between the LMW SOA components, since the majority of these compounds usually contain more than one functional group, as it was shown in Section 1.4.1.

Table 1.14 Liquid – phase reactions that were proposed to lead to observed HMW α -pinene SOA components formation

Reaction number	Reaction type	Reference
1.27	Aldol condensation	136-140,143,145
1.28	Gem-diol and acetals formation	125,135-139,141,143,145,152
1.29	Esterification	136,141-143,146,147

Aldol condensation (reaction 1.27) was frequently proposed as possible linking mechanism between the carbonyl compounds. This reaction product is characterized by the elimination of the 18 Da fragment from the parent ion, corresponding to the neutral loss of water.¹⁴¹ Aldol condensation reaction between pinonaldehyde and pinonic acid is shown in Fig. 1.16, reaction 1.27.¹⁴⁵

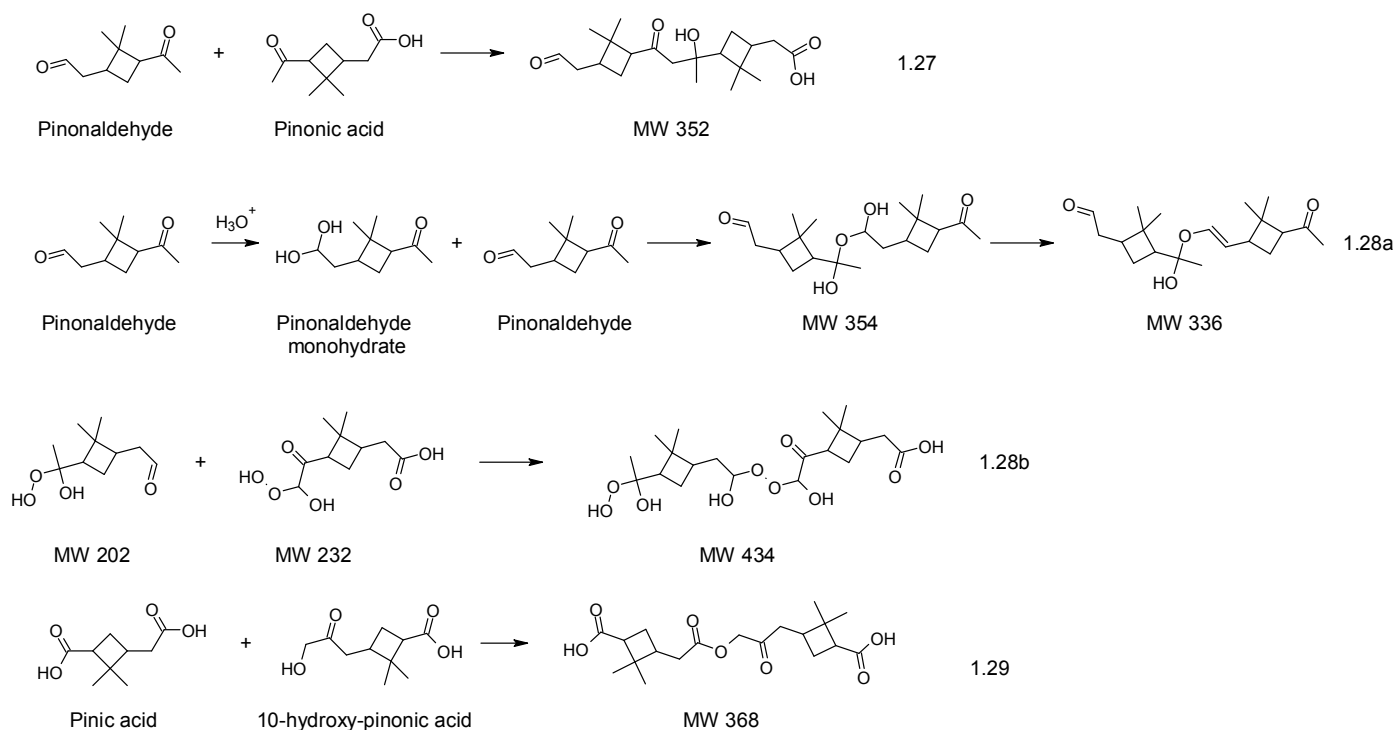


Figure 1.16 Particle – phase reactions leading to the formation of α -pinene HMW SOA components

Hemiacetal formation (reaction 1.28a) is also proposed as a coupling mechanism for carbonyl compounds. If the carbonyl compound initially undergoes hydration reaction, gem-diol (hydrate) is formed. Afterwards, generated OH group can react with another carbonyl group to form a hemiacetal with MW 354 Da, and subsequently MW 336 Da, as a result of water elimination.¹³⁹

Formation of peroxyhemiacetals (reaction 1.28b) was also proposed as a possible association mechanism between carbonyl compounds and molecules with hydroperoxide moiety. An example of peroxyhemiacetal formation proposed by Hall et al.¹⁴⁵ was also included in Fig. 1.16, showing the proposed formation of the compound with MW 434 Da.

Example of pinic and 10-hydroxy-pinonic acid association via esterification (reaction 1.29), proposed by Camredon et al.¹⁴³ is also shown in Fig. 1.16. Generally, this HMW SOA components formation mechanism can be operational, when the two molecules under consideration contain carboxylic and hydroxyl groups. Please note that only one possible structure of this product was

included for clarity. Also, water elimination is characteristic for ester formation, thus the mass of the resulting product differ from the sum of the masses of substrates by 18 Da.

It is important to underline that, a large number of possible association reactions between the multifunctional monomers, makes the identification of the specific formation mechanism of observed HMW compounds very difficult. Association of the two stable products can lead to a number of compounds and the two molecules can react via a number of possible mechanisms. Therefore, in the majority of the currently available studies, unambiguous identification of the specific reaction mechanism was not possible, and presented evidence was rarely conclusive see section 1.4.3.

1.4.3.4.2. Gas – phase reactions

Besides coupling of the monomers in the particle-phase, reactions in the gas-phase leading to the HMW components of SOA were also proposed. Summary of the proposed gas-phase reactions, leading to the formation of the oligomers is presented in Table 1.15. The majority of the gas-phase formation pathways of the HMW compounds involve reactions of SCIs with the stable products, such as those listed in Section 1.4.1. Reactions 1.30 - 1.32 involves SCI association with aldehydes, carboxylic acids and SCI self reaction. Reaction 1.33 is association of the two carboxylic acids in the gas-phase to form non-covalently bonded dimer. Some of these reactions were proposed to produce nucleation – inducing species, as discussed in Section 1.4.4.

Table 1.15 List of substrates that were proposed to react in the gas-phase to form HMW α -pinene SOA components

Reaction number	Reactant 1	Reactant 2	Product	Reference
1.30	SCI	Aldehyde	Secondary ozonide	145,150,152,155
1.31	SCI	Carboxylic acid	Acyloxyhydroperoxides	93,117,150,152,155
1.32	SCI	SCI	Oligoperoxide	155
1.33	Carboxylic acid	Carboxylic acid	Non-covalently bonded dimer	133,145,172

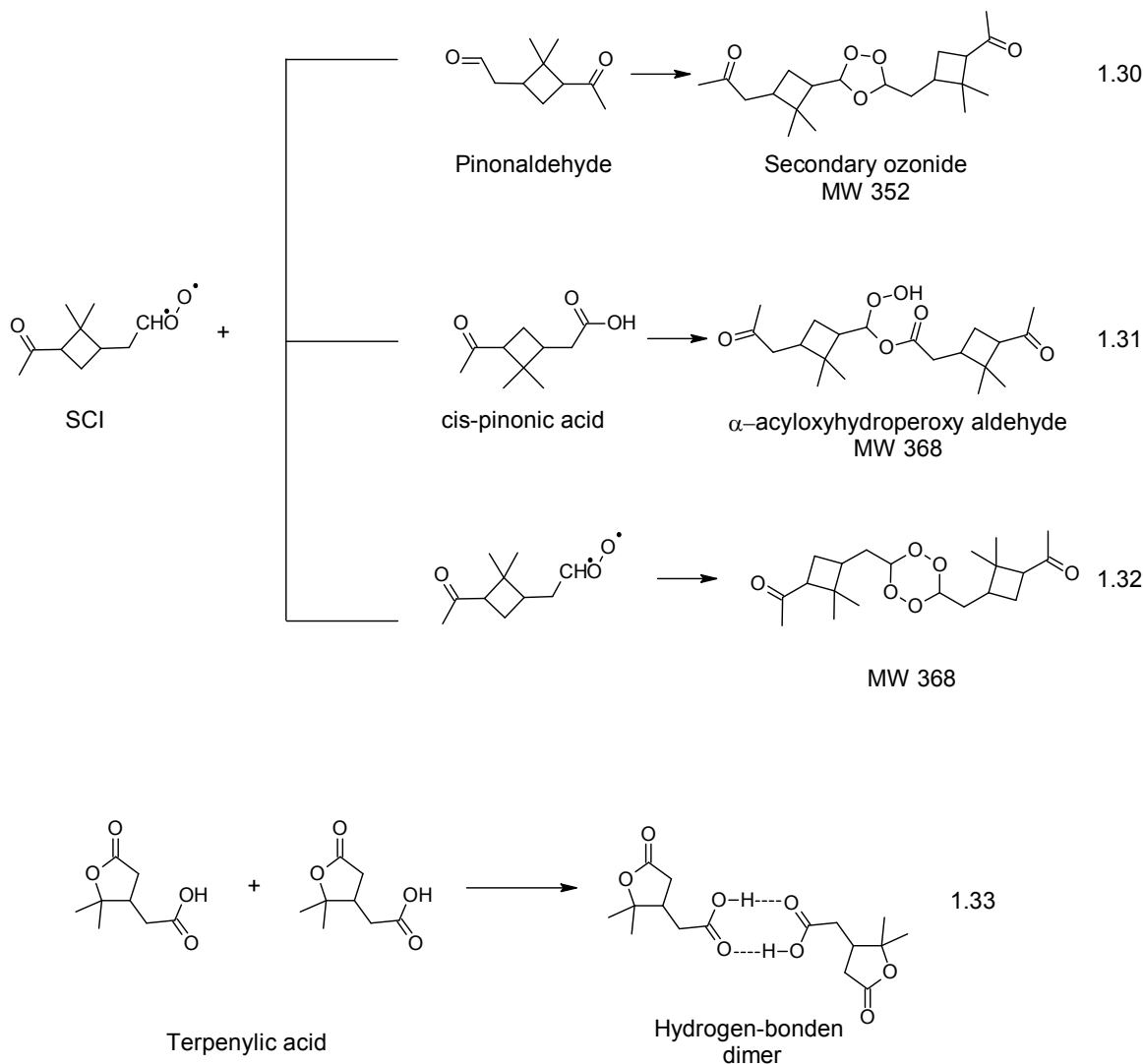


Figure 1.17 Gas – phase reactions leading to the formation of α -pinene HMW SOA components

Examples of the proposed reactions listed in Table 1.15, leading to the formation of HMW compounds in the α -pinene/ozone system are shown in Fig. 1.17. Since, as already discussed in Section 1.4.1, two SCIs can be produced from α -pinene, only one possible structure was included for clarity.

Reaction 1.30 involves the SCI association with the pinonaldehyde to produce secondary ozonide.¹⁷² Reaction 1.31 is the SCI reaction with cis-pinonic acid to produce α -acyloxyhydroperoxy aldehyde.¹²⁴ Both reaction 1.30 and 1.31 are considered important for the

SOA nucleation process, as will be discussed in the section 1.4.4. Reaction 1.32 involves association of two SCIs¹⁵⁵ The first two reactions were proven to occur in the gas-phase, and they involve SCI reactions with scavengers, reacting a few orders of magnitude faster than reaction with water.

The gas-phase formation of the terpenylic acids dimers was concluded to be energetically favorable, with the dimerization energies comparable to acetic acid.¹⁷⁵ Therefore, gas-phase dimerization of terpenylic acid via hydrogen bonding of the two carboxyl groups appears to be reasonable.

Reactions summarized in section are believed to compose a fraction of HMW SOA components; however, formation of the potential nucleation – inducing species via reactions 1.30 and 1.31 was also proposed, as discussed in section 1.4.4. As already discussed in the 1.4.3.3, up-to date, very limited analytical evidence, supporting the formation reactions 1.30 and 1.31 products have been presented.

1.4.4. Proposed nucleation precursors

In this section, current theories of the SOA nucleation in the α -pinene/ozone system are discussed. In the earlier publications, it was speculated that dicarboxylic acids were initiating the SOA nucleation, due to their lowest vapor pressures, out of all known α -pinene oxidation products at that time. Currently published results strongly indicate that this theory was incorrect,^{93,133,139,150,181} and thus it will not be discussed here. Instead, results of the most recent investigations of the SOA nucleation in the α -pinene/ozone system will be summarized. Up-to-date, there is no generally accepted nucleation mechanism, although in a number of studies, similar theories were presented.

Kamens et al.⁹³ in their model study assumed that the α -pinene/ozone SOA self-nucleation will proceed via SCI addition to the pinonaldehyde, producing the secondary ozonide. It was argued, that since the secondary ozonide is most probably extremely non-volatile, it will enable the SOA self-nucleation pathway in the model simulation. This assumption was based on the

earlier observation of the secondary ozonides formation during the ozonolysis of simple alkenes, such as propylene and isobutene. In the subsequent study, Kamens and Jaoui¹¹⁷, in addition to the formation of the nucleation seeds via reaction of SCI with pinonaldehyde, reaction with the carboxylic acids were also included as the possible formation pathway of the nucleating species, thus the formation of α -acyloxyhydroperoxy aldehydes was assumed. Also, as compared to the previous model, gas-phase association of the two dicarboxylic acids was included as the possible formation of the nucleating species. It was argued that such nucleation mechanism is reasonable, based on the investigations available at that time, reporting the formation of large molecules from SCI association with carboxylic acids and carbonyls for simple alkenes, such as ethene. As concluded by Kamens and Jaoui,¹¹⁷ both modeling studies agreed reasonably well with the experimental data. However, no evidence of the HMW compounds formation, assumed to be acting as the nucleating species in the developed model was presented.

Bonn et al.¹⁸¹ investigated the influence of the water vapor on the SOA nucleation for both α and β -pinene and other monoterpenes. For α and β -pinene it was found that water addition suppressed the SOA formation. For the α -pinene experiments, when the higher reactants concentrations were used, no effect of water vapor on SOA formation was initially observed, as opposed to the experiments with β -pinene. Similar effect for the α -pinene experiments was observed after lowering the concentrations of both ozone and the precursor by about an order of magnitude, effectively increasing the water concentration, relative to other two reactants. It was concluded that for both α and β -pinene water reduced the nucleation precursor concentration and, consequently, suppressed the SOA formation. For α -pinene, and endocyclic alkenes, suppression of SOA formation by water was less pronounced than for exocyclic alkenes. Also, the addition of formic acid to the reaction system, much more reactive SCI scavenger, led to much stronger suppression of the SOA nucleation than the addition of water. These results pointed out on the SCI-mediated nucleation mechanism, similar to other studies, listed in Table 1.16. Two possible nucleating agents were proposed for the exocyclic and endocyclic alkenes, based on the acquired data. For the exocyclic alkenes, such as β -pinene, it was proposed that the secondary ozonide, formed by the reaction of C_9 -SCI with a carbonyl compound can initiate the SOA nucleation. For the α -pinene, an intramolecular secondary ozonide was proposed. Since the water

suppressing effects was much weaker for the endocyclic alkenes, Bonn et al.¹⁸¹ have argued that the formation of the intramolecular secondary ozonide is much faster, hence observed suppression effect on SOA formation was weaker, than in the case of β -pinene. It is however important to underline, that the proposed nucleation precursors were not observed directly. Also, Lee and Kamens,¹⁵⁰ after calculating the vapor pressure of the intramolecular secondary ozonide formed from α -pinene SCI, concluded that this compound is much too volatile, thus it is unlikely to act as a nucleating agent.

Lee and Kamens¹⁵⁰ studied SOA formation by adding high concentration of LMW SCI scavengers to the α -pinene/ozone system. It was concluded, that SOA formation was significantly suppressed in experiments with the SCI scavengers. In case of α -pinene ozonolysis a number of products of the SCI reaction with the first generation products was proposed as the possible nucleation precursors. The compounds proposed by Lee and Kamens¹⁵⁰ are shown in Fig. 1.18. Please note that for the non-symmetrical alkene, such as α -pinene, two possible SCIs can be produced (see sections 1.3.3. and 1.4.1). For simplicity, only one possible reaction product with the SCI scavenger, also listed in Fig. 1.18, was shown.

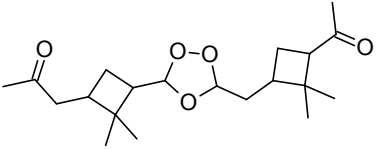
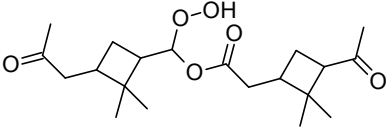
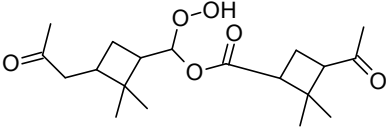
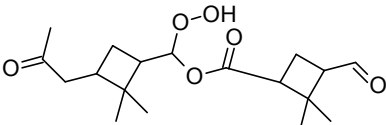
Structure	Molecular weight (Da)	SCI scavenger
	352	cis-pinonaldehyde
	368	cis-pinonic acid
	354	norpinonic acid
	340	pinilic-4-acid

Figure 1.18 Structures and the molecular masses of the possible nucleation precursors proposed by Lee and Kamens.¹⁵⁰

Aside from studying the impact of addition of LMW SCI scavengers on SOA formation yield, Lee and Kamens¹⁵⁰ also studied the first generation aerosol composition produced in a very short time scale 0.4-6 s. The SOA composition was studied with GC/MS after appropriate derivatization procedure was performed on filter extracts. Such approach does not allow detecting the HMW SOA components, as already discussed in Section 1.4.3. However, it was possible to eliminate the formation of the dicarboxylic acids such as pinic acid in this short time-scale, since this acid was not detected in the filter extract. Thus, pinic acid was not included as the potential SCI scavenger, and such product was not considered as the possible nucleation precursor. For every compound shown in Fig. 1.18, vapor pressure was calculated. It was concluded, that products of the SCI reaction with the α -acyloxyhydroperoxy aldehydes have the vapor pressures approx. two orders of magnitude lower than the vapor pressure for secondary ozonide, thus suggesting that the latter class of compounds are better candidates for the potential nucleation precursors. It was also concluded that intramolecular, secondary ozonide, produced from the SCI self – reaction is much too volatile as compared to the other compounds shown in Fig. 1.18 to be considered as the potential nucleation precursor, as already discussed earlier in this section. It is however important to underline, that no experimental evidence for presence of the compounds considered as the nucleation precursors in the discussed study was presented.

Tolocka et al.¹⁵⁵ also studied ozone-initiated α -pinene SOA formation on a short time scale of 3 – 22 s. Photoionization aerosol mass spectrometer (PIAMS) was used for the online analysis of the SOA molecular composition. A number of oligomers were concluded to be produced within the time scale of the experiment, based on the PIAMS mass spectrum. The acquired data suggested the formation of the secondary ozonide proposed by Lee and Kamens¹⁵⁰ – see Fig. 1.18. Ions indicating the formation of the other secondary ozonides were also detected. However, as stated by Tolocka et al,¹⁵⁵ it is difficult to obtain unambiguous identification of the SOA components, based on the PIAMS mass spectrum. Therefore, alternative mechanisms for the formation of the observed HMW ions were proposed. The oligomers were proposed to be formed by association of

the two SCIs followed by elimination reaction, and/or fragmentation of the ions with the highest m/z . It was also hypothesized that PIAMS may selectively detect the secondary ozonides, over α -acyloxyhydroperoxy aldehydes, and thus the ions indicating the formation of the latter class of compounds were not observed.

Claeys et al.¹⁷⁷ have proposed that clusters of the terpenylic acid, a molecule with strong tendencies to form a non-covalently bonded dimers is likely to initiated SOA nucleation. Claeys et al.¹⁷⁷ concluded that this compound was present in the smog-chamber generated SOA, as well as in ambient SOA samples. The identification was based on the mass spectra interpretation, as well as on the actual standard synthesis. Based on the quantum calculations as well as experiments performed with LC-ESI/MS, it was concluded that terpenylic acids formed dimers, while under the same conditions, no dimer formation was observed from the *cis*-pinonic acid. It was argued that terpenylic acid dimer have sufficiently low vapor pressure as well as appropriate size to be a good candidate for the nucleation precursor. Additionally, in a number of previously published studies, this specific acid was concluded to be produced in the early stages of SOA formation. The presented theory is well supported by the analytical as well as theoretical experimental results. However, it is important to underline that there is no direct, analytical evidence, proving that the terpenylic acid clusters initiated SOA nucleation during gas-phase, ozone initiated oxidation of α -pinene.

Viitanen et al.¹⁸² used ion mobility spectrometer (IMS) to study the SOA nucleation in the α -pinene/ozone system. It was concluded that the large molecule or most likely dimer with the MW 355 ± 71 Da was responsible for initiating the SOA formation. The Viitanen et al.¹⁸² justified this conclusion as follow: the small cluster of molecules, below the detection limit of the scanning mobility particle sizer (SMPS), which was used to monitor particles size distribution, was detected well before the nucleation was observed with SMPS. The two peaks, detected with IMS were assumed to be responsible for the SOA nucleation, since they were the only indication of the reaction mixture composition change before the particles formation were observed with SMPS. As stated by Viitanen, et al.¹⁸² IMS cannot measure the mass to charge ratio directly, thus some approximation were made, resulting in significant uncertainty of the reported MW of suspected

nucleating species. However, the molecular identity of the suspected nucleation precursor could not be elucidated, based on the acquired experimental data.¹⁸² Also, it was underlined that this cluster can consist of two or more HMW species.

Significantly different results were reported by Gao et al.¹⁷⁴ where SOA composition was studied over a time scale of 23 s in the flow-tube reactor. It was concluded that under the experimental conditions used by Gao et al.¹⁷⁴ the compound with MW 358 was a dominant component of the freshly formed aerosol in the α -pinene/ozone system. This dimer was previously identified as an ester of diaterpenylic acid and pinic acid – see section 1.4.3.3.1.^{146,147,175} Thus, it was concluded that this ester is a key intermediate in the nucleation process. In the study by Gao et al.¹⁷⁴ it was also concluded that the particles formation was not limited by the gas-phase dimer formation. This was confirmed by investigating the dependence of particle number concentration from the ozone concentration. The particle number concentration was found to increase linearly with the ozone concentrations, thus strongly indicating that the new particles formation was not initiated by the gas-phase dimerization. It is also important to underline, that Gao et al.¹⁷⁴ presented clear experimental evidence of SOA composition analysis, supporting the hypothesis that the previously observed ester with MW 358 is the key intermediate for the new particles formation.

Wolf et al.⁸⁸ studied the aerosol formation from a number of alkenes ozonolysis, including 1-methyl-cyclohexene, methylene-cyclohexane, α -pinene, β -pinene etc. In the study by Wolf et al,⁸⁸ SOA formation was studied as a function of pressure. As the pressure was decreased, the SOA yield was also reduced. Also, formation of the specific decomposition products was observed at lower pressures, suggesting that the lower SOA yield was a result of the reduced ECI stabilization. However, as discussed by Wolf et al,⁸⁸ a detailed modeling study is necessary to draw any definitive conclusions.

Winkler et al.¹⁸³ studied SOA formation during the gas-phase α -pinene ozonolysis in the flow tube reactor at the time scale ranging between 15 and 60 s. SOA particles composition was analyzed with thermal desorption chemical ionization mass spectrometer (TDCIMS). As stated by the Winkler et al,¹⁸³ this instruments is unable to analyze oligomers, due to the sampling method

employed in the TDCIMS, they most likely decompose into the respective monomers. It was found that there is a significant difference between the chemical composition of the smallest particles (10 and 20 μm in diameter) and the particles with diameters of 40 μm . The dominant components of the smallest particles were carboxylic acids, while the larger particles consisted primarily of carbonyl compounds and LMW carboxylic acids. However, the decomposition of the less stable oligomers during analysis raises the question, if the observed monomers indeed origin directly from the simple decomposition of the parent compound. It is however possible, that the fragments of the HMW parent compound, produced in TDCIMS further isomerize and/or rearrange to form the observed ions. The simple bond cleavage is not always the dominant fragmentation mechanism. Also, suggestion that pinic acids could participate in the new particles formation is in direct opposition to the results presented by Lee and Kamens,¹⁵⁰ suggesting that pinic acid is not produced during the very early stages of SOA formation.

Zhao et al.¹⁴⁸ have used chemical ionization mass spectrometry (CIMS) to probe the composition of α -pinene SOA on the early stage of particles formation. It was found that a group of compounds with molecular masses ranging from 490 – 630 Da participated in the new particles formation. This conclusion was based on the observed correlation between the concentration of a specific group of HMW compounds and the formation of the smallest particles, with diameters 10 – 20 μm . It is important to underline, that the presented experimental results strongly indicated that the initially formed particles contain oligomers, and the LMW compounds were not detected in significant quantities suggesting that HMW species were responsible for the initial particles formation. The Zhao et al.¹⁴⁸ concluded that the compounds with the molecular masses between 490 and 630 Da most probably initiated the SOA nucleation. However, specific molecular identities of the suspected nucleation precursors could not be elucidated based on the acquired experimental data. As stated by the Zhao et al,¹⁴⁸ additional investigation of the initially formed particles composition is necessary to present any definitive conclusions.

Table 1.16 Summary of the α -pinene/ozone SOA nucleation studies

Proposed nucleation mechanism	Experimental evidence	Ref.	Year of publication
SCI – mediated nucleation mechanism and association of the acids adducts in the gas-phase	The products of SCI association with carbonyls were sufficiently low-volatile to induce the system self-nucleation	^{93,117}	1999 and 2001
SCI – mediated nucleation mechanism	Water vapor and formic acid (LMW SCI scavengers) suppressed SOA formation	¹⁸¹	2002
SCI – mediated nucleation mechanism	Reduced SOA yield with addition of the high – concentration of LMW SCI scavengers	¹⁵⁰	2005
SCI – mediated nucleation mechanism	Masses of the oligomers formed in the early stages of SOA formation corresponded to the SCI addition to the primary oxidation products	¹⁵⁵	2006
Clusters of terpenylic acids and related compound participated in the nucleation process	The compounds under consideration showed strong dimer forming properties in ESI, supported by the quantum chemical calculations	¹⁷⁷	2009
Compound with MW. = 355 ± 70 was responsible for SOA nucleation	Very small particles consisting of dimers with approx. 355 Da were observed before SOA nucleation	¹⁸²	2010

Ester of terpenylic acid and <i>cis</i> -pinic acid acting as the nucleation precursor	Analysis of the molecular composition of particles, produced in the flow-tube reactor revealed the compound with MW. = 358 as the dominant component	¹⁷⁴	2010
SCI – mediated nucleation mechanism	Both SOA yield and SCI stabilization was reduced as the pressure was lowered	⁸⁸	2011
Ester of terpenylic acid and <i>cis</i> -pinic acid acting as the nucleation precursor	The two carboxylic acids were detected as the main components of the smallest particles, as opposed to the particles with larger diameters	¹⁸³	2012
Different compounds, with molecular masses between 490 and 630 Da initiated particles formation	Correlation between formation of compounds with m/z with that specific range and formation of the smallest SOA particles	¹⁴⁸	2013

As summarized in Table 1.16, a variety of experimental results indicated a different nucleation mechanism. Formation mechanism as well as molecular identity of the SOA nucleation precursors in the α -pinene/ozone system is currently unclear. Some studies report that the single compound, such as ester, secondary ozonide and/or α -acyloxyhydroperoxy aldehyde can initiate the SOA nucleation. On the other hand, there is considerable number of published results, indicating that more than one compound is responsible for the new particle formation. Most of the studies, summarized in Table 1.16, provided indirect evidence for the SCI participation in the formation of the nucleation precursors. SCI association with first generation oxidation products such as carbonyl compounds and carboxylic acids was proposed to lead to the formation of HWM oligomers. Such molecules are good candidates for the potential nucleating species, since they are extremely low-volatile.

On the other hand, a number of more recent investigations indicate participation of the carboxylic acids clusters and/or dimers in the nucleation process. Such dimers were observed directly, with soft-ionization techniques like ESI in the early stages of SOA formation. Monomers, corresponding to carboxylic acids, were also observed in the small, newly formed particles.

Despite a large number of published studies, still little is known about the SOA nucleation process in the α -pinene/ozone system. Also, up-to date, there is no commonly accepted nucleation mechanism; the formation mechanism and structures of the nucleation precursors or precursor are particularly ambiguous, as can be concluded from the results of the previously published studies, summarized in this section.

2. Aim of this work

The main goal of this work was to study the SOA composition on the early stages of aerosol formation, focusing mainly on the currently poorly characterized HMW compounds.^{20, 136-139,141,142,144,145,147,151,152,170,172} Formation of the α -acyloxyhydroperoxy aldehydes was postulated in a number of previously published investigations as the possible nucleation precursors of SOA formed in the α -pinene/ozone system.^{20,117,150,155}

Also, according to a number of studies, they can compose a fraction of the HMW SOA components.^{20,145} Even though that the formation of these compounds during α -pinene gas-phase ozonolysis was previously proposed, no direct, analytical evidence confirming or excluding the formation of α -acyloxyhydroperoxy aldehydes was presented.^{20,117,150,152,155}

Therefore, the investigation of α -acyloxyhydroperoxy aldehydes formation during gas-phase ozone-initiated oxidation of α -pinene with the appropriate analytical techniques would provide valuable insights into the importance of these compounds for the SOA formation. The additional goal was to study the SOA composition on the early stage of particles formation with the instrumental technique that, up-to date, provided the most detailed information on the molecular identity of the HMW α -pinene SOA components, as discussed in Section 1.4.3.2.

Since it was previously reported that water, present in large quantities in the atmosphere, could have significant impact on the proposed SCI-mediated nucleation mechanism,^{20,150,181} an additional objective of this study was to investigate the humidity impact on the SOA composition.

The experimental work described in this thesis can be divided into three sections:

(I) Standards preparation and analysis method development for the α -acyloxyhydroperoxy aldehydes was the initial step of the presented investigation. Standards of the α -acyloxyhydroperoxy aldehydes were generated by liquid – phase ozonolysis of cyclohexene and α -pinene in the presence of the selected carboxylic acids. The next stage of this work was to develop a universal method to identify a whole class of α -acyloxyhydroperoxy aldehydes and to optimize the LC/MS conditions for their analysis. Cyclohexene was used as a model precursor, in addition to

the synthesis of the α -acyloxyhydroperoxy aldehydes using α -pinene. Standards of the α -acyloxyhydroperoxy aldehydes were prepared as described in Section 3.3. Development of the α -acyloxyhydroperoxy aldehydes analysis method is described in Section 4.1.2.

(II) The second part of this work was a design and construction of the flow-tube reactor. In the past, similar flow-tube reactors as the one constructed, here were used to generate SOA by the gas-phase α -pinene ozonolysis on a short time scale.^{150,155,135,151,152,154,156,157} Therefore, flow – tube reactor was concluded to be most suitable to study SOA composition on the early stages of particles formation, as opposed to the aerosol generation in a smog-chamber or in a Teflon bag. If, as postulated in a number of previous studies,^{20,117,150,155} α -acyloxyhydroperoxy aldehydes are the compounds initiating the SOA formation, it is reasonable to assume that they should be one of the main HMW components of the newly formed aerosol. Flow – tube reactor constructed and used in this work is described in Section 3.4.

(III) In the last part of this work, the method developed was used to study a formation of α -acyloxyhydroperoxy aldehydes in the SOA samples from the α -pinene and cyclohexene ozonolysis using the flow-tube reactor, as described in Section 4.3.1.2. and Section 4.3.2.2. Aside from investigating the formation of α -acyloxyhydroperoxy aldehydes, the investigation of the HMW cyclohexene and α -pinene components of SOA, produced during the early stages of aerosol formation from these two precursors was also carried out.

3. Experimental

In this section, detailed description of the experimental setup is given while reagents are listed in section 3.1. Afterwards, description of the LC/MS and GC/FID apparatus and analysis conditions is given in Section 3.2. Standards synthesis is described in section 3.3. Detailed description of the flow – tube reactor experimental setup is provided in Section 3.4.

3.1. Reagents

Pentanoic acid ($\geq 99.8\%$) was purchased from Fluka, Sigma - Aldrich (Schnelldorf, Germany). Levulinic acid ($\geq 98.0\%$), 5-oxohexanoic acid ($\geq 97.0\%$), hexanoic acid ($\geq 99.5\%$), heptanoic acid ($\geq 99.0\%$), octanoic acid ($\geq 98.0\%$), decanoic acid ($\geq 98.0\%$), succinic acid ($\geq 99.0\%$), glutaric acid ($\geq 99.0\%$), adipic acid ($\geq 99.0\%$), pimelic acid ($\geq 98.0\%$), suberic acid ($\geq 98.0\%$), cis-pinonic acid (\geq), pinic acid (\geq), ammonium acetate-d7 ($\geq 98.0\%$ D), hexanoic acid-6,6,6-d₃ ($\geq 99.0\%$ D atom), cyclohexene ($\geq 99.0\%$), α -pinene ($\geq 98.0\%$), as well as LC - MS grade solvents and eluent additives; acetonitrile ($\geq 99.9\%$), ammonium acetate ($\geq 99.0\%$), formic acid and acetic acid ($\geq 99.5\%$), were all purchased from Sigma - Aldrich (Schnelldorf, Germany). Deionized water (18 M Ω ×cm⁻¹) was prepared using Direct - Q3 Ultrapure Water System (Millipore). Nonanoic acid was purchased from AlfaAesar, Chemat (Gdańsk, Poland). Cyclohexene - d₁₀ ($\geq 98.0\%$ D atom) was purchased from C/D/N Isotopes, Dr. Ehrenstorfer (Augsburg, Germany). Deuterium oxide ($\geq 99.5\%$ D) was purchased from Armar, AMX (Łódź, Poland). Pentane ($\geq 99.0\%$), methanol ($\geq 99.0\%$) and acetone ($\geq 99.0\%$) were purchased from POCH, Gliwice, Poland. Synthetic zero air for FID (≤ 3 ppmv of H₂O, ≤ 0.1 ppmv of hydrocarbons), H₂ for FID ($\geq 99,999\%$) and ultra-high purity (UHP) He for GC ($\geq 99,999\%$) were supplied by Multax (Stare Babice, Poland).

3.2. Apparatus

In this section experimental conditions for the chromatographic and/or mass spectrometric characterization of the specific compounds are presented. Initially, direct infusion MSⁿ experimental conditions are provided in Section 3.2.1. MS², MS³ as well as optimization of the MRM conditions was performed in the direct infusion mode. Cyclohexene and α -pinene SOA composition was studied with LC-ESI/MSⁿ. LC-ESI/MSⁿ experimental conditions for the analysis of

cyclohexene and α -pinene SOA composition are provided in Sections 3.2.2.1, 3.2.2.2, 3.2.2.3 and 3.2.2.4. Elemental formulas of the synthesized α -acyloxyhydroperoxy aldehydes were confirmed with ESI-HR-MS and the experimental conditions for these measurements are provided in Section 3.2.2.5. GC/FID conditions used for monitoring cyclohexene and α -pinene gas-phase concentrations in the flow-tube reactor are reported in Section 3.2.2.6.

3.2.1. Direct infusion electrospray tandem mass spectrometry (ESI-MSⁿ)

Investigation of the fragmentation mechanism of the synthesized α -acyloxyhydroperoxy aldehydes, as well as optimization of the MS/MS conditions for the multiple reaction monitoring (MRM) mode were performed by introducing the sample directly into the ion source of QTRAP 3200 mass spectrometer (AB Sciex). Mass spectrometer was equipped with the exchangeable ESI and APCI probes. Samples were delivered to the ion source with the Harvard Apparatus syringe pump at a flow rate of 10 μ L/min. ESI conditions were as follows: source temperature 200 °C, curtain, nebulizer and auxiliary gas (N₂): 0.07 MPa, source voltage 4.0 kV, declustering (DP) and entrance (EP) potentials were set to 20 and 10 V, respectively. Spectra were registered in the mass range: 50 - 1000 m/z in the positive or negative ionization mode. In the MS² experiments selected precursor ion was subjected to the collision - induced dissociation (CID) in the collision cell (Q2) and the collision energy (CE) - dependent fragments were monitored using the third quadrupole (Q3). In the MS³ experiments, the 1st precursor ion was subjected to CID in Q2 and one of the fragment ions produced, the 2nd precursor, was trapped in the ion trap (Q3) and fragmentation was induced by applying excitation energy (AF2). Conditions for the MRM mode were also optimized by directly introducing the sample into the mass spectrometer ion source. For the selected precursor ion, potentials: EP, DP, collision cell entrance potential (CEP), CE, and collision cell exit potential (CXP) were optimized.

3.2.2. Liquid chromatography coupled to the electrospray ionization tandem mass spectrometry (LC-ESI/MSⁿ)

LC/MS experiments were performed by coupling the tandem mass spectrometer with LC20 liquid chromatograph (Shimadzu). Separation was carried out with Zorbax (Agilent) C8 column (150 mm \times 2.1 mm, 3 μ m) kept at 40°C; the mobile phase was delivered at a flow rate of 0.2

mL/min. 2 μ l of the sample was injected into the liquid chromatograph. LC/MS analysis conditions varied, and are listed below.

3.2.2.1. Carboxylic acids produced by gas-phase ozonolysis of cyclohexene

For the analysis of the acidic fraction of the cyclohexene (including cyclohexene-d₁₀) SOA, the analysis conditions were as follows. Formic acid (pH = 3.28) and ACN (eluent B) were used as the mobile phase components, and the following gradient elution program was used: 0 - 8 min, 5% B, 8 -12 min 50% B, 12-15 min, 50% B, 15 – 21 min 90%, 21 - 25 min 90% B, 25 - 27 min 5% B, 27 - 35 min 5% B. Mass spectrometer was operating in the MRM mode and the mass spectra were simultaneously obtained in the range 50 – 300 m/z in both positive and negative ionization modes. ESI conditions were as follows: capillary temperature was 450 °C, curtain gas was 1.7 atm, nebulizer and auxiliary gas were 3.0 atm, spray voltages were 5.5 kV in positive and 4.5 kV in the negative ionization mode, DP and EP were set to 30 and 10 V respectively.

3.2.2.2. α -acyloxyhydroperoxy aldehydes synthesized using cyclohexene

The same gradient elution as for the acidic fraction was used for the analysis of the α -acyloxyhydroperoxy aldehydes, synthesized using cyclohexene as a precursor. Ammonium formate (pH = 3.4) was used as eluent component A and ACN as eluent component B. Mass spectrometer was operating in the MRM mode and the mass spectra were simultaneously obtained in the range 50 – 300 m/z in both positive and negative ionization modes. ESI conditions were as follows: capillary temperature was 450 °C, curtain gas was 2.7 atm, nebulizer and auxiliary gas were introduced at pressure of 3.0 atm, spray voltages were 5.5 kV in positive and 4.5 kV in the negative ionization mode, DP and EP were set to 30 and 10 V, respectively.

3.2.2.3. Carboxylic acids produced by gas-phase ozonolysis of α -pinene

For the analysis of the acidic fraction of the α -pinene SOA, the analysis conditions were as follows. Formic acid (pH = 4) and ACN (eluent B) were used as the mobile phase components, and the following gradient elution program was used: from 0 - 8 min, 10% B, 8 – 18 min 50% B, 18 – 20 min, 50% B, 20 – 27 min 10% B, 27 – 35 min 10% B. Mass spectrometer was operating in the MRM mode and the mass spectra were simultaneously obtained in the range 50 – 500 m/z in both

positive and negative ionization modes. ESI conditions were as follows: capillary temperature was 450 °C, curtain gas was 2.4 atm, nebulizer and auxiliary gas were introduced at pressure of 3.0 atm, spray voltages were 5.5 kV in positive and 4.5 kV in the negative ionization mode, DP and EP were set to 20 and 10 V respectively.

3.2.2.4. α -acyloxyhydroperoxy aldehydes synthesized using α -pinene as the precursor

The same gradient elution as for the acidic fraction, was used for analysis of the α -acyloxyhydroperoxy aldehydes, synthesized using α -pinene as the precursor. Ammonium formate (pH = 4) was used as eluent A component and ACN as eluent B component. Mass spectrometer was operating in the MRM mode and the mass spectra were simultaneously obtained in the range 50 – 500 m/z in both positive and negative ionization modes. ESI conditions were as follows: capillary temperature was 450 °C, curtain gas was introduced at pressure of 2.0 atm, nebulizer and auxiliary gas were introduced at pressure of 3.0 atm, spray voltages were 5.5 kV in positive and 4.5 kV in the negative ionization mode, DP and EP were set to 20 and 10 V respectively.

during direct infusion experiments.

3.2.3. Elemental formula assigned for the synthesized α -acyloxyhydroperoxy aldehydes with high-resolution mass spectrometry (HR-MS)

High-resolution mass spectrometry (HR-MS) experiments were performed with LCT TOF mass spectrometer (Waters). Apparatus was equipped with the ESI probe and the ionization condition were as follows; spray voltage was 4.5 kV, nebulizer gas was introduced at pressure of 2.0 atm and cone voltage was 10 V. Spectra were acquired in the mass range 50 – 1500 m/z in the positive ionization mode. Samples were introduced into the ion source with the Harvard Apparatus syringe pump at a flow rate of 10 μ L/min. Reaction mixtures were diluted with water and acetonitrile (ACN) (1:1 v/v). Sodium acetate was used as a mass calibration standard. Elemental formulas of the sodium adducts for the compounds of the α -acyloxyhydroperoxy aldehydes were fitted within the tolerance of \pm 5.0 mDa.

3.2.4. α -pinene and cyclohexene quantification with GC/FID

Gas chromatograph (HP 5890 Series II, Hewlett Packard) equipped with the flame ionization detector (FID) was used to monitor the concentrations of both α -pinene and cyclohexene during the SOA generation experiments in the flow-tube reactor. Gas samples from the flow-tube were drawn from the sampling port (see Section 3.4.1) with the gas – tight syringe; 100 μ l of the sample was injected into GC.

For the cyclohexene quantification, GC was equipped with SPB-1 fused silica capillary column (60 m, 0.32 mm, 1 μ m). Column was kept at a constant temperature of 75°C and the analysis conditions were as follows: Injector temperature 120°C, FID temperature 180°C, column head pressure 1.38 atm. Ultrapure He was used as carrier gas. For the α -pinene quantification GC was equipped with DB-5 fused silica capillary column (30 m, 0.32 mm, 0.25 μ m) kept at 90°C, injector and detector temperatures were 150°C and 180°C, respectively. Carrier gas pressure was 0.59 atm.

3.3. Standards synthesis

Standards of the α -acyloxyhydroperoxy aldehydes were prepared by liquid phase ozonolysis of cyclohexene in the presence of carboxylic acids. Reaction mixtures were prepared by dissolving 0.1 mM of cyclohexene and 0.2 mM of the carboxylic acid in 2 ml of ACN. Ozone/air mixture (0.6 % v/v) was bubbled through the solution for 4 minutes, resulting in the α -acyloxyhydroperoxy aldehyde concentration of approximately 1.25×10^{-2} M/L. All the synthesized α -acyloxyhydroperoxy aldehydes together with their elemental formulas and the carboxylic acids used as the SCI scavengers are listed in Section 4.1.2.1.

After synthesis, 10 μ l of the sample was diluted with 1ml of the solvent and injected into mass spectrometer. For the LC/MS experiments, 2 μ l of the sample was injected into liquid chromatograph.

3.4. Flow tube reactor

In this section, detailed description of the flow tube reactor experimental setup is given. Outline of the flow tube reactor is presented in Section 3.4.1, including description of the critical

reaction parameters monitoring; precursor and ozone concentrations as well as relative humidity (RH). Description of the SOA generation procedure is given in section 3.4.2. Aerosol filter sampling and sample preparation prior to analysis by LC/MS is described in section 3.4.3. Reactor cleanup procedure is described in section 3.4.4.

3.4.1. Flow tube reactor experimental setup

Outline of the flow tube reactor is shown in Fig. 3.1. Reactor consisted of 60 mm O.D. and 75 cm long glass tube with two Teflon covers. The carrier gas was sealed inside the reactor by two Viton o-rings located between the glass and the Teflon in each cover. The whole experimental setup, including the filter holder, flow meters, humidifier and small precursor bubbler was leak-tested up to approx. 1.5 atm.

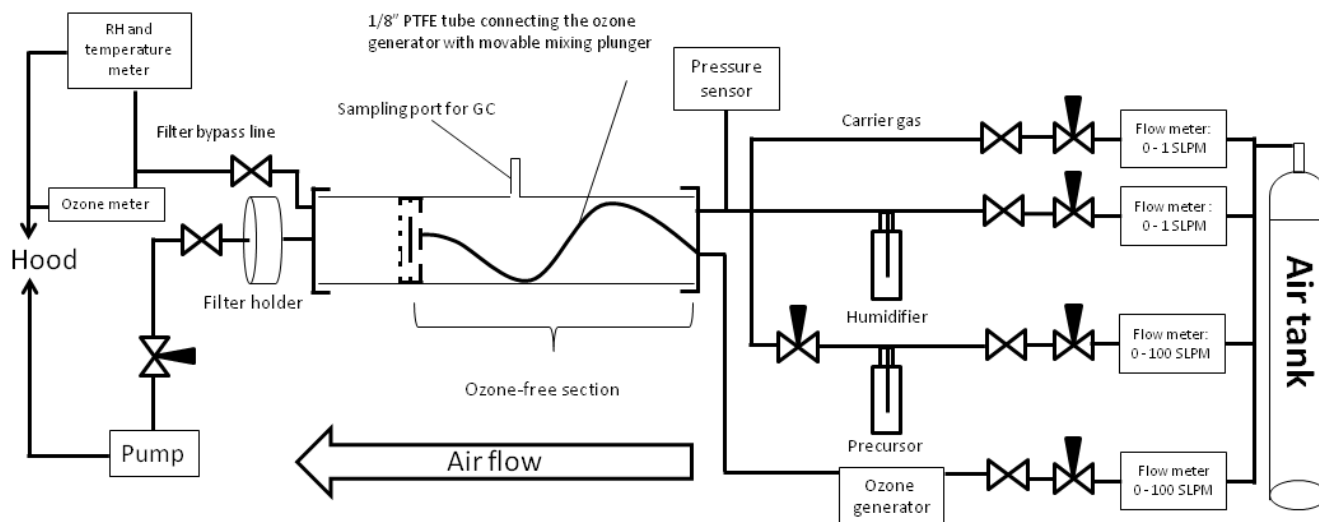


Figure 3.1 Schematic of the flow reactor

As shown in Fig. 3.1, before entering the reactor, carrier gas (UHP synthetic air) from the tank was directed through a four-way flow divider, connected to the four mass flow meters (Sierra). Carrier gas, precursor and humidified air were mixed before entering the reactor in the $\frac{1}{4}$ " cross connector and introduced into the flow tube via one of the two inlet ports in the Teflon cover - Fig. 3.1. Picture of a part of experimental setup is shown in Fig. 3.2. It includes the 500 ml water bubbler (humidifier), the small precursor bubbler, the heating jacket (used in α -

pinene experiments only, see later in this section), the four mass flow meters, the pressure sensor and the Teflon cover with two inlet ports.

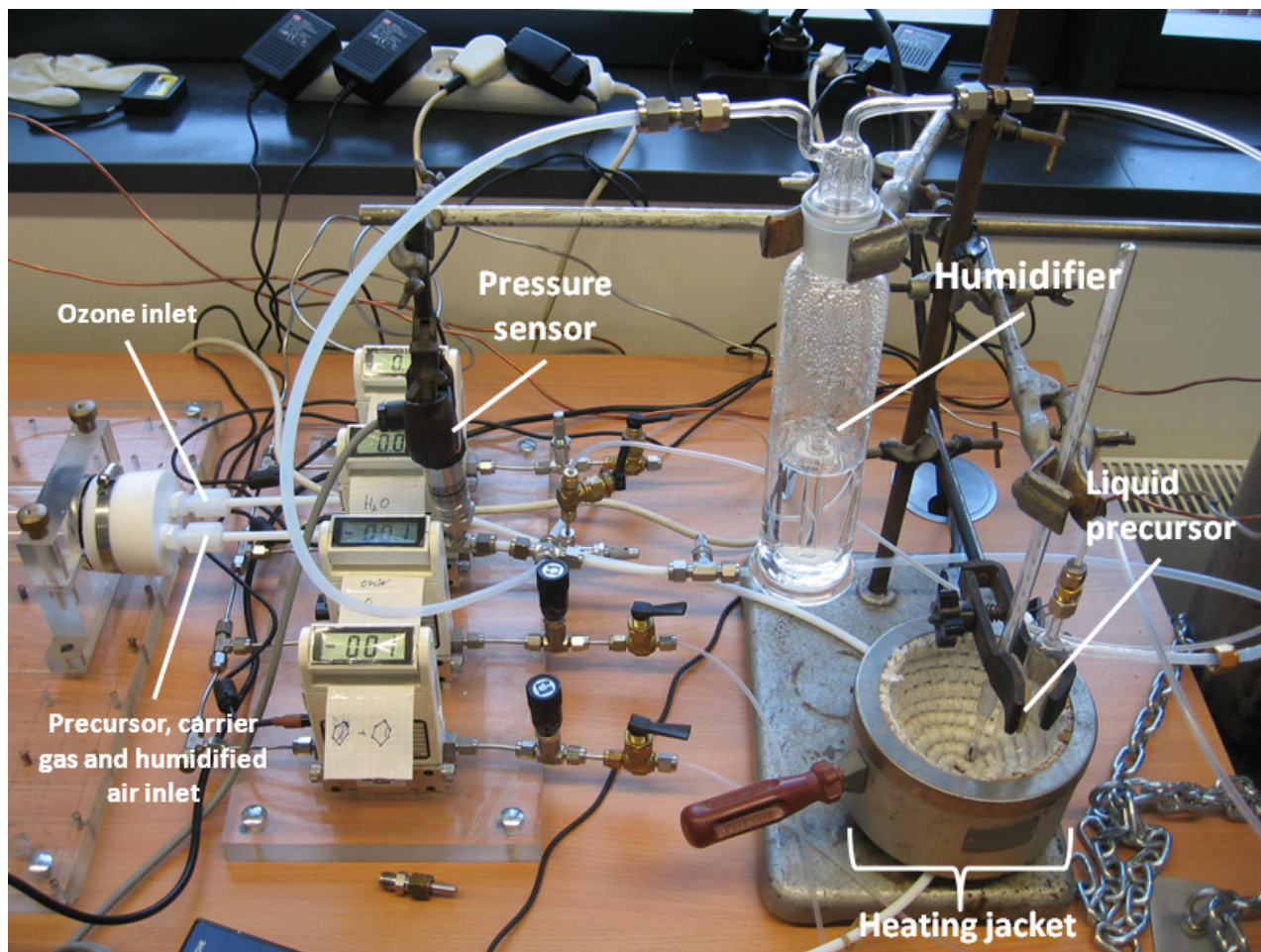


Figure 3.2 The inlet side of the flow reactor

For the experiments under both dry and humid conditions, RH was adjusted by bubbling air through a 500 ml bubbler filled with approx. 200 ml of distilled water. Relative humidity, and temperature were monitored with thermo hygrometer (model 701, LAB-EL), connected to the outlet of the reactor. Pressure was monitored with capacitance manometer (model MP 221, Elvac) and adjusted to exactly 1 atm. using a rotary vacuum pump (model BL15P; Unitra) connected to the exit of the reactor, as shown in Fig. 3.1. Pressure adjustment using vacuum pump was necessary in order to avoid pressure rise inside the reactor due to the restriction of flowing air through the filter sampling assembly.

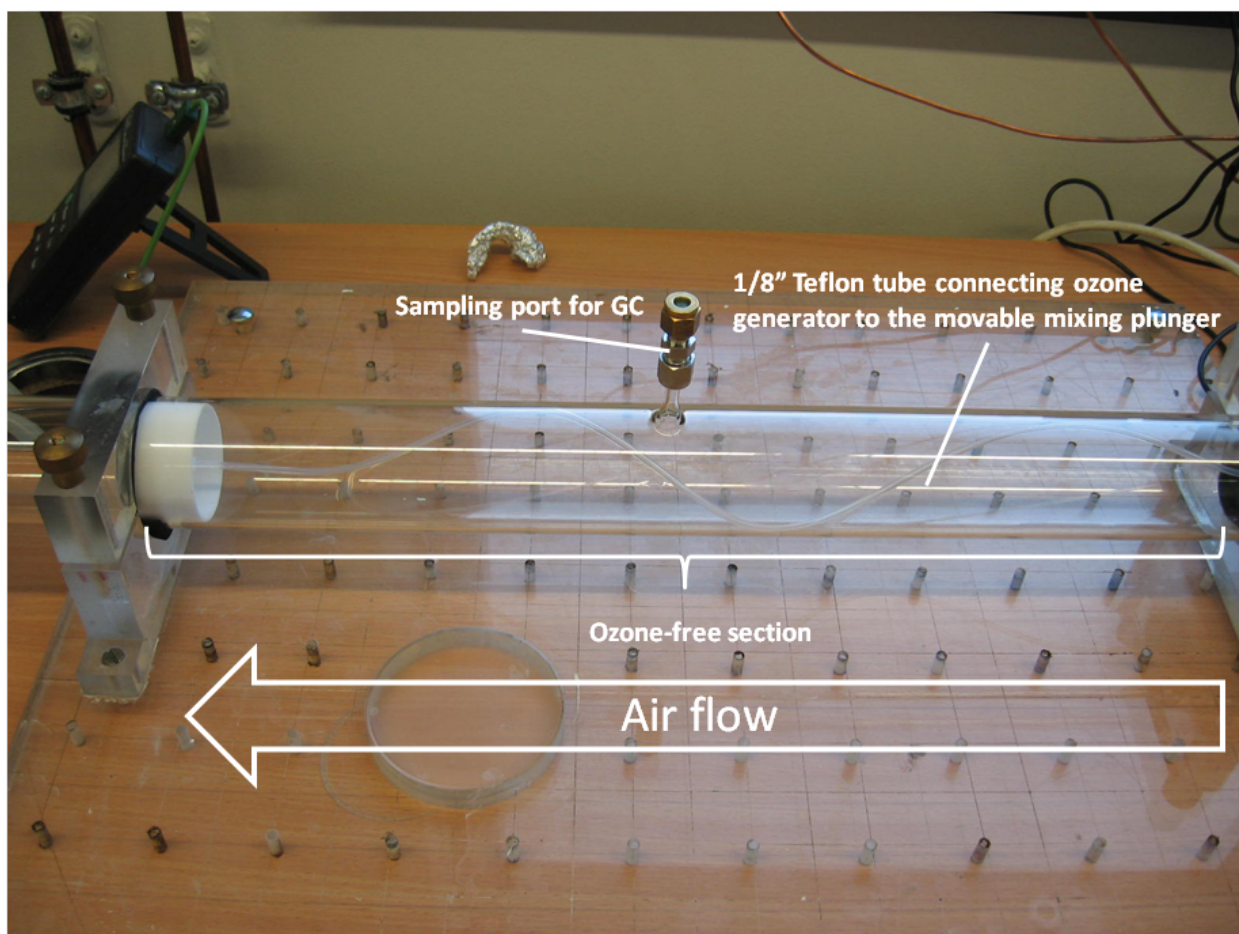


Figure 3.3 The middle section of the reactor

As shown in Fig. 3.1 and Fig. 3.2, ozone was introduced separately via the second inlet port. 1/8" Teflon tube, shown in Fig. 3.3, was used to connect ozone generator with the movable Teflon mixing plunger, thus avoiding ozone contact with the precursor before reaching the mixer and initiating the ozonolysis reaction. Movable mixing plunger design schematic and photograph are shown in Fig. 3.4A and Fig. 3.4B, respectively.

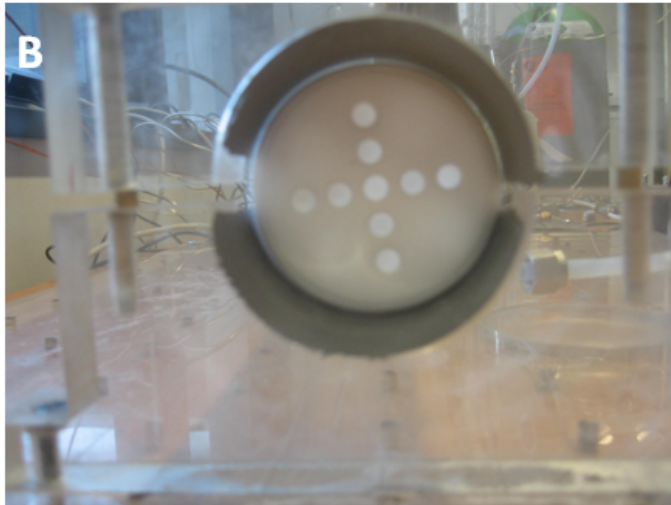
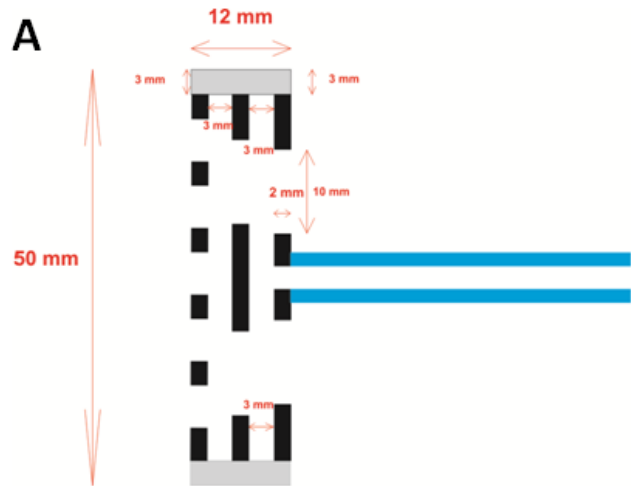


Figure 3.4 Detailed design schematic of the movable mixing plunger (A) and the photograph of the plunger front side, installed inside the flow tube (B)

Mixing plunger consisted of three, 2 mm thick Teflon discs, mounted inside the 50 mm O.D. Teflon housing, as shown in Fig. 3.5.

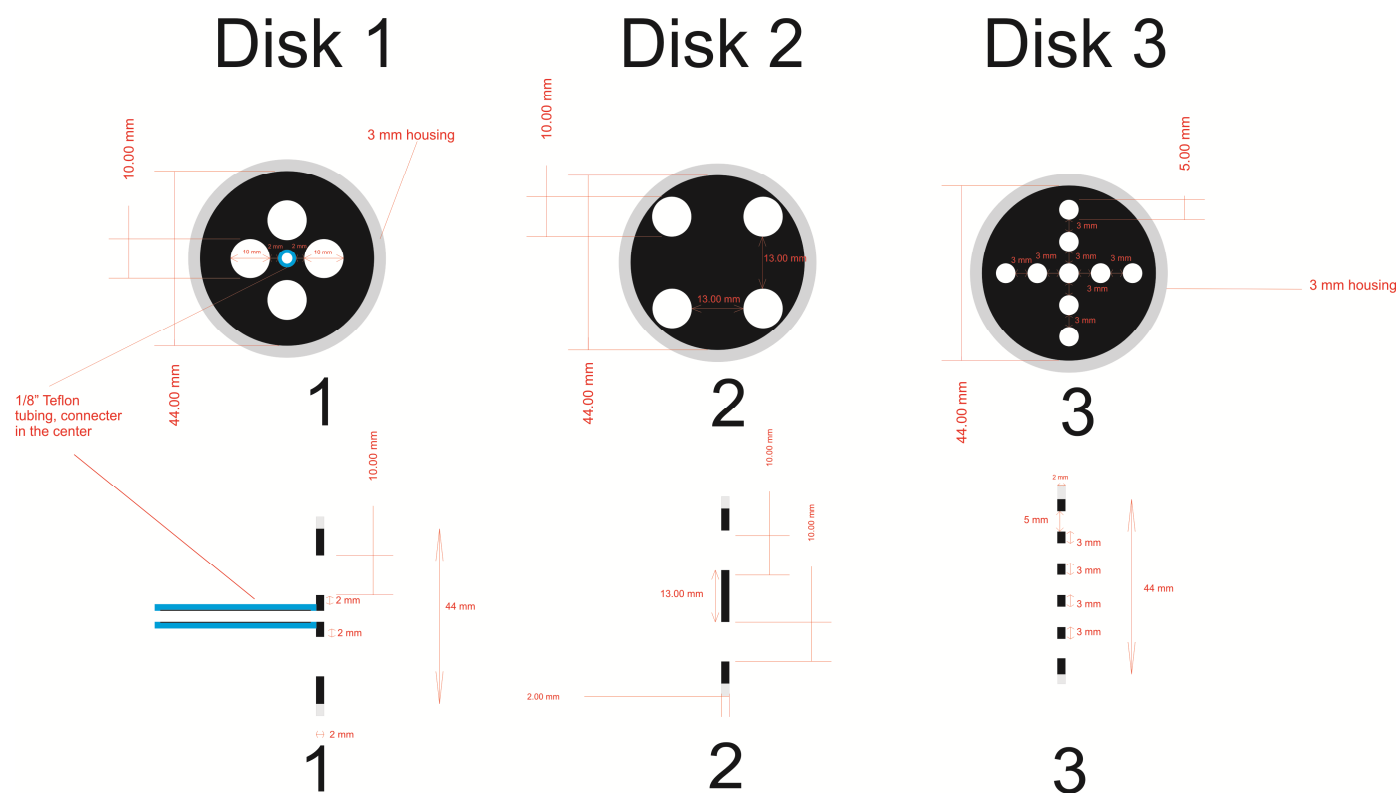


Figure 3.5 Detailed design schematic of the three disks, mounted inside the housing of the movable mixing plunger

The plunger was designed to mix the precursor with ozone and generate uniform stream of gas on the outlet side of the mixer. Ozone entered the mixing plunger via 1/8" Teflon tubing. Precursor entered the plunger via the four 10 mm holes, together with the carrier gas. The holes in the second disk, forced the gas flow to circulate inside the plunger and thus mixing of the ozone with the precursor. Mixed gases, exited the mixing plunger via the holes in the third disk as a uniform stream, as shown in Fig. 3.4 and Fig. 3.5.

As illustrated in Fig. 3.3, the initial part of the reactor was ozone-free section, and contained only precursor mixed with humidified air. Ozone concentration was monitored with ozone sensor (A-212X, Eco Sensors), connected to the exit of the reactor. Ozone was generated using Ozone 25 generator (Aqua Medic), (see Fig. 3.1 and Fig. 3.6).

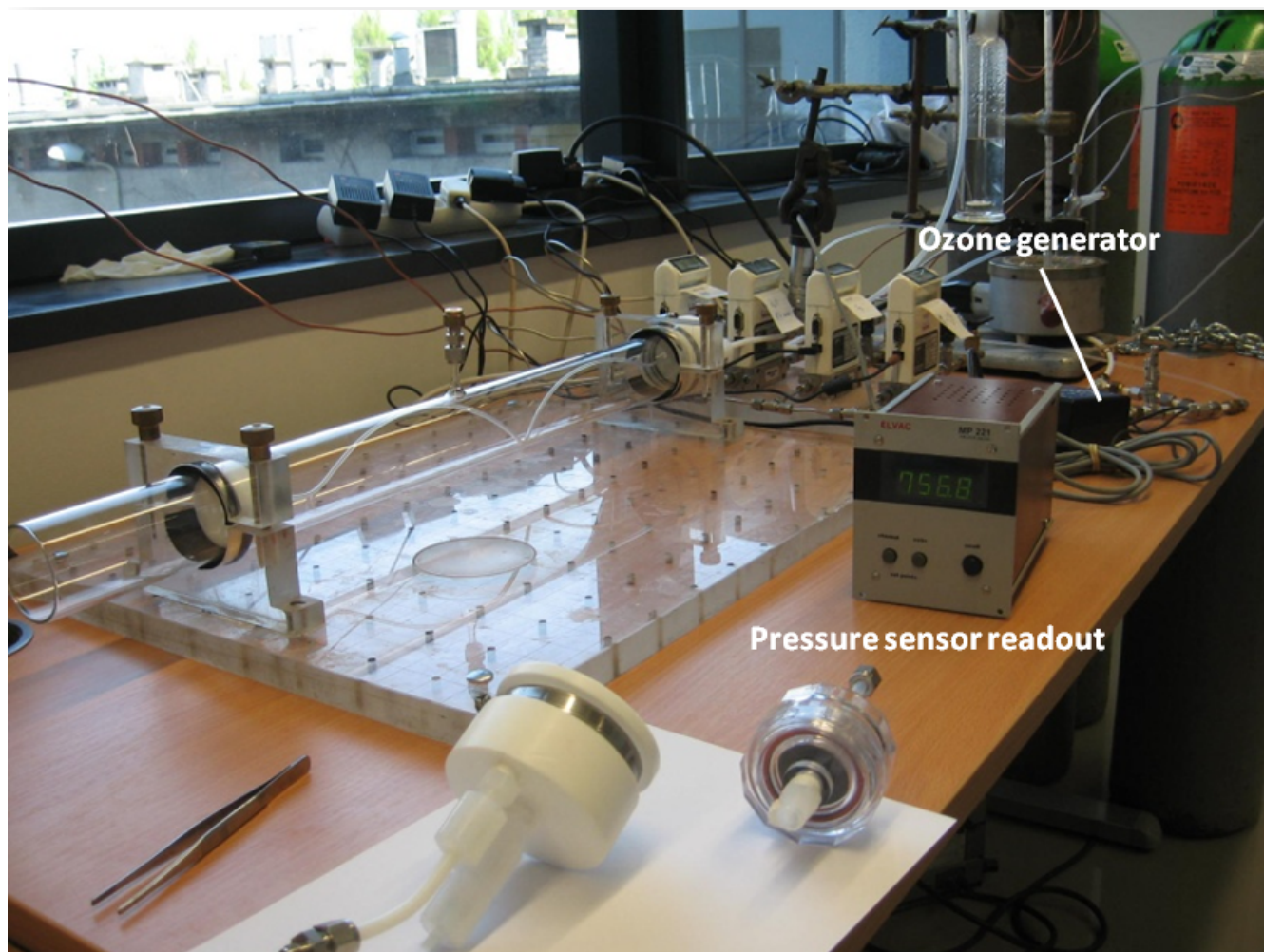


Figure 3.6 Photograph of the flow – tube reactor

Both cyclohexene and α -pinene were added to the reactor by passing a stream of air over the pure liquid surface (Fig. 3.2), with, of course, the only one precursor present at a given experiment. α -Pinene was gently heated to about 45°C to achieve high enough concentration, since the amount of this compound, introduced into the reactor at room temperature was insufficient. Cyclohexene was kept at room temperature, due to much higher vapor pressure of this compound, heating was not necessary. Precursors concentrations were monitored using a gas chromatograph, as described in Section 3.2.4. Samples were drawn from the reactor via the sampling port positioned in the middle as shown in Fig. 3.1, Fig. 3.3 and Fig. 3.6.

3.4.2. Conditions for the SOA generation

Experimental conditions for SOA generation are reported in Table 3.1; all experiments were performed at room temperature and under dark conditions, i.e. after shielding the reactor from the outside irradiation by black cloth. As listed in Table 3.1, precursor and ozone concentrations varied slightly between experiments. Uncertainties, listed in Table 3.1, are standard deviations calculated from the experiments under given conditions. Ozone and precursor concentrations were always kept at the levels that ensured almost complete ozone consumption by the excess of alkene before it could reach the filter holder – see section 4.2.2.

Table 3.1 Experimental conditions for SOA generation

Precursor	Precursor concentration (ppm)	Ozone concentration (ppm)	Temperature	Relative humidity (%)	Extraction solvent
Cyclohexene	278 ± 36	3.6 ± 0.4	Room temperature, approx. 20°C	40.8 ± 0.5	ACN/H ₂ O (1:4, v/v)
				3.3 ± 0.2	
α-pinene	434 ± 46	3.4 ± 0.3		3.5 ± 0.2	ACN/H ₂ O (1:1, v/v)
				40.9 ± 0.6	

The procedure of SOA generation was as follows:

- Reactor was assembled after cleaning (see section 3.4.4) and the whole system was leak tested.
- After approx. 30 min flushing with clean air, the air composition inside the reactor was monitored with GC/FID; the traces of the precursor left from the previous experiments would interfere with the ozone concentration measurement.
- Filter was placed inside the filter holder, and the bypass line was opened for RH adjustment.

- After adjusting the RH, ozone was introduced into the reactor and its concentration was set to about 3.5 ppm - see Table 3.1.
- Both needle valves on the precursor supply line were opened (see Fig. 3.1) and precursor was added into the reactor. Filter line remained closed until the precursor reached sufficient concentration; the airflow was forced through the bypass line.
- After the alkene concentration was sufficiently high to consume all of the ozone (see section 4.2.2), the bypass line was closed and air was pumped through the filter; pressure was adjusted to exactly 1 atm.
- Aerosol was collected for 2 h.
- Precursor concentration was monitored for the entire time of aerosol collection using GC/FID in 5 min intervals.
- After 2 h, ozone generator was shut down, and precursor was allowed to consume all of the leftover ozone.
- Afterwards, filter line was closed and the bypass line was opened.
- Before removing the filter holder, precursor and humidifier lines were closed and reactor was flushed with clean air for 10 min.
- Filter was removed and extracted with the solvent – see Table 3.1.
- Reactor was cleaned after each experiment, including blank experiments (section 3.4.5.)

3.4.3. SOA sampling

Aerosol was collected with in-line polycarbonate filter holder. Photograph of the filter holder is shown in Fig. 3.7A and Fig. 3.7C. Interior side of the Teflon front cover, with two Viton o-rings is shown in Fig. 3.7B. As shown in Fig. 3.7C, filter holder consisted of the polycarbonate body, support screen and silicone o-ring, making the filter capsule gas-tight up to 3.35 atm.¹⁸⁴

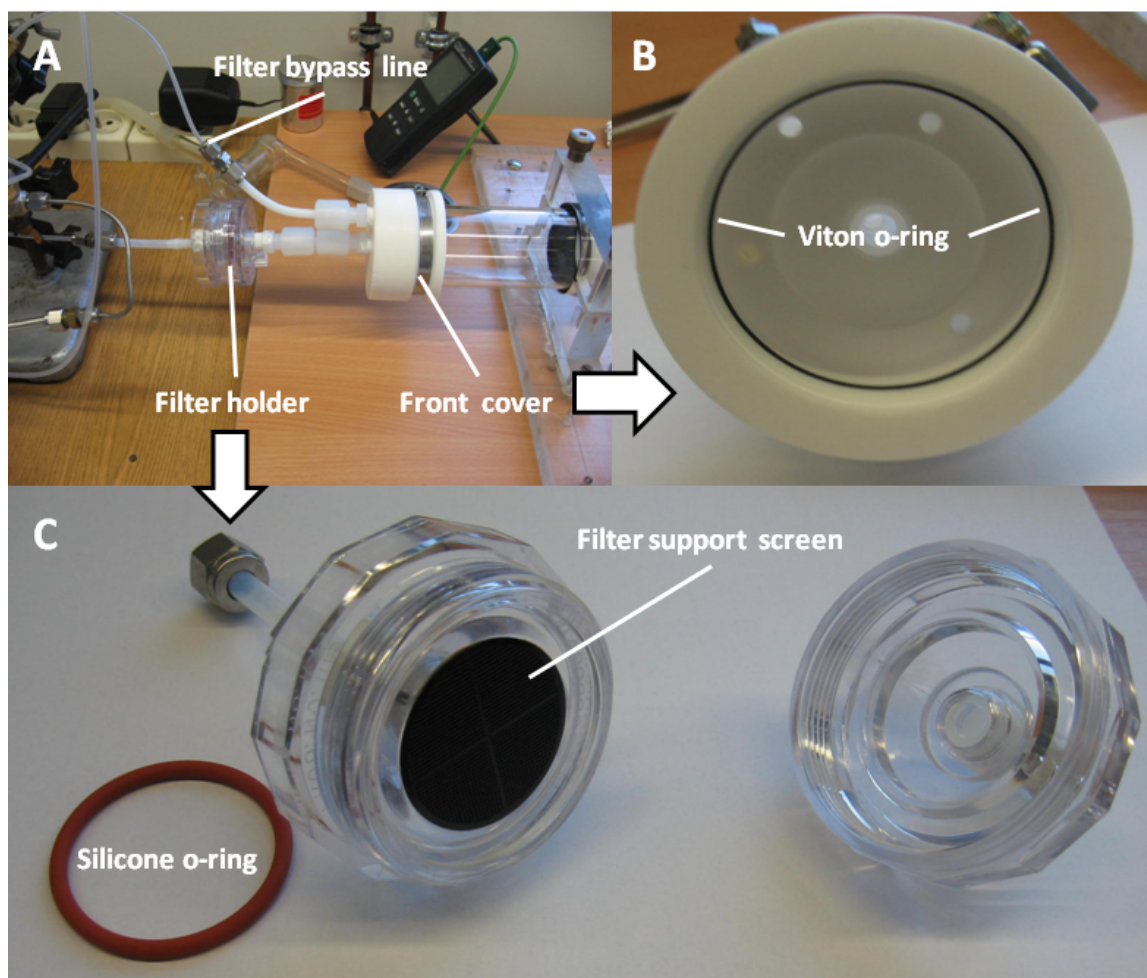


Figure 3.7 The exit side of the flow-tube reactor (A); reactor front cover (B) and filter holder (C)

Filter holder was connected to the exit of the reactor with $\frac{1}{4}$ " PTFE tube and positioned immediately after the Teflon cover, as shown in Fig. 3.1 and Fig. 3.7A. Particles were collected by the 47 mm borosilicate glass fiber filter coated with fluorocarbon (T60A20), Pall Corporation. After particle collection, each filter was extracted with 1.5 ml of the solvent for 15 min in the ultrasonic bath. Extraction solvents, used in experiments with both precursors are listed in Table 3.4. After extraction, samples were filtered with 0.2 μm pore size, nylon syringe filter and subjected to the LC/MS analysis, as described in section 3.2. Please note that filter extracts were not evaporated to dryness and redissolved, to minimize analyte losses and possible secondary reactions.

3.4.4. Reactor cleaning

After each experiment (including blank experiments), the front cover of the reactor was removed, and the glass tube was cleaned with acetone and methanol. Movable mixing plunger was also thoroughly cleaned with both solvents. Front reactor cover and filter holder were cleaned with detergent, thoroughly rinsed with distilled water and dried overnight at 50°C. After cleaning, the reactor was assembled and leak tested. Before each experiment, flow-tube was flushed with air until FID signals for the solvents (acetone and methanol) and traces of precursor were indistinguishable from the background noise.

4. Results and discussion

In this section, the results from the performed experiments are reported and discussed. Initially, the development of the LC/MS analysis methods for carboxylic acids analysis (Section 4.1.1) and the α -acyloxyhydroperoxy aldehydes analysis (section 4.1.2) is described. Afterwards, the SOA formation in the flow-tube reactor is described (section 4.2). In Section 4.3 results of the SOA samples analysis are reported and discussed.

4.1. Development of the SOA composition analysis method using liquid chromatography coupled to electrospray ionization tandem mass spectrometry (LC-ESI/MSⁿ)

In this section, optimization of the LC/MS analysis conditions for the SOA samples analysis is described. Carboxylic acid LC/MS analysis method is described in Section 4.1.1. That method was used for the analysis of carboxylic acids produced during gas-phase ozone initiated oxidation of a model compound - cyclohexene (Section 4.1.1.1) and α -pinene (Section 4.1.1.2). Calibration curves were optimized for both deprotonated pseudo-molecular ions as well as selected fragment ions.

Development of the α -acyloxyhydroperoxy aldehydes analysis method is described in Section 4.1.2. Development of the analysis method included evaluation of the ionization conditions (Section 4.1.2.3) followed by confirmation of the synthesized compounds elemental formulas (Section 4.1.2.4). Afterwards, the detailed investigation of the fragmentation mechanism (Section 4.1.2.5), including analysis of the isotopically labeled analogs (Section 4.1.2.6) was performed. α -Acyloxyhydroperoxy aldehydes prepared using cyclohexene as well as α -pinene shared the common fragmentation mechanism, as described in Section 4.1.2.5 and section 4.1.2.7. General mechanism allowed predicting the mass spectrum of different α -acyloxyhydroperoxy aldehydes that could not be synthesized due to the lack of appropriate substrates, is described in Section 4.1.2.8.

4.1.1. Carboxylic acids analysis method

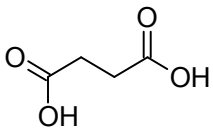
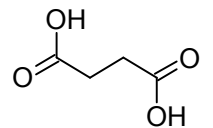
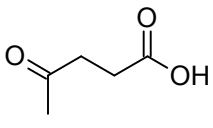
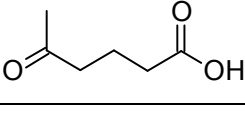
Carboxylic acids are known particle-phase components for aerosol (SOA) generated from both precursors under study; cyclohexene as well as α -pinene. As opposed to the α -

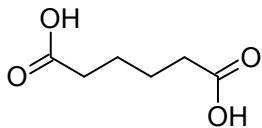
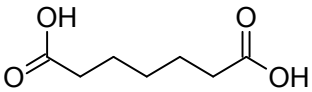
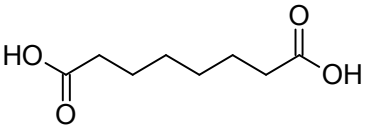
acyloxyhydroperoxy aldehydes, standards for a number of carboxylic acids were commercially available, and thus synthesis was not necessary. LC/MS analysis conditions for each set of carboxylic acids are described in Section 3.2.2. In the following sections, carboxylic acids analysis method optimization is discussed separately for the model precursor - cyclohexene (section 4.1.1.1) and α -pinene (section 4.1.1.2).

4.1.1.1. Carboxylic acids obtained by cyclohexene ozonolysis

LC/MS analysis conditions for the carboxylic acids obtained by cyclohexene ozonolysis are listed in section 3.2.2.1. List of carboxylic acids selected for the LC/MS analysis method of cyclohexene SOA is provided in Table 4.1; structures and molecular masses of the standards were also included.

Table 4.1 Carboxylic acids selected as standards for the analysis of SOA samples, generated by cyclohexene ozonolysis

Name	Structure	Molecular weight (Da)
Succinic acid		118
Glutaric acid		132
Levulinic acid		116
5-oxohexanoic acid		130

Adipic acid		146
Pimelic acid		160
Suberic acid		174

As listed in Table 4.1, seven commercially available carboxylic acids were selected as standards or surrogate standards for the known ozonolysis products of cyclohexene.^{136,170,185} The selected carboxylic acids were two carboxylic acids containing carbonyl group and five dicarboxylic acids. This set of carboxylic acids was selected to react with SCI, formed by ozone reaction with cyclohexene in the liquid phase, to synthesize compounds VII – XIII (see Table 4.7 and Fig. 4.8). Synthesis of the α -acyloxyhydroperoxy aldehydes standards is described in Section 3.3.

It was also possible to detect the deprotonated pseudo-molecular ions for the compounds of interest, in addition to the selected Q1/Q3 transitions, monitored in the MRM mode, as described below. MS conditions were optimized, so the $M-H^-$ ions for the carboxylic acids listed in Table 4.1 had the highest sensitivity. Extracted ion current (EIC) chromatograms for all carboxylic acids listed in Table 4.1 are shown in Fig. 4.1.

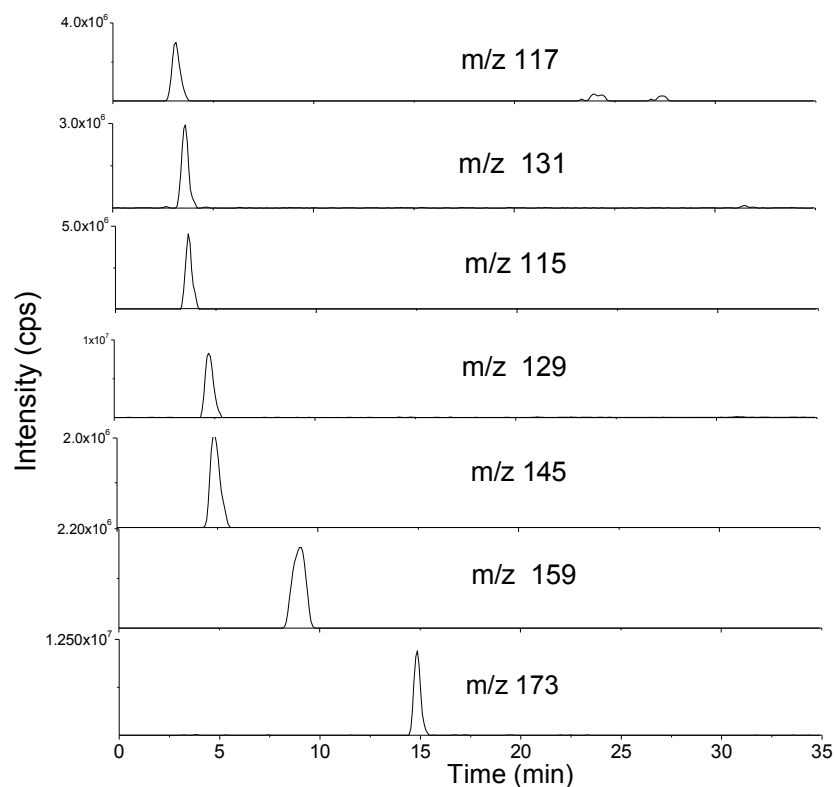


Figure 4.1 EIC's for the carboxylic acids standards listed in Table 4.1.

As shown in Fig. 4.1, $M-H^-$ ions were detected for all compounds of interest. Acidic eluent was used in order to enhance the retention of the carboxylic acids on the used C8 RP stationary phase (see section 3.2.2). Even though the carboxylic acids were retained sufficiently to be eluted after the void peak, the majority of peaks shown in Fig. 4.1 are not separated to the baseline. This can be attributed to the weak retention of the LMW compounds with the carboxylic functional groups, such as the acids listed in Table 4.1. However, since the MS was used as the detector, full chromatographic separation was not necessary. As shown in Fig. 4.1 the compounds under study can be quantified separately due to the different molecular masses. The use of the MRM mode further enhanced selectivity of the developed method.

Analysis conditions for the MRM mode were optimized by directly introducing standard solutions for each carboxylic acid into the MS ion source and swapping the values of the individual ion lenses voltages for the highest sensitivity. MS conditions for the direct-infusion experiments are reported in Section 3.2.1. Afterwards, CE was optimized for the fragment ions, and one or two

most efficient Q1/Q3 transitions were selected for the final method. Examples of the CE optimization for the adipic acid and 5-oxohexanoic acid are shown in Fig. 4.2A and Fig. 4.2B, respectively.

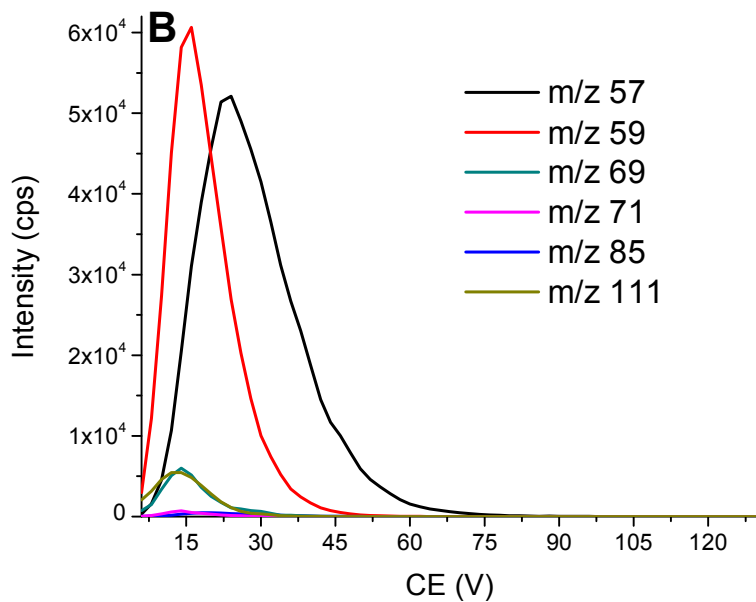
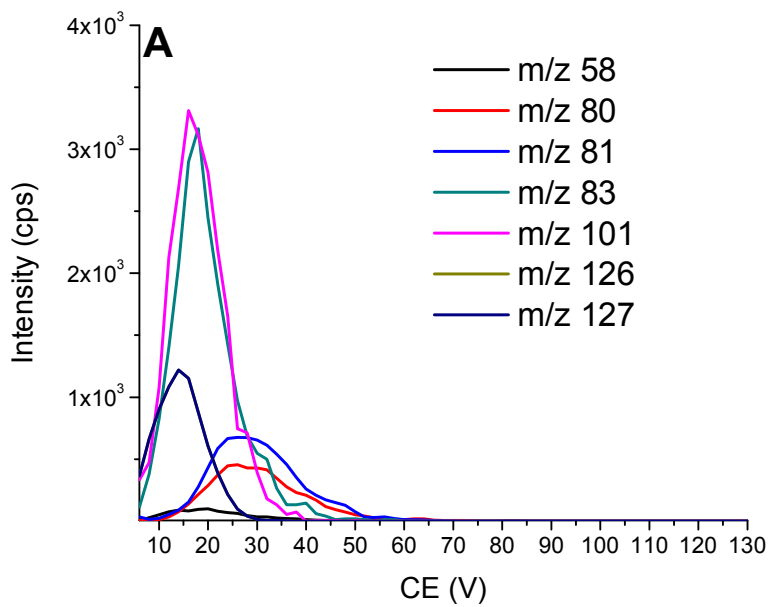


Figure 4.2 Optimization of the CE for the adipic acid, m/z 145 Da (A) and 5-oxohexanoic acid m/z 129 Da (B)

As shown in Fig. 4.2, the two carboxylic acids produced different sets of fragment ions. For the adipic acid (Fig. 4.2A), the most intense Q1/Q3 transitions were 145/101 and 145/83, as listed in Table 4.2. For the 5-oxohexanoic acid (Fig. 4.2B) the two Q1/Q3 transitions selected for the final method were 129/57 and 129/59 also listed in Table 4.2. Results of the MRM conditions optimization for each carboxylic acid from Table 4.1 are listed in Table 4.2; it includes optimal values of DP, EP and CE.

Table 4.2 Optimal MRM parameters for the analyzed carboxylic acids

Name	MRM (s)	Retention time (min)	DP (V)	EP (V)	CE (V)
Succinic acid	117/73	3.08	25	4.5	16
Glutaric acid	131/87	3.54	25	5.5	16
Levulinic acid	115/97	3.62	25	6.5	14
5-oxohexanoic acid	129/57	4.68	25	9.5	16
	129/59		25	9.5	24
Adipic acid	145/101	4.88	25	4.5	16
	145/83		25	4.5	18
Pimelic acid	159/97	8.80	25	8.5	18
Suberic acid	173/111	14.76	30	6.5	20

As listed in Table 4.2, one or two Q1/Q3 transitions (MRMs) were selected for each carboxylic acid. Mass spectrometer operating in the MRM mode is much more sensitive than in the TIC mode due to significantly lower background noise. Also, in addition to the molecular

masses of the compounds of interests, monitoring specific fragment ions is possible, which further enhances the selectivity of the MS detection. MRM chromatograms for the selected Q1/Q3 transitions (Table 4.2) are shown in Fig. 4.3.

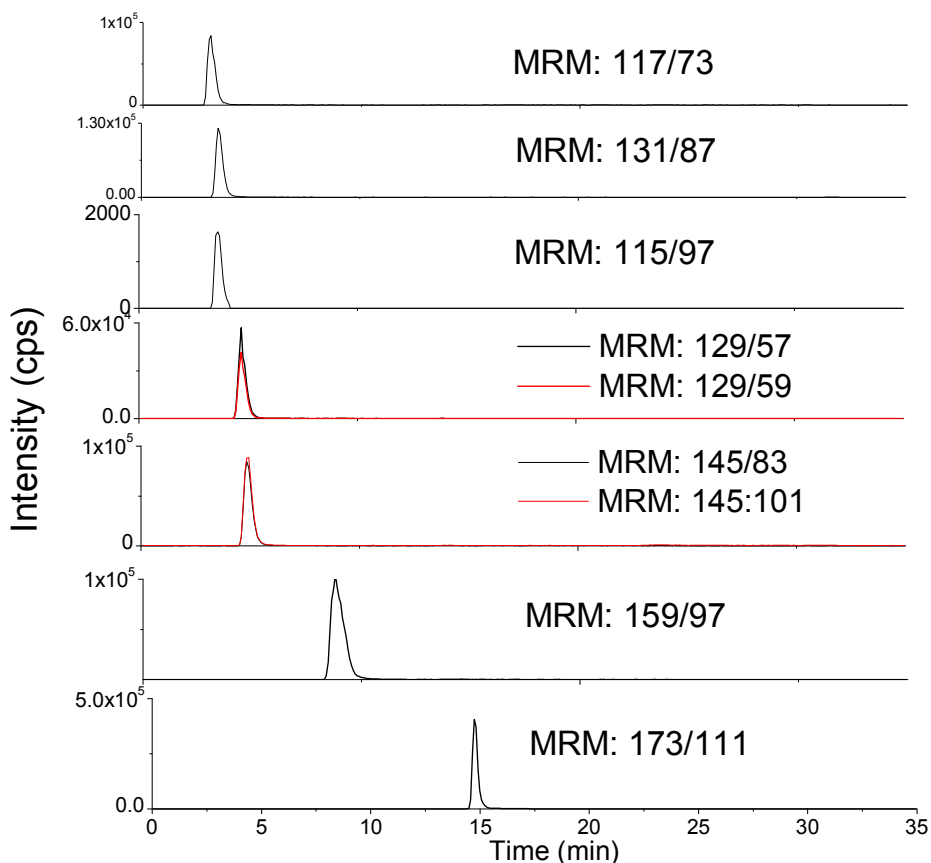


Figure 4.3 MRM's for the carboxylic acids listed in Table 4.2.

As shown in Fig. 4.3, retention times of the monitored Q1/Q3 transitions (MRMs) are in excellent agreement with the retention times of the peaks detected for the $M-H^-$ ions. However, this mode of detection is much more selective towards the compounds under study, since only specific Q1/Q3 transitions are monitored. However, as discussed in Section 4.3.1.1, if similar, isobaric carboxylic acid is present in the sample, it may produce different fragment ions than the standard compound.

Therefore, peak areas from both MRMs and deprotonated pseudo-molecular ions were used as dependent variable for the linear regression analysis. Standard solution of the carboxylic

acids was prepared over the concentration range: 0.001 – 0.03 mg/ml, and each sample was analyzed three times. Plot of the analyte peak area versus concentrations of the standard solutions is shown in Fig. 4.4A (for the MRM pairs listed in Table 4.2) and Fig. 4.4B, (deprotonated pseudo-molecular ions).

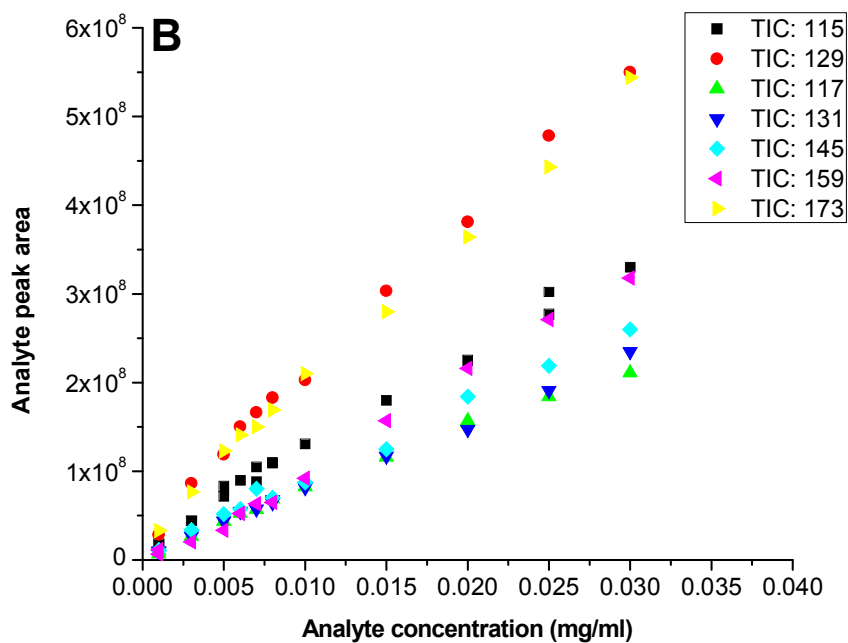
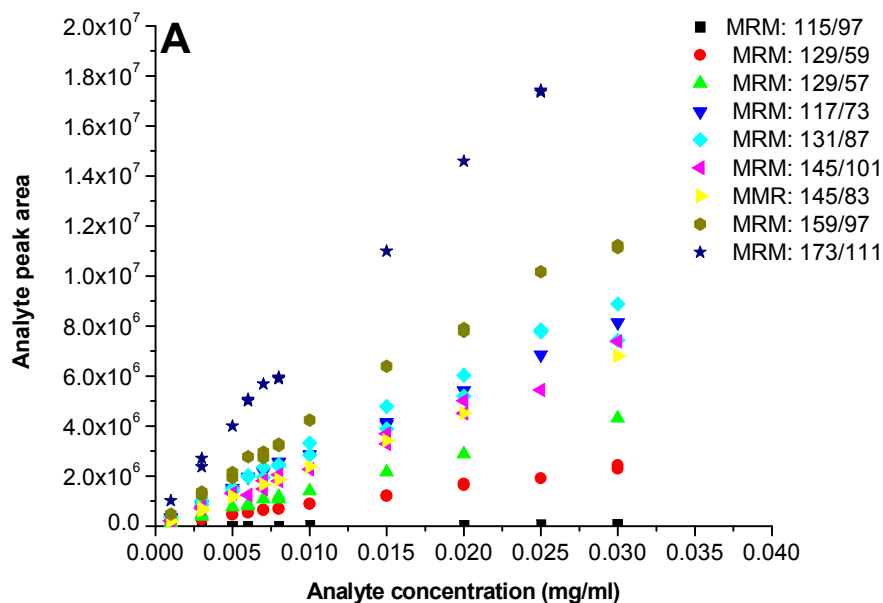


Figure 4.4 Plot of the analyte peak area versus concentrations for the selected MRM pairs (A) and deprotonated pseudo-molecular ions (B)

As shown in Fig. 4.4 in both quantification modes, sensitivity increases with the increasing MW of the analyte. Using the data shown in Fig. 4.4A and Fig. 4.4B, linear regression analysis was performed. The results of the linear regression analysis are summarized in Table 4.3. Two squared linear regression coefficients and two equations are listed when additional MRM was selected.

Table 4.3 The results of linear regression analysis

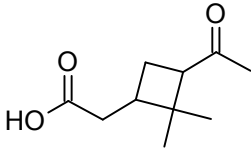
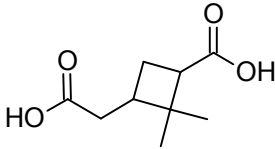
Name	R ² (MRM)	Regression equation (MRM)	R ² (M-H)	Regression equation (M-H)
Succinic acid	0.9983	(MRM) $2.67 \times 10^8 + 1.72 \times 10^5$	0.9971	$7.12 \times 10^9 + 7.46 \times 10^6$
Glutaric acid	0.9984	(MRM) $3.04 \times 10^8 + 6.16 \times 10^4$	0.9987	$7.51 \times 10^9 + 5.01 \times 10^6$
Levulinic acid	0.9992	(MRM) $2.8 \times 10^6 + 2.2 \times 10^3$	0.9973	$1.06 \times 10^{10} + 1.6 \times 10^7$
5-oxohexanoic acid	0.9975	(MRM) $7.71 \times 10^7 + 6.87 \times 10^4$	0.9981	$1.76 \times 10 + 3.32 \times 10^7$
	0.9993	(MRM1) $1.44 \times 10^8 - 1.71 \times 10^3$		
Adipic acid	0.9949	(MRM) $2.35 \times 10^8 + 5.45 \times 10^3$	0.9971	$8.51 \times 10^9 + 6.27 \times 10^6$
	0.9949	(MRM1) $2.27 \times 10^8 - 2.56 \times 10^4$		
Pimelic acid	0.9977	(MRM) $3.77 \times 10^8 + 2.615 \times 10^5$	0.9988	$1.13 \times 10^{10} - 1.6 \times 10^7$
Suberic acid	0.9990	(MRM) $6.72 \times 10^8 + 6.67 \times 10^5$	0.9987	$1.69 \times 10^{10} + 3.09 \times 10^7$

As listed in Table 4.3, values of the squared linear regression ≥ 0.99 were obtained, thus proving linear response of the MS detector in the studied concentration range. It is important to underline, that no weighting method was used during the linear regression analysis.

4.1.1.2. Carboxylic acids obtained by α -pinene ozonolysis

LC/MS analysis conditions for the carboxylic acids obtained by α -pinene ozonolysis are listed in Section 3.2.2.3. List of carboxylic acids selected for the LC/MS method analysis of α -pinene SOA is provided in Table 4.4; structures and molecular masses were also included.

Table 4.4 Carboxylic acids selected as standards for the analysis of SOA samples, generated by α -pinene ozonolysis

Name	Structure	Molecular weight (Da)
Cis-pinonic acid		184
Pinic acid		186

Two commercially available carboxylic acids (Table 4.4) were selected as standards or surrogate standards (see section 4.3.2.1) for the known ozonolysis products of α -pinene. For the remainder of carboxylic acids produced by ozone-initiated α -pinene oxidation, standards were not commercially available. The selected carboxylic acids included one carboxylic acid containing a carbonyl group: cis-pinonic acid and one dicarboxylic acid: pinic acid. These two acids were used as the SCI scavengers, for the synthesis of the α -acyloxyhydroperoxy aldehydes as described in Section 3.3: compounds XIV and XV listed in Table 4.7 and shown in Fig. 4.9. Thus, investigating the carboxylic acids production was the initial step of the α -acyloxyhydroperoxy aldehydes formation analysis, since they can subsequently react with SCI to form the potential α -pinene SOA nucleation precursors.

Mass spectra were acquired continuously in the mass range 50 - 500 m/z see section 3.2.2.3. Therefore, it was possible to detect the deprotonated, pseudo-molecular ions for both

carboxylic acids, in addition to the Q1/Q3 transitions, monitored in the MRM mode, as described below. MS conditions were optimized, so the deprotonated pseudo-molecular ions $M-H^-$ for the two carboxylic acids, listed in Table 4.4 had the highest sensitivity. Extracted ion current (EIC) chromatograms for the pinic and cis-pinonic acids are shown in Fig. 4.5A and Fig. 4.5B, respectively.

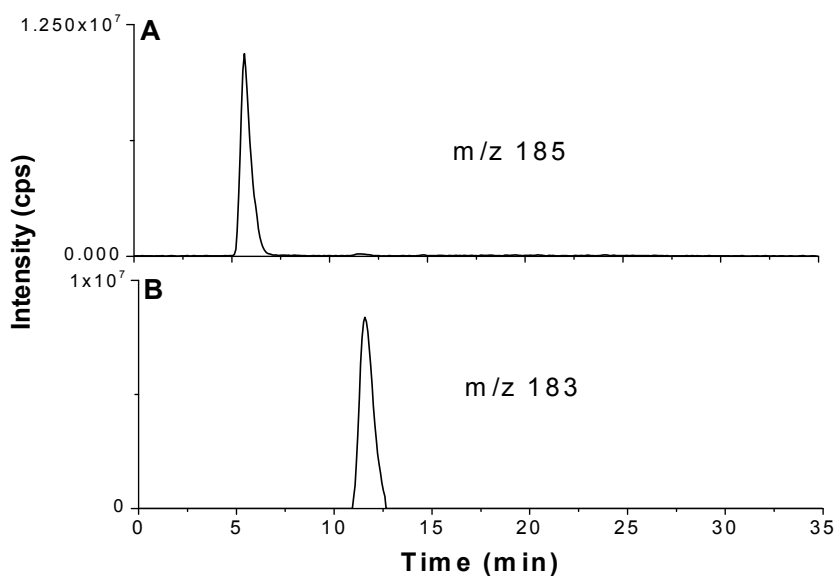


Figure 4.5 EIC's for the α -pinene carboxylic acids standard solution

As shown in Fig. 4.5, $M-H^-$ ions were detected for both pinic and cis-pinonic acid. Acidic eluent was used to enhance the retention of the carboxylic acids on the used RP (C8) stationary phase. However, pH was less acidic, than for the analysis of cyclohexene carboxylic acids (pH=4 as compared to pH=3, see section 3.2.2.1 and section 3.2.2.3). Also, for both carboxylic acids listed in Table 4.4 it was possible to obtain baseline separation. This can be attributed to the better retention of the pinonic acid and cis-pinonic acid as compared to the carboxylic acids produced during gas-phase ozone-initiated oxidation of cyclohexene. Better retention is most probably a result of higher molecular masses and larger number of carbon atoms in the molecule for the pinic acid and cis-pinonic acid, making these two compounds significantly less polar, as compared to the LMW carboxylic acids, listed in Table 4.1. Also, since the MS was used, it is possible to quantify co-eluting carboxylic acids with different MWs as discussed in Section 4.3.2.1.

Analysis conditions for the MRM mode were optimized in the direct infusion mode, as described in Section 3.2.1. Afterwards, CE was optimized for the ion products, and one or two most intense Q1/Q3 transitions were selected for the final method. Example of the CE optimization for the cis-pinonic acid is shown in Fig. 4.6.

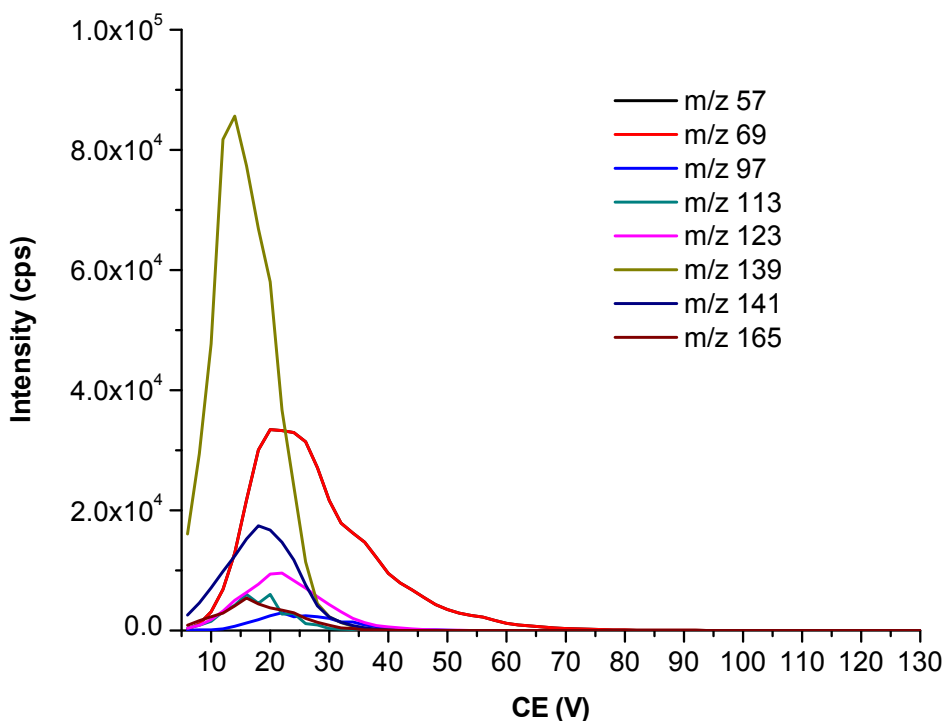


Figure 4.6 CE optimization for the cis-pinonic acid: m/z 183

As shown in Fig. 4.6, CID of cis-pinonic acid produced several CE - dependent fragments. For the cis-pinonic acid as well as for pinic acid, the most intense Q1/Q3 transitions were selected for the final method, as listed in Table 4.5. As reported in Section 3.2.1, for each MRM, individual ion lenses voltages were optimized to achieve highest sensitivity. The results of the MRM conditions optimization for both carboxylic acids are listed in Table 4.5; optimal values of DP, EP and CE are also included.

Table 4.5 The optimal parameters for pinic and cis-pinonic acids MS analysis

Name	MRMs	Retention time (min)	DP (V)	EP (V)	CE (V)
Pinic acid	183/141	6.20	30	9	18
	183/139		30	9	16
	183/57		30	9	20
Cis-pinonic acid	185/167	12.30	35	8.5	18
	185/141		35	8.5	20
	185/123		35	8.5	22

As listed in Table 4.5, three MRMs were selected for each carboxylic acid. Linear regression analysis was performed to calculate MS response for the pinic acid as well as cis-pinonic acid. Both acids were quantified in the α -pinene SOA samples, as described in section 4.3.2.1. Response factors of the MS detector calculated for the deprotonated, pseudo-molecular ions were used for the quantification of the remainder of carboxylic acids formed during α -pinene ozone initiated gas-phase oxidation, for which standards were not available – see section 4.3.2.1. Peak areas from both MRMs and deprotonated pseudo-molecular ions were used as dependent variable for the linear regression analysis. Standard solution for both carboxylic acids was prepared over the concentration range 0.006 – 0.03 mg/ml, and each sample was analyzed three times. MRM chromatograms for the selected Q1/Q3 transitions (Table 4.5) are shown in Fig. 4.7.

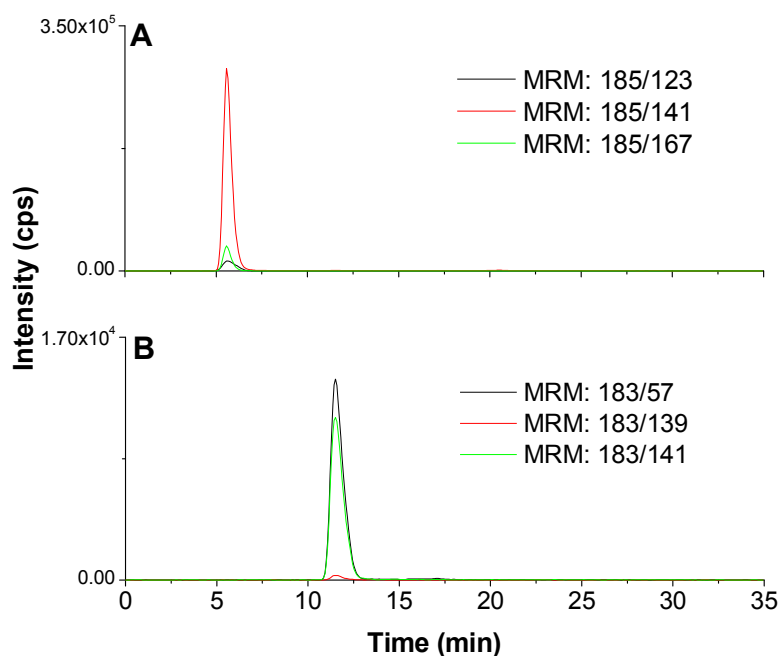


Figure 4.7 MRMs for the cis-pinonic acid (A) and pinic acid (B) in standard solution (0.01mg/ml)

As shown in Fig. 4.7A and Fig. 4.7B, retention times of the monitored MRM pairs match those for the EICs for the M-H⁻ ions shown in Fig. 4.5. Similar to the analysis of cyclohexene, the use of MRM mode significantly enhanced sensitivity and selectivity of the MS detector for the analysis of the cis-pinonic acid as well as the pinic acid.

Plot of the analytes peak areas versus concentrations of the standard solution is shown in Fig. 4.8A and Fig. 4.8B, for the six Q1/Q3 transitions (MRMs) listed in Table 4.5 and deprotonated pseudo-molecular ions, respectively. Linear regression analysis results for both deprotonated pseudo-molecular ions as well as six MRM pairs were used to calculate the cis-pinonic acid and pinic acid concentrations in the SOA samples. Linear regression analysis results obtained for deprotonated pseudo-molecular ions were used to calculate the concentrations for the remainder of carboxylic acids, detected in the SOA samples – see section 4.3.2.1.

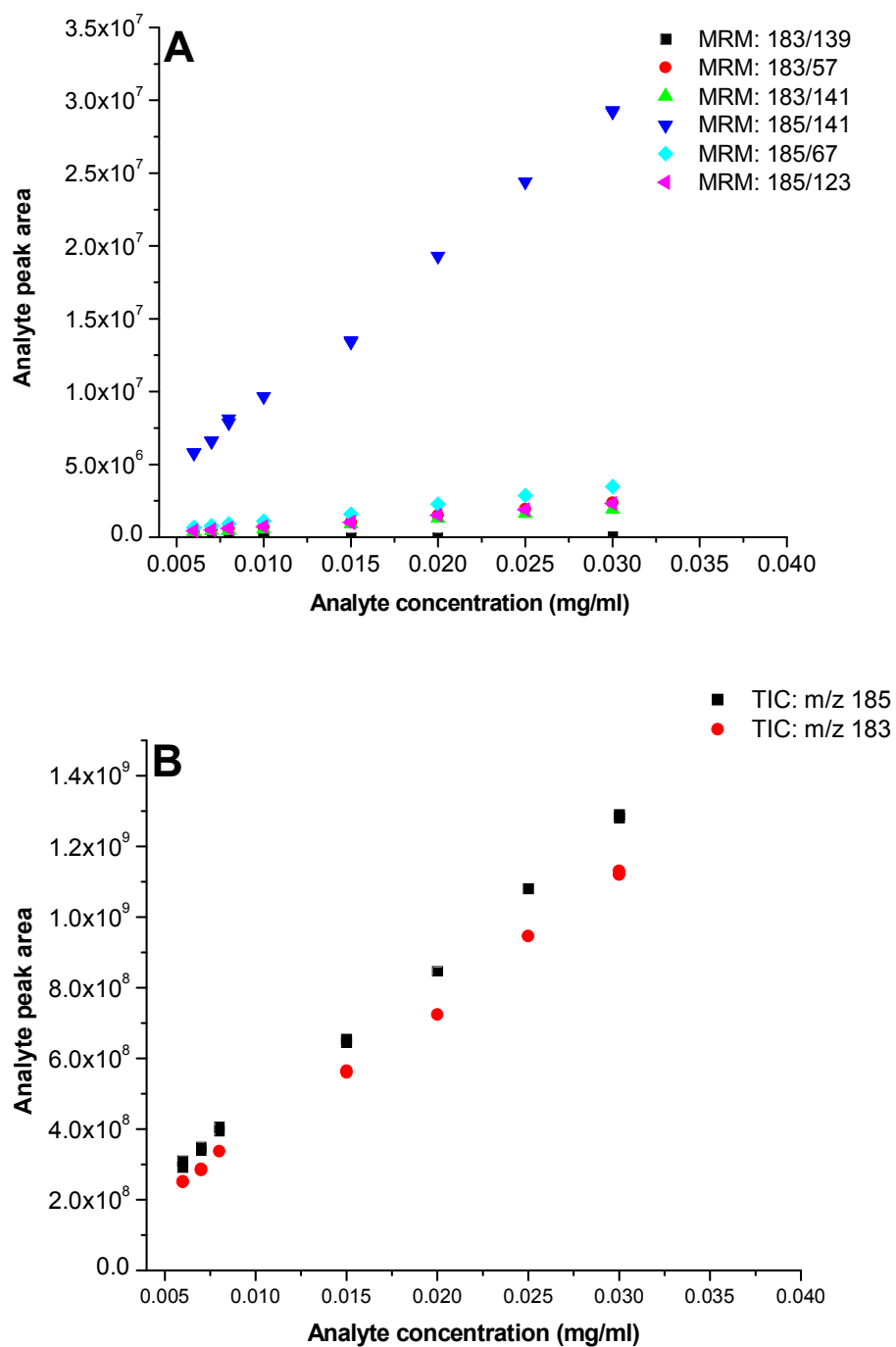


Figure 4.8 Plot of the analyte peak area versus concentrations for the selected MRM pairs (A) and deprotonated pseudo-molecular ions (B)

As shown in Fig. 4.8, MS response for the two carboxylic acids, listed in Table 4.4 was of similar order. For the MRM mode MS response differed more significantly (Fig. 4.8A), the MRM 185/141 being the most sensitive, out of the six Q1/Q3 transitions, listed in Table 4.5.

Using the data shown in Fig. 4.8A and Fig. 4.8B, linear regression analysis was performed. The results of the linear regression analysis are summarized in Table 4.6. Three squared linear regression coefficients and equations are listed for every carboxylic acid, since three MRM pairs were selected, as listed in Table 4.5.

Table 4.6 Linear regression analysis results

Name	R ² (MRM)	Regression equation (MRM)	R ² (M-H)	Regression equation (M-H)
Pinic acid	0.9991	(MRM) $1.37 \times 10^6 - 2.03 \times 10^3$	0.9993	$4.06 \times 10^{10} + 5.86 \times 10^7$
	0.9959	(MRM1) $7.94 \times 10^7 - 7.25 \times 10^4$		
	0.9984	(MRM2) $6.55 \times 10^7 - 3.7 \times 10^4$		
Cis-pinonic acid	0.9987	(MRM) $9.75 \times 10^8 - 2.11 \times 10^5$	0.9992	$3.62 \times 10^{10} + 3.05 \times 10^7$
	0.9995	(MRM1) $1.17 \times 10^8 - 5.79 \times 10^4$		
	0.9988	(MRM2) $7.71 \times 10^7 - 3.26 \times 10^4$		

As listed in Table 4.6, values of the squared linear regression ≥ 0.99 were obtained, thus proving linear response of the MS detector in the studied concentration range. Similar as for the analysis of the carboxylic acids formed during ozone initiated, gas-phase oxidation of cyclohexene, no weighting method was used for linear regression analysis.

4.1.2. α -acyloxyhydroperoxy aldehydes analysis method

In this section, a development of the LC/MSⁿ analysis method of the α -acyloxyhydroperoxy aldehydes is described. Since the standards for these compounds are not commercially available, development of the analysis method was much more complex, as compared to the carboxylic acids. Initially, standards were synthesized, as described in Section 4.1.2.1. Also, appropriate solvent had to be selected as the reaction medium as described in Section 4.1.2.2. Afterwards, ionization conditions were evaluated, as described in Section 4.1.2.3. Elemental formulas of the synthesized standards were confirmed using HR-MS, as described in Section 4.1.2.4. Fragmentation mechanism was thoroughly investigated, as described in Section 4.1.2.5, including analysis of a series of isotopically labeled analogs, described in Section 4.1.2.6. Afterwards, two α -acyloxyhydroperoxy aldehydes synthesized using α -pinene were analyzed – Section 4.1.2.7. It was concluded that the fragmentation spectrum of a more complex α -acyloxyhydroperoxy aldehydes can be predicted, based on the analysis of simpler analogues, as described in Section 4.1.2.8.

4.1.2.1. Synthesis of the α -acyloxyhydroperoxy aldehydes standards

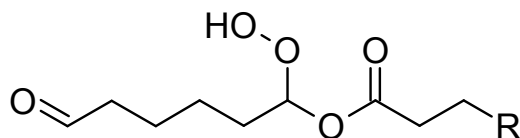
α -acyloxyhydroperoxy aldehydes were synthesized as described in section 3.3. Structures of the synthesized compounds are shown in Fig 4.9; molecular masses and elemental compositions of the synthesized α -acyloxyhydroperoxy aldehydes together with the names and molecular masses of carboxylic acids used as the SCI scavengers are listed in Table 4.7.

Table 4.7 Synthesized α -acyloxyhydroperoxy aldehydes standards

Compound number	Molecular weight (Da)	Elemental composition	Name of the SCI scavenger	Molecular weight of the SCI scavenger (Da)
I	232	C ₁₁ H ₂₀ O ₅	Pentanoic acid	102
II	246	C ₁₂ H ₂₂ O ₅	Hexanoic acid	116
III	260	C ₁₃ H ₂₄ O ₅	Heptanoic acid	130
IV	274	C ₁₄ H ₂₆ O ₅	Octanoic acid	144
V	288	C ₁₅ H ₂₈ O ₅	Nonanoic acid	158
VI	302	C ₁₆ H ₃₀ O ₅	Decanoic acid	172
VII	246	C ₁₁ H ₁₈ O ₆	4-Oxopentanoic acid	116

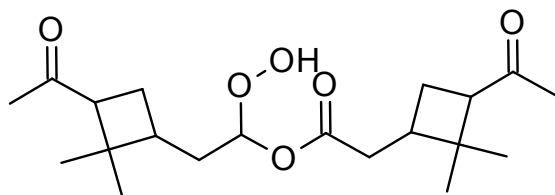
VIII	260	C ₁₂ H ₂₀ O ₆	5-Oxohexanoic acid	130
IX	248	C ₁₀ H ₁₆ O ₇	Succinic acid	118
X	262	C ₁₁ H ₁₈ O ₇	Glutaric acid	132
XI	276	C ₁₂ H ₂₀ O ₇	Adipic acid	146
XII	290	C ₁₃ H ₂₂ O ₇	Pimelic acid	160
XIII	304	C ₁₄ H ₂₄ O ₇	Suberic acid	174
XIV	368	C ₂₀ H ₃₂ O ₆	cis-Pinonic acid	184
XV	370	C ₁₉ H ₃₀ O ₇	Pinic acid	186

Linear carboxylic acids were used as SCI scavengers for the synthesis of the compounds I - VI. Compounds VII - XIII were prepared using the carboxylic acids previously identified as components of SOA from the cyclohexene ozonolysis, as already discussed in section 4.1.1.1. The same procedure was used to prepare compounds XIV and XV, with α -pinene as a precursor and *cis*-pinonic and pinic acids as the SCI scavengers. Structures of the studied α -acyloxyhydroperoxy aldehydes are shown in Fig. 4.9.

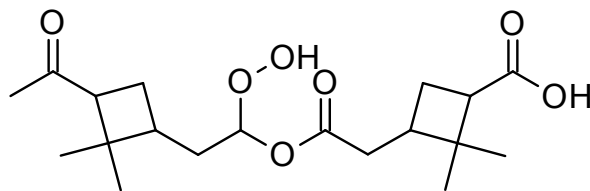


I) R=C₂H₅ II) R=C₃H₇ III) R=C₄H₉ IV) R=C₅H₁₁ V) R=C₆H₁₃ VI) R=C₇H₁₅ VII) R=C(O)CH₃

VIII) R=CH₃(CO)CH₃ IX) R=COOH X) R=CH₃COOH XI) R=C₂H₅COOH XII) R=C₃H₇COOH XIII) R=C₄H₉COOH



XIV



XV

Figure 4.9 Structures of the synthesized α - acyloxyhydroperoxy aldehydes

Liquid phase ozonolysis of the alkenes in the presence of carboxylic acids and alcohols is known as very efficient method for preparation of the α -acyloxy and α -alkoxy hydroperoxides, as described in section 1.4.3.^{89,91,110,112-115,186-189} For the cyclic alkenes, the resulting α -acyloxyhydroperoxy aldehydes contains both hydroperoxy and aldehyde moiety, therefore compounds shown in Fig. 4.9 can potentially form cyclic peroxyhemiacetals. However, as reported by Ziemann,⁸⁹ the cyclization of alkoxy hydroperoxyaldehydes synthesized from a series of cyclic alkenes occurred only in the gas – phase and under the thermal conditions. The reaction of SCI with the carboxylic acids used for the synthesis of compounds I – VI and IX - XIII could only yield one possible product. However, the two carboxylic acids containing carbonyl group used for the synthesis of the compounds VII and VIII can potentially yield two isobaric products: hydroperoxide and the secondary ozonide. Relative rate coefficients for the reactions of formic acid with the C1 and C13 SCIs were reported to be approx. 2.5¹⁰⁴ and 20⁹¹ times faster than for formaldehyde (see section 1.3.3). Those values would correspond to the secondary ozonide product yields of 0.4 and 0.05 comparing to the yields of hydroperoxide products, respectively. Therefore, it is difficult to predict if the secondary ozonides are the significant side - products under the experimental conditions used in this work. However, the results presented in section 4.1.2.5 strongly indicate that the secondary ozonides were not formed in significant quantities. No significant differences between the MS² spectra of the compounds VII and VIII and the rest of α -acyloxyhydroperoxy aldehydes were observed. Those results strongly indicated that secondary ozonides were not significant side – products under the experimental conditions used in this work.

4.1.2.2. Liquid phase ozonolysis solvent

In the previously published studies, both cyclohexane^{91,114} and hexane¹¹⁰ were used as non - participating solvents for the ozonolysis of 1-tetradecene in the presence of carboxylic acids – see section 1.3.4. However, it was concluded that the solubility of carboxylic acids containing carbonyl group and dicarboxylic acids in the most popular, non – participating ozonolysis solvents was insufficient to carry out the synthesis of the compounds VI – XIII. Therefore, ACN was used as the most suitable ozonolysis solvent, since it dissolved the required carboxylic acids in sufficient quantities. Acetonitrile was previously used as the reaction medium for the liquid – phase ozonolysis of verbenone and it can be also considered a non – participating solvent.¹⁰⁸ In order to

confirm that the use of ACN did not affect the products distribution, synthesis of the compounds I - VI was carried out in both ACN and cyclohexane. Analysis of the MS and MS² spectra of the compounds I – VI synthesized in both solvents has confirmed that use of ACN had no impact on the course of reaction. MS² spectra of the compound IV synthesized in cyclohexane and ACN are shown in Fig. 4.10.

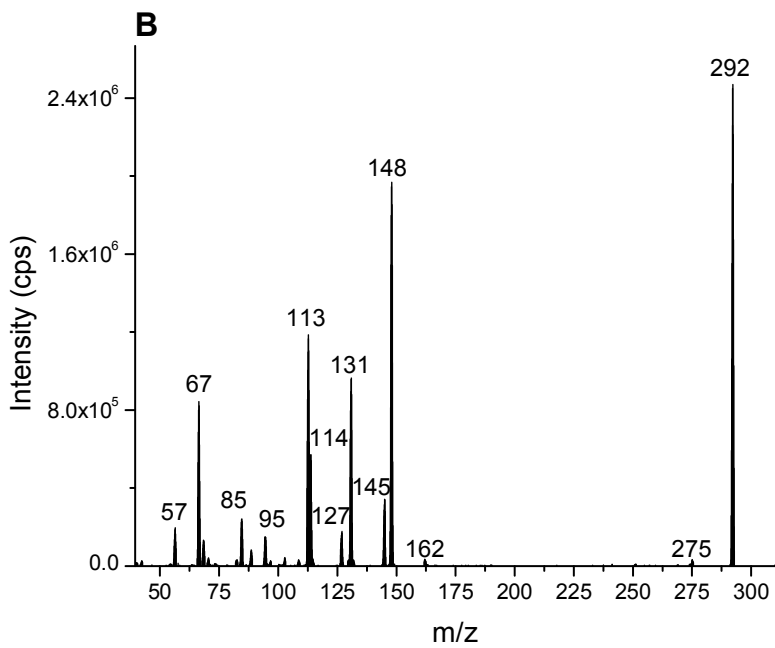
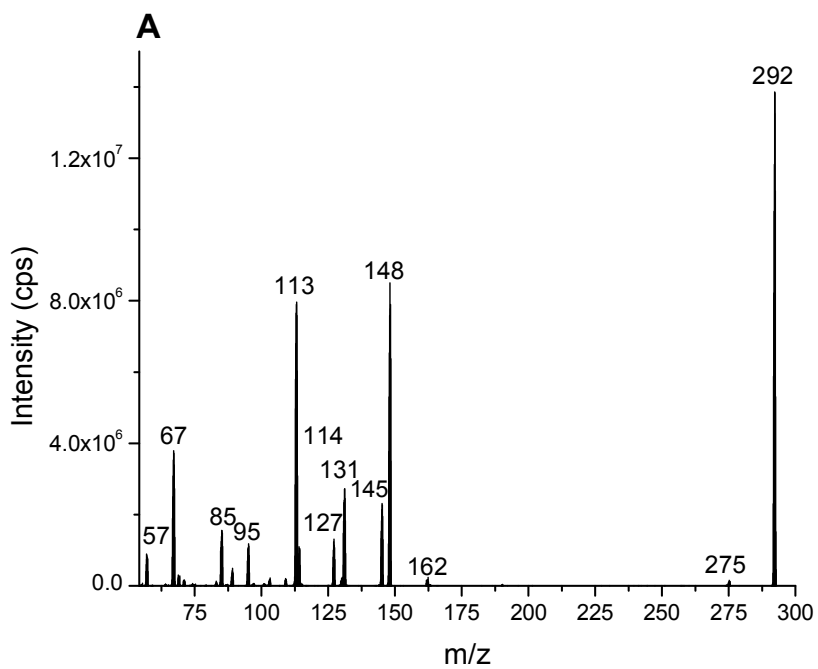


Figure 4.10 MS² spectra of compound IV (identified as M + NH₄⁺ ion) synthesized using cyclohexane (A) and acetonitrile (B) as the reaction medium

As shown in Fig. 4.10, the comparison of the two MS² spectra of the compound IV synthesized proved that ACN didn't affect the product formation. This agrees with the previously published studies, reporting very similar products yields when liquid phase ozonolysis of verbenone was performed in ACN and CH₂Cl₂.¹⁰⁸

4.1.2.3. Evaluation of the ionization conditions

Analysis of the organic peroxides and hydroperoxides using ESI and APCI is problematic and only few papers on the subject can be found in the literature.^{116,176,178,190-198} Results of the previously published studies have shown that hydroperoxy group is not a favorable protonation or deprotonation site.^{176,190-193} However, it was tentatively concluded that some hydroperoxides produced relatively abundant M + H⁺ ions in APCI.¹⁷⁸ In the majority of the published studies, protonation of the hydroperoxy group has led to the neutral losses of water and hydrogen peroxide, thus suppressing the M + H⁺ ions formation.^{176,190-193} Therefore, if no ionization sites are present,¹⁷⁶ detection has to rely on the formation of adduct ions. Hydroperoxides produced during cholesterol ozonolysis were analyzed with ESI as their ammonia and acetate adducts.^{116,194} Formation of sodium and ammonia adducts was utilized for the detection of the triacetone triperoxide.^{195,196} Ammonia and silver adducts were used for the detection and structural analysis of diacyl peroxides with ESI.^{197,198}

Ionization conditions were investigated in order to determine the optimal detection method and solvent composition. Two ionization methods as well as six solvent compositions listed in Table 4.8 were studied. Samples were prepared as described in section 3.3 and delivered directly into the mass spectrometer ion source.

Table 4.8 Solvents used during the investigation of ionization conditions

Solvent composition (1:1 v/v)	pH
H ₂ O + ACN	7
H ₂ O + MeOH	
2 mM ammonium acetate (H ₂ O) + ACN	

2 mM ammonium acetate (H ₂ O) + MeOH	3
8 mM formic acid (H ₂ O) + ACN	
8 mM formic acid (H ₂ O) + MeOH	

4.1.2.3.1. Atmospheric pressure chemical ionization (APCI)

All of the analyzed compounds failed to produce $M + H^+$ ions when APCI was used. Additionally, mass spectra obtained using APCI indicated significant decomposition of the analyte in the ion source. Those results were expected, since it is known that APCI is not suitable for ionization of the large, thermally labile molecules.¹⁷³ Thus, indirect ionization of the α -acyloxyhydroperoxy aldehydes by ammonia adducts formation with ESI was concluded to be necessary, similar to the ionization conditions reported in other studies of the different organic peroxides and hydroperoxides.

4.1.2.3.2. Electrospray ionization (ESI)

The use of ESI led to the following conclusions. As expected, all of the analyzed compounds failed to produce protonated pseudo-molecular ions. When solvent containing water and methanol or acetonitrile was used, only the formation of sodium and potassium adducts ions was observed. Similar spectra distribution was observed when aqueous solution of formic acid (pH = 3) was used as the solvent component. Formation of the deprotonated pseudo-molecular ions $M-H^-$ was observed for the compounds IX - XIII due to the presence of the non-derivatized carboxylic group, as shown in Fig. 4.8. Formation of these ions was observed in all of the tested solvents, and it was most efficient when ammonium acetate was used. A number of dicarboxylic acids were reported as the components of SOA from ozonolysis of cyclohexene and α -pinene. However, variety of carboxylic acids detected in the SOA sample also contains hydroxyl and carbonyl groups. Therefore, a method for detecting a single group of α -acyloxyhydroperoxy aldehydes would be far from universal. It was concluded that formation of the ammonia adducts was the most versatile ionization method. This method was proven to be efficient for the e.g. diacyl peroxides and hydroperoxides produced during ozonolysis of cholesterol.^{116,194,198} Also, all of the studied α -

acyloxyhydroperoxy aldehydes can be ionized in this manner. Solvents containing 2mM ammonium acetate gave similar spectra distribution, when ACN and methanol were used. However, acetonitrile and ammonium acetate were chosen as the optimal solvent components since in ACN the $M + NH_4^+$ ions had significantly higher intensity compared to methanol. Also, the use of alcohol as a solvent carried a risk of hemiacetal formation, since all of the compounds shown in Fig. 4.8 had one or two (compounds VII and VIII) carbonyl groups.

4.1.2.4. Confirmation of the elemental formulas of α -acyloxyhydroperoxy aldehydes with HR-MS

The elemental formulas of the synthesized standards of α -acyloxyhydroperoxy aldehydes were confirmed with HR-MS. Sample preparation and conditions of the HR-MS experiments are described in section 3.2.3.

In order to validate the method, elemental formulas of the compounds synthesized using model precursor – cyclohexene - were confirmed. Results of the HR-MS experiments are reported in Table 4.9. C, H, O, Na and N were the elements included in the elemental formulas assignment, even though the only source of nitrogen was the inert solvent (ACN). Molecular formulas of the compounds VII-XIII were confirmed with the HR-MS, since synthesis of these compounds was concluded to be potentially most problematic, due to presence of the two reactive sites in the SCI scavengers molecules, as already discussed in section 1.3.3.

Table 4.9 Results of the HR-MS measurements of the compounds VII - XIII

Compound number	Scavenger	Elemental formula	Calculated molecular weight	Calculated $M+Na^+$ mass	Measured $M+Na^+$ mass	Matching formulas +/- 5 mDa
VII	Levulinic 116	$C_{11}H_{18}O_6$	246.1103	269.1001	269.1033	$C_{14}H_{16}NO_3Na$ $C_{13}H_{17}O_6$ $C_{16}H_{15}NO_3$ $C_{11}H_{15}N_3O_5$ $C_{11}H_{18}O_6Na$ $C_9H_{16}N_3O_5Na$ $C_8H_{17}N_2O_8$
VIII	5-oxohexanoic	$C_{12}H_{20}O_6$	260.1259	283.1158	283.1131	$C_9H_{19}N_2O_8$ $C_{10}H_{18}N_3O_5Na$

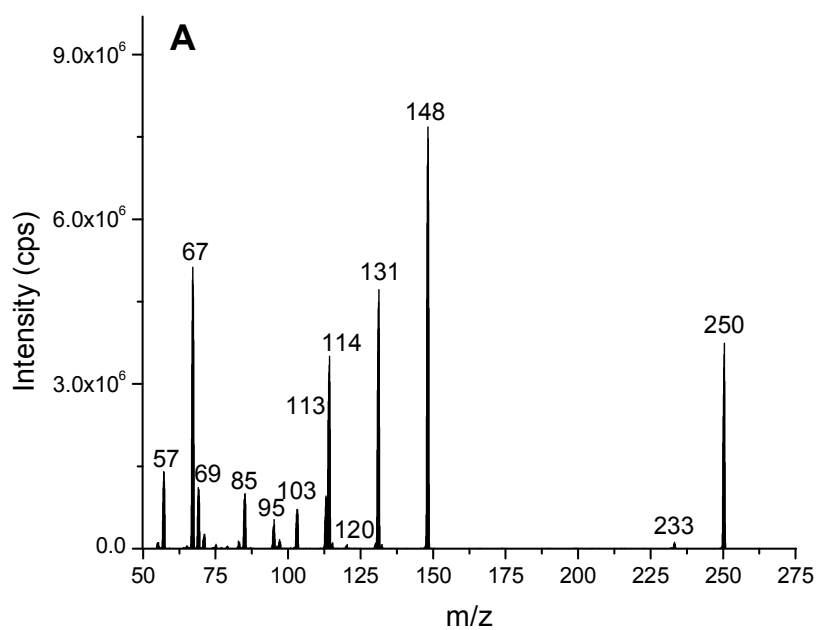
	130					C₁₂H₂₀O₆Na C ₁₂ H ₁₇ N ₃ O ₅ C ₁₆ H ₁₅ N ₂ O ₃
IX	Succinic 118	C ₁₀ H ₁₆ O ₇	248.0895	271.0794	271.0763	C ₇ H ₁₅ N ₂ O ₉ C ₈ H ₁₄ N ₃ O ₆ Na C₁₀H₁₆O₇Na C ₁₄ H ₁₁ N ₂ O ₄
X	Glutaric 132	C ₁₁ H ₁₈ O ₇	262.1052	285.0950	285.0912	C ₈ H ₁₇ N ₂ O ₉ C ₉ H ₁₆ N ₃ O ₆ Na C ₁₅ H ₁₃ N ₂ O ₄ C₁₁H₁₈O₇Na C ₁₁ H ₁₅ N ₃ O ₆
XI	Adipic 146	C ₁₂ H ₂₀ O ₇	276.1208	299.1107	299.1087	C ₉ H ₁₉ N ₂ O ₉ C ₁₀ H ₁₈ N ₃ O ₆ Na C₁₂H₂₀O₇Na C ₁₄ H ₁₉ O ₇ C ₁₅ H ₁₈ NO ₄ Na
XII	pimelic 160	C ₁₃ H ₂₂ O ₇	290.1365	313.1263	313.1270	C ₁₃ H ₁₉ N ₃ O ₆ C₁₃H₂₂O₇Na C ₁₅ H ₂₁ O ₇ C ₁₆ H ₂₀ NO ₄ Na C ₁₁ H ₂₀ N ₃ O ₆ Na C ₁₀ H ₂₁ N ₂ O ₉ C ₁₈ H ₁₉ NO ₄
XIII	Suberic 174	C ₁₄ H ₂₄ O ₇	304.1521	327.1413	327.1392	C ₁₈ H ₁₉ N ₂ O ₄ C ₁₁ H ₂₃ N ₂ O ₉ C ₁₇ H ₂₂ N ₁ O ₄ Na C₁₄H₂₄O₇Na C ₉ H ₂₄ N ₂ O ₉ Na

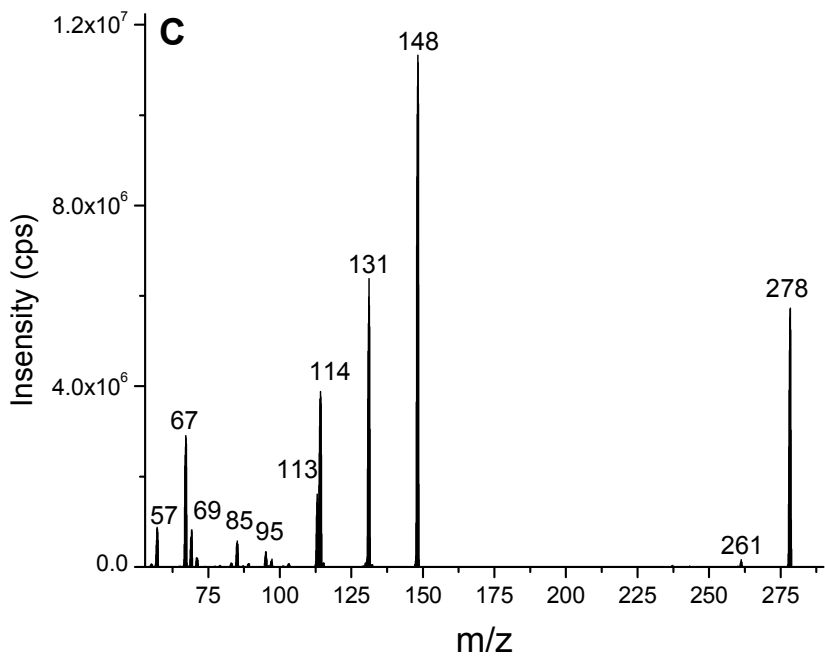
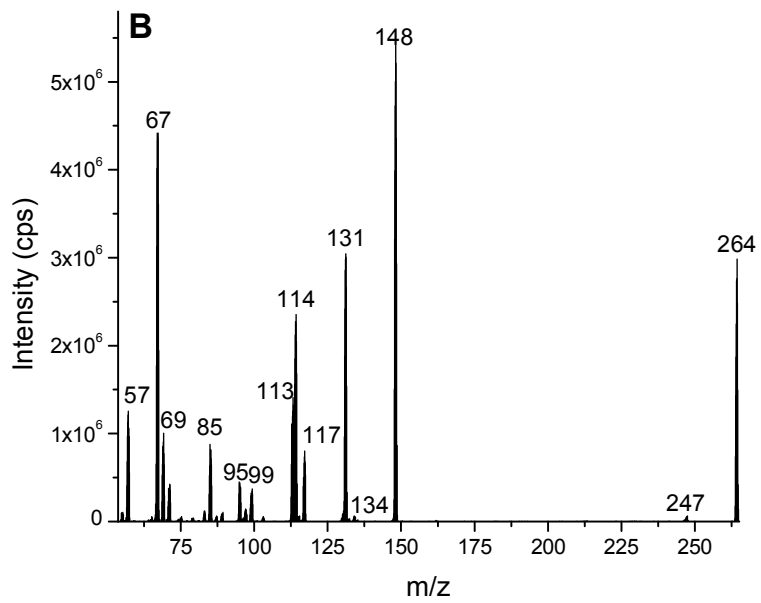
Formulas listed in Table 4.9 had the exact masses closest to the experimental data. As shown in Table 4.9, when only sodium adducts of the compounds without nitrogen are considered, elemental formulas for all of the synthesized standards were confirmed within the uncertainty of the measurement (shown in bold).

4.1.2.5. Investigation of the fragmentation mechanism

Investigation of the fragmentation pathways of the ammonium cationized pseudo-molecular ions of the compounds I – XIII was carried out as follows. Initially, MS² spectra of the M + NH₄⁺ ions were acquired and the structures of the major fragmentation ions were investigated by recording their MS³ spectra. General fragmentation mechanism was elucidated using acquired tandem mass spectra and confirmed with analysis of the isotopically labeled analogs (see section

4.1.2.6). MS² spectra of the M + NH₄⁺ ammonia adducts of compounds I, II, III, V and VI are shown in Fig. 4.11. Spectrum of the compound IV is shown in Fig. 4.10.





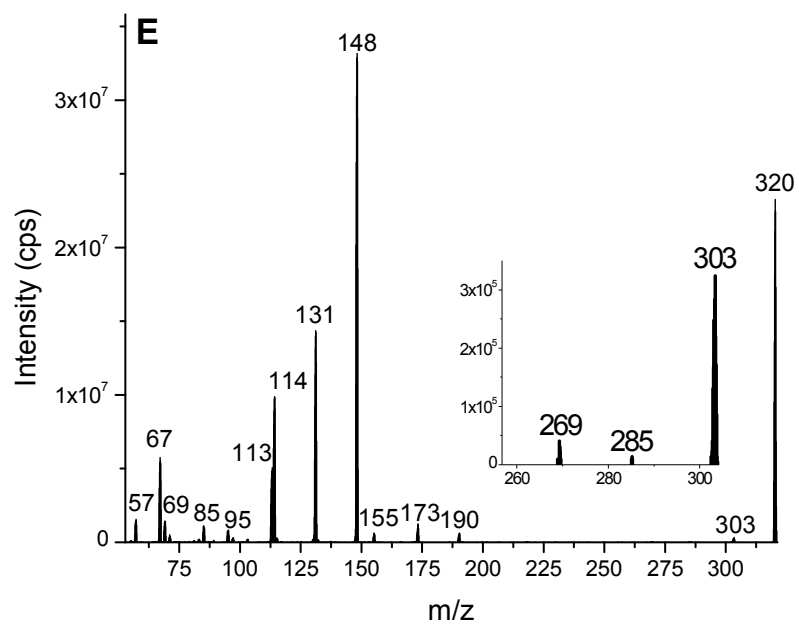
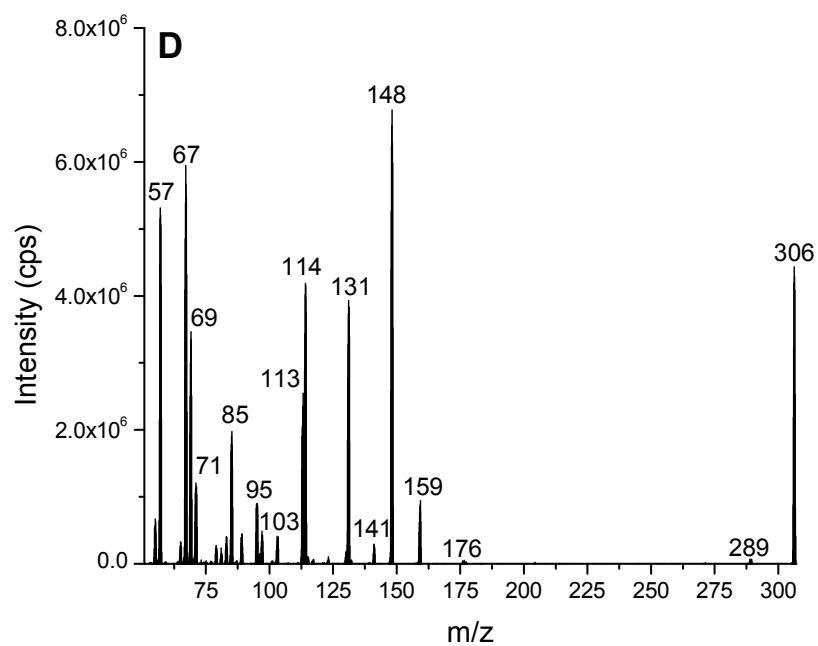


Figure 4.11 MS² spectrum of the M + NH₄⁺ ion of the compound I (A), II (B), III (C), V (D) and VI (E)

As shown in Fig. 4.11, all of the compounds synthesized with linear carboxylic acids shared the same fragmentation patterns, strongly indicating the same fragmentation mechanism. The

MS^2 spectra of the compounds I – VI differ only by the scavenger - specific fragment ions, as discussed later in this section. Based on the interpretation of the tandem mass spectra as well as analysis of the isotopically labeled analogs (see section 4.1.2.3), general fragmentation mechanism for the ammonium cationized α - acyloxyhydroperoxy aldehydes was proposed.

Bond homolysis has been previously proposed as a major fragmentation mechanism for some ammonium cationized diacyl peroxides.¹⁹⁸ However, this mechanism appears to be unlikely for the ammonium cationized α - acyloxyhydroperoxy aldehydes studied in this work. If the bond dissociation between the atoms 2 and 5 occurred via homolysis mechanism, the major resulting fragment ions would be radical cations: m/z 149 for the peroxide side of the molecule and m/z $M_{\text{scavenger}} + 17$ for the fragment ions originating from the SCI scavenger. Instead of bond homolysis, two mechanisms of the bond dissociation between carbon 2 and oxygen 5 are proposed. Both fragmentation pathways involve McLafferty – like hydrogen rearrangements as shown in Fig. 4.12.

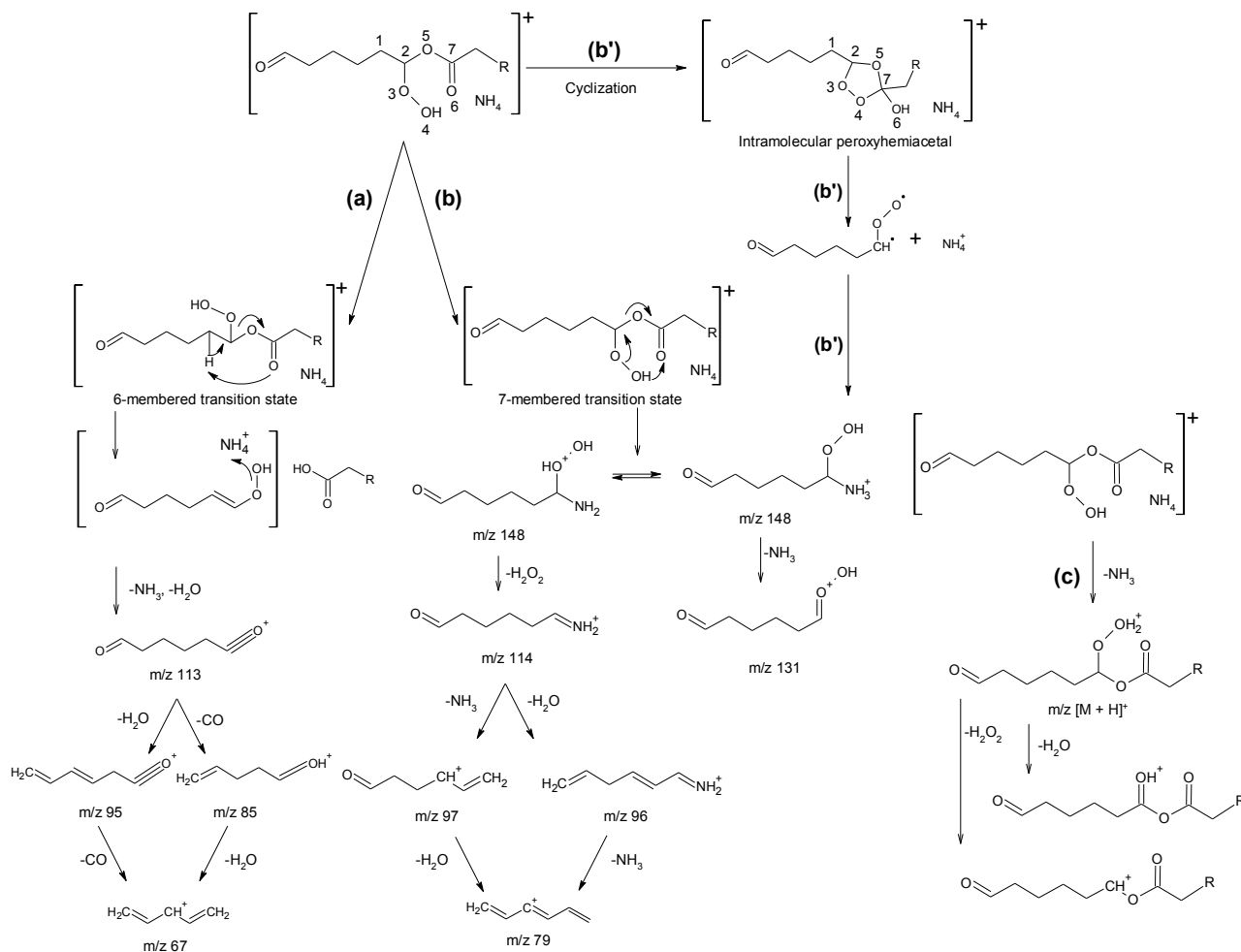


Figure 4.12 Proposed fragmentation mechanism of the ammonium cationized α -acyloxyhydroperoxy aldehydes

An alternate mechanism, involving the formation of intramolecular, peroxyhemiacetal is also proposed. Please note that hydrogen rearrangements accompanying the formation of a number of ions shown in Fig. 4.12 were omitted for clarity. Pathway (a) leads to the formation of the m/z 113 ion by the hydrogen rearrangement via six membered transition state. Very similar fragmentation mechanism was previously reported for ammonium cationized, alkyl-substituted diacyl peroxides.¹⁹⁸ After the transfer of hydrogen atom adjacent to the carbon atom 1 to the oxygen atom 6 the ion m/z 113 is formed by the subsequent elimination of water and ammonia molecules. MS^2 spectrum of compound II, along with the MS^3 spectra of the major fragmentation ions are shown in Fig. 4.13.

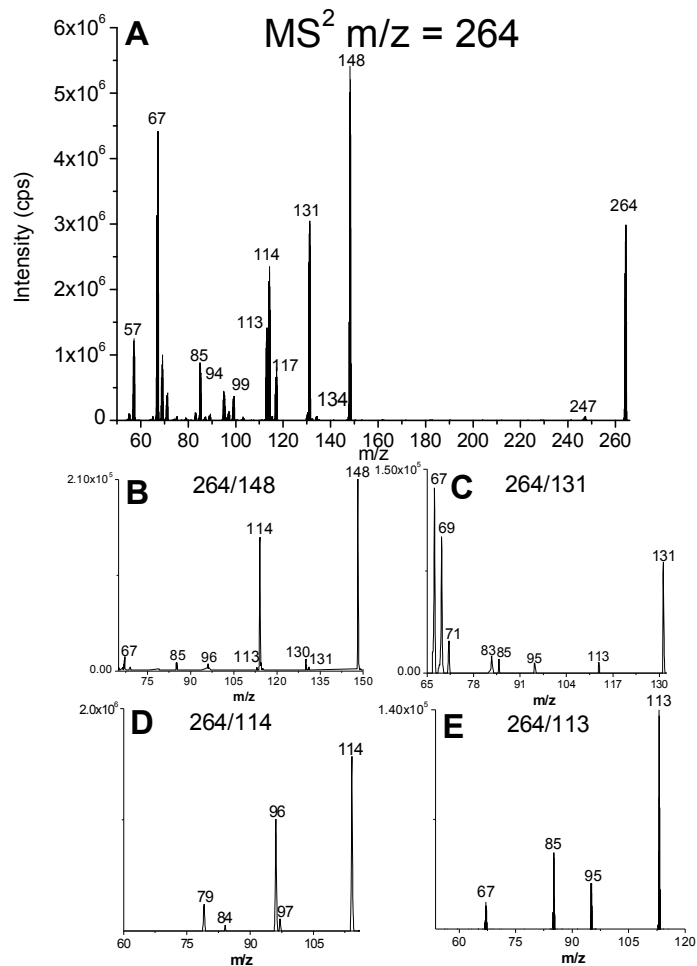


Figure 4.13 M + NH₄⁺ ion MS² spectrum of the compound II – m/z 264 (A); MS³ spectra of the major fragment ions: m/z 148 (B), m/z 131 (C), m/z 114 (D) and m/z 113 (E)

Ions produced from fragmentation of the m/z 113 ion, shown in Fig. 4.13 E, are formed by subsequent elimination of water and/or carbon oxide molecules. This leads to the formation of the m/z 95, 85 and ultimately m/z 67 ions.

Formation of the m/z 114 ion is also proposed to occur via McLafferty - like rearrangement. The hydrogen atom adjacent to the oxygen atom 4 is transferred to the oxygen atom 6 via seven – membered transition state; pathway (b) shown in Fig. 4.12. Fragmentation via pathway (b) initially leads to the formation of the m/z 148 ion, which subsequently produces ion m/z 114 (Fig. 4.13 B)

by loss of 34 mass units, it is consistent with the elimination of hydrogen peroxide. Subsequent fragmentation (MS^3) of the m/z 114 ion has led to the formation of the m/z 97, 96, 79 ions and minor fragment m/z 84 ion as shown in Fig. 4.13 D. Formation of the ions m/z 97 and 96 can be attributed to the loss of water molecule or ammonia. Elimination of both water and ammonia leads to the formation of m/z 79 ion. M/z 84 fragment ion is proposed to be formed by the neutral loss of formaldehyde. Unfortunately, this conclusion could not be confirmed based on acquired experimental data.

Since seven membered transition states are known to be very uncommon in mass spectrometry,¹⁹⁹⁻²⁰¹ an alternate mechanism for the generation of the fragment m/z 148 is proposed. The second possible mechanism, denoted as pathway (b') in Fig. 4.12 involves the formation of the intramolecular, cyclic peroxyhemiacetal in the gas phase,⁸⁹ structurally very similar to the secondary ozonide. Fragmentation of the 5 – membered ozonide ring can lead to the regeneration of the Criegee intermediate, as it was concluded in the previously published studies.^{202,203} For example, the bond dissociations between atoms 2-5 and 4-7, will lead to the regeneration of the Criegee intermediate as well as the scavenger-specific ion formation, as reported previously.^{202,203} The Criegee intermediate can subsequently react with ammonia to generate one of the possible structures of the m/z 148 ion. After the formation of m/z 148 ion, fragmentation via both proposed pathways proceed by the common mechanism. Unfortunately, the fragmentation via pathway (b) or (b') cannot be concluded as the major path based on the experimental data acquired in this study. However, as discussed in section 4.1.2.6, analysis of the compounds synthesized with cyclohexene- d_{10} as the precursor strongly indicated the fragmentation mechanism involving the transfer of non – aliphatic hydrogen from the peroxide side of the molecule to the acidic fragment. This can only be accomplished by either seven – membered transition state (b) or by formation of an intramolecular peroxyhemiacetal (b').

In addition to the two major fragmentation pathways, (a) and (b), pathway (c) shown in Fig. 4.12 was a minor one (approx. 5% of the relative intensity). Weakly abundant protonated, pseudo-molecular ions were detected in the MS^2 spectra for all of the synthesized standards. An example of formation of the ions via pathway (c) is shown in Fig. 4.14, for the compound VI. Please note the difference in the Y axis scale between the frame and the remainder of the mass spectrum.

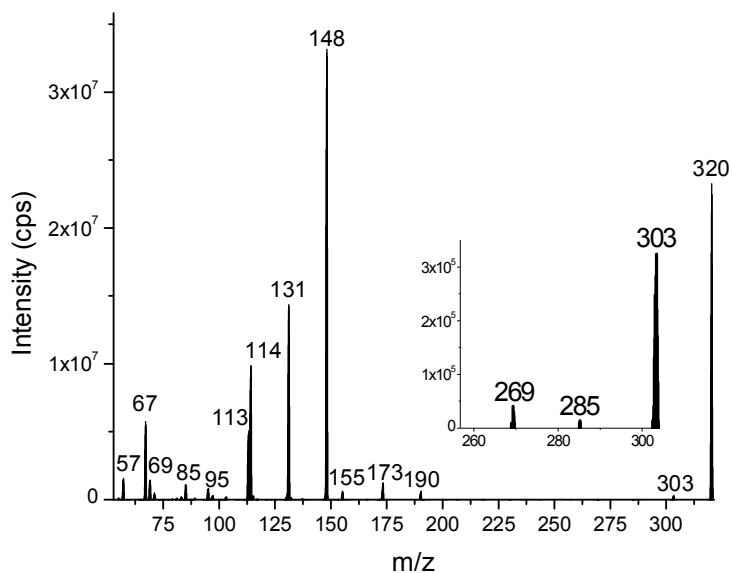
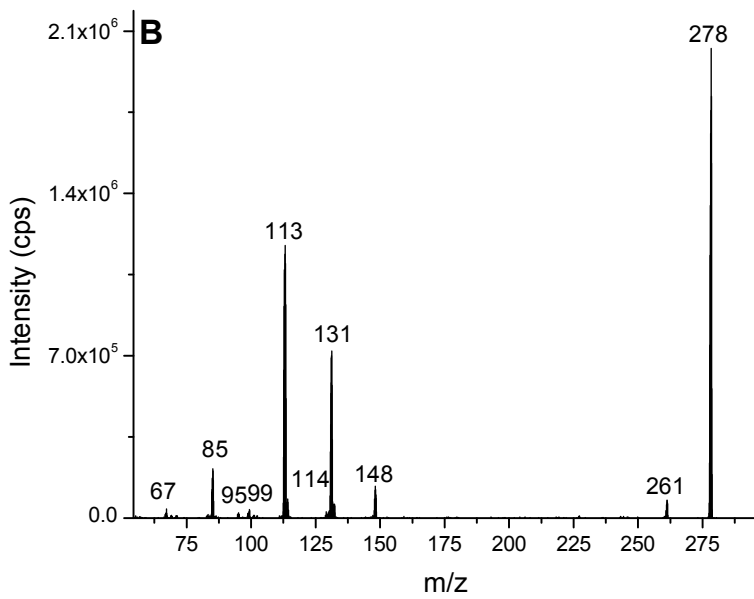
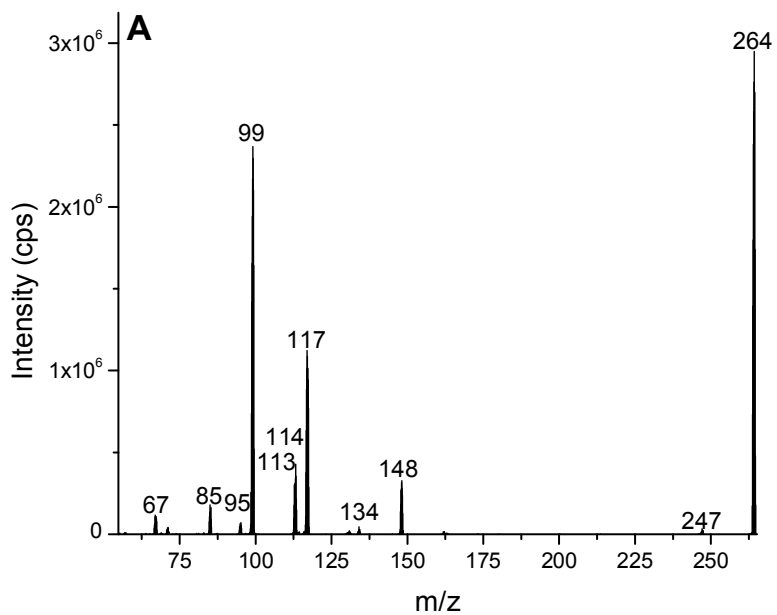
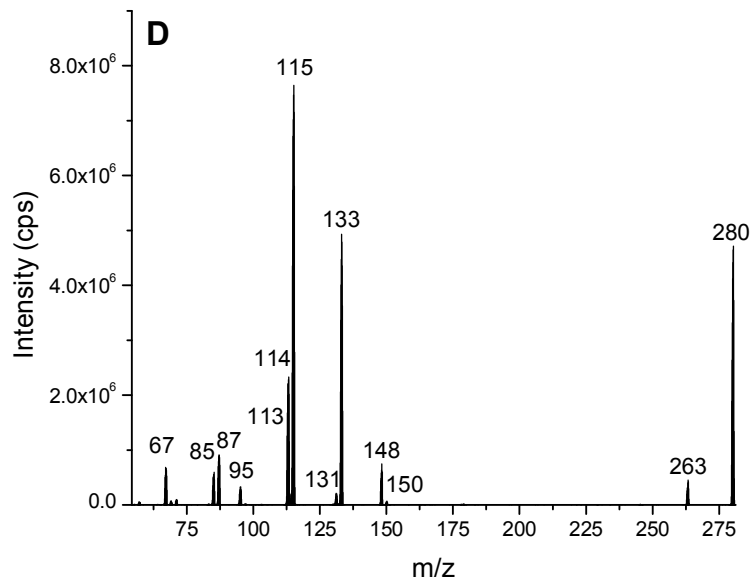
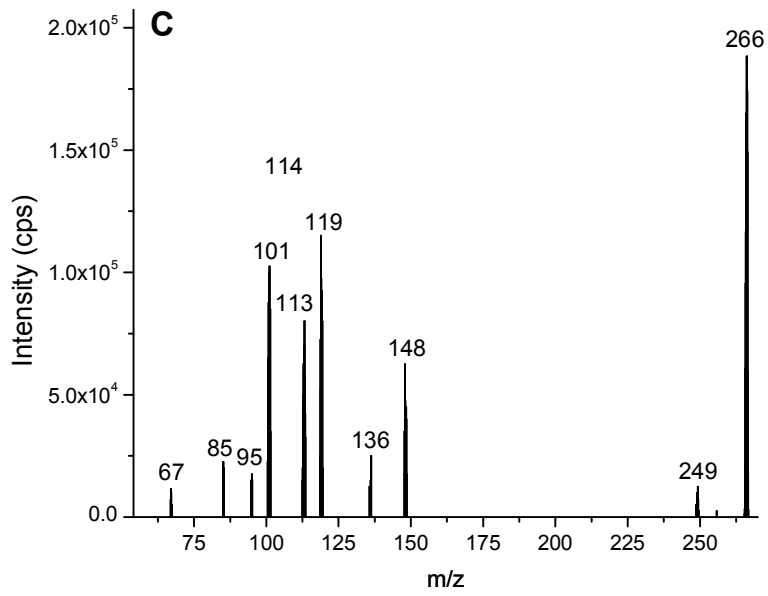


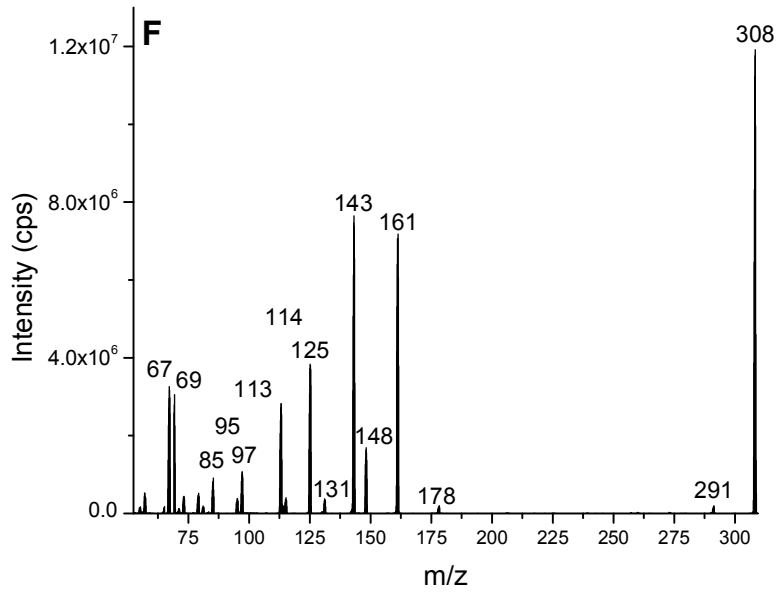
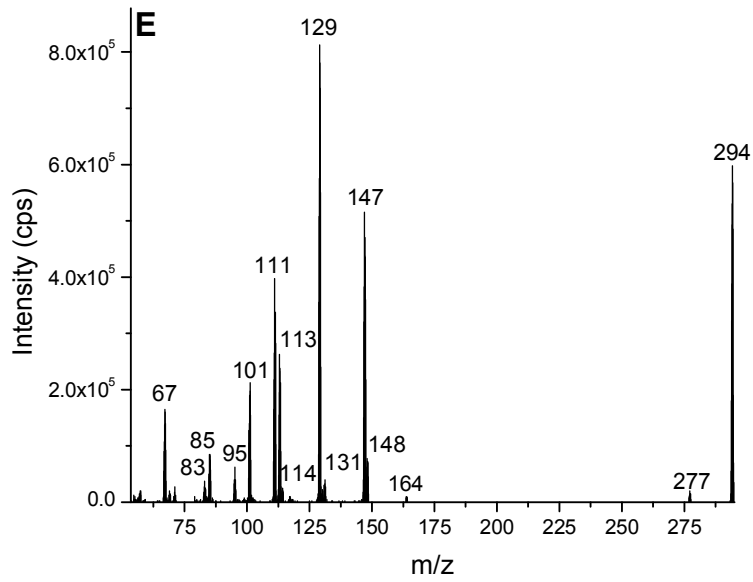
Figure 4.14 MS² spectrum of the M + NH₄⁺ ion of compound VI

As shown in Fig. 4.14, fragments corresponding to the neutral losses of H₂O and H₂O₂ from the M + H⁺ ions were also detected. It is also important to notice, that loss of the hydrogen peroxide molecule from the protonated pseudo-molecular ions as well as from the ion m/z 148 in the pathway (b) additionally confirmed the presence of the –OOH moiety.

In both proposed fragmentation pathways, ammonia can be coordinated by either hydroperoxide – fragment of the molecule or by the scavenger (acidic) fragment. MS² spectra of the M + NH₄⁺ ions for the compounds synthesized using carbonyl containing carboxylic acids as well as dicarboxylic acids are shown in Fig. 4.15. Spectra for the compounds VII and VIII, synthesized using carboxylic acids containing carbonyl groups are shown in Fig. 4.15A and Fig. 4.15B; spectra of the compounds IX, X, XI, XII, XIII are shown in Fig. 4.15C, Fig, 4.15D, Fig, 4.15E, Fig. 4.15F and Fig. 4.15G.







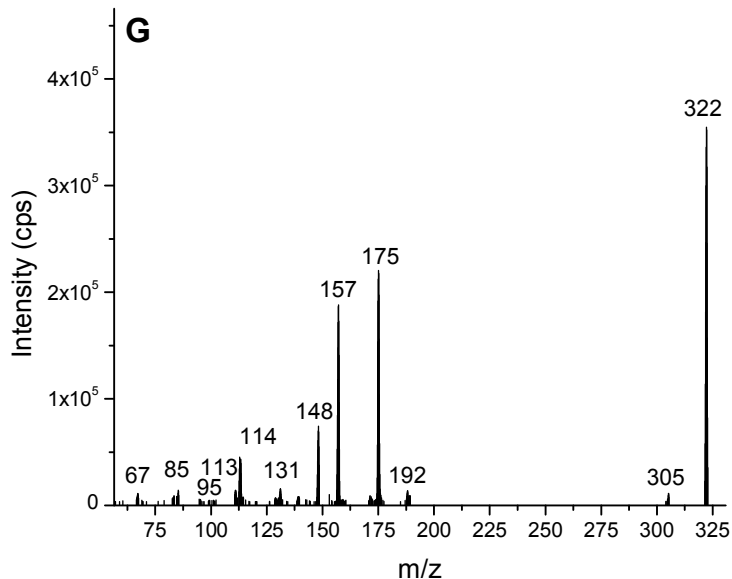


Figure 4.15 MS² spectrum of the M + NH₄⁺ ion of the compound VII (A), VIII (B), IX (C), X (D), XI (E), XII (F) and XIII (G)

The relative intensities of the major fragment ions for the compounds I – XIII are summarized in Table 4.10.

Table 4.10 Relative abundances (%) of the ions formed via two major fragmentation pathways – (a) and (b) in the MS² spectra of the synthesized standards

Compound number	Mass to charge ratio of the major fragment ions						
	148	131	114	113	67	Scavenger+1	Scavenger+1-H ₂ O
I*	11.3%	10.8%	11.1%	0.4%	63.0%	1.1%	2.2%
II	17.9%	8.0%	13.6%	1.2%	58.0%	0.6%	0.6%
III**	5.8%	7.5%	9.1%	3.2%	63.7%	7.5%	3.2%
IV	11.2%	7.2%	7.9%	5.9%	64.4%	2.4%	1.0%

V	23.7%	16.8%	13.4%	2.2%	42.5%	1.0%	0.4%
VI	12.2%	11.6%	12.5%	1.6%	61.7%	0.4%	0.1%
VII	6.2%	3.9%	4.1%	1.7%	25.6%	14.7%	43.8%
VIII**	4.1%	18.0%	0.8%	29.0%	1.2%	18.0%	29.0%
IX	3.7%	1.5%	1.4%	5.2%	33.6%	9.8%	44.8%
X	2.9%	1.5%	4.7%	5.6%	27.3%	13.9%	44.0%
XI	5.3%	4.3%	5.1%	3.6%	33.5%	19.3%	29.0%
XII	7.6%	4.6%	4.9%	3.6%	41.3%	15.6%	22.4%
XIII	6.9%	3.5%	5.0%	5.0%	41.5%	10.7%	27.4%

*For the compound I dehydrated SCI scavenger ion was overlapping with the m/z 85 ion, produced via pathway (a) from m/z 113 ion

**Please note that for the compounds III and VIII ions produced from the SCI scavenger and peroxide side of the molecule are isobaric and thus cannot be distinguished

As shown in Fig. 4.11 and Fig. 4.15, as well as in Table 4.10, relative intensities of the scavenger's specific fragments differ significantly between the compounds synthesized using linear carboxylic acids, and those synthesized with carboxylic acids containing carbonyl group as well as dicarboxylic acids. The scavenger's specific fragments are the most abundant peaks in the MS² spectra of the compounds VII – XIII, as opposed to the compounds I – VI.

Ability to produce more intense scavenger fragments in the MS² spectrum is most likely a result of higher oxygen content in the carboxylic acids containing carbonyl group as well as dicarboxylic acids. The larger number of oxygen atoms in those carboxylic acids results in a better coordination of the NH₄⁺ and H⁺ ions, and thus higher intensity of the ions originating from the SCI scavengers.

4.1.2.6. Isotope study

As already discussed in section 4.1.2.5, proposed fragmentation mechanism for α -acyloxyhydroperoxy aldehydes is supported by the analysis of isotopically labeled analogs. Shifts of the major mass peaks in the MS² spectra of the isotopically labeled analogs are summarized in

Table 4.11; ions for the non-labeled standards were added for reference. As listed in Table 4.11, for each compound under study, MS^2 and MS^3 spectra of the $M + ND_4^+$ as well as $M + N^{15}H_4^+$ ions were acquired and analyzed. Compounds I – XIII were also prepared with the cyclohexene- d_{10} . Compound II, was prepared using hexanoic acid-6,6,6- d_3 , and was omitted in the summary, presented in Table 4.11, since that was the only experiment with the isotopically labeled scavenger.

Table 4.11 Mass to charge ratio of the major mass peaks in the MS^2 spectra of the isotopically labeled analogs

The most abundant ions produced upon CID of the ammonium cationized standards (m/z)				
Description	Non- labeled standards	Ammonium acetate – d7	Ammonium acetate – N¹⁵	Cyclohexene - d₁₀
Ammonium cationized fragment	148	152	149	158
Protonated fragment	131	132	131	141
Ion produced via pathway (a)	113	113	113	122
Fragments originating from m/z 113, pathway (a)	95	95	95	102
	85	85	85	94
	67	67	67	74
Ion produced via pathway (b)	114	116	115	124
Fragments originating from ion m/z 114	79	79,80,81	79	84,85,86
	96	97,98	97	104,105
	97	98,99	97	106,107
For the compounds VII – XIII the fragment ions originating from the SCl scavengers were the major mass peaks in the MS^2 spectrum; refer to section 4.1.2.5 for the discussion	Scavenger+1	Scavenger+2	Scavenger+1	Scavenger+1 and scavenger +2
	Scavenger +18	Scavenger +22	Scavenger +19	Scavenger +18 and +19

In following paragraphs, analysis results for the each isotopically labeled analog, listed in Table 4.11 are discussed separately.

Hexanoic acid-6,6,6-d₃ was used to confirm the formation of the scavenger - specific fragments. The mass spectrum of the compound II, synthesized with isotopically labeled hexanoic acid is shown in Fig. 4.16

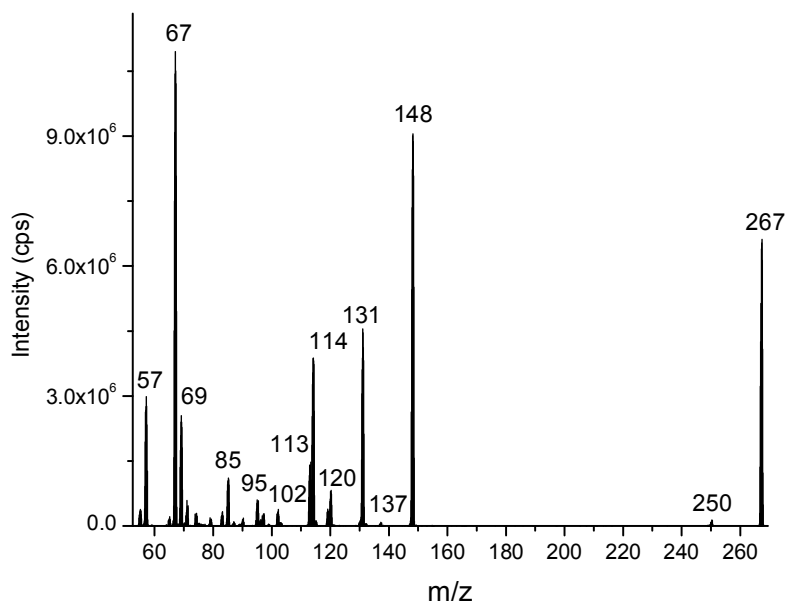


Figure 4.16 MS² spectrum of the M + NH₄⁺ ion of the compound II prepared using hexanoic acid – d₃ as the SCI scavenger

As shown in Fig. 4.16A, the MW of compound II shifted by 3 mass units, unambiguously confirms the occurrence of SCI reaction with the carboxylic acid. The shift of the acidic fragments m/z by three mass units, confirmed that these ions were indeed scavenger's specific fragments. For the compound II, the scavenger's fragments can be observed at m/z 117 and m/z 134, for the protonated and ammonium cationized ions, respectively, as shown in Fig. 4.13A. These ions are shifted to the m/z 120 and 137, as it can be seen in Fig. 4.16. The shift in molecular mass for these ions by 3 mass units also indicates that the initial fragmentation of the α -acyloxyhydroperoxy

aldehydes didn't involve the formation of the scavenger's specific ions and confirms the proposed fragmentation mechanism described in section 4.1.2.5.

Ammonium acetate labeled with deuterium (d7) allowed to distinguish the protonated and ammonium cationized fragments. Measurements with the deuterium labeled ammonium acetate were performed in D₂O/ACN instead of H₂O/ACN, due to fast exchange of labile hydrogens with the solvent if H₂O was used. Note that the use of D₂O was only necessary when ND₄⁺ was used, since it contained solvent - exchangeable deuterium atoms. MS² spectrum of the M + ND₄⁺ ion of the compound II is shown in Fig. 4.17.

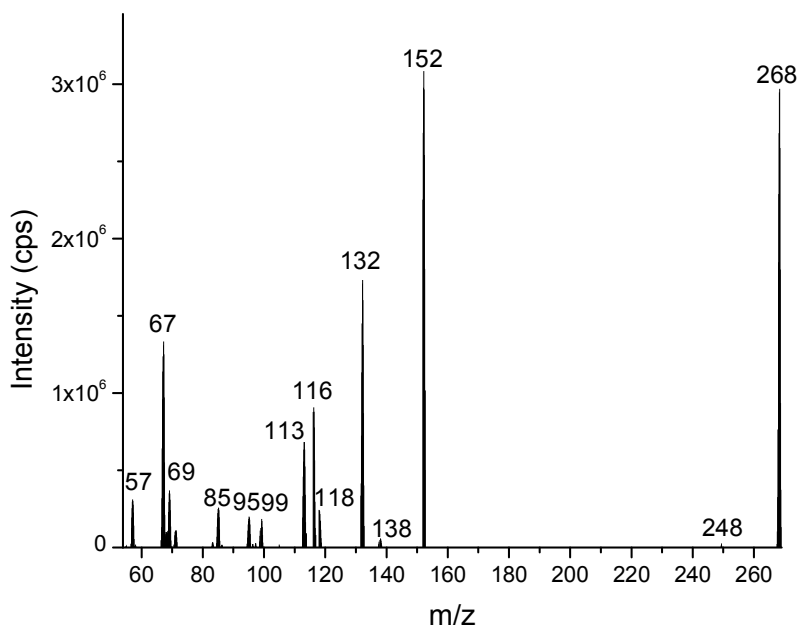


Figure 4.17 MS² spectrum of the M + ND₄⁺ ion of the compound II

Distinguishing the protonated and ammonium cationized fragment ions was crucial for the correct interpretation of the MS² and MS³ spectra and for proposing the fragmentation mechanism. Before the mass shift of the fragment ions in the MS² spectrum is discussed, it is important to underline that the parent ion shifted by 4 mass units, unambiguously confirming that the ions under study were indeed ammonia adducts of the compounds of interest. As listed in Table 4.11, fragment ion m/z 148 was the only mass peak that shifted by 4 mass units, confirming

that NH_4^+ was the charge carrier in this fragment. Ion m/z 131 shifted by 1 mass unit, thus confirming that this fragment was the protonated ion. Ion $m/z = 114$ is shifted to $m/z = 116$ suggesting that two ammonia hydrogen atoms are transferred to this fragment during fragmentation process. This can be explained by the formation of the new nitrogen – carbon bond, as shown in Fig. 4.12. Also, when MS^3 spectrum of the ion m/z 116 was acquired, a higher number of fragment ions were observed, as compared to the spectrum of the m/z 114 ion when non-labeled analogs were analyzed. This has led to the conclusion, that fragment ions m/z 96 and m/z 97 produced from the ion m/z 114 via pathway b (Fig. 4.12) can be formed via different hydrogen rearmament mechanism, involving exchange between the two original NH_4 hydrogen atoms and aliphatic hydrogen atoms of the m/z 114 ion. Ions $m/z=113$ and 95, 85 and 67 remained unaffected by the substitution of NH_4^+ with ND_4^+ ; proving that these ions were most likely carbocations. This conclusion is consistent with the fragmentation via pathway (a). As also listed in Table 4.11, scavenger's specific ions shifted by 1 and 4 mass units, respectively, proving the formation of protonated and ammonium cationized acidic fragments. For the compound II the ions originating from the hexanoic acid are shifted from m/z 117 and m/z 132 to m/z 118 and m/z 138, respectively, as shown in Fig. 4.17.

The use of N^{15} labeled ammonia also allowed to confirm the formation of ammonium cationized parent ion. The mass of the parent ion is shifted by 1 mass unit, again confirming that the ions under study were ammonia adducts. MS^2 spectrum of the $\text{M} + \text{N}^{15}\text{H}_4^+$ ion of the compound II is shown in Fig. 4.18.

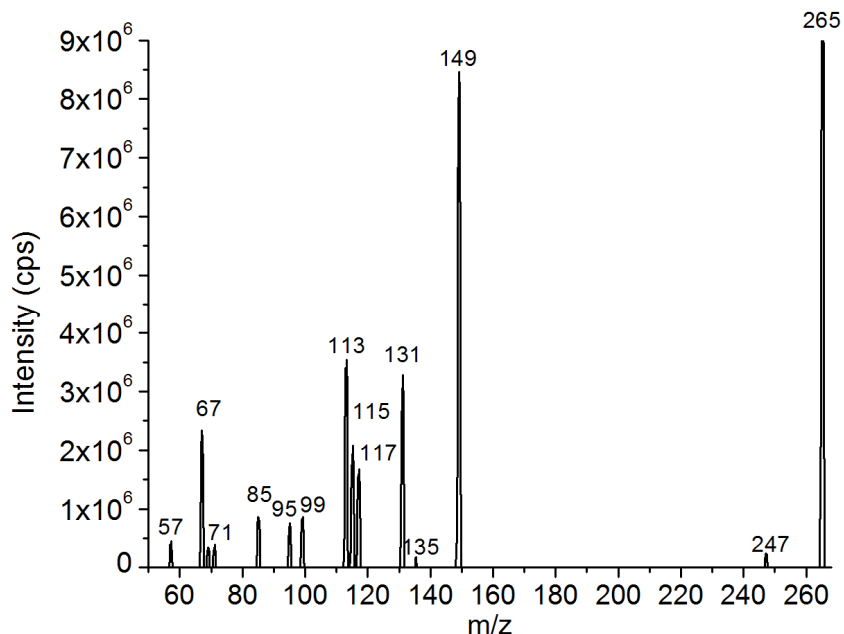
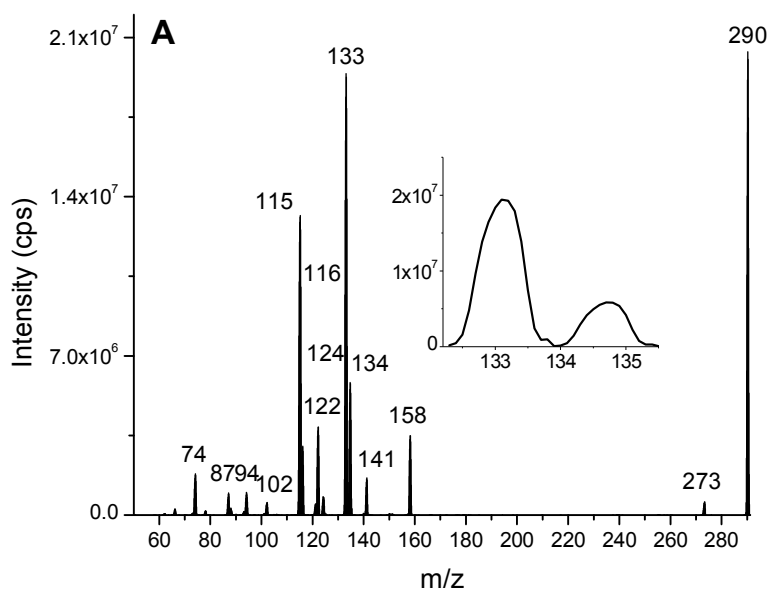


Figure 4.18 MS² spectrum of the M + N¹⁵H₄⁺ ion of the compound II

As shown in Fig. 4.18, and listed in Table 4.11, ions m/z 148 and m/z 114 shifted by 1 mass unit, confirming the presence of the nitrogen atom in this ion. Shift of the ion m/z 114 confirmed the nitrogen presence in this fragment, which in turn indicates the formation of the new carbon-nitrogen bond, consistent with the fragmentation pathway (b) as shown in Fig. 4.12 Also, the elimination of the 18 mass units from the parent ion created an ambiguity, since when non-isotopically labeled standards were analyzed. It was unclear whether neutral ammonia or OH radical was eliminated from the parent ion. Elimination of OH radicals during fragmentation process was even more likely, due to presence of the -OOH moiety. However, when ammonia labeled with N¹⁵ was used, exclusive loss of 19 mass units was observed, thereby excluding OH radical elimination from the parent ion. The same reasoning can be applied to the elimination of the 19 mass units from the fragment ion m/z 149, leading to the formation of the ion m/z 131, consistent with the fragmentation pathway (b). As listed in Table 4.11, ions formed via fragmentation pathway (a), m/z 113, 95, 85 and 67 were unaffected by substitution of regular ammonia with ammonia labeled with N¹⁵, which is also consistent with the proposed fragmentation mechanism – section 4.1.2.5.

The use of cyclohexene-d₁₀ as the precursor instead of the regular cyclohexene provided additional insights into some hydrogen rearrangements as well as enabled to calculate the number of aliphatic hydrogen atoms in the individual fragments. The use of cyclohexene-d₁₀ also confirmed that the observed ions were indeed reaction products of the SCI with carboxylic acids, since the mass of the parent ions shifted by 10 mass units. MS² spectra of the compound X and VI are shown in Fig. 4.19A and Fig. 4.19B.



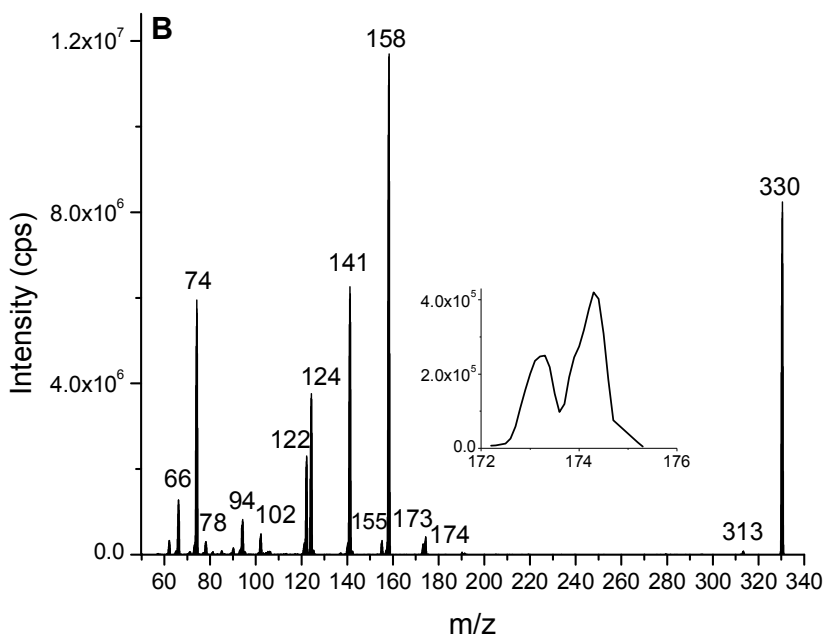


Figure 4.19 MS² spectrum of the M + NH₄⁺ ion of the compound X (A) and compound VI (B) synthesized using cyclohexene-d₁₀

As shown in Fig. 4.19A and Fig. 4.19B, when cyclohexene-d₁₀ and regular ammonia were used, ions m/z 148, 131 and 114 are shifted by 10 mass units, yielding fragments at m/z 158, 141 and 124 respectively. Therefore, these fragments are likely to be formed via the same pathway. Also, the use of cyclohexene-d₁₀ as the precursor resulted in a split of the protonated scavenger ions into two peaks. For the compound X, the mass peak of the protonated scavenger splits into m/z 133 and 134; analogically, for the compound VI, the mass for protonated scavenger ion splits into m/z 173 and m/z 174, as shown in Fig. 4.19A and Fig. 4.19B. These observations strongly indicated fragmentation mechanism involving the transfer of non – aliphatic hydrogen from the peroxide side of the molecule to the acidic fragment. This can only be accomplished by either seven – membered transition state (b) or by formation of an intramolecular peroxyhemiacetal (b'), as shown in Fig. 4.12. Also, in the MS³ spectrum of the ion m/z 124, instead of the same number of peaks as in the spectrum of ion m/z 114, groups of ions spaced by 1 m/z were observed – see Table 4.11. This suggested that most likely several hydrogen rearrangements were involved in the

formation of those fragment ions, which is in line with the same conclusion, drawn when ND_4^+ was used, as it was already discussed above. Ion m/z 113 was shifted to m/z 122, indicating the fragmentation mechanism, involving the transfer of the aliphatic hydrogen from the peroxide side of the molecule to the acidic fragment. This is consistent with the fragmentation mechanism via pathway (a). Also, fragments produced as a result of ion m/z 113 fragmentation, m/z 95, 85 and 67 were shifted to m/z 102, 94 and 74, which indicates the presence of 7, 9 and 7 aliphatic precursor hydrogen presence in these ions.. This is consistent with the fragmentation mechanism via pathway (a) involving elimination of H_2O and CO from the ion m/z 113 to produce the detected fragment ions. Also, it is important to underline that the substitution of the regular cyclohexene with cyclohexene- d_{10} didn't resulted in splitting of the fragment ions produced via pathway (a) into several peaks, similar as for the ions produced via pathway (b). This observation additionally confirmed that ion m/z 113 was indeed carbocation, and not protonated ion.

The experiments with the isotopically labeled analogs provided very valuable insights into the fragmentation mechanism of the ammonium cationized α -acyloxyhydroperoxy aldehydes. The results presented in this section allowed proposing the fragmentation mechanism, common for all of the compounds under study. It is important to underline, that whether pathway (b) or (b') was the main fragmentation mechanism, could not be concluded, based on the data presented here. However, analysis of the isotopically labeled analogs greatly aided in the correct data interpretation providing unambiguous confirmation of the number of proposed fragmentation reactions. Such definitive conclusions could not be presented based only on analysis results for non-labeled standards.

4.1.2.7. Analysis of the ammonium cationized α -acyloxyhydroperoxy aldehydes synthesized using α -pinene

After establishing the general fragmentation mechanism, two α -acyloxyhydroperoxy aldehydes related to the BSOA chemistry were analyzed. For the synthesis of the compounds XIV and XV *cis*-pinonic acid and pinic acid were used. Compound XIV was proposed by Lee et al.¹⁵⁰ as a possible SOA nucleation precursor in the α -pinene/ozone system, as described in section 1.4.4. Compound XV was excluded as a possible nucleation precursor, since it was concluded that the

time required for pinic acid formation is longer than the time necessary for SOA formation. Compound XV was synthesized, since pinic acid and cis-pinonic acid were the only commercially available standards for the known α -pinene LMW SOA components. Also, confirmation of the proposed fragmentation mechanism, based only on one compound analysis would not allow for presenting any meaningful conclusions. Even though the compound XV was tentatively excluded as a possible nucleation precursor, it could be produced during subsequent SCI reactions, after initial nucleation steps.

Two SCIs can be produced from non – symmetric precursor like α -pinene (see section 1.3.3), therefore leading to the two possible α -acyloxyhydroperoxy aldehydes.¹⁵⁰ For clarity, only one possible structure of the compounds XIV and XV was included in Fig. 4.9. The formation ratio for the two ECIs is 6:4, favoring the methyl substituted ECI with the stabilization yields of about 0.15 for both ECIs, as described in section 1.3.3. The mechanism was reported for the gas-phase ozonolysis and it is unclear whether these findings also apply to the reaction in the liquid-phase. However, the degree of stabilization seems to be much higher in the liquid, since the α -acyloxyhydroperoxy aldehydes formed during liquid-phase ozonolysis of the alkenes were reported to be produced in nearly quantitative yields, as it was already discussed in section 1.3.4.⁸⁹ It is therefore reasonable to assume that both possible structures of compounds XIV and XV will give very similar spectra distribution and undergo fragmentation pathways (a), (b) and (c), as shown in section 4.1.2.5.

For both compounds XIV and XV fragmentation of the ammonium cationized pseudo-molecular ions via pathway (a) will lead to the formation of the m/z 167 ion, and m/z 139, 149 and 121 ions due to the neutral loss of carbon oxide and water. M/z 202 ion is expected to be formed via pathway (b) and yield m/z 168 and 185 ions by the neutral loss of hydrogen peroxide and ammonia, respectively. Neutral loss of water and ammonia from the m/z 168 ion will produce m/z 151, 150 and m/z 133 ions. MS^2 spectra of the $M + NH_4^+$ ions for the compound XIV and compound XV are shown in Fig. 4.20A and Fig. 4.20B

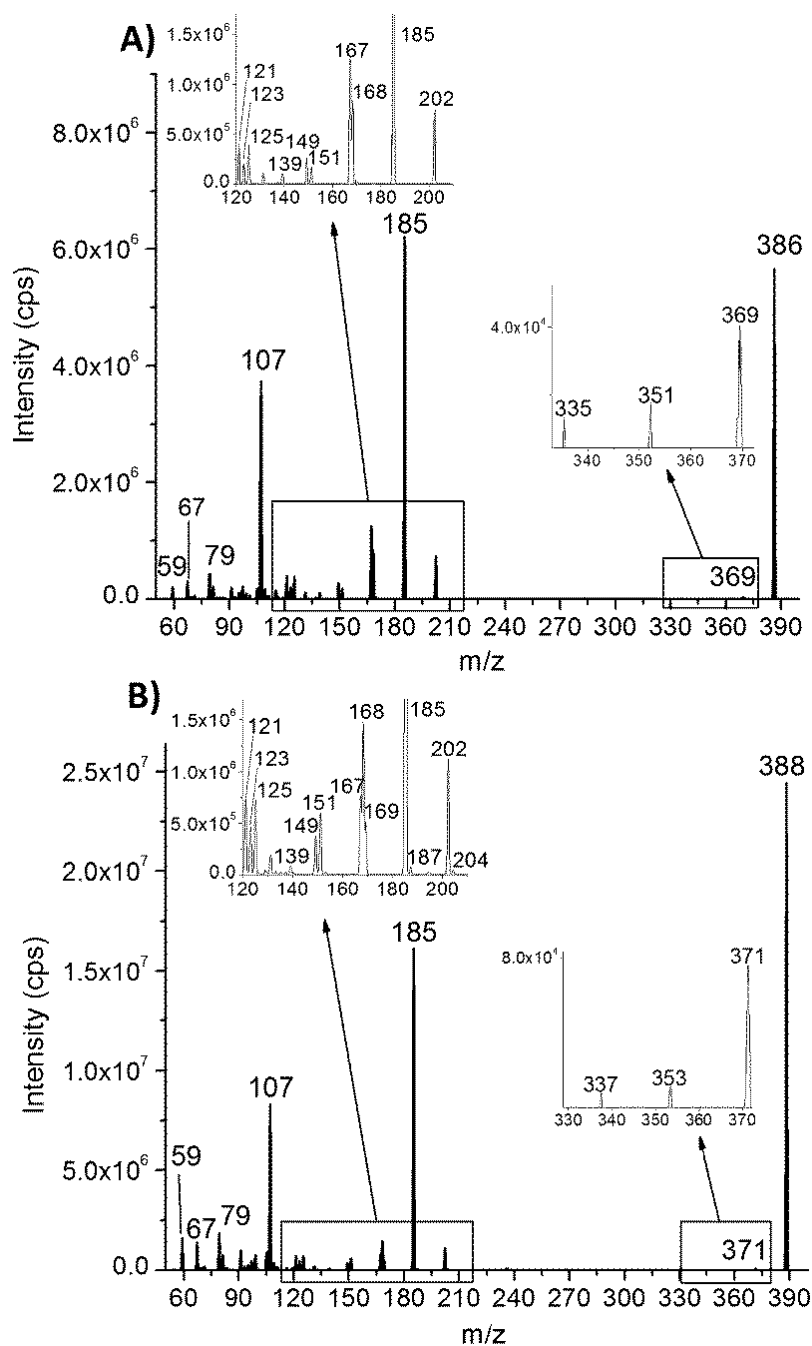


Figure 4.20 MS² spectra of the M + NH₄⁺ ions for the compound XIV (A) and XV (B)

As shown in Fig. 4.20A and Fig. 4.20B, the experimental data are in very good agreement with the predicted fragmentation. Unfortunately, for the compound XIV, similar to the compounds III and VIII, fragments originating from the SCI scavenger overlap with those obtained from the fragmentation of the peroxide side of the molecule via pathway (b). Ion of the protonated *cis*-

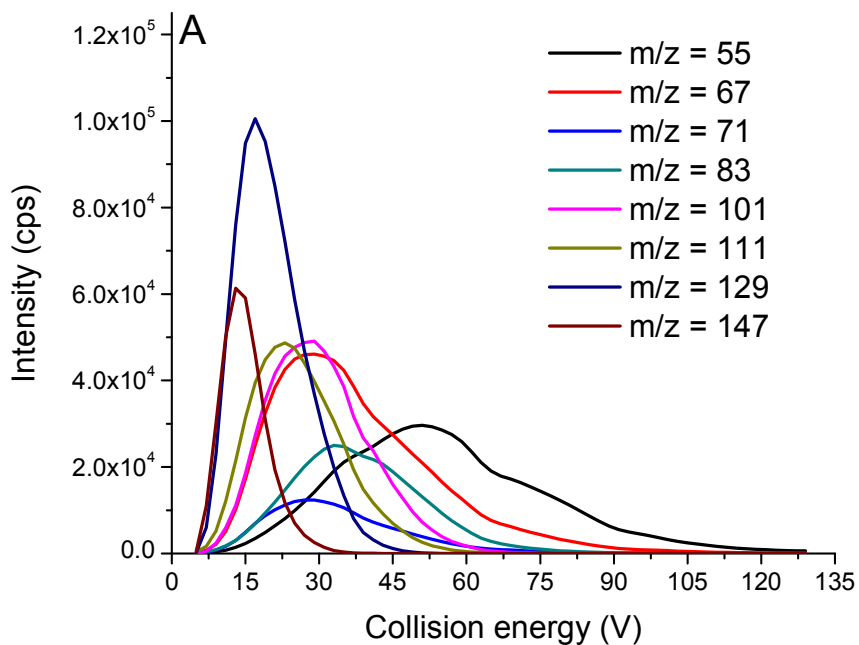
pinonic acid, m/z 185 will most likely undergo fragmentation by the elimination of water and carboxylic group, producing m/z 167 and 139 ions. However, under the experimental conditions employed in this work, fragments originating from the *cis*-pinonic acid could not be distinguished from those produced by the peroxide side of the molecule. For the compound XV, weakly abundant, but clearly present ions corresponding to the protonated (m/z 187), ammonium cationized (m/z 204) and dehydrated (m/z 169) pinic acid were observed as shown in Fig. 4.20B. In addition to the fragments produced via pathways (a) and (b), weakly – abundant ions formed via pathway (c) were observed. Fragments corresponding to the neutral loss of water and hydrogen peroxide molecules from the $M_{XIV}+H^+$ and $M_{XV}+H^+$ ions were detected as shown in Fig. 4.20A and Fig. 4.20B. The m/z 107 ion was most abundant in the spectrum of both compound XIV and XV. The m/z 107 ion formation can be attributed to the loss of the 42 mass units from the m/z 149 ion, most likely due to the fragmentation of cyclobutane ring. This fragmentation mechanism was not possible for the compounds I - XIII. However, it is important to note that the formation of the majority of fragments produced by CID of the $M+NH_4^+$ ions for both compound XIV and XV was predicted accurately.

4.1.2.8. Optimization of the MS/MS conditions and predicted MRM (pMRM) method

After the general fragmentation mechanism was established (section 4.1.2.5) using standards synthesized with the model precursor (cyclohexene), it was confirmed that the mass spectrum of a more complex α -acyloxyhydroperoxy aldehydes can be accurately predicted. Therefore, if the structure of the α -acyloxyhydroperoxy aldehyde under consideration is known, the mass spectrum of the ammonium adduct can be accurately predicted without the need for standard synthesis, as it was concluded in Sections 4.1.2.5 and 4.1.2.6.

After investigating the fragmentation mechanism, MRM conditions for the compounds VII – XV were optimized. Compounds I – VI were not selected for the LC/MS method, since the linear carboxylic acids were not reported to be produced in significant quantities during gas-phase cyclohexene ozonolysis,¹³⁶ as already discussed in Section 4.1.1.1. The MRM conditions optimization procedure was the same, as for the carboxylic acids – see section 3.2.1. Positive

ionization mode was used to detect the ammonia adducts the synthesized standards shown in Fig. 4.9. Potentials: EP, DP, CEP, CE and CXP were swapped and optimal values for each MRM pairs were determined. Afterwards, CE was optimized for the ion products, and the most intense Q1/Q3 transitions were selected for the final method. Examples of the CE optimization for compound XI and compound XIV are shown in Fig. 4.21A and Fig. 4.21B.



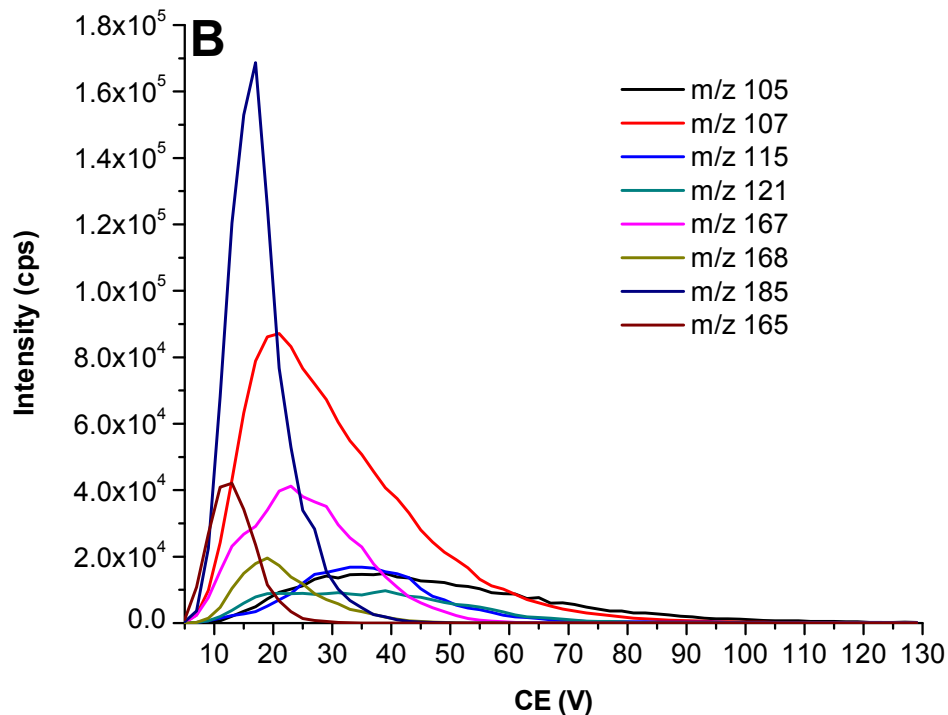


Figure 4.21 Optimization of the CE for the compound XI(A) and compound XIV(B)

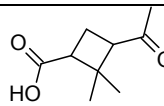
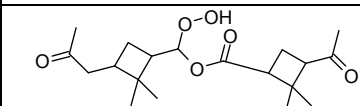
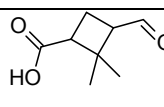
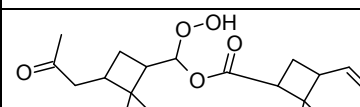
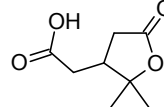
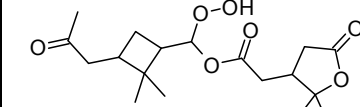
As shown in Fig. 4.21, the compounds XI and XIV produced different sets of fragment ions. For the compound XI (Fig. 4.21A), the most intense Q1/Q3 transitions were 294/147 and 294/129, 294/111 and 294/101 as listed in Table 4.12. For the compound XIV (Fig. 4.21B) four Q1/Q3 transitions selected for the final method were 386/202 and 386/185, 386/168 and 386/107, as also listed in Table 4.12. The first three fragment ions can be either scavenger – specific ions (cis-pinonic acid) or the ions produced by fragmentation of the peroxide side of the molecule, as already discussed in Section 4.1.3.5. The transition 386/107 was common for the compounds XIV and XV, and can be considered a marker of the cyclobutane ring presence, as already discussed in section 4.1.3.7. Results of the MRM conditions optimization for the synthesized compounds, listed in Table 4.7 are reported in Table 4.12.

Table 4.12 The most abundant Q1/Q3 transitions for the α -acyloxyhydroperoxy aldehydes selected for the final method

Compound number	Molecular weight (Da)	M+NH ₄ ⁺ m/z	MRMs
VII	246	264	117,99,71,67
VIII	260	278	148, 131, 114, 85
IX	248	266	119, 101, 113, 67
X	262	280	133, 115, 87, 67
XI	276	294	147, 129, 111, 101
XII	290	308	161, 143, 125, 67
XIII	304	322	175, 157, 83, 67
XIV	368	386	202, 185, 168, 107
XV	370	388	185, 168, 107, 105

As listed in Table 4.12, for the compounds VII – XIII scavenger's specific ions were the most abundant fragment, with the exception of the compound VIII, as discussed in Section 4.1.3.4. As already discussed in Section 4.1.3.6, m/z 202, 185 and 107 ions are most likely being produced as a result of the peroxide side fragmentation. It is therefore reasonable to assume, that the ammonium cationized ions of the compounds XVI – XVIII will produce the same set of ions, when the fragmentation of the peroxide side of the molecule is considered. As concluded in Section 4.1.3.6 the scavenger's specific fragment ions can be formed as a result of the ammonia adducts CID of the α -acyloxyhydroperoxy aldehydes formed from the reactions of α -pinene SCI with a different carboxylic acids. Based on the detailed evaluation of the fragmentation mechanism (section 4.1.2.5) and analysis of the compounds XIV and XV (section 4.1.2.6), fragment ions for a set of α -acyloxyhydroperoxy aldehydes listed in Table 4.13 were predicted.

Table 4.13 Predicted fragmentations of the α -acyloxyhydroperoxy aldehydes produced from α -pinene SCI and three carboxylic acids

Compound number	SCI scavenger	α -Acyloxyhydroperoxy aldehyde structure	Molecular weight (Da)	$M+NH_4^+$ m/z	Predicted major fragment ions
XVI	 Norpinonic acid MW 170 Da		354	372	185, 107, 202, 171, 189
XVII	 Pinalic-4-acid MW 156 Da		340	358	185, 107, 202, 157, 175
XVIII	 Terpenylic acid MW 172 Da		356	374	185, 107, 202, 173, 191

Five fragment ions for each compound listed in Table 4.13 were proposed. The first three fragments, listed in Table 4.13 are most likely to be formed as a result of the molecule peroxide side fragmentation. The next two ions corresponding to the protonated and ammonium cationized ions of the carboxylic acids (SCI scavengers) were also included in Table 4.13. The protonated and ammonium cationized acidic fragment ions were 171 and 189, 157 and 175, 173 and 191 for the norpinonic acid, pinalic-4-acid and terpenylic acid, respectively. Compounds XVI and XVII were proposed as potential nucleation precursors, as discussed in Section 1.4.4.^{117,150} Compound XVIII is the product of the reaction of SCI with the terpenylic acid. Terpenylic acid was recently proven to be produced in the early stages in SOA formation, as discussed in section 1.4.4.^{174,177,183} Since it was impossible to optimize the MRM conditions for the compounds listed in Table 4.13, the same ion-lenses voltages were used as for the analysis for the compounds XIV and XV. Therefore, MS/MS analysis conditions for the analysis of the compounds listed in Table 4.13 were not

optimized for the highest possible sensitivity. However, it is reasonable to assume that individual ion lenses voltages and CE for the compounds XIV and XV and the α -acyloxyhydroperoxy aldehydes presented in Table 4.13 did not differ significantly, due to very similar structures of these compounds.

4.2. SOA formation in the flow – tube reactor

Details of the flow tube reactor experimental setup are provided in section 3.4. In the flow-tube reactor precursor, cyclohexene or α -pinene was mixed with ozone to initiate SOA formation. Reactor schematic is presented in Section 3.4.2; reactor was designed in a similar manner to the flow tube reactors described in the studies published previously, summarized in Section 1.4.2.2. Movable plunger was used to shorten the reaction time without increasing the carrier gas flow rate and for reactants mixing. Reactants residence time and concentrations were also comparable with those used in the experiments, described in the literature - see Section 1.4.2.2. SOA generation conditions are described in Section 3.4.3. SOA was generated for both precursors under both low and high humidity conditions, as described in Section 3.4.3.

SOA was sampled onto a filter, extracted with a solvent and subjected to the LC/MS analysis as described in Section 3.4.3. LC/MS analysis conditions for the SOA samples are described in Section 3.2.2. During the SOA formation experiments, aerosol particles formation and growth were not monitored directly. Thus, the only indication of the SOA formation in the flow tube reactor was the detection of the particle-phase products with LC/MS. In the flow-tube reactor, pressure was controlled with the vacuum pump (see sections 3.4.1 and 3.4.2), thus pressure rise inside the reactor due to clogging of the filter was not observed. In Section 4.3, results of the SOA samples analysis with LC/MS are described.

All experiments under dry and humid conditions and with both precursors were performed at least three times, to ensure that the results were reproducible. Blank experiments for each set of the experimental parameters were also carried out, in the absence of the precursor or ozone. Experiments with cyclohexene-d10 (see section 4.3.1.1) were performed under the same conditions, as for the regular cyclohexene.

Reynolds number was calculated for the used set of experimental conditions to confirm that the SOA formation in the flow-tube reactor was performed under laminar flow conditions - see section 4.2.1. In order to minimize the possibility of the filter artifacts formation, the reactants concentrations were adjusted so that the ozone was almost completely consumed before reaching the filter capsule – section 4.2.2. Also, no OH radicals scavengers were used in this study, since the use of such scavengers was concluded to alter the original product distribution, as discussed in Sections 4.2.3 and 1.4.2.3.

4.2.1. Flow conditions calculations

Flow rates of the carrier gas, air flowing through bubblers filled with water and liquid precursor as well as through ozone generator are listed in Table 4.14. Such flow rates were necessary to obtain the desired concentrations of the water vapor, the precursor and the ozone inside the reactor. The total flow rate was 800 ml/min.

Table 4.14 Flow rates through the flow-tube reactor

RH conditions and precursor		Flow rates (ml/min)			
Precursor	RH (%)	Carrier gas	Humidifier	Precursor	Ozone
Cyclohexene	4	790	3	5	10
	40	410	370	5	10
α -pinene	4	690	3	100	10
	40	690	370	100	10

In order to determine if reaction in the flow tube will take place under laminar or turbulent conditions, Reynolds number for a set of experimental conditions used in this study was calculated, according to Eq. 4.1:

$$Re = \frac{Q \cdot D_H}{v \cdot A} \quad (4.1)$$

Where:

A: tube cross-sectional area - (m²)

Q: volumetric flow rate - (m³s⁻¹)

D_H : hydraulic diameter of the pipe - (m)

ν : air kinematic viscosity - (m^2s^{-1})

Values used for Reynolds number calculations were as follows: $A=0.028 \text{ m}^2$, $Q=1.667 \times 10^{-5} \text{ m}^3/\text{s}$ – see Table 3.1, $D_H=0.0595 \text{ m}$, $\nu=1.51 \times 10^{-5} \text{ m}^2/\text{s}$, yielding the Reynolds number of 24, thus proving that reaction was performed under laminar conditions. Since the plunger was positioned 15 cm before the outlet of the reactor, the mean reaction time was calculated to be approx. 33 seconds, under laminar flow conditions

4.2.2. Box model calculations

Box model simulations were performed in order to confirm that the ozone was completely consumed before reaching the end of the reactor, as well as for calculating the amount of precursor consumed during a single experimental run.

In order to ensure that the ozone will be almost completely consumed before reaching the end of the reactor, calculations were performed using the reactants concentrations and reaction time reported in Table 4.3. Calculated ozone temporal profiles in both experiments are shown in Fig. 4.22A and Fig. 4.22B. Reaction rate coefficients in Table 4.15 were mean values, calculated using the numbers listed in the NIST Chemical Kinetics Database.¹⁰¹

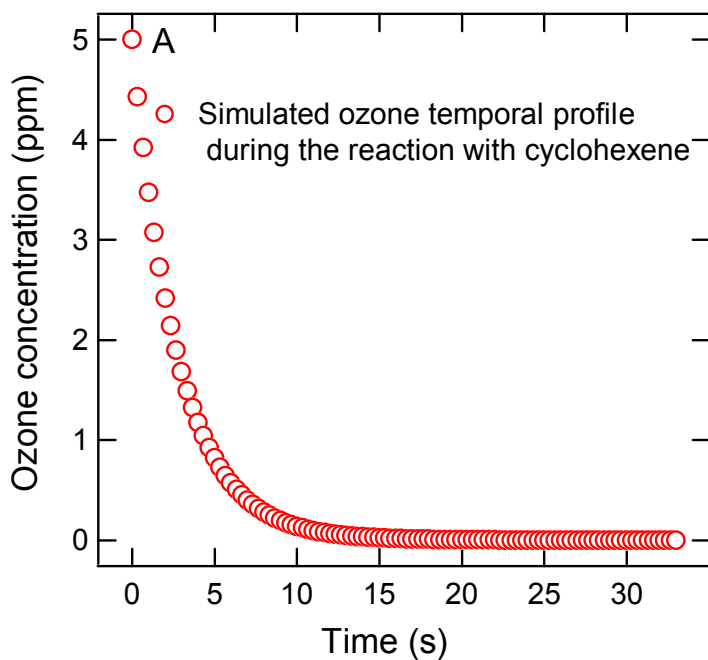
Table 4.15 Ozonolysis reaction rate coefficients for cyclohexene and α -pinene reported in the literature

Precursor	Reaction rate coefficient with O_3 ($\text{cm}^3 \text{ molecule}^{-1} \text{ s}^{-1}$) at 298 K	Reference
α -pinene	8.11×10^{-17}	Khamaganov and Hites ⁹⁸
	8.00×10^{-17}	Munshi et al. ⁹⁹
	8.09×10^{-17}	Atkinson et al. ¹⁰⁵
Cyclohexene	7.44×10^{-17}	Treacy et al. ²⁰⁴
	7.46×10^{-17} (296 K)	Greene and Atkinson ²⁰⁵
	7.80×10^{-17} (297 K)	Nolting et al. ²⁰⁶

As shown in Table 4.15, for both cyclohexene and α -pinene the reaction rate coefficients with ozone are well established, and discrepancies between the values reported in the literature are relatively low. For convenience, the numbers in $\text{cm}^3 \text{ molecule}^{-1} \text{ s}^{-1}$ were converted to the $\text{ppm}^{-1} \text{ s}^{-1}$ listed in Table 3.3. The conversion was performed using the formula given by Kamens et al.⁹³

Table 4.16 Concentrations of the reactants and reaction rate coefficients used for calculations

Precursor	Precursor concentration (ppm)	Ozone concentration (ppm)	Reaction rate coefficient ($\text{ppm}^{-1} \text{ s}^{-1}$)	Reaction time (s)	Consumed ozone (%)
Cyclohexene	220	5	0.00183	33	>99.999
α -Pinene	220	5	0.00213		>99.999



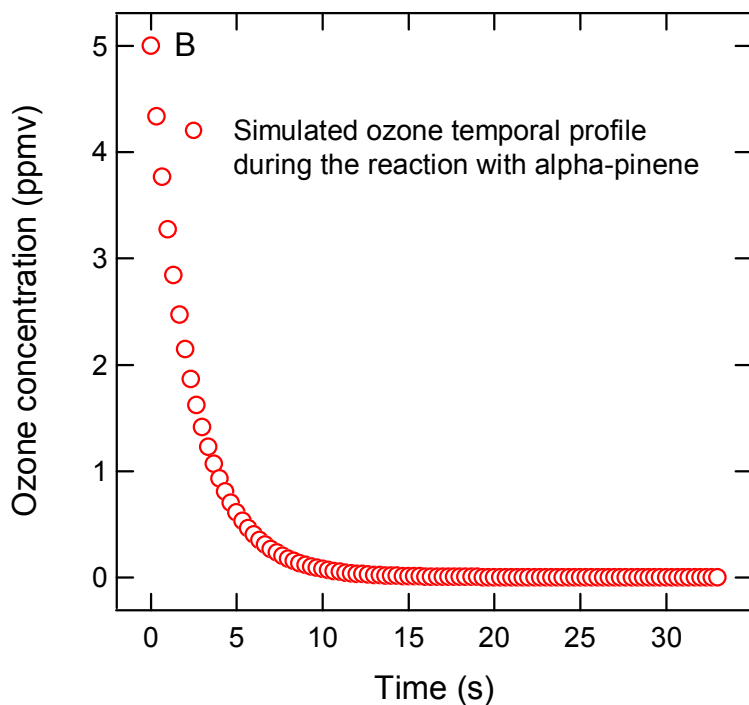


Figure 4.22 Simulated temporal profiles of ozone under experimental conditions listed in Table 3.3 during the reaction with cyclohexene (A) and α -pinene (B).

As shown in Fig 4.22A and Fig 4.22B, under experimental conditions employed in this work, 99.999% of ozone was consumed after 33 s of the reaction (also, see Table 4.16). Therefore, it can be assumed that only negligible amount of ozone was passing through the filter during the SOA collection. Based on the box model simulations, the following conclusions can be made. Taking into account accuracy of the ozone and precursors concentration measurements, ozone concentration was adjusted to about 3.5 ppmv – see Table 3.1. Also, sufficient excess of the precursor has to be present to consume all of the ozone, and avoid artifacts formation during sampling. As reported in Section 3.4.2 both precursors concentrations were higher than 200 ppmv used for box model calculations, and always kept well above this threshold concentration.

As already discussed in Section 1.3.3 and Section 1.4.1, during the ozonolysis of alkenes, high amounts of OH radicals are formed. Therefore, in order to calculate the molar yields of the detected LMW and HMW products, reported in Section 4.3.1.1, Section 4.3.1.4.1, Section 4.3.2.1

and Section 4.3.2.4.1, the total amount of the precursor, oxidized during each experiment is needed.

Table 4.17 Kinetic calculations input parameters, used for calculating the total amount of consumed precursor

Precursor	Concentration (ppm)	Ozone concentration	OH radicals yield	Reaction rate coefficient with OH ($\text{ppm}^{-1} \text{s}^{-1}$)
Cyclohexene	220	3.5	0.55	1659
α -pinene	220	3.5	0.85	1312

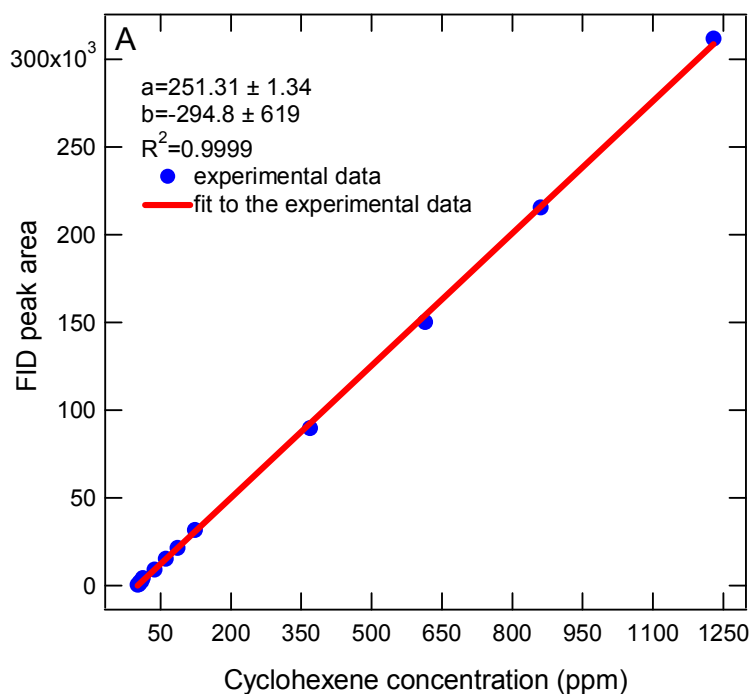
The OH yields and reaction rate coefficients listed in Table 4.17 were taken from summaries published by Atkinson¹⁵⁸ and Finlayson-Pitts and Pitts jr.¹ Concentrations of the precursor used for the simulations (Table 4.16) were lower than those used in the actual experiments (see Table 3.1). However, it was concluded that as long as the high excess of the precursor was present in the flow-tube reactor, the amount of the reacted alkene remained constant. Ozone concentration during each experiment was approx. 3.5 ppm, as listed in Section 3.4.2. It is known that one ozone molecule reacts with one alkene molecule (section 1.3.3). Also, single OH radical reacts with the single alkene molecule. Using the input values listed in Table 4.17, it was calculated, that 5.4 ppm of cyclohexene and 6.48 ppm of α -pinene was consumed during 33s of reactants residence time inside the reactor. Knowing the reaction vessel volume, the amount of the precursors consumed during 2 h of the experimental run was calculated to be approx. 2.22×10^{-5} M of cyclohexene and 2.66×10^{-5} M of α -pinene. These values include precursor oxidation by the ozone and OH radicals, generated as a result of gas-phase alkene ozonolysis.

4.2.3. Precursors concentrations monitoring

During the SOA formation experiments, concentration of α -pinene and cyclohexene was monitored with GC/FID. GC/FID conditions for the analysis of cyclohexene and α -pinene are

reported in section 3.2.4. Samples were taken from the sampling port positioned in the middle of the reactor, as described in Section 3.4.1.

For both precursors, GC/FID was calibrated over the range from 1 to 1000 ppmv. Standard solutions were prepared by diluting different volumes of cyclohexene and α -pinene (1 – 100 μ l) with n-pentane to reach the total volume of 1 ml. Afterwards, 1 μ l of each standard solution was added to the 20.3 ml gas-tight headspace vial and thermostated for 10 min in water bath at 35°C. Alkene concentration was calculated using ideal gas-law after correcting for temperature; pressure inside the headspace vial was assumed to be unaffected by expansion of 1 μ l of the pentane solution. After cooling down to room temperature, 100 μ l of air from the vial was injected into the GC using gas-tight syringe and each sample was analyzed only once. Solutions for each concentration were prepared and analyzed three times. Calibration curves were calculated using FID peak areas and analyte concentration in ppm. Squared correlation coefficients (R^2) \geq 0.999 were obtained for both compounds. Calibration curves are shown in Fig. 4.23A for cyclohexene and Fig. 4.23B for α -pinene.



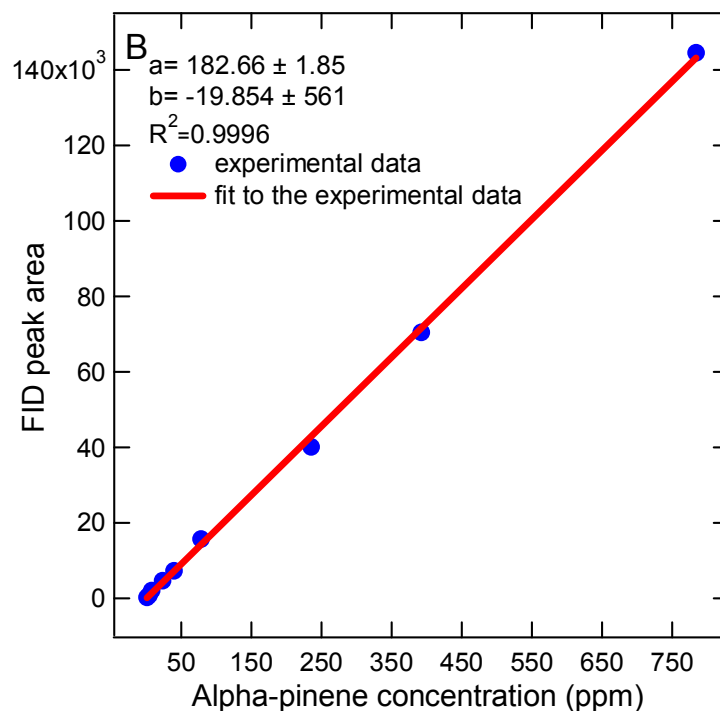


Figure 4.23 GC calibration curves for cyclohexene (A) and α -pinene (B)

Equations, obtained from linear regression analysis used for calculating the precursor concentration in the flow – tube are shown in Fig. 4.23A and Fig. 4.23B. Concentration of cyclohexene-d10 was calculated using the FID response factor for the regular cyclohexene. The results of the SOA generation experiments using cyclohexene-d10 are described in Section 4.3.1.1.1 and section 4.3.1.3.1.

4.2.4. OH radicals scavengers

Large amounts of the highly reactive OH radicals are known to be formed during ozonolysis of the alkenes, as already discussed in Section 1.3.3, Section 1.4.1 and Section 1.4.2.3. Therefore, frequently, high concentrations of the OH radicals scavengers are used during the laboratory studies of SOA formation (see section 1.4.2.3). However, it was concluded that the use of OH radicals scavengers influences the SOA formation mechanism and thus alters the original products distribution, as discussed in section 1.4.2.3.

It was previously reported, that the use of OH radicals scavengers alter the LMW products distributions, formed during the gas phase ozone initiated oxidation of α -pinene.^{120,159 160} It is also

important to underline, that, up-to date, it was not examined, if the formation yields of the HMW α -pinene SOA components are affected by the OH radical's scavengers. However, it was unambiguously proven that the SOA yields, as well as yields of the individual LMW products are dependent on the OH radical scavenger type and concentration.^{120,159,160}

Therefore, it is straightforward to assume that, since the LMW SOA components are the building blocks for the HMW compounds (see section 1.4.3.4 and section 1.4.3), that the formation yields of these HMW compounds are also scavengers dependent.

Taking into account the previously published results, discussed above and in section 1.4.2.3, it can be concluded, that the presence of the OH radicals scavengers significantly alter the SOA generation mechanism from ozone – initiated α -pinene oxidation. In the ambient atmosphere, both α -pinene oxidation channels, by O_3 and OH radicals, are operational. Therefore, performing the laboratory studies in the absence of the OH radicals scavengers is more representative, when the SOA formation in the ambient atmosphere is considered. Also, high amounts of some OH radicals scavengers can act as the SCI scavengers, as it was concluded in the previously published studies.^{125,129,149,150,156} Also, products of the reaction of the most frequently used OH radicals scavengers are often carbonyl compounds or alcohols; such compounds can also potentially act as the SCI scavengers.

Thus, in order to obtain more reliable data, no OH radicals scavengers were used during the SOA generation experiments in the flow-tube reactor conducted in this work.

4.3. Analysis of SOA samples generated in the flow tube reactor

In this section analysis of SOA samples generated in a flow-tube reactor with the developed LC/MS analysis method is described. LC/MS analysis conditions are described in section 3.2.2. SOA sample in each set of experimental conditions (see section 3.4.2) was prepared and analyzed three times to confirm the results reproducibility. Every result presented in this section was confirmed by analysis of the blank sample, generated in the absence of the ozone or precursor, as described in Section 3.4.2.

4.3.1. SOA produced from ozonolysis of the model compound – cyclohexene

Globally, cyclohexene SOA forming potential is very low when the ambient atmosphere is considered, as compared to the monoterpenes – see section 1.3.1.

However, very frequently cyclic alkenes, like cyclohexene and 1-methylcyclohexene, are used as the simpler analogues of α -pinene. Those simple cyclic alkenes can be considered model compounds for all the endocyclic monoterpenes. Investigation of the simpler precursors have provided very valuable insight in the mechanism and chemical composition of SOA generated in the more complex monoterpenes/ozone systems.^{88,136,142,170,171,176,185,207,208} Therefore, SOA composition, produced from the ozone initiated oxidation of a model compound - cyclohexene was initially investigated.

Carboxylic acids analysis in the SOA samples is described in Section 4.3.1.1 and section 4.3.1.1.1, for the cyclohexene and cyclohexene-d10, respectively. Carboxylic acids produced during cyclohexene ozonolysis were analyzed as described in Section 4.1.1.1.

Afterwards, investigation of the α -acyloxyhydroperoxy aldehydes formation is discussed in Section 4.3.1.2. α -acyloxyhydroperoxy aldehydes were analyzed as described in section 4.1.2. Aside from α -acyloxyhydroperoxy aldehyde, formation of other HMW SOA components was investigated in section 4.3.1.3. Using the data acquired for the deuterated analogs of the LMW SOA components generated during the cyclohexene ozonolysis, structures of the detected HMW SOA components (section 4.3.1.3) were proposed, as described in section 4.3.1.3.1.

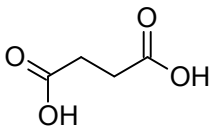
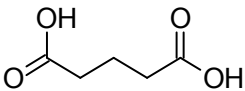
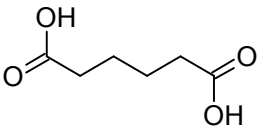
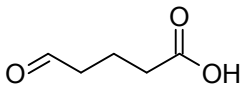
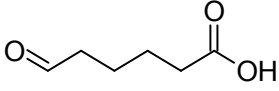
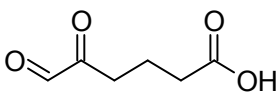
RH influence on SOA composition is discussed in sections 4.3.1.4, including the impact of higher water concentration on the formation of carboxylic acids (section 4.3.1.4.1), α -acyloxyhydroperoxy aldehydes (section 4.3.1.4.2) and other high-molecular weight SOA components (section 4.3.1.4.3).

4.3.1.1. Carboxylic acids identification

In this section, investigation of the carboxylic acids formation during the SOA generation by cyclohexene ozonolysis is described. Carboxylic acids detected in the SOA samples formed by

ozone-initiated cyclohexene oxidation in the flow-tube reactor under low humidity conditions (RH \approx 3%) are listed in Table 4.18.

Table 4.18 Carboxylic acids identified in the SOA samples formed by ozone-initiated cyclohexene oxidation under dry conditions (RH \approx 3%)

Name	Structure	Molecular weight (Da)
Succinic acid		118
Glutaric acid		132
Adipic acid		146
5-oxopentanoic acid		116
6-oxohexanoic acid		130
4,5-dioxopentanoic acid		144

Succinic, adipic and glutaric acids listed in Table 4.18 were identified based on the comparison with the actual standards. MRM and EIC chromatograms of the cyclohexene SOA samples for these three carboxylic acids are shown in Fig. 4.21.

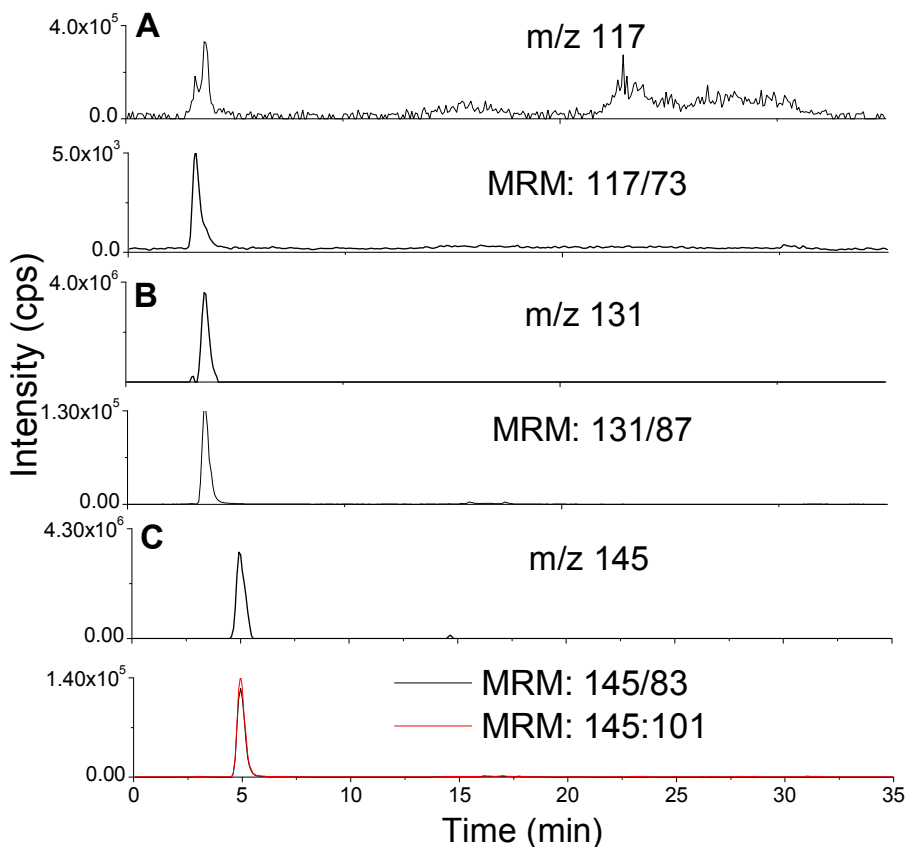


Figure 4.24 ECI and MRM chromatograms for succinic acid (A), glutaric acid (B) and adipic acid (C) in the SOA sample

For the succinic acid (Fig. 4.24A), glutaric acid (Fig. 4.24B), and adipic acid (Fig. 4.24C) both MRMs and deprotonated pseudo-molecular ions were detected, unambiguously confirming the presence of these three acids in SOA samples formed by cyclohexene ozonolysis.

On the other hand, both α -carboxylic acids containing carbonyl group listed in Table 4.2, levulinic and 5-oxohexanoic acids were concluded to be absent in the aerosol samples. However, intense peaks for the deprotonated pseudo-molecular ions for these two carboxylic acids were detected, as shown in Fig. 4.25.

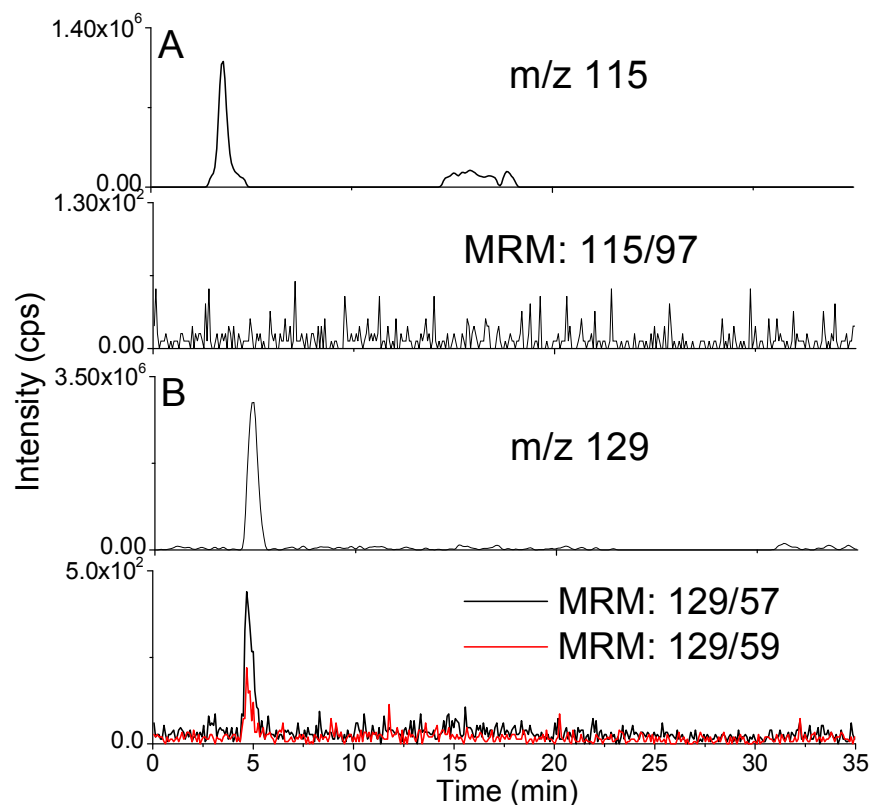


Fig. 4.25 ECI and MRM chromatograms for levulinic acid (A) and 5-oxohexanoic acid (B) in the SOA sample

The absence of the specific fragment ions for the levulinic acid (Fig. 4.25A) and only very minor MRM peaks for the 5-oxohexanoic acid (Fig. 4.25B) while the parent ions were clearly present can be explained by the presence of structurally different carboxylic acids with the same MWs as the analyzed standards. Based on the mechanistic implications and previously published data^{136,209-211} these compounds can be identified as 5-oxopentanoic and 6-oxohexanoic.^{137,210-212}

The structural information for the compound with MW 144 Da was less conclusive. However, intense peak, most likely originating from the deprotonated, pseudo-molecular ion m/z 143 was also detected. EIC for the m/z 143 is shown in Fig.4.26.

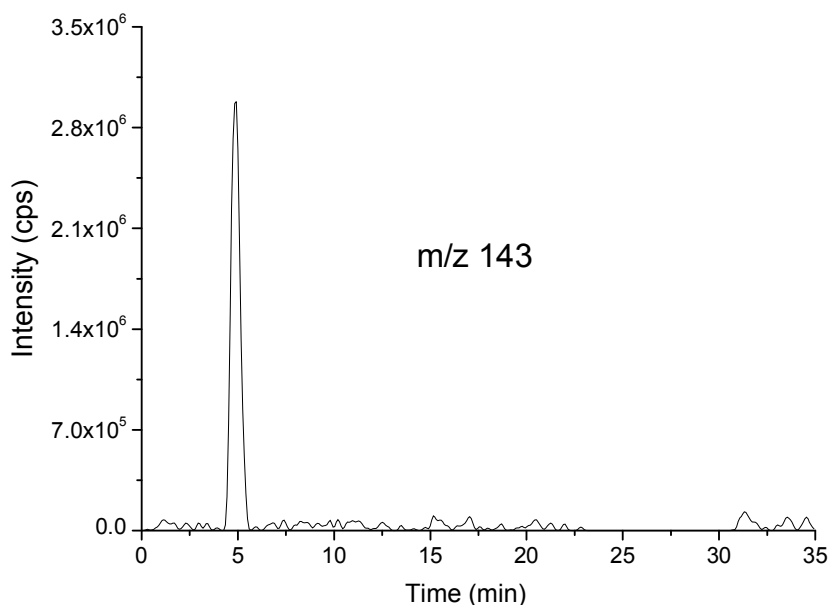


Fig. 4.26 ECI chromatogram for m/z 143 in the SOA sample

As shown in Fig. 4.26, short retention time of this compound suggested that it was most likely carboxylic acid with additional oxygen-containing functional group, making the compound under consideration more polar than for instance carboxylic acid with lower MW, such as 5-oxopentanoic acid.

Using the calibration curves, listed in Section 4.1.1.1, concentration of each carboxylic acid in the SOA sample was calculated. For the 5-oxopentanoic and 6-oxohexanoic calibration curves obtained for the levulinic acid and 5-oxohexanoic acids were used. For the compound with the MW 144 Da, mean MS response factor for the carboxylic acids containing carbonyl group was used. Concentrations of the carboxylic acids were subsequently used to calculate their molar yields, listed in Table 4.19. Amount of the cyclohexene consumed during a single experimental run, as a result of oxidation by both ozone and OH radicals was calculated as described in Section 4.2.2.

Table 4.19 Molar yields of the carboxylic acids identified in the SOA samples formed by ozone-initiated cyclohexene oxidation under dry conditions (RH \approx 3%)

Name	M-H ⁻	Retention time (min)	Molar yield
Succinic acid	117	3.08	$(2.8 \pm 0.4) \times 10^{-4}$
4.5-dioxopentanoic acid*	143	3.14	$(4.0 \pm 0.3) \times 10^{-4}$
5-oxopentanoic acid	115	3.5	$(1.6 \pm 0.4) \times 10^{-3}$
Glutaric acid	131	3.58	$(5.1 \pm 0.4) \times 10^{-3}$
6-oxohexanoic acid	129	4.79	$(2.4 \pm 0.3) \times 10^{-3}$
Adipic acid	145	4.99	$(5.9 \pm 1.0) \times 10^{-3}$

Molar yields, listed in Table 4.19 are the cyclohexene molar yields, representing the fraction of cyclohexene molecules converted into the given carboxylic acid. Unfortunately, the experimental setup used in this work (see section 3.4) was not equipped with the instrument, capable of measuring particles size distribution, such as SMPS. Therefore, it was not possible to estimate the portion of SOA mass corresponding to the carboxylic acids listed in Table 4.18.

Adipic and glutaric acids were produced with highest yields, which is consistent with the literature data.^{136,210,211} Relative yields of the succinic acids are also in good agreement with previously reported values¹³⁶. 4.5-dioxopentanoic acid formation yield differ more significantly from the literature data,¹³⁶ as compared to the formation yields for dicarboxylic acids. Due to the lack of the standard, this compound may have been incorrectly identified. This difference in yield can be attributed to a shorter reaction time-scale in the flow-tube as compared to the reaction in the smog-chamber. Once formed, 6-oxohexanoic, as well as other carboxylic acids, can undergo subsequent reactions to form a variety of different products, similar to e.g. adipic acid (see below). 6-oxohexanoic formation mechanism is most likely analogous to the formation mechanism of the cis-pinonic acid. It can be generated directly from the SCI via ester channel or by SCI reaction with water. Thus, it is likely to be produced in the early stages of SOA formation in larger quantities.

No peaks suggesting the presence of the higher MW carboxylic acids, such as pimelic and suberic acids, were detected in cyclohexene SOA samples. It is important to underline that no carboxylic acid containing more carbon atoms than the original alkene was detected. Also, it is important to note, that in the study by Gao et al,¹³⁶ significantly larger number of carboxylic acids were detected in the cyclohexene SOA samples, including pimelic and adipic acid derivatives, such as 2-hydroxyadipic acid. The lack of higher-MW carboxylic acids can also be explained by the short formation time-scale of the SOA formation used in this work. This agrees well with the relatively simple composition of the freshly formed cyclohexene SOA, reported by Nojgaard et al.²¹¹ The formation mechanism of pimelic and suberic acids as well as of other carboxylic acids previously detected in cyclohexene SOA samples,^{136,210} is more complex, and consequently slower. In general, the LMW compounds found in SOA samples, formed during ozone-initiated cyclohexene oxidation under dry conditions (RH ≈ 3%) found in this work agreed very well with the previously published data.^{136,210,211}

4.3.1.1.1. Isotope study

Cyclohexene-d10 SOA was generated under the same conditions as for regular cyclohexene, as described in Section 3.4.4. Standards for the deuterated analogs of the carboxylic acids listed in Table 4.18 were not available. Carboxylic acids detected in the cyclohexene-d10 SOA are listed in Table 4.20. Deprotonated, pseudo-molecular ions for the non-labeled carboxylic acids and their deuterated analogs are also listed in Table 4.20.

Table 4.20 Carboxylic acids obtained from the gas-phase ozonolysis of cyclohexene-d10

Carboxylic acid	Retention time (cyclohexene)	M-H ⁻ (cyclohexene)	M-H ⁻ (cyclohexene-D10)	Retention time (cyclohexene-D10)	Number of original precursor hydrogen
Succinic acid	3.08	117	121	3.20	4

4.5-dioxopentanoic acid	3.14	143	150	3.10	7
5-oxopentanoic acid	3.5	115	122	3.40	7
Glutaric acid	3.58	131	137	3.61	6
6-oxohexanoic acid	4.79	129	138	4.52	9
Adipic acid	4.99	145	153	5.00	8

EIC's chromatograms of the cyclohexene-d₁₀ SOA samples for the m/z 121, 150, 122, 137, 138 and 153 ions listed in Table 4.20 are shown in Fig. 4.27.

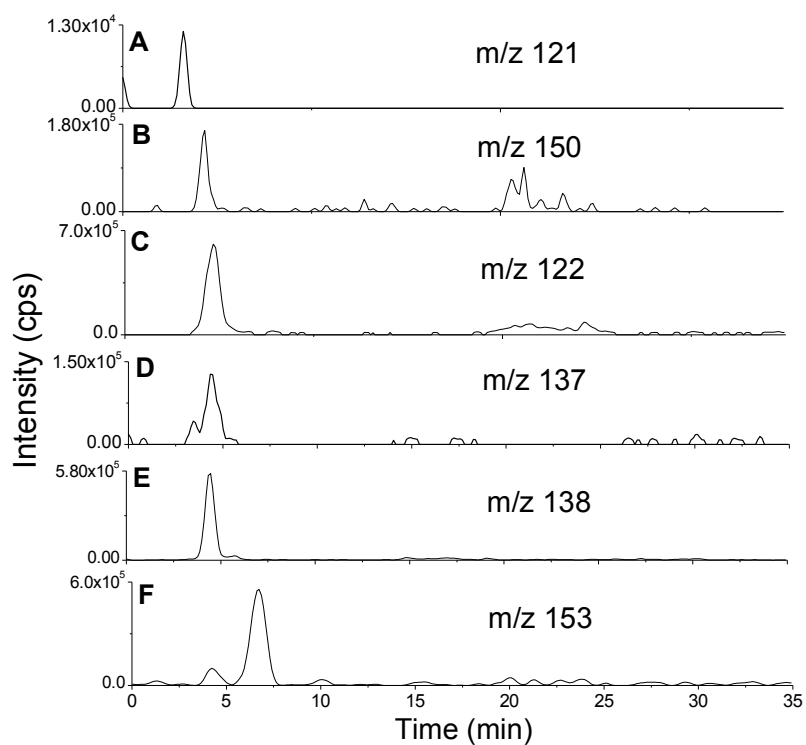


Figure 4.27 EIC's chromatograms of the cyclohexene-d10 carboxylic: m/z 121 (A), 150 (B), 122(C), 137 (D), 138 (E) and 153 (F) acids in the SOA sample

As can be seen in Fig. 4.27 (A), peak for EIC m/z 121 was detected at a retention time of 3.20 in the cyclohexene-d10 SOA sample, most likely corresponding to the deuterated succinic acid. Succinic acid $M-H^-$ ion was shifted by 4 mass units, equal to the number of the aliphatic hydrogen in this acid molecule. Since the retention times of compounds with MW 123 Da and 151 Da, corresponding to mass peaks with m/z 122 and 150 were very similar, there may be some confusion, which m/z corresponds to the specific carboxylic acid. The following reasoning can be used to resolve this ambiguity. Both m/z 122 and 150 cannot correspond to the deuterated succinic acid, because the mass shift of 5 and 33 is too large, since there are only 4 aliphatic hydrogens present in the succinic acid molecule. By the same logic, m/z 150 is not a deuterated 5-oxopentanoic acid. Thus, m/z 150 can be assigned to the deprotonated pseudo-molecular ion for the deuterated 4,5-dioxopentanoic acid. By analogy the deuterated ion of 5-oxopentanoic acid can be found at m/z 122. These assumptions agree with the number of aliphatic hydrogen atoms in molecules of those acids, as listed in Table 4.20. It is important to underline at this point, that the compound structure detected with m/z 143 (see section 4.3.1.1 and Table 4.19) cannot be unambiguously confirmed, based on the stable isotope study discussed in this section. This compound was tentatively identified as 4,5-dioxopentanoic acid, based on the experimental data obtained for experiments with cyclohexene – see section 4.3.1.1. However, there are still different structural isomers of this acid, and definitive conclusions cannot be presented, based on the experimental data acquired in this study.

For the deuterated glutaric acid, the ion m/z 137 was partially overlapping with the EIC from m/z 138, as shown in Fig. 4.27D and Fig. 4.27E. However, weakly intense but clearly present peak at retention time 3.61 min was detected, corresponding to the deprotonated, pseudo-molecular ion for glutaric acid, shifted by 6 mass units, which is in line with the number of aliphatic hydrogen atoms present in this molecule.

Intense peak for ion m/z 138 was found at retention time 4.52 min., most likely corresponding to the deuterated 6-oxohexanoic acid. This ion is shifted by 9 mass units, equal to the number of aliphatic hydrogen atoms in the 6-oxohexanoic acid molecule.

Intense peak for m/z 153 was also detected in cyclohexene-d10 SOA at retention time 5.10 min, most likely corresponding to the deuterated adipic acid, and thus shifted by 8 mass units. Mass shift of the $M-H^-$ ion of adipic acid corresponds to the number of aliphatic hydrogen atoms in this acid molecule.

By generating SOA in the flow-tube reactor, using cyclohexene-d10 instead of regular cyclohexene, it was possible to draw several important conclusions regarding the formation of the carboxylic acids listed in Table 4.18. Mass shifts of the carboxylic acids listed in Table 4.18 were equal to the number of original precursor hydrogen, when cyclohexene was substituted with cyclohexene-d10. The results presented in this section have shown that aliphatic hydrogens in the detected carboxylic acid molecules are not dissociated during the precursor oxidation and formation of the detected carboxylic acids.

4.3.1.2. Investigation of α -acyloxyhydroperoxy aldehydes formation

In this section, investigation of the α -acyloxyhydroperoxy aldehyde formation during cyclohexene SOA generation is described. During the initial experimental run, MRMs for the compounds VII – X were monitored. Carboxylic acids used for the synthesis of the compounds IX – XI were detected in SOA samples as described in Section 4.3.1.2. Also, isobaric carboxylic acids as those used for the synthesis of the compounds VII and VIII, were also detected in the aerosol samples.

EIC and MRM chromatograms for the compounds VII, IX, and X are shown in Fig. 4.28A, Fig. 4.28B and Fig. 4.28C.

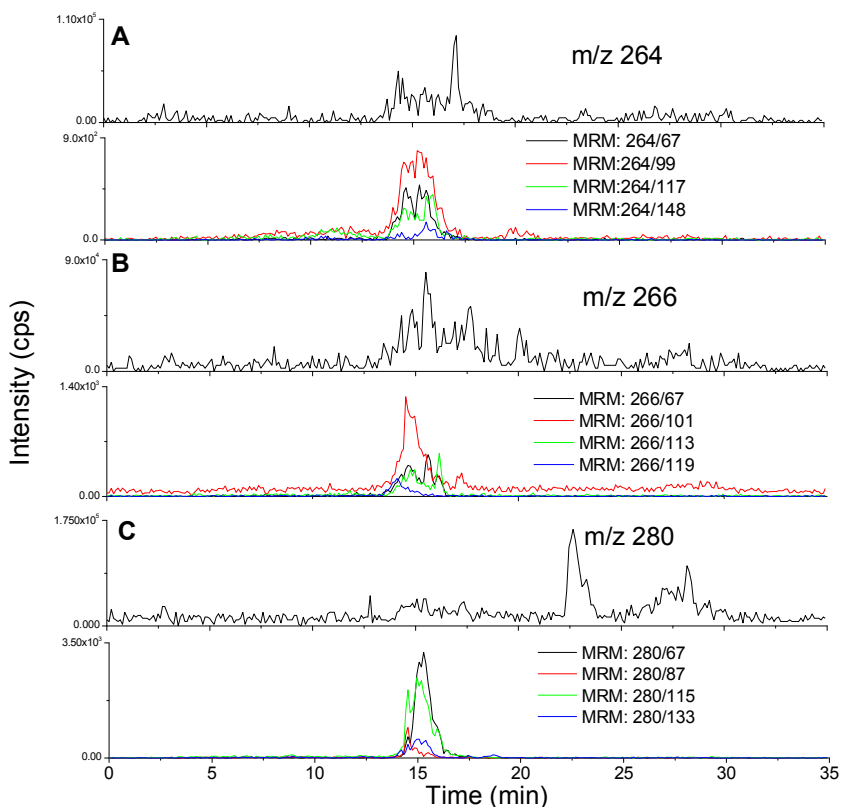


Figure 4.28 ECI and MRM chromatograms for the compound VII (A), IX (B), and X (C) from the SOA sample

As shown in Fig. 4.28, for the compounds VII, IX and X, the ammonium cationized ions were not detected, and only background signals were observed. Also, weakly intense peaks for the monitored MRM's for these compounds are visible. However, the intensities and shape of these peaks strongly indicated that these were only the background noise. Therefore, it was concluded, that compounds VII, IX and X were not present in the cyclohexene SOA samples.

EIC and MRM chromatograms for the compounds VIII, and XI are shown in Fig. 4.29A, Fig. 4.29B.

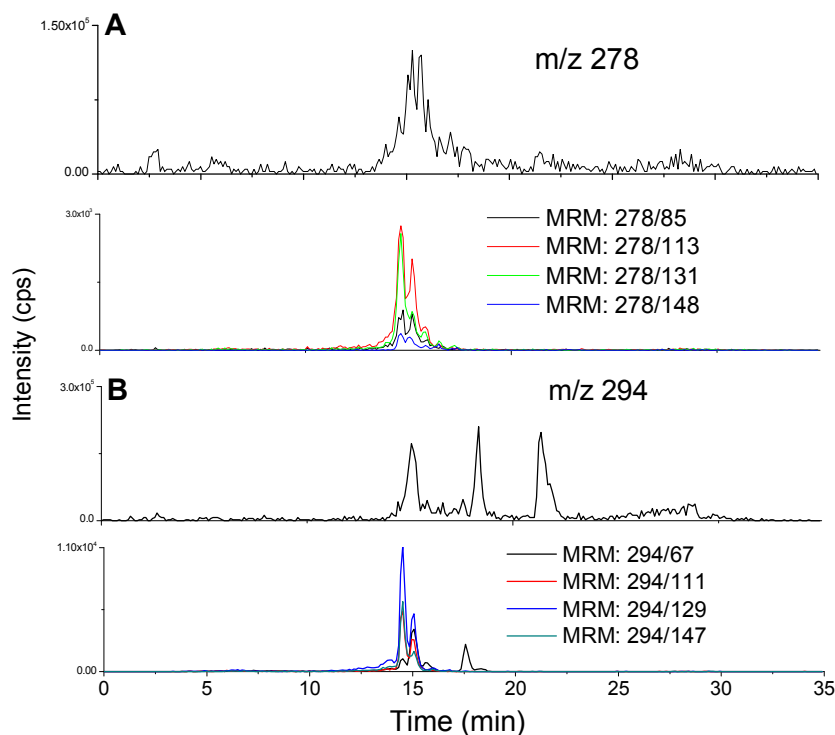


Figure 4.29 M ECI and MRM chromatograms for the compound VIII (A), and XI (B) in the SOA sample

As it can be seen in Fig. 4.29 minor peaks for both ammonium cationized ions and MRM's were detected in the SOA samples. Although these peaks were also comparable with the background noise, similar for the compounds VII, IX and X, however, significantly higher intensity of the peaks shown in Fig. 4.29 created an ambiguity, whether the minor quantities of the compounds VIII and XI were present in the cyclohexene SOA samples. In order to resolve this ambiguity, LC/MS analysis of the standards for the compounds VIII and XI was performed. EIC and MRM chromatograms for the standards of the compounds VIII, and XI are shown in Fig. 4.30A, Fig. 4.30B, respectively.

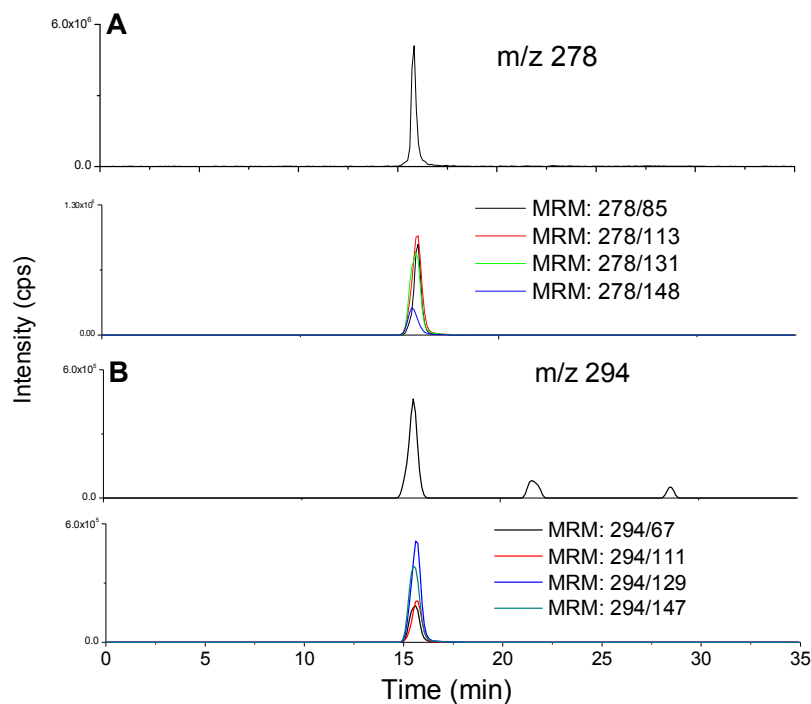


Figure 4.30 ECI and MRM chromatograms for the compound VIII (A), and XI (B) in the standard samples

By comparing the ECI and MRM chromatograms, the retention times of the peaks detected in the SOA samples (14:52 min) and synthesized standard (15:73 min) differ significantly. Also, comparison of the MS^2 spectra of the m/z 294 in the standard sample and SOA sample was performed. MS^2 spectra of the m/z 294 in the standard sample (A) and cyclohexene SOA (B) is shown in Fig. 4.31. Please note that background spectrum was subtracted from both spectra shown in Fig. 4.31.

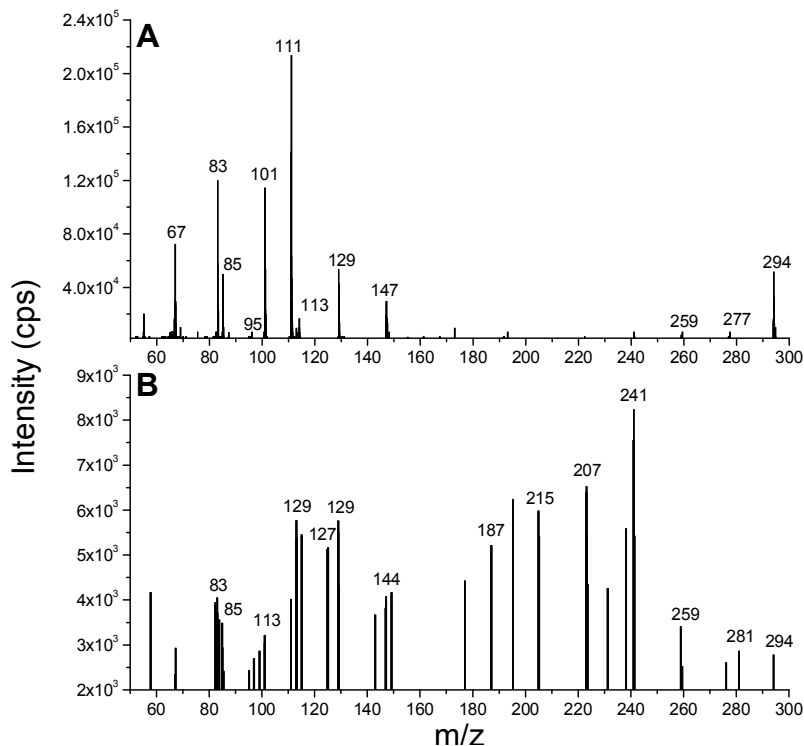


Figure 4.31 MS² spectra of the m/z 294 from the LC/MS analysis of the compound XI standard (A) and in the SOA sample (B)

As shown in Fig. 4.31A, MS² of the m/z 294 in the standard sample is in excellent agreement with the spectrum of the compound XI acquired in the direct infusion mode – see Fig. 4.15E. Also, fragmentation spectrum of the ion m/z 294 in the SOA sample differ significantly from the spectrum of the standard compound, as could be seen in Fig. 4.31B. Of course, in the SOA sample, the additional compound with m/z 294 may be present at the same retention time. However, if the MS² spectrum of the compound XI, present in the SOA sample, was overlapping with the spectrum of another, isobaric compound, the spectrum seen in Fig. 4.31B should be composed of fragments, shown in Fig. 4.31A. However, only few ions are common for the spectra presented in Fig. 4.31A and Fig. 4.31B. Thus the unambiguous confirmation of the presence of the compound XI is not possible.

However, a presence of the α -acyloxyhydroperoxy aldehyde formed by SCl reaction with 6-oxohexanoic acid could not be confirmed by comparison of the retention times with the compound VIII. Compound VIII was synthesized using 5-oxohexanoic acid, and this acid was not

detected in SOA samples formed by ozone-initiated oxidation of cyclohexene, as already discussed in Section 4.3.1.1. Instead, isobaric carboxylic acid, 6-oxohexanoic acid was detected in significant quantities. Therefore, retention times of the compound VIII and α -acyloxyhydroperoxy aldehyde formed by SCI association with 6-oxohexanoic acid are expected to be different. Moreover, as already discussed in section 4.1.2.5, both isobaric α -acyloxyhydroperoxy aldehydes should produce the same fragment ions. Therefore, the comparison of the MS² spectra for the m/z 278 ion of the standard and in the SOA samples should allow confirming or eliminating the formation of α -acyloxyhydroperoxy aldehyde with MW 278 Da during gas-phase cyclohexene ozonolysis. MS² spectra of the m/z 278 in the standard sample (A) and cyclohexene SOA (B) are shown in Fig. 4.32.

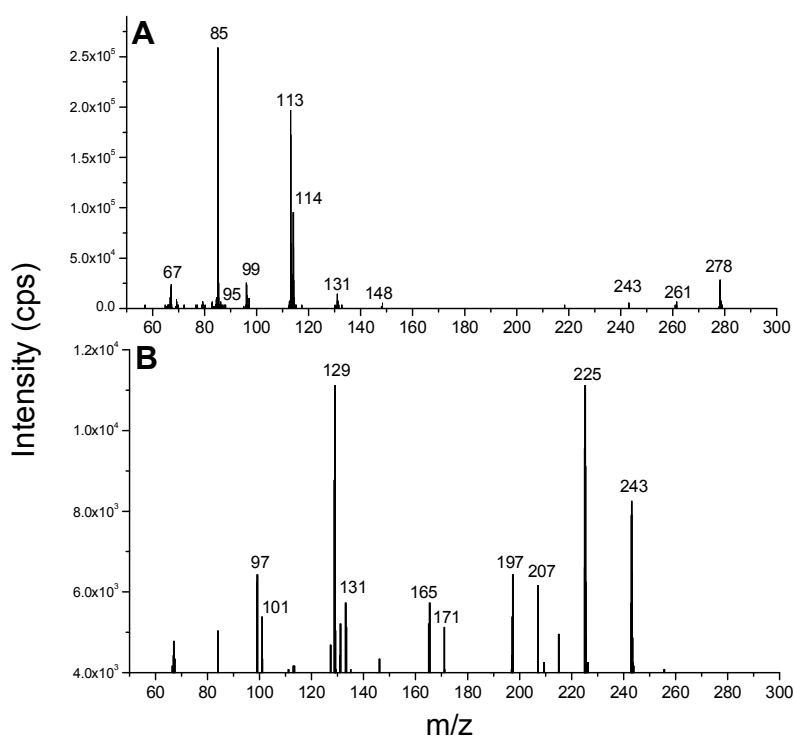


Figure 4.32 MS² spectra of the m/z 278 from the LC/MS analysis of the compound VIII standard (A) and in the SOA sample (B)

As shown in Fig. 4.32(B) spectra of the m/z 278 in the SOA sample, differ significantly from the standard spectra shown in Fig. 4.32A. Thus, most likely the ion peaks seen in the MRM chromatograms, presented in Fig. 4.29, originated from different aerosol components and/or from the background signal, but not from the α -acyloxyhydroperoxy aldehydes.

Thus, it can be concluded, that α -acyloxyhydroperoxy aldehydes are not formed during the ozone-initiated SOA formation from cyclohexene in significant quantities, as compared to the other LMW and HMW components, described in Sections 4.3.1.1 and 4.3.1.3. It is important to note that some minor quantities of the α -acyloxyhydroperoxy aldehydes may still be produced during the SOA formation from cyclohexene ozonolysis, but it is unlikely that such low quantities would have any influence on the aerosol formation.

4.3.1.3. Formation of other high-molecular weight SOA components

In this section, investigation of the other high-molecular weight compounds formation during cyclohexene SOA generation is described. In addition to the carboxylic acids, listed in Table 4.18, a number of HMW compounds were also detected in the cyclohexene SOA samples. These peaks were detected using negative ionization mode; LC/MS analysis conditions were the same as for the analysis of carboxylic acids, listed in Table 4.18. EIC chromatograms for the compound with MW 230 Da ($t_r = 15.24$ min) and the compound with MW 244 Da ($t_r = 15.61$ min) are shown in Fig. 4.33A and 4.33B.

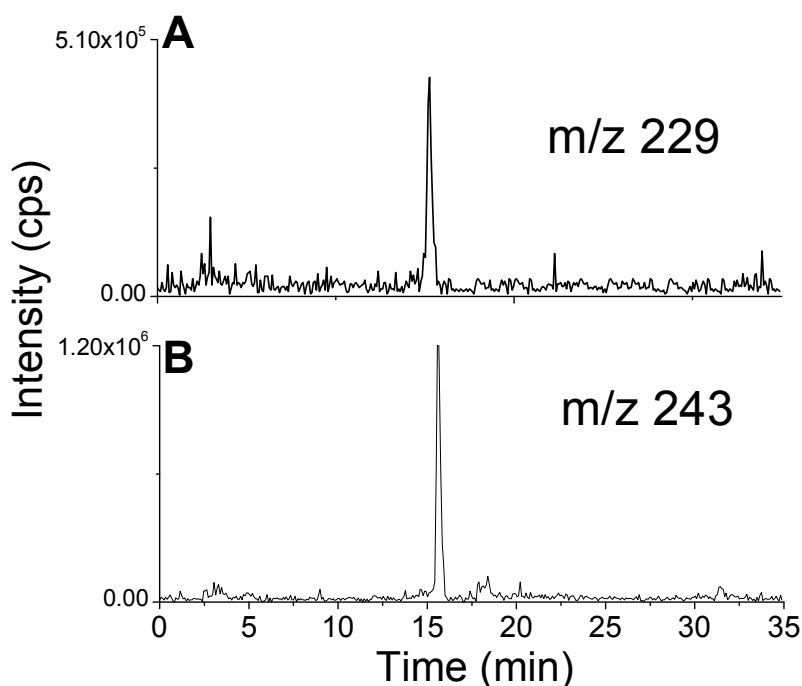


Figure 4.33 ECI chromatograms for the m/z 229 (A) and 243 (B) in the SOA sample

As shown in Fig. 4.33, compounds with molecular masses 230 and 244 were the major HMW components of the cyclohexene SOA samples. Peaks from the compound with MWs 288 Da and 294 Da were also detected. However, these peaks were barely distinguishable from the background noise. Also, the formation of these additional peaks was not reproducible. For these two HMW cyclohexene SOA based on molecular weights and known association mechanisms of the LMW SOA components (see section 1.4.3.4), a number of possible structure was proposed. The possible structures and formation pathways of the compounds with MWs 230 Da and 244 Da are shown in Fig. 4.34.

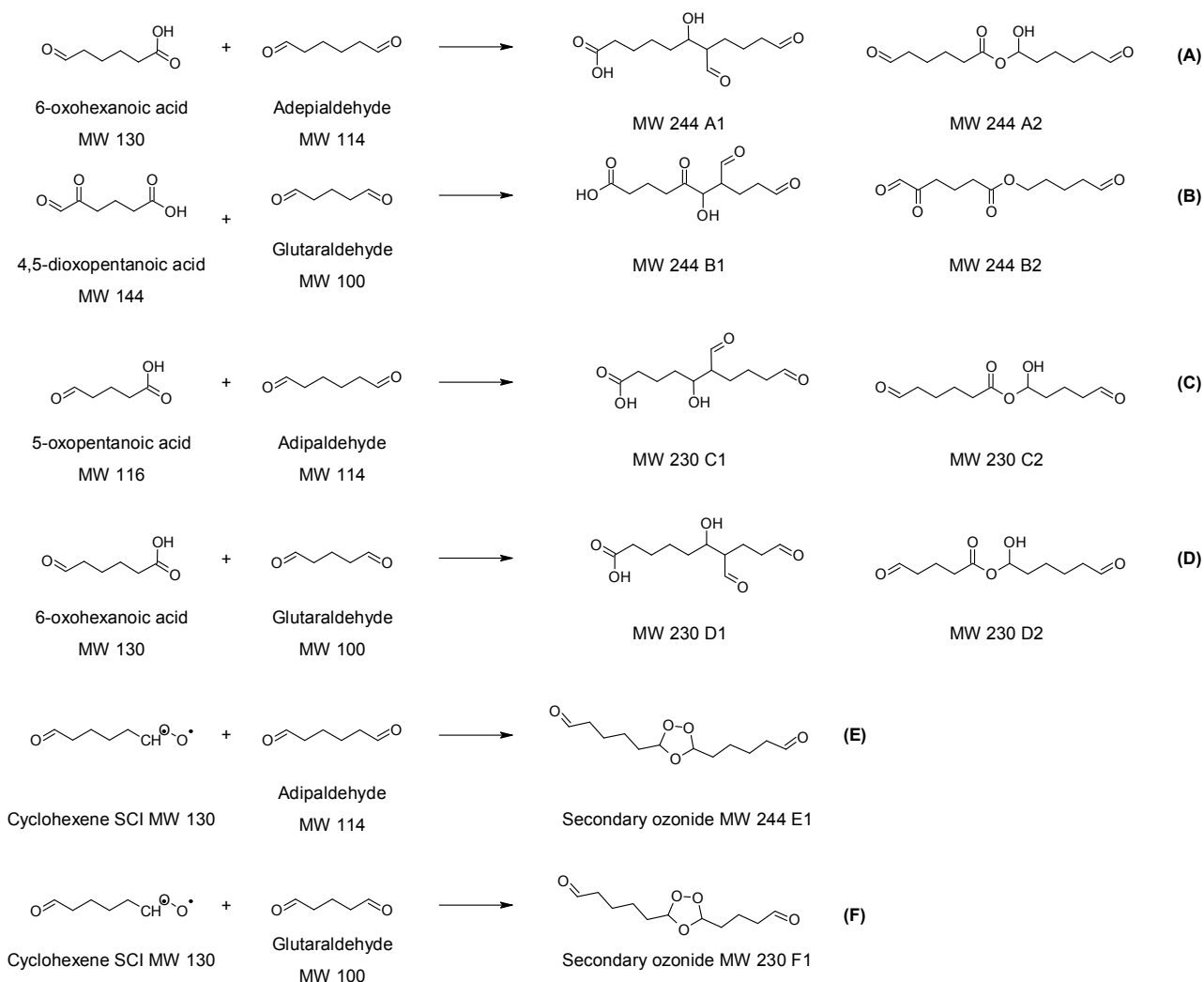


Figure 4.34 Possible structures and formation pathways for the compounds with MW 244 and 230

It is important to notice, that the molecular mass of the compounds with MW 230 Da and 244 Da does not correspond to the sum of mass of any two LMW cyclohexene SOA components, listed in Table 4.18. Therefore, additional building blocks of the observed HMW cyclohexene SOA components have to be considered. It is well known, that large quantities of adipaldehyde (MW 114 Da) and glutaraldehyde (MW 100 Da) are formed during gas-phase ozonolysis of cyclohexene.²¹¹⁻²¹³ These two carbonyl compounds are also known to partition between gas and particle phase. As already discussed in Section 1.4.3.2, when ESI is used, detection of carbonyl compounds is usually not possible, and thus formation of these two aldehydes was not experimentally confirmed in this work. However, it is well known that adipaldehyde and glutaraldehyde are one of the major LMW components of the SOA formed by cyclohexene ozonolysis. Thus, it is reasonable to assume that they can both act as potential building blocks for the HMW compounds. Taking this assumption into account, a number of potential structures for compounds with MW 230 Da and 244 Da is shown in Fig. 4.34. Pathway A shown in Fig. 4.34 involves association of 6-oxohexanoic acid with adipaldehyde by either aldol condensation reaction or hydration followed by esterification, leading to the formation of products AI and AII, respectively. Pathway B involves analogous reaction between 4,5-dioxopentanoic acid (or another dicarbonyl carboxylic acid) and glutaraldehyde, leading to the formation of products BI and BII. Pathway C shows association between 5-oxopentanoic acid and adipaldehyde, also via either aldol condensation (C1) or hydration followed by esterification (C2). Product with MW 230 Da can be also formed by reaction of glutaraldehyde with 6-oxohexanoic acid by either of the two mechanisms – products D1 and D2.

Pathways E and F shows the reaction of SCI association with adipaldehyde (E) and glutaraldehyde (F), leading to the formation of the secondary ozonide. The reaction E and F are most likely to occur in the gas phase (see section 1.4.3.4.2).

The number of possible structures for the two most prominent HMW components of SOA formed by cyclohexene ozonolysis creates an ambiguity, since standards for these compounds were not available. The detection of these two compounds in the negative ionization mode suggests the presence of the carboxyl group, thus tentatively eliminating the formation of compounds A2, B2, C2 and D2, since they do not contain any apparent proton dissociation sites.

Also, it is unclear if secondary ozonides can be detected in the negative ionization mode – compounds E1 and F1. A number of papers, describing secondary ozonides detection using ESI operating in the negative ionization mode can be found in the currently available literature.^{202,214-216} However, these publications describe analysis of secondary ozonides, also containing other functional groups, acting as the ionization sites. Therefore, it is highly unlikely, that the ozonides such as compounds E1 and F1 would directly ionize in the negative ESI since no currently published data supports such hypothesis.

The ambiguity, regarding the structures of the detected HMW components of SOA formed by cyclohexene ozonolysis has been resolved based on the comparison with the analysis of the deuterated analogs, and is going to be discussed in Section 4.3.1.3.1.

It is also important to underline that in this study analysis of the HMW components of SOA formed by cyclohexene ozonolysis was carried out by LC/MS and not by directly introducing the sample into the ion source. As already discussed in Section 1.4.3.2, the important limitation of ESI is the in-source formation of analytes adducts ions.^{141,145,170} Direct introduction of a complex mixture of organic compounds into the ion source, can result in formation molecular clusters, mimicking the formation of dimers, trimers and tetramers, even if those are not actually present in the sample.¹⁷³ As demonstrated by Muller et al,¹⁷⁰ when adipic and pinic acids mixture was directly introduced into ESI ion source, the resulting mass spectrum contained a large number of adduct ions. When mixture of unknown compounds is analyzed, the formation of these cluster ions can be easily misinterpreted as a confirmation of dimers presence in the sample. Those clusters cannot be distinguished from the actual, covalently bonded dimers even by HR-MS, since their elemental formulas are often identical. This can be avoided by adjustment of the proper parameters and calibrating the system with standard “monomer” solutions.^{141,145,170} The cluster ions can also be unambiguously distinguished from the covalently bonded molecules by performing LC analysis,^{146,170} before introducing the samples into the ion source. When LC analysis is performed, LMW and HMW sample components are not present in the ions source at the same time, and thus it can be easily deduced which of the observed ions are covalently and non-covalently bonded molecules.

4.3.1.3.1. Isotope study and identification of the HMW compounds

The mass peaks corresponding to the detected HMW components of SOA formed by cyclohexene ozonolysis were also detected in the cyclohexene-d10 SOA. The detected cyclohexene-d10 HMW SOA components are listed in Table 4.21. Additionally, the ion peaks corresponding to the two most prominent HMW components of SOA formed by cyclohexene ozonolysis were added for reference.

Table 4.21 Detected HMW compounds in cyclohexene and cyclohexene-d10 SOA

M-H⁻ (cyclohexene)	Retention time (cyclohexene)	M-H⁻ (cyclohexene- d10)	Retention time (cyclohexene- d10)	Mass shift (Da)
229	15.24	245	15.20	16
243	15.61	261	15.51	18

EIC chromatograms for the compounds detected in the cyclohexene-d10 SOA listed in Table 4.21 are shown in Fig. 4.35A and 4.35B.

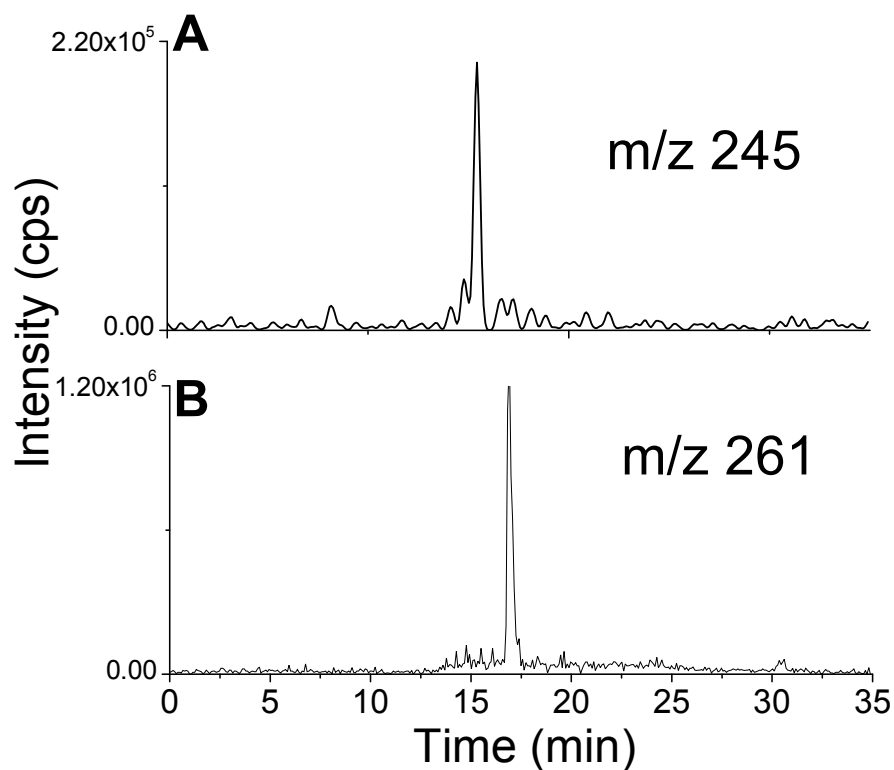


Figure 4.35 ECI chromatograms for the m/z 245 (A) and 261 (B) in the cyclohexene-d10 SOA sample

As presented in Table 4.21, the compounds with MWs 230 Da and 244 Da are shifted by 16 and 18 mass units. Based on the mass shift of the ion corresponding to the specific HMW compound it was possible to elucidate its formation mechanism, given certain assumptions. As discussed in Section 4.3.1.1.1, experimental data acquired in this study show that aliphatic precursor hydrogen atoms do not participate in the formation of the carboxylic acids listed in Table 4.18. Thus, when cyclohexene was substituted with the cyclohexene-d10 during the SOA formation experiments in the flow-tube reactor, mass of the ions of detected carboxylic acids shifted by the values corresponding to the number of aliphatic hydrogens in their molecules.

However, before evaluating the mass shifts for the two most prominent SOA cyclohexene SOA components, adipaldehyde formation mechanism needs to be presented. Since this compound was not observed experimentally in this work, the number of the original precursor hydrogen atoms in this compound has to be evaluated, based on the available literature data.

Adipaldehyde, similar to the pinonaldehyde (section 1.4.1) is formed via ozonolysis, as well as the reaction of OH with the cyclohexene.^{211,212} Both formation mechanisms are shown in Fig. 4.36A and Fig. 4.36B, for the ozone and OH-initiated adipaldehyde formation mechanism, respectively.

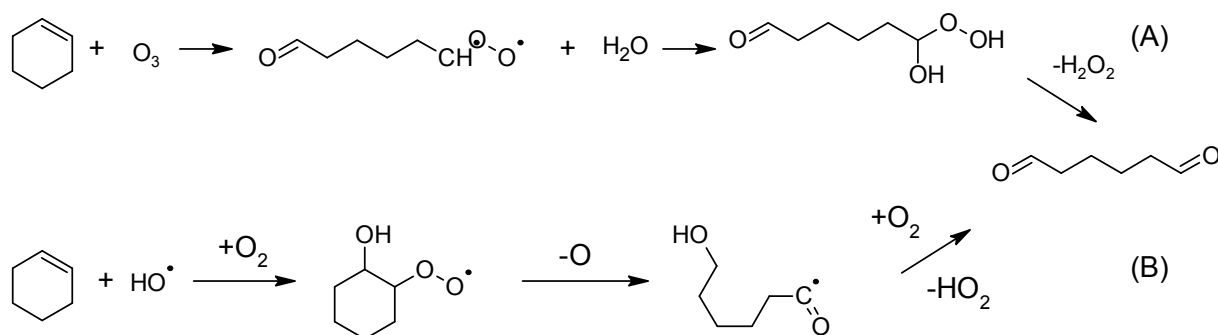


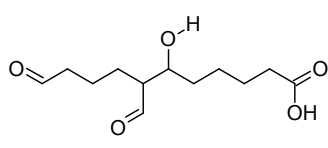
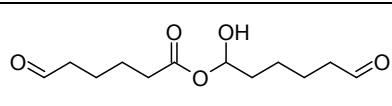
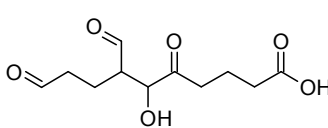
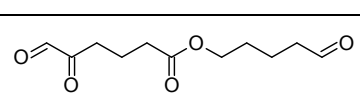
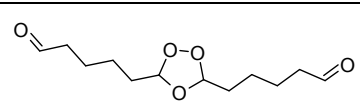
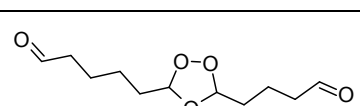
Figure 4.36 Adipaldehyde formation pathways via cyclohexene oxidation by ozone (A) and OH radicals (B)

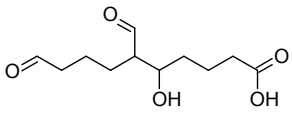
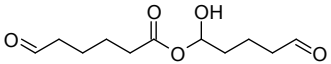
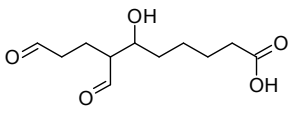
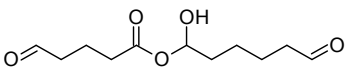
Both formation pathways for the adipaldehyde are analogous to the formation pathways of the pinonaldehyde, described in section 1.4.1. Pathway A shown in Fig. 4.36 involves SCl reaction with water and subsequent elimination of hydrogen peroxide to yield adipaldehyde. It is reasonable to assume that the aliphatic hydrogens do not participate in this reaction, and only water hydrogen atoms are eliminated from the formed hydroxyl hydroperoxide. When OH initiated oxidation is considered, the initial step is the addition to the carbon-carbon double bond and the formation of the radical product, followed by addition of O₂. Next, the original double bond breaks in the following step, involving elimination of oxygen atom (by e.g. oxidation of NO to NO₂, see section 1.3.3) and isomerization of the resulting radical product. Afterwards, adipaldehyde is formed via elimination of HO₂ and addition of oxygen molecule. These reaction steps involve addition and/or elimination of O₂, OH and HO₂ radicals. Thus, it is also reasonable to assume that aliphatic precursor hydrogen atoms do not participate in the reactions shown in Fig. 4.36B. As already discussed in section 4.3.1.3, glutaraldehyde alongside adipaldehyde was also reported to be formed in large quantities during gas-phase ozonolysis of cyclohexene.²¹¹⁻²¹³ Mass of the glutaraldehyde should shift by 8 mass units, equal to the number of aliphatic hydrogens, present in this molecule, when cyclohexene is substituted with the cyclohexene-d₁₀. These

conclusions are in excellent agreement with the study by Aschmann et al.²¹² In the study by Aschmann et al,²¹² SOA composition from the ozonolysis of cyclohexene and cyclohexene-d10 was investigated and it was reported that the peaks for adipaldehyde and glutaraldehyde are shifted by 10 and 8 mass units, respectively. It is important to note, that the study by Aschmann et al.²¹² was carried out in the presence of the OH radical scavengers. There are also no experimental indications, suggesting that the cyclohexene hydrogen atoms are exchanged when adipaldehyde and glutaraldehyde are produced by the gas-phase ozone initiated oxidation of cyclohexene.

Given the assumption described above, the mass shift of the two HMW cyclohexene SOA components allows eliminating a number of structures shown in Fig. 4.34, as listed in Table 4.22.

Table 4.22 Number of aliphatic hydrogen atoms for the compounds shown in Fig. 4.34

Structure in Fig. 4.34	Compound number	Molecular weight (Da)	Number of aliphatic hydrogen atoms
	A1	244	18
	A2	244	19
	B1	244	14
	B2	244	16
	E1	244	20
	F1	230	18

	C1	230	16
	C2	230	17
	D1	230	16
	D2	230	17

As listed in Table 4.22, a number of aliphatic hydrogen atoms in the individual molecules allows eliminating most of possible structures for the compounds with MWs 230 Da and 244 Da. The formation of secondary ozonides, structures E1 and F1, can be eliminated since the reaction of SCI with adipaldehyde and glutaraldehyde would lead to the mass shift of the product by 20 and 18 mass units, instead of the observed 18 and 16 mass units. Also, as noted above, it is very unlikely that secondary ozonides would directly ionize in ESI, in the negative ionization mode. Structures B1 and B2 for the compound with MW 244 Da can also be eliminated, as these molecules are not containing a sufficient number of aliphatic hydrogen atoms to explain the observed mass shift. Therefore, the only possible structures of the compound with MW 244 Da are the aldol product (A1) and ester (A2), formed from the association of the 6-oxohexanoic acid and adipaldehyde.

The experimental data acquired in this study, strongly indicate that the observed compound was an aldol condensation product (A1), instead of an ester (A2). As already discussed in Section 4.3.1.1, the detection of the compound A2 is most likely not possible using ESI in the negative ionization mode, due to the lack of the ionization site, namely the carboxylic group. Also, the formation of an ester does not involve the exchange of one of the aliphatic hydrogen atoms with the solvent, as discussed below, and thus the mass shift of the observed product would be 19 instead of the 18. Additionally, if the hydration followed by esterification was the dominant

oligomer formation pathway, additional esters of the adipaldehyde and e.g. adipic acid would be observed, since dicarboxylic acids were also detected in significant quantities, as described in Section 4.3.1.1.

Therefore, the only mechanism explaining the observed shift by 18 mass units is the aldol condensation between adipaldehyde and 6-oxohexanoic acid, as shown in Fig. 4.37.

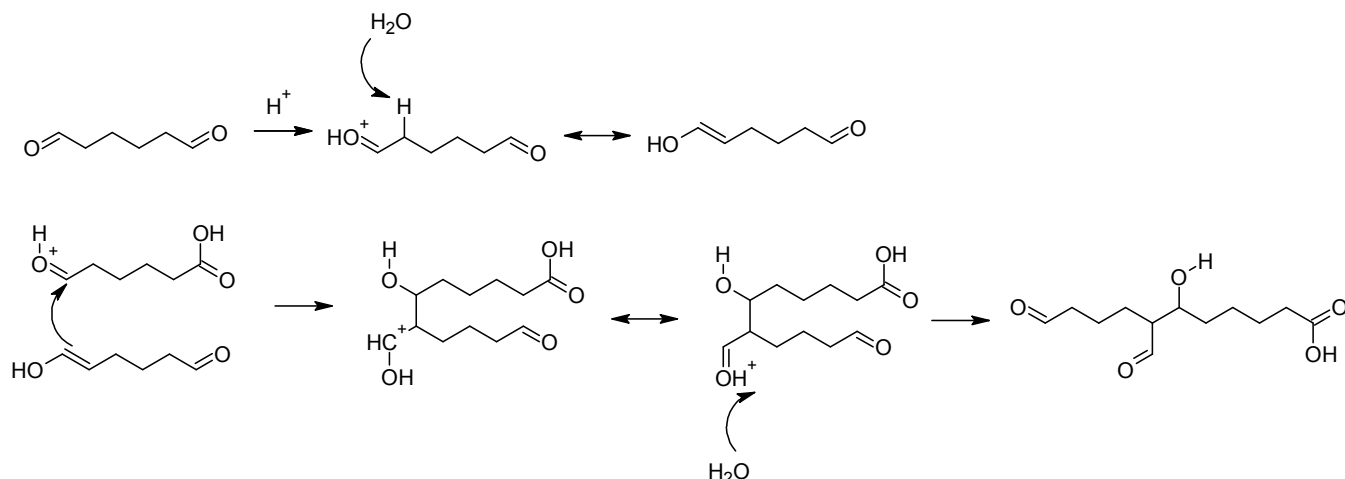


Figure 4.37 Proposed formation mechanism of the compound with MW 244 Da

It was concluded in the previously published papers,^{20,125,135,179} that the particle – phase reactions leading to the portion of the observed HMW SOA components are most likely acid-catalyzed – see section 1.4.3.4.1. Thus, the aldol reaction shown in Fig. 4.37 is acid catalyzed variant of the aldol condensation.¹⁸⁰ Protonation can occur on carbonyl group of adipaldehyde or 6-oxohexanoic acid leading to the two isomers of the compound A1; for simplicity only one mechanism and the resulting product is shown in Fig. 4.37. The number of aliphatic hydrogen atoms for the substrates of compound A1 is 19, with the 10 original cyclohexene hydrogens for the adipaldehyde, as discussed above in this section, and 9 hydrogens for the 6-oxohexanoic acid, as confirmed by the acquired experimental data, reported in Section 4.3.1.1.1. As a result of the aldol condensation between these two compounds, one of the aliphatic hydrogen atoms of either adipaldehyde or 6-oxohexanoic acid is exchanged with the water hydrogen, thus leading to the observed mass shift by 18 mass units. Initially, the carbonyl group is protonated by the acid, followed by the abstraction of the α -carbon hydrogen, leading to the enol formation. In this step, the exchange of the one of aliphatic hydrogen occurs, leading to the observed mass shift by 18

mass units. Aliphatic hydrogen atoms are not involved in the subsequent steps of the new carbon-carbon double bond formation between the adipaldehyde α -carbon and the carbonyl carbon of the 6-oxohexanoic acid, followed by deprotonation of the carbonyl group and formation of the product. The presented mechanism agrees well with the experimental data, acquired from the SOA formation in this study as a result of cyclohexene-d10 ozone initiated oxidation.

For the compounds with MW 230 Da, using the same arguments, as for compound with MW 244 Da, the structures D2 and C2 can be eliminated, together with the formation of the secondary ozonide (F1). Structures C1 and D1 can be presented for the compound with the MW 230 Da. This compound is formed as a result of either the aldol condensation between 5-oxopentanoic acid with adipaldehyde or 6-oxohexanoic acid with glutaraldehyde, structures D1 and C1, respectively. Unfortunately, since these two compounds have the same molecular masses and are formed via the same mechanism, whether the structure C1 or D1 is the major product cannot be concluded. It is also possible that chromatographic resolution was insufficient to separate the two isomers, and there were two isomers of the compound with MW 230 Da present in the sample.

In the study by Muller et al.¹⁷⁰ SOA formation from cyclohexene ozone-initiated oxidation was studied in a 100 L reaction vessel. HMW SOA components were subsequently analyzed using ESI-FTICR-MS as well as LC-ESI/MSⁿ. A number of HMW SOA components were detected by Muller et al.¹⁷⁰ using ESI in the negative ionization mode. Compounds with MWs 230 Da and 244 Da were also detected by Muller et al.¹⁷⁰ and their elemental formulas agree with the elemental formulas of the compound A1, for the species with MW 244 Da, and with compounds C1 and D1 for the compound with MW 230 Da. The same two compounds were detected by Sato,¹⁸⁵ however, the structures were not proposed.

Several different HMW SOA components from cyclohexene ozonolysis were detected previously in the other studies.^{136,142,185,210} Right now, it is not clear which compound is the major HMW component of SOA, formed during ozone initiated oxidation of cyclohexene. Due to the lack of standards, it cannot be confirmed if compounds A1, C1 and D1 are ionized much more efficiently, as compared to the other HMW species. The preferable ionization of the aldol

condensation products is unlikely, but it cannot be completely excluded. However, assuming that the ionization efficiency does not differ significantly for the carboxyl group-containing compounds, the two compounds detected in this work (MW 230 Da and 244 Da) appear to be the major HMW components of the freshly formed SOA, in addition to some minor components, as noted in Section 4.3.1.3. These compounds were detected previously,^{170,185} proving that they are not artifacts, formed exclusively in the experimental setup used in this work, or during the extraction procedure. However, the structures for these two SOA components were not previously proposed.^{170,185} They were also never reported to be the major components of the freshly formed cyclohexene SOA. A number of other compounds, most likely the derivatives of dicarboxylic acids (e.g. compounds with MW 246 Da tentatively identified as a derivative of adipic acid) was reported to compose the “aged” SOA formed in the cyclohexene ozonolysis during the smog chamber studies.^{137,142,170,185,209,210} This leads to the conclusion that the two compounds, identified in this work, are characteristic for the freshly formed aerosol. Based on the results discussed in this section, it can be concluded that the early stages of SOA particles formation most likely involve the reactive uptake of the carbonyl compounds and oligomer formation by the aldol condensation reactions.

4.3.1.4. Relative humidity influence on the composition of SOA resulted from cyclohexene ozonolysis

In this section, RH influence on composition of SOA formed by gas-phase cyclohexene ozonolysis is discussed. SOA samples were prepared in humidified air (40% RH), as described in Section 3.4.2.

4.3.1.4.1. Carboxylic acids

Carboxylic acids were identified as described in Section 4.3.1.1. The same set of carboxylic acids was detected in SOA samples generated under dry and humid conditions. Therefore, increased humidity did not influence the cyclohexene SOA composition, when the formation of LMW carboxylic acids is considered.

Molar yields of the individual carboxylic acids were calculated as described in Section 4.3.1.1. Comparison of the carboxylic acids cyclohexene molar yields calculated for the experiments performed under dry and humid conditions are presented in Table 4.23.

Table 4.23 Molar yields of the carboxylic acids formed under dry and humid conditions

Name	M-H ⁻	Molar yield (3% RH)	Molar yield (40% RH)
Succinic acid	117	$(2.8 \pm 0.4) \times 10^{-4}$	$(4.2 \pm 0.6) \times 10^{-4}$
4.5-dioxopentanoic acid*	143	$(4.0 \pm 0.3) \times 10^{-4}$	$(1.03 \pm 0.2) \times 10^{-3}$
5-oxopentanoic acid	115	$(1.6 \pm 0.4) \times 10^{-3}$	$(2.20 \pm 0.6) \times 10^{-3}$
Glutaric acid	131	$(5.1 \pm 0.4) \times 10^{-3}$	$(8.4 \pm 1.0) \times 10^{-3}$
6-oxohexanoic acid	129	$(2.4 \pm 0.3) \times 10^{-3}$	$(6.8 \pm 1.0) \times 10^{-3}$
Adipic acid	145	$(5.9 \pm 1.0) \times 10^{-3}$	$(1.19 \pm 0.3) \times 10^{-2}$

As listed in Table 4.23, significant increase in the molar yields for all of the carboxylic acids detected in the cyclohexene SOA samples was observed.

The RH influence on SOA formation produced by gas-phase ozone initiated oxidation of cyclohexene was not previously investigated. However, results reporting investigation of RH influence on SOA formation in the α -pinene/ozone system can be found in the literature.^{150,181,217} Therefore, the results of the RH influence on SOA formation by cyclohexene ozonolysis were evaluated, by comparison with the data available for α -pinene.

According to the previously published studies^{150,181,217} increased RH has led to the uptake of water molecules onto the SOA particles formed as a result of ozone-initiated α -pinene oxidation. It was also reported, that for the SOA formation in the α -pinene/ozone system, increased water content lead to the increase in the SOA mass^{160,217} and volume concentration¹⁸¹ Total aerosol volume also increased with increasing RH.¹⁸¹ Also, as already discussed in Section 1.4.4 and section 2, water influences the α -pinene ozonolysis mechanism, e.g. by acting as the SCI scavenger.^{20,150,181}

The results of the SOA formation experiments performed in the flow tube reactor at 40 % RH indicate that formation of all of the LMW compounds is enhanced by increased water content.

This suggests increase in the SOA mass with increasing RH. As already discussed in Section 4.3.1.1, it is not clear what portion of the SOA mass corresponds to the compounds listed in Table 4.18. However, as reported previously from smog-chamber experiment, LMW compounds correspond to about 31% of the total SOA mass.¹³⁶ Thus, it seem to be reasonable to assume, that the compounds listed in Table 4.18 compose a significant SOA fraction, and thus increase in their formation yields indicate the increase in aerosol yields under humid conditions, as compared to the experiments performed under dry conditions.

4.3.1.4.2. α-acyloxyhydroperoxy aldehydes

Formation of the α-acyloxyhydroperoxy aldehydes was investigated as described in section 4.3.1.2. Similar to the experiments under dry conditions, it was concluded that no α-acyloxyhydroperoxy aldehydes were produced when cyclohexene ozonolysis under humid conditions was performed.

4.3.1.4.3. Other high-molecular weight SOA components

No additional HMW compounds were detected in the SOA samples generated under humid conditions. However, it is important to underline, that formation of the different products under dry and humid conditions cannot be completely excluded. Since the reactants concentrations used here were much higher, as compared to the smog-chamber investigations as well as to those encountered in the ambient atmosphere. Therefore, the increased RH impact on the SOA composition may be more pronounced, when lower reactants concentrations are used, effectively increasing the relative water concentration, as compared to the other reactants. This assumption agrees with the results published by Bonn et al.¹⁸¹ In the study by Bonn et al,¹⁸¹ the α-pinene SOA formation was initially unaffected by increased RH; however, when reactants concentrations were lowered by about a factor of 10, the aerosol nucleation was suppressed. These results point out, that a careful evaluation of the laboratory results is necessary, before any meaningful conclusions can be presented, and extrapolated to the ambient conditions.

4.3.2. SOA produced from α -pinene ozonolysis

Carboxylic acids identification in the SOA samples obtained by α -pinene ozonolysis is described in Section 4.3.2.1. Afterwards, investigation of the α -acyloxyhydroperoxy aldehydes formation is discussed in section 4.3.2.2. The α -acyloxyhydroperoxy aldehydes analysis is described in Section 4.1.3; predicted MRM method used for the analysis of the α -pinene SOA samples is described in Section 4.1.3.8.

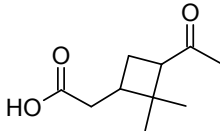
The formation of other HMW SOA components is described in Section 4.3.2.3. Using the data acquired for the model precursor - cyclohexene, structures of the detected HMW α -pinene SOA components were proposed.

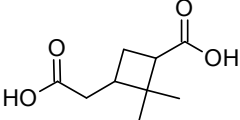
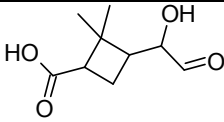
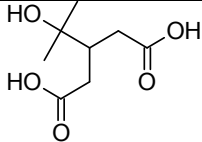
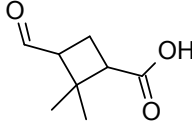
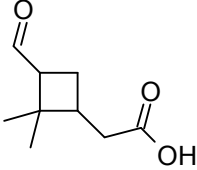
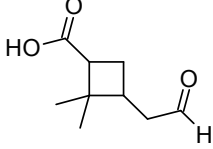
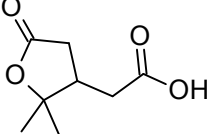
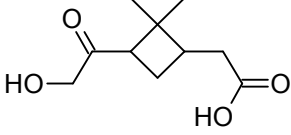
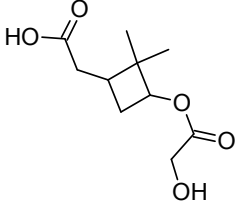
RH influence on SOA composition is discussed in Sections 4.3.2.4, including impact of the higher water concentration on the formation of carboxylic acids (Section 4.3.2.4.1), α -acyloxyhydroperoxy aldehydes (Section 4.3.2.4.2) and other high-molecular weight SOA components (Section 4.3.2.4.3).

4.3.2.1. Carboxylic acids identification

In this section, investigation of the carboxylic acids formed by α -pinene ozonolysis is described. Carboxylic acids detected in the α -pinene SOA samples, generated under dry conditions (RH \approx 3%) are listed in Table 4.24.

Table 4.24 Carboxylic acids identified in the SOA samples formed by ozone-initiated α -pinene oxidation under dry conditions (RH \approx 3%)

Name	Structure	Molecular weight (Da)
Cis-pinonic acid		184

Pinic acid		186
4-hydroxy-pinalic-3-acid		186
Diaterpenylic acid		190
Norpinalic acid		156
Pinalic acid		170
Norpinonic acid		170
Terpenylic acid		172
10-hydroxy pinonic acid		200
		216

cis-Pinonic acid and pinic acid were identified based on the comparison with the actual standards. MRM and EIC chromatograms of the α -pinene SOA samples for these two carboxylic acids are shown in Fig. 4.38.

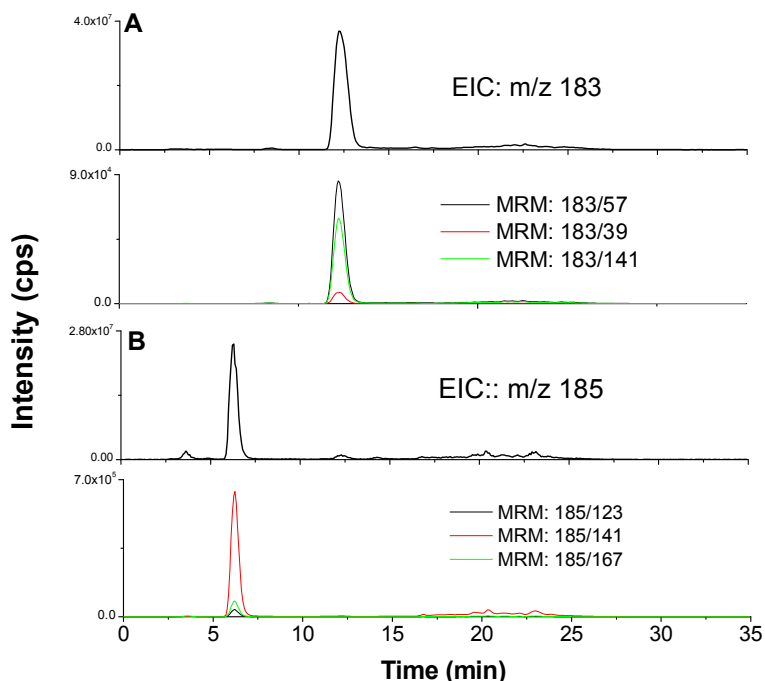


Fig. 4.38 ECI and MRM chromatograms for cis-pinonic acid (A) and pinic acid (B) in the SOA sample

For the cis-pinonic acid (Fig. 4.38A) and pinic acid (Fig. 4.38B) both MRMs and deprotonated pseudo-molecular ions were detected, unambiguously confirming the presence of these two acids in α -pinene SOA samples. Both cis-pinonic^{120,122,138,147,150,155} and pinic acids^{120,122,137,138,147,155,170,174,175,183} are known as α -pinene SOA particle phase components. For the rest of carboxylic acids LMW compounds the standards were not available. Therefore, the structures listed in Table 4.24 are based on the previously published data.^{120,122,134,137,138,143,146,147,155,170,174,175,177,183}

As shown in Fig. 4.38B the small peak at retention time 3.62 min for the m/z 185 was detected. For the compound, isobaric to pinic acid, a number of structures were proposed by Winterhalter et al.¹²² However, out of the proposed structures, only pinic acid was detected in the negative ESI. The structure of the 4-hydroxy-pinalic-3-acid, listed in Table 4.24 was tentatively

identified by Ma et al.¹²⁰ EIC chromatograms for the ions listed in Table 4.24 are shown in Fig. 4.39.

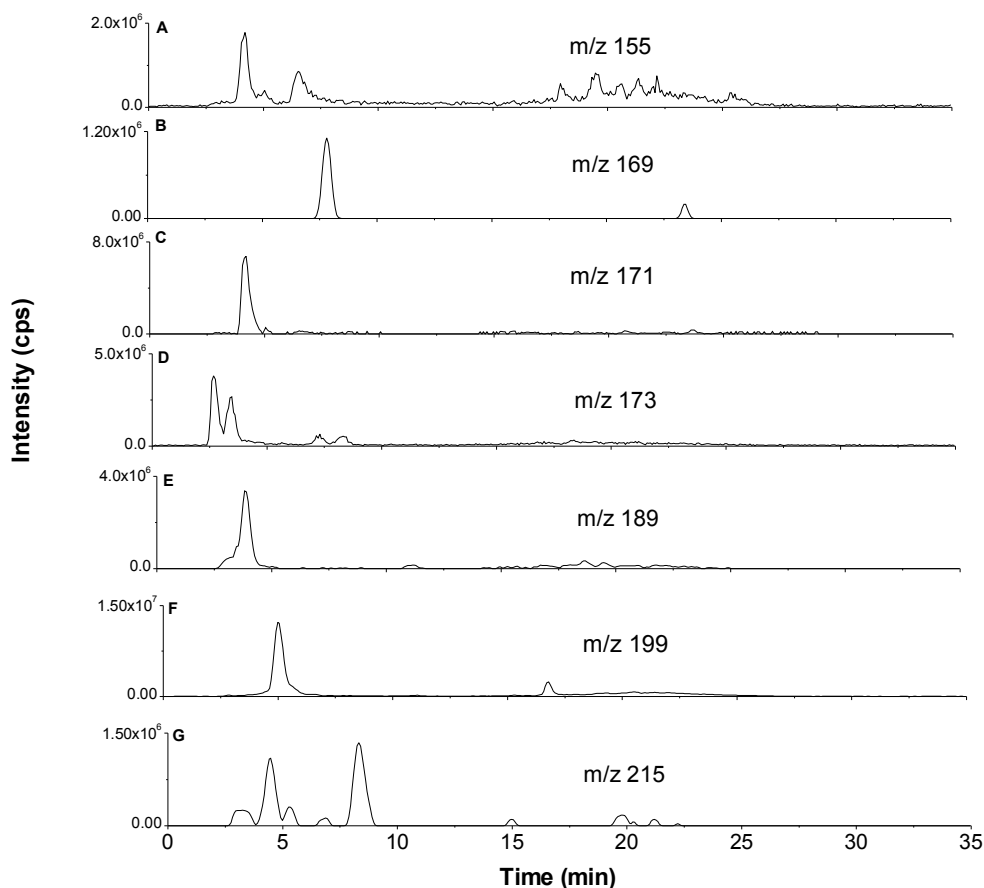


Figure 4.39 EIC chromatograms for the m/z 155 (A), m/z 169 (B), m/z 171 (C), m/z 173 (D), m/z 189 (E), m/z 199 (F) and m/z 215 (G)

As shown in Fig. 4.39A, for the m/z 155 there were two peaks present at $t_r = 2.72$ min and $t_r = 5.54$ min. The second peak was concluded to be a background signal, since it was also present in the blank sample. However, the first signal can be attributed to the carboxylic acid with MW 156 Da, identified in the earlier studies as norpinalic acid.^{120,143,150}

As shown in Fig. 4.39B, two peaks for m/z 169 were detected. The carboxylic acids with MWs 170 Da were detected in a number of previous studies.^{120,122,150,155} These compounds have been tentatively identified as pinalic acid^{122,218} or norpinonic acid.^{122,150,218} The two carboxylic acids had the same MWs and both produced deprotonated, pseudo-molecular ions with m/z 169.

Therefore, it was not possible to distinguish pinalic acid and norpinonic acid, based on the acquired experimental data.

A single ion peak, corresponding to the compound with MW 172 Da was detected, as shown in Fig. 4.39C. Compound with MW 172 Da was detected in a number of previously published studies.^{120,122,137,172,174} Two possible structures were proposed for this compound; earlier it was tentatively identified as norpinic acid.^{120,122,137} However, in the most recent investigations, it was concluded that compound with MW 172 Da is most likely a molecule containing a lactone moiety; terpenylic acid.^{147,174,175,177,183} These two acids cannot be distinguished even with HR-MS due to the same elemental formulas.¹⁷¹ However, it is important to note, that terpenylic acid was shown to be produced in large quantities in the early stages of SOA formation.^{174,177,183} Also, terpenylic acid hydrolysis product – diaterpenylic acid was identified as a building block of dimer with MW 358 Da, a potential nucleating agent. Compound with MW 358 Da (see section 4.3.2.3) as well as diaterpenylic acid were detected in significant quantities in this study. Also, high concentrations of norpinic acid were concluded to characterize an aged α -pinene SOA.¹⁴⁶ Thus, it is very reasonable to assume that norpinic acid should not be present in the freshly formed α -pinene SOA in significant quantities. Therefore, compound with MW 172 Da detected in this study was identified as terpenylic acid. At the same time, the formation of norpinic acid under the experimental conditions used in this work cannot be completely excluded, due to e.g. insufficient chromatographic resolution and/or very large concentration difference between the two, isobaric compounds. However, assuming that the detected compound with MW 172 Da was terpenylic acid, norpinic acid was not formed in significant quantities.

Two ion peaks were detected for the compound with the MW 174 Da; the first ion peak originated from the background signal. However, the ion peak eluting at t_r 3.44 min indicated the presence of the previously unidentified carboxylic acid. It is also unlikely that this ion peak is result of in-source fragmentation, since its retention time doesn't correspond to the retention time of any other compound, as listed in Table 4.22. The presence of the carboxylic acid with this particular mass was reported by Muller et al.¹⁷⁰ and assigned elemental formula for this

compound shown the presence of four oxygen atoms. However, the structure for this compound could not be proposed, based on the experimental data acquired in this study.

Ion peak shown in Fig. 4.39E (MW 190 Da) most likely corresponded to the diaterpenylic acid, a hydrolysis product of the terpenylic acid. This compound was detected in a number of previously published studies.^{147,170,175}

The compound with MW 200 Da (Fig. 4.39F) was also detected in a number of previously published studies.^{120,122,137,138,143,146,147,155,170} This compound was tentatively identified as hydroxypinonic acid. Three of possible isomers for this acid were proposed by Winterhalter et al.¹²² In the few studies, reporting the detection of this or isobaric carboxylic acid, specific structure was not proposed.^{138,155,170} However, in a number of studies, the structure of the 10-hydroxy pinonic acid was proposed as the most probable structure of this compound. Thus, the structure of this acid is shown in Table 4.24.^{120,137,143,146,147} Also, it is important to note that 10-hydroxy pinonic acid was identified as one of the building blocks of the ester with MW 368 Da, also identified as the SOA component produced in the flow tube reactor – see section 4.3.2.3. Using similar reasoning as for the formation of terpenylic acid and norpinic acid, the formation of additional isomers cannot be completely excluded.

Two ion peaks with m/z 215 were detected at $t_r = 4.20$ min and 8.19 min as shown in Fig. 4.39G. The first ion peak can be attributed to the cluster of terpenylic acid and eluent additive – formic acid (section 3.2.2.3). Formation of such abundant adduct ions with eluent additive is common in ESI (see section 1.4.1.3) but was not observed for the rest of the carboxylic acids. This can be explained by the strong cluster-forming properties of the terpenylic acid.¹⁷⁷ It was proven by theoretical calculations¹⁷⁷ that terpenylic acid possess strong dimer forming properties.

The ion peak eluting at $t_r = 8.19$ min indicated the presence of the compound with MW 216 Da. The formation of this compound was reported to be enhanced by the presence of acidic seed.¹³⁸ The elemental formula, assigned by HR-MS measurement, indicated that this molecule contain five oxygen atoms.¹⁷⁰ The structure listed in Table 4.24 was proposed by Warscheid and Hoffmann,¹³⁴ based on on-line α -pinene SOA composition study. The elemental formula of the molecule listed in Table 4.24 also agrees with the experimental data, reported by Muller et al.¹⁷⁰

After proposing the structures for the detected LMW α -pinene SOA components, their relative concentrations were estimated by calculating the molar yields listed in Table 4.25. Concentrations of the cis-pinonic acid and pinic acid were calculated using calibration curves (see Section 4.1.1.2). No standards were available for the rest of the carboxylic acids, listed in Table 4.24. Therefore, the concentrations of these carboxylic acids were estimated by using the MS response calculated for cis-pinonic acid and pinic-acid, for the monocarboxylic acids and diaterpenylic acid, respectively. Of course, utilizing such approach leads to the increased uncertainty, regarding the α -pinene molar yields for these compounds. Amount of the α -pinene consumed during a single experimental run, as a result of oxidation by both ozone and OH radicals was calculated as described in Section 4.2.2. Concentrations of the carboxylic acids were subsequently used to calculate their molar yields listed in Table 4.25.

Table 4.25 Molar yields of the carboxylic acids identified in the SOA samples formed during ozone-initiated α -pinene oxidation under dry conditions (RH \approx 3%)

Name	M-H ⁻	Retention time (min)	Carboxylic acids molar yield
cis-Pinonic acid	183	12.26	$(2.8 \pm 0.1) \times 10^{-3}$
Pinic acid	185	6.29	$(7.4 \pm 0.9) \times 10^{-4}$
10-hydroxy pinonic acid	199	5.01	$(4.8 \pm 0.4) \times 10^{-4}$
Pinalic acid/Norpinalic acid	169	4.48	$(1.2 \pm 0.1) \times 10^{-3}$
Diaterpenylic acid	189	3.84	$(2.9 \pm 0.4) \times 10^{-4}$
Terpenylic acid	171	4.17	$(1.2 \pm 0.1) \times 10^{-3}$
4-Hydroxy-pinalic-3-acid	185	3.62	$(7.0 \pm 0.4) \times 10^{-5}$
Norpinalic acid	155	2.72	$(9.0 \pm 2) \times 10^{-5}$
MW 216 Da	215	8.19	$(1.3 \pm 0.4) \times 10^{-4}$

Molar yields, listed in Table 4.25 are the fraction of α -pinene molecules, converted into the carboxylic acids as a result of oxidation in the flow-tube reactor. As already discussed in Section

4.3.1.1, the yields reported in the literature are SOA mass yields, it is therefore difficult to compare the data acquired in this study with the values available in the literature.

As listed in Table 4.25, cis-pinonic acid was the main LMW α -pinene SOA component, formed under experimental conditions used in this work. It is currently known that cis-pinonic acid is one of the main constituents of the newly formed SOA.^{150,155,174} Cis-pinonic acid was present in significant quantities in the aerosol generated in the smog-chamber experiments.^{120,138} As already discussed in section 1.4.1, cis-pinonic acid is formed by the direct rearrangement of the α -pinene SCI via ester channel and by SCI reaction with water. Thus, it is expected that the large quantities of this compound would be present in the freshly formed SOA.

Pinic acid was found in this work to be present in the freshly formed SOA samples in significant quantities, as shown in Table 4.25. Lee and Kamens¹⁵⁰ reported that this carboxylic acid was not produced during very early stages of α -pinene SOA formation. On the other hand, pinic acid was also reported to be formed during early stages of SOA formation.^{155,183} However, pinic acid was found to be an important oligomer building block, in particular for the compound with the MW 358 Da,^{146,147,170,174,175,219} proposed as the potential nucleating agent¹⁷⁴ – see section 1.4.4.

Both terpenylic acid and diaterpenylic acid were shown to be formed in significant quantities during the early stages of SOA formation.^{122,172,174} The amount of terpenylic acid was shown to decrease as a result of SOA aging, indicating that the presence of this acid is characteristic for the freshly formed aerosol.¹⁴⁶ This agrees very well with the results obtained in this study. Also, as it was already discussed in section 1.4.4, the gas-phase terpenylic acid dimer was proposed to participate in the α -pinene SOA nucleation process. The significant amount of terpenylic acid, detected in the SOA samples generated under the experimental conditions used in this work, support this hypothesis. However, in this as well as in the previously published studies,¹⁷⁷ no experimental evidence supporting the stable terpenylic acid dimer production in the early stages of α -pinene SOA formation can be presented – see section 1.4.4. It is important to note, that the presence of diaterpenylic acid acetate (MW 232 Da) was also reported, alongside the underivatized acid.^{147,175} However, compound with the MW 232 Da was not detected in significant

quantities in the SOA particles, produced in this work. This is consistent with the conclusions presented by Yasmeeen et al,¹⁴⁶ where diaterpenylic acid acetate was identified as one of the traces of α -pinene SOA chemical aging.

10-Hydroxy pinonic acid was previously detected in the SOA samples generated in smog chamber experiments.^{120,122,138} The compound with MW 200 Da was also detected in the freshly formed SOA.¹⁵⁵ The concentration of this acid decreased as a result of chemical aging,¹⁷⁵ thus it is unlikely to be a product of the SOA subsequent aerosol transformation reactions. Therefore, the presence of significant quantities of 10-hydroxy pinonic acid in the freshly formed SOA found in this work agrees very well with the previously published data.¹⁵⁵

One of the structural isomers of the carboxylic acid with MW 170 Da was also reported to be present in the freshly formed α -pinene SOA.^{150,155} This agrees with the experimental data obtained in this work. As noted above, this compound may be one of the two isomers: pinalic acid or norpinalic acid.

The α -pinene molar yields for the rest of the detected carboxylic acids; 4-hydroxy-pinalic-3-acid, norpinalic acid as well as for the compound with the MW 216 were calculated to be less than approx. 0.0001. Therefore, these compounds were present in significantly lower quantities than other SOA components listed in Table 4.24. Due to significantly lower concentrations, these compounds were unlikely to participate in the SOA nucleation either directly or as the oligomers building blocks - see below.

The formation of 4-hydroxy-pinalic-3-acid was reported for the SOA generated in smog-chamber experiments, and there are no results indicating the participation of this acid in the aerosol nucleation process.¹²⁰ The molar yield of the unknown compound with MW 174 Da was approx. 0.00005 (not included in Table 4.25). Compound with the MW 216 Da was also detected in a number of smog chamber studies.^{122,134,138,170} There is no published data indicating the formation of large quantities of the acids with MWs 174, 4-hydroxy-pinalic-3-acid as well as norpinalic acid during the early stages of α -pinene SOA formation and growth. The results acquired in this work also confirmed that the acids with MWs 174, 4-hydroxy-pinalic-3-acid as well as norpinalic acid

were not present in the freshly formed SOA formed by gas-phase α -pinene ozonolysis in large quantities.

Norpinalic acid was reported to be present in significant quantities in the freshly generated SOA samples.¹⁵¹ In this study, this carboxylic acid was found to be a minor LMW SOA component. This difference may be due to different time-scale of the SOA formation in this study and in the study by Lee and Kamens.¹⁵¹ Also, Lee and Kamens used GC/MS for the LMW products quantification. Since norpinalic acid standard was not available, it is difficult to estimate the ESI response for this acid under the experimental conditions used in this work. Also, using cis-pinonic acid as the surrogate standard for the quantification led to the significant uncertainty in the calculated molar yield of norpinalic acid. Since significant quantities of norpinalic acid were not detected in the SOA samples studied in this work, it was unlikely that this compound was the important monomer building block under the experimental conditions used in this work.

Results reported in this section are in excellent agreement with the previously published data,^{120,122,134,137,138,143,146,147,155,170,174,175,177,183} which can be regarded as a validation of the experimental setup used in this work. Analysis of the LMW α -pinene aerosol fraction provided little insights into the nucleation mechanism, with the exception of terpenylic acid. It is currently well established that carboxylic acids are very unlikely to initiate α -pinene SOA nucleation (it was discussed in Section 1.4.4). The main LMW SOA components, produced in large quantities during early stages of aerosol formation, can be regarded as the potential building blocks for the HMW components. These HMW compounds can either initiate the SOA formation or participate in the early stages of aerosol growth. Formation of these HMW compounds is discussed in Section 4.3.2.2 and Section 4.3.2.3.

4.3.2.2. Investigation of α -acyloxyhydroperoxy aldehydes formation

In this section, investigation of the α -acyloxyhydroperoxy aldehyde formation during α -pinene SOA generation is described. During the initial experimental run, MRMs for the compounds XIV – XVIII were monitored. Carboxylic acids used for the synthesis of the compounds XIV - XV were detected in SOA samples as described in section 4.3.2.1. MRMs for the α -acyloxyhydroperoxy

aldehydes that can potentially be produced as a result of the SCI reaction with the norpinonic acid (compound XVI), pinalic-4 acid (compound XVII) and terpenylic acid (compound XVIII) were predicted, as described in section 4.1.2.8. Compounds XIV, XVI and XVII were previously proposed as potential nucleation precursors of the SOA formed in the α -pinene/ozone system, as described in Section 1.4.4.

Compounds XIV and XV were synthesized and MRM conditions were optimized for these two α -acyloxyhydroperoxy aldehydes, as described in Section 4.1.2.8. Since compounds XVI, XVII and XVIII could not be synthesized, their MRM conditions were predicted based on the results of the MRM conditions optimization for the compounds XIV and XV (see section 4.1.2.8). The carboxylic acids used for the synthesis of the compounds XIV and XV were the two major LMW SOA components, as listed in Table 4.25. EIC and MRM chromatograms for the compounds XIV and XV are shown in Fig. 4.40A and Fig. 4.40B.

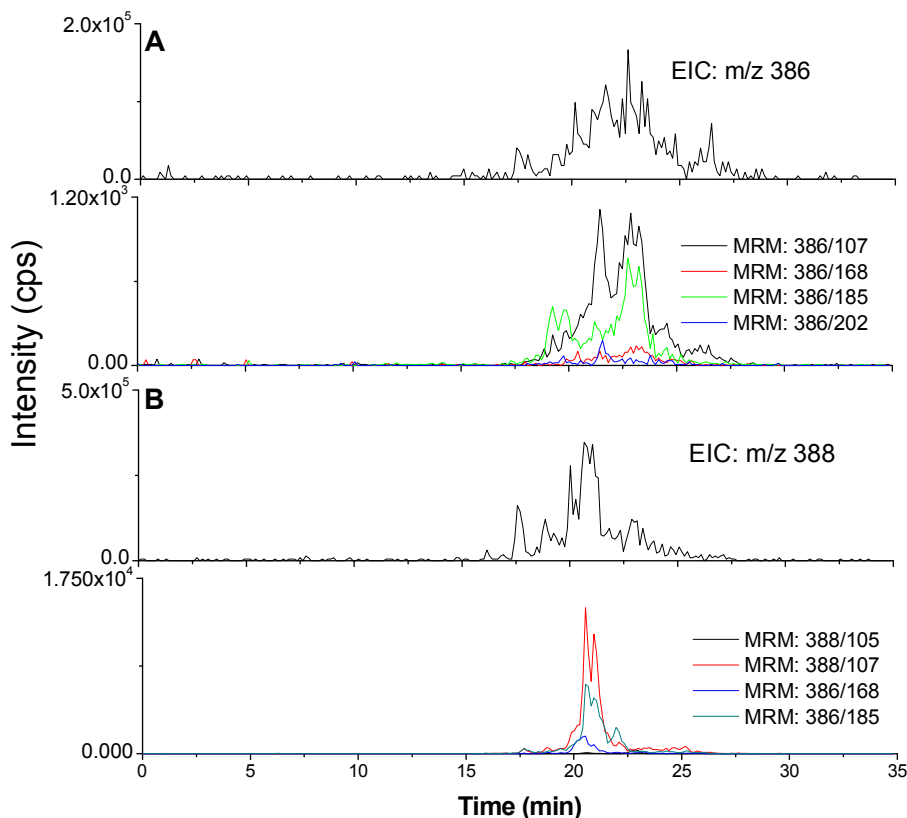


Figure 4.40 EIC and MRM chromatograms for the compound XIV (A), and XV (B) in the SOA sample

As shown in Fig. 4.40A and Fig. 4.40B, for both compound XIV and XV, the characteristic ion peaks for the ammonium cationized parent ions as well as monitored MRMs were not detected. Small peak was detected for the compound XV, however the retention time of this peak differ significantly from the retention time of the synthesized standard (see below). Also, the shape of the peak shown in Fig. 4.40B strongly indicated that this signal was a result of the background noise.

To confirm the absence of the compound XIV and the compound XV in the α -pinene SOA sample, LC/MS analysis of the synthesized standards was performed. EIC and MRM chromatograms for the standards of the compounds XIV and XV are shown in Fig. 4.41A, Fig. 4.41B, respectively.

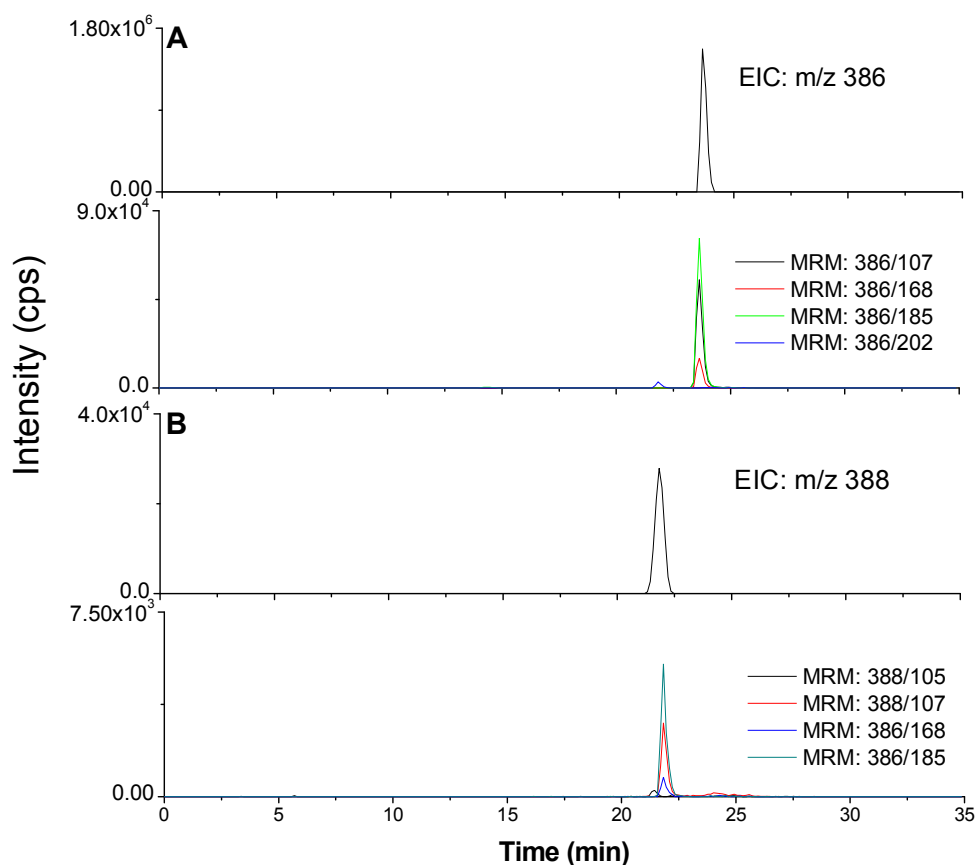


Figure 4.41 ECI and MRM chromatograms for the synthesized standards of the compounds XIV (A) and XV (B)

As shown in Fig. 4.41A, for the compound XIV, ion peaks for both ammonium cationized parent ion as well as fragments monitored in the MRM mode were detected at t_r 23.20. Also, as shown in Fig. 4.41, no distinctive peak was present at this retention time in the SOA sample unambiguously proving that compound XIV was not present in the SOA sample.

Similarly, as shown in Fig. 4.41B, for the compound XV, the ion peak was detected at t_r 21.48. As shown in Fig. 4.40B, no signal with this retention time was detected in the SOA samples, thus proving that compound XV was also not present in the flow tube reactor aerosol samples.

As already discussed in Section 4.1.3.8, no standards were available for the compounds XVI, XVII and XVIII. EIC and MRM chromatograms for the compounds XVI, XVII and XVIII are shown in Fig. 4.42A, Fig. 4.42B and Fig. 4.42C.

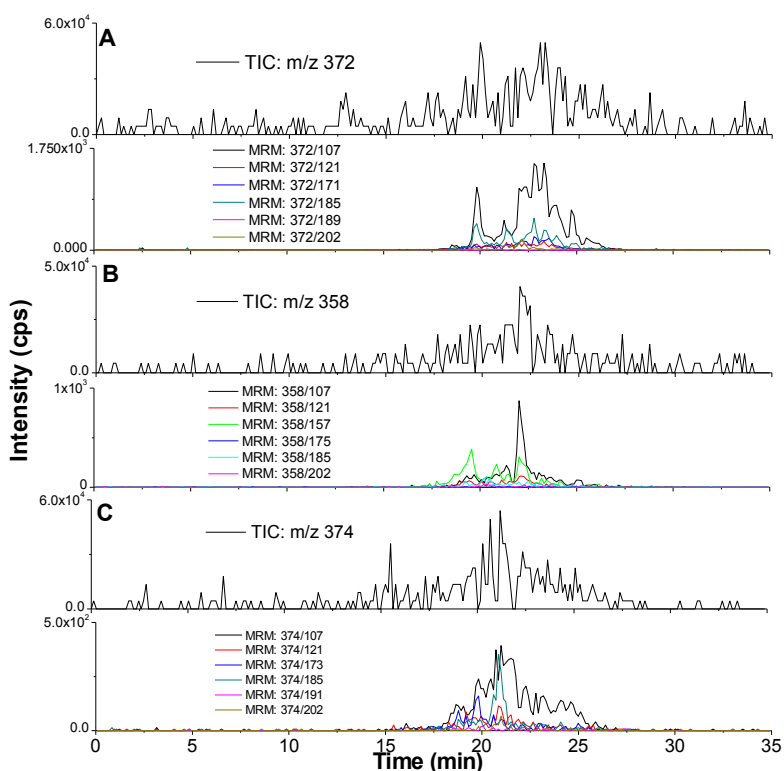


Figure 4.42 EIC and MRM chromatograms for the compounds EIC and MRM chromatograms for the compounds XVI(A), XVII(B) and XVIII(C)

As shown in Fig. 4.42, for the compounds XVI, XVII and XVIII, the ammonium cationized ions were not detected, and only background signals were observed. Weakly intense ion peaks for the monitored MRMs for these compounds are visible. However, the intensities and shape of these ion peaks strongly indicated that these were only background signals. As shown in Fig. 4.42B, for the compound XVIII, distinctive peaks for MRM pairs 358/107 and 358/157 were detected. However, the absence of ion peaks for the rest of the MRMs predicted for this compound strongly indicated that the observed signals were also the result of the presence of the compound similar to the α -acyloxyhydroperoxy aldehyde – see section 4.3.2.3. Therefore, the compounds XVI, XVII and XVIII were not present in the α -pinene SOA samples.

Thus, it was concluded, that α -acyloxyhydroperoxy aldehydes were not formed during the early stage of the ozone-initiated SOA formation from α -pinene in significant quantities, in contrast to LMW and HMW components - see sections 4.3.2.1 and 4.3.2.3. These results are in excellent agreement with those obtained for the model precursor – cyclohexene, as described in section 4.3.1.2.

As already discussed in Section 4.3.1.2, it is important to note that some minor quantities of the α -acyloxyhydroperoxy aldehydes may still be produced during the cyclohexene and α -pinene SOA formation, but it is unlikely that such low yields would have any influence on the aerosol formation. These results undermine the previous assumptions about the key role of the α -acyloxyhydroperoxy aldehydes in the α -pinene SOA nucleation process. As already discussed in section 1.4.4, up-to-date, no direct, analytical evidence were presented, confirming or contradicting this hypothesis. Thus, the results presented in this section are the first, direct analytical evidence, showing that the α -acyloxyhydroperoxy aldehydes are not the main components of the freshly formed SOA in the α -pinene/ozone system. The analysis results reported in this section strongly indicate that the α -acyloxyhydroperoxy aldehydes are unlikely to be the important nucleating agents for the α -pinene SOA.

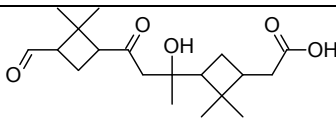
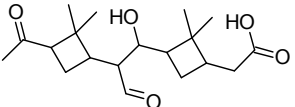
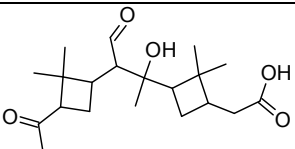
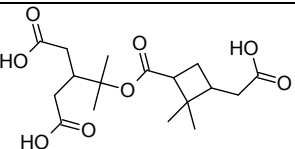
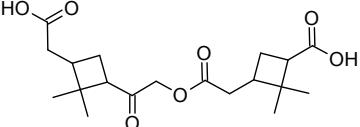
Also, HMW compounds detected in the negative ionization mode are in perfect agreement with the recently published nucleation theories,^{174,177,183} arguing against the gas-phase formation

of the nucleating agents. The formation of HMW compounds, most likely responsible for the SOA formation and growths is discussed in Section 4.3.2.3.

4.3.2.3. Formation of other high-molecular weight SOA components

In this section, investigation of the HMW compound formation during α -pinene SOA generation is described. In addition to the carboxylic acids, listed in Table 4.24, a number of HMW compounds were also detected in the α -pinene SOA samples. These experiments were carried out in the negative ionization mode; LC/MS carboxylic acids analysis conditions are described in Section 3.2.2.3. Mass to charge ratio (m/z) for the $M-H^-$ ions of the detected HMW α -pinene SOA components, together with their retention times are listed in Table 4.26; names (if known) and structures were also included.

Table 4.26 HMW compounds detected in SOA samples formed during ozone-initiated α -pinene oxidation under dry conditions (RH \approx 3%)

Name	M-H ⁻	Structure	Retention time (min)
Aldol condensation products	337	 and 	19.46
		21.44	
Unknown	341	Experimental data was insufficient to propose the structure for this compound	18.14
Aldol condensation product	351		20.80
Piny-diterpenylic ester	357		17.30
Pinonyl-piny ester	367		19.47

EIC chromatograms for the compounds listed in Table 4.26 are shown in Fig. 4.43.

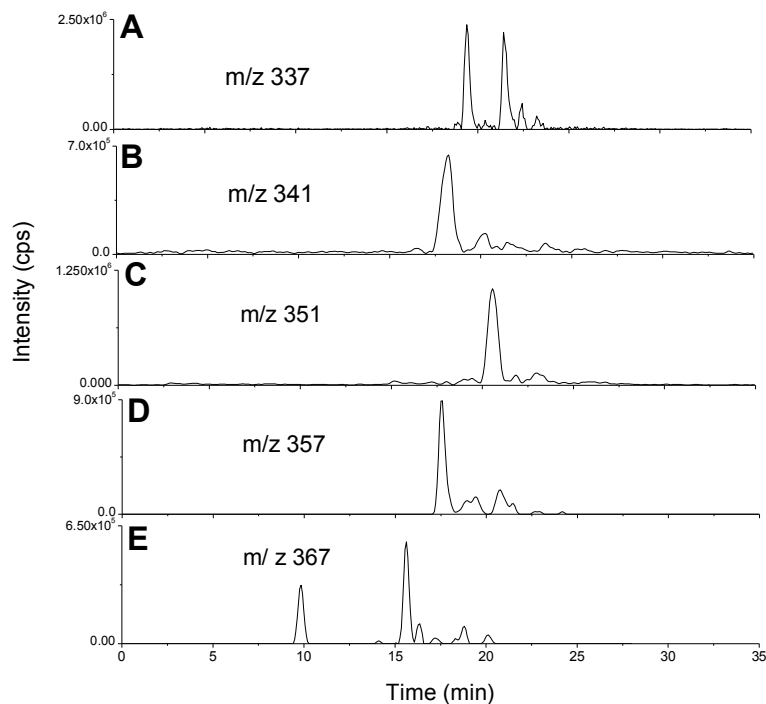


Figure 4.43 ECI chromatograms for the m/z 337(A), 341(B), 351(C), 357(D) and 367(E) in the α -pinene SOA sample

As shown in Fig. 4.43A, two peaks were detected for the m/z 337, showing the presence of the two isomers of the compound with MW 338 Da. The formation of this compound in the α -pinene SOA generated in smog-chamber experiment was reported by Tolocka et al,¹³⁹ but no structure was proposed. The formation of this compound in the early stages of aerosol formation produced in the flow-tube reactors was also reported.^{155,174} The compound with MW 338 Da detected in the ambient SOA samples was identified as a dimer product and elemental formula assigned for this compound using HR-MS was $C_{19}H_{30}O_5$.²¹⁹ Therefore, this compound appears to be an unknown, important intermediate for the early stage α -pinene SOA formation. There are a number of possible structures for this compound, taking into account the possible formation mechanism, as discussed in Section 1.4.3.4 and Section 4.3.1.3. However, using the data acquired for the analysis of the model precursor, cyclohexene and cyclohexene-d10 it is possible to propose the specific structure. As described in Section 4.3.1.3, there were two intense dimer peaks detected in the cyclohexene and cyclohexene-d10 SOA samples. After detailed evaluation of the data obtained for the deuterated precursor, these two compounds were concluded to be the aldol

condensation products of carboxylic acids containing carbonyl group with adipaldehyde and/or glutaraldehyde. It is therefore reasonable to assume the same formation mechanism for the dimers formed during α -pinene ozonolysis. In order to apply such reasoning, it has to be assumed that the carbonyl compounds are formed in large quantities during ozone – initiated α -pinene oxidation. This agrees with the previously published studies, reporting that pinonaldehyde and norpinonaldehyde were the major products of the gas-phase α -pinene ozone-initiated oxidation. 120,143,150,183

Taking this into account, the compound with MW 338 Da detected in this study is most likely produced by association of cis-pinonic acid with norpinonaldehyde and pinalic acid/norpinonic acid with pinonaldehyde. Both cis-pinonic acid and carboxylic acid with MW 170 Da were concluded to be major LMW SOA components, as reported in section 4.3.2.1. The possible formation mechanism for the compounds with MW 338 Da detected in this study is shown in Fig. 4.44.

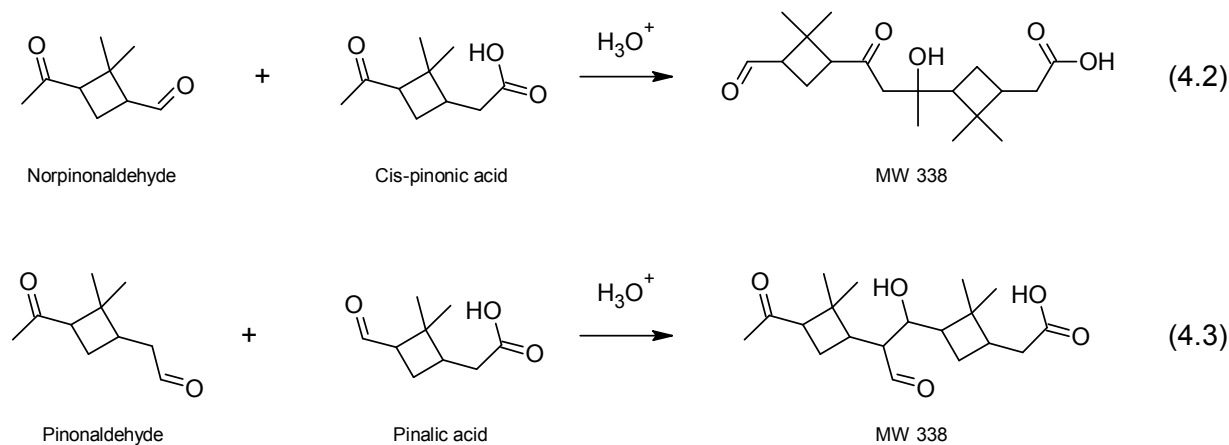


Figure 4.44 Mechanism of formation of the compounds with MW 338 Da via aldol condensation reaction

Reaction 4.2 and 4.3 are aldol condensation reactions between norpinonaldehyde and cis-pinonic acid and pinonaldehyde and cis-pinonic acid, respectively. Since, as the substrates shown in Fig. 4.44 are non-symmetric molecules, there are a number of possible isomers for the products of the reaction 4.2 and reaction 4.3. Only one possible product is shown for clarity. The retention time corresponding to the specific isomer of the compound with MW 338 Da cannot be

elucidated, based on the experimental data obtained in this study. Also, it is important to underline, that elemental formulas for the compound with the MW 338 Da, reported by Wozniak et al.²¹⁹ matches the elemental formulas of the compounds shown in Fig. 4.44.

For the α -pinene SOA, there are two pathways leading to the formation of the compounds with MW 338 Da. On the other hand, only one peak for the compound with MW 230 Da was detected in the cyclohexene - SOA samples – as reported in Section 4.3.1.3. This can be attributed to the lower chromatographic resolution of the cyclohexene dimers, and thus the two isomers were not separated. For the α -pinene, the retention on the C8, RP column is much more efficient, due to higher number of carbons in the precursor molecule, and consequently in the oxidation products, making the baseline separation of the two isomers possible.

The same argument can be used to identify the structure of the compounds with MW 352 Da. This compound was also detected in the number of studies^{139,155,219} and identified as an early stage HMW α -pinene SOA component.¹⁵⁵ This compound was tentatively identified as secondary ozonide,¹⁵⁵ but no experimental evidence, supporting these assumptions were presented. However, as already discussed in Section 4.3.1.3 no experimental results, proving that the secondary ozonides can be detected in the negative ESI are currently available. Also, it is reasonable to assume that the formation mechanism of the compound with MW 352 Da is analogous to the formation mechanism of the compound with MW 244 Da, detected in the cyclohexene SOA samples. Therefore, the compound with MW 352 Da is most likely formed via aldol condensation of cis-pinonic acid and pinonaldehyde, as shown in Fig. 4.45.

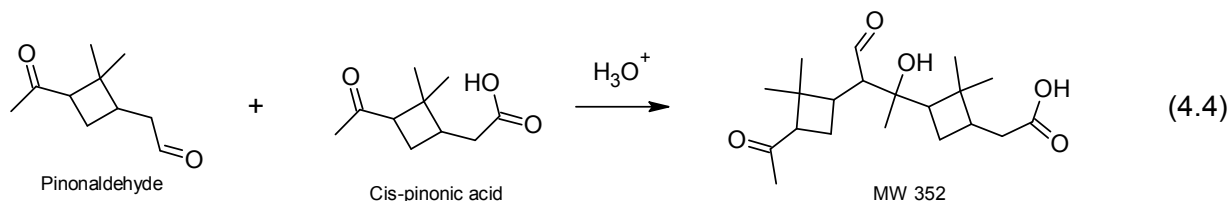


Figure 4.45 Possible formation mechanism of the compound with MW 352 Da via aldol condensation reaction

As shown in Fig. 4.43C, only one peak for the m/z 351 was detected, strongly indicating that only one formation pathway for this compound exists. Also, similar to the compounds with MWs 338 Da, the elemental formula of the aldol condensation product shown in Fig. 4.45 agrees with the elemental formula for the compound with MW 352 Da, reported by Wozniak et al: $C_{20}H_{32}O_5$.²¹⁹

As shown in Fig. 4.43D, ion peak with m/z 357 in the EIC was also detected in the SOA sample. As already discussed in Section 1.4.3.3.1 and Section 4.3.2.1, this compound was detected in a number of studies and it is now considered an important α -pinene SOA tracer.^{146,147,170,174,175,219} As already discussed in section 1.4.3.3.1, the structure of this compound is now considered to be well established, and corresponds to the ester of pinic acid and diaterpenylic acid. This is in excellent agreement with the results reported in section 4.3.2.1, since both these acids were concluded to be the major LMW components of α -pinene SOA, produced under the experimental conditions used in this work. Most importantly, this compound was reported to be the dominant component of the smallest particles, generated on short time-scale in a flow-tube reactor by Gao et al.¹⁷⁴ The results of investigation presented in this work are in excellent agreement with those reported by Gao et al.¹⁷⁴

Two ion peaks for m/z 367 were detected in the α -pinene SOA samples, at retention times $t_r=12.30$ min and $t_r=19.47$ min, as shown in Fig. 4.43E. The first ion peak corresponds to the non-covalently bonded dimer of cis-pinonic acid, based on the retention time of cis-pinonic acid standard – see section 4.1.1.2. The second peak most likely corresponds to the acidic compound with MW 368 Da. The compound with MW 368 Da was previously detected in the SOA samples, generated by ozonolysis of α -pinene in the smog-chamber.^{147,170,174,175} This compound was proposed to be esterification product of the pinic acid and 10-hydroxy pinonic acid.^{147,175} This is in excellent agreement with the results reported in section 4.3.2.1. Both 10-hydroxy pinonic acid and pinic acid were identified as the major LMW components of SOA generated in this study. The formation of the compound with MW 368 Da during the early stages of α -pinene SOA formation agrees with the results published by Gao et al.¹⁷⁴

As shown in Fig. 4.43B, large ion peak corresponding to the compound with MW 342 Da was detected at $t_r=18.14$ min. The formation of this compound has been reported by Gao et al,¹⁷⁴ and elemental formula assigned to this deprotonated peak was $C_{17}H_{25}O_7$. The same elemental formula was assigned to the deprotonated ion for this compound by Muller et al.¹⁷⁰ Although the formation of this compound during the early stages of SOA formation agrees with the previously published data, the structure could not be proposed, based on the experimental data acquired in this work.

It is difficult to estimate the concentrations of the HMW SOA components listed in Table 4.26, due to lack of standards. Similarly to the carboxylic acids listed in Table 4.24, response of the MS detector for the cis-pinonic acid and pinic acid can be used for such estimation. However, since the ESI signal is strongly dependent on the eluent composition, this estimation is very likely to lead to the overestimation of the HMW compounds concentration yields. The HMW compounds listed in Table 4.26 are strongly retained on the C8 stationary phase and thus are introduced into the ion source in solvent containing high portion of ACN due to used gradient elution (see section 3.2.2.3). It should also be noted that assuming the similar ionization efficient for the carboxylic acids and their dimers leads to an additional increase in the experimental uncertainty.

Taking this into account, the molar yields for the compounds listed in Table 4.26 should be in the range of the minor LMW components (5.0 to 1.0×10^{-5}). The realistic estimate of the uncertainty for these values can be as high as a factor of 10. Similar yields were obtained by directly comparing the ion peak areas for the HMW and LMW components; such method was utilized by Gao et al.¹⁷⁴ However, in their study¹⁷⁴ the peak area for the dimers were reported to be about 20 time greater than the peak areas of the corresponding monomers. Such discrepancies can be a result of several factors. Initially, it should be noted that comparing the ion peak areas, obtained for the two different LC/MS systems must be performed very carefully. The relative ratios of the peak areas in this study can be easily reversed by changing e.g. the ESI parameters. Reaction time of 23 s used in the flow-tube reactor by Gao et al.¹⁷⁴ was very similar to the reaction time used in this work - 33 s. (see section 3.4). Therefore different reaction time is unlikely to be a source of the aforementioned discrepancies. However, significantly lower reactant

concentrations used by Gao et al.¹⁷⁴ and the measurement of the size-dependent particles composition are likely to be a reason for the different concentration ratios of the LMW and HMW components of SOA. Also, since size-dependent SOA composition was not measured in this study, the reported results apply to the bulk of aerosol particles, including particles with larger diameters.

On the other hand, results presented in this work provided important insights into subsequent α -pinene SOA growth mechanism, while confirming the participation of the compound with MW 358 Da in the nucleation process. Also, it may be possible that more than one chemical individual is responsible for the SOA self-nucleation. This agrees with the results reported by Zhao et al.¹⁴⁸ The number of different compounds was found in the smallest particles. Similar conclusions were presented by Viitanen et al.¹⁸²

In this work, for the first time, the analytical evidence shows that the reactive uptake of the carbonyl compounds is an important growth mechanism for the freshly formed SOA, produced by gas-phase ozonolysis of α -pinene. This was supported by proposing the structures for the previously unidentified HMW products. The conclusion that aldol condensation products may be responsible for the subsequent SOA particles growth is in excellent agreement with the results published by Winkler et al.¹⁸³ In their study, it was shown that the smallest particles composed mostly of carboxylic acids while the larger particles were characterized by the higher concentrations of the carbonyl compounds. Also, as discussed by Winkler et al,¹⁸³ the used analytical method has most likely led to the thermal decomposition of the oligomers into the corresponding monomers. Therefore, it is reasonable to assume that thermal decomposition of the aldol condensation products would lead to the regeneration of the carbonyl building blocks. The results reported by Winkler et al.¹⁸³ strongly indicate that carbonyl compounds were responsible for the subsequent SOA particles growth. This is in excellent agreement with the experimental data acquired in this work, where both esters and aldol products were identified in the freshly formed SOA, produced in the α -pinene/ozone system. Similar results were obtained by studying the uptake of pinonaldehyde onto the particles composed of H_2SO_4 and $(\text{NH}_4)_2\text{SO}_4$.²²⁰ It was concluded that the reactive uptake on aerosol grain with the subsequent oligomer formation

were the major carbonyl compounds partitioning mechanisms. However, for the first time, results supporting such growth mechanism for the freshly formed SOA in the α -pinene/ozone system were presented.

The results presented in this study indicate that the SOA nucleation mechanism (in the absence of seed particles) assuming formation of the α -acyloxyhydroperoxy aldehydes needs to be revised. Under the experimental conditions used in this work, significant quantities of the α -acyloxyhydroperoxy aldehydes were absent in the freshly formed SOA as compared to the other possible nucleating agents. Therefore, the results presented in this work strongly indicate that α -acyloxyhydroperoxy aldehydes are not responsible for the self – nucleation of aerosol formed in the α -pinene/ozone system.

4.3.2.4. Relative humidity influence on SOA composition

In this section, RH influence on SOA composition is discussed. α -pinene SOA samples were prepared in humidified air (40% RH), as described in Section 3.4.4.

4.3.2.4.1. Carboxylic acids

Carboxylic acids were identified as described in Section 4.3.2.1. The same carboxylic acids were detected in SOA samples generated under dry and humid conditions. Therefore, increased humidity did not influence the α -pinene SOA composition, when the formation of the LMW carboxylic acids is considered.

Molar yields of the individual carboxylic acids were calculated as described in section 4.3.2.1. Comparison of the molar yields calculated for the experiments performed under dry and humid conditions are presented in Table 4.27.

Table 4.27 Molar yields of the α -pinene carboxylic acids formed under dry and humid conditions

Name	M-H ⁻	Molar yield (3% RH)	Molar yield (40% RH)
cis-Pinonic acid	183	$(2.8 \pm 0.1) \times 10^{-3}$	$(1.1 \pm 0.2) \times 10^{-2}$
Pinic acid	185	$(7.4 \pm 0.9) \times 10^{-4}$	$(3.2 \pm 0.4) \times 10^{-3}$

10-hydroxy pinonic acid	199	$(4.8 \pm 0.4) \times 10^{-4}$	$(1.4 \pm 0.1) \times 10^{-3}$
Pinalic acid/Norpinalic acid	169	$(1.2 \pm 0.1) \times 10^{-3}$	$(1.0 \pm 0.2) \times 10^{-2}$
Diaterpenylic acid	189	$(2.9 \pm 0.4) \times 10^{-4}$	$(5.8 \pm 0.4) \times 10^{-4}$
Terpenylic acid	171	$(1.2 \pm 0.1) \times 10^{-3}$	$(1.4 \pm 0.2) \times 10^{-3}$
4-Hydroxy-pinalic-3-acid	185	$(7.0 \pm 0.4) \times 10^{-5}$	$(1.5 \pm 0.3) \times 10^{-4}$
Norpinalic acid	155	$(9.0 \pm 2) \times 10^{-5}$	$(1.8 \pm 0.3) \times 10^{-4}$
MW 216 Da	215	$(1.3 \pm 0.4) \times 10^{-4}$	$(3.2 \pm 0.08) \times 10^{-4}$

As listed in Table 4.27, significant increase in the molar yields for all of the carboxylic acids detected in the α -pinene SOA samples was observed, within the experimental uncertainty. Similar to the data obtained for the cyclohexene SOA experiments, discussed in section 4.3.1.4, the results reported in this section indicate that formation of all of the LMW compounds is enhanced by increased amount of water vapor during the SOA formation in the flow-tube reactor. This suggests that most likely the SOA mass increases with increasing RH under the experimental conditions used in this work. This is in very good agreement with the results reported in a number of the previously published investigations. As already discussed in Section 4.3.1.4 the increased humidity leads to an increase in the SOA mass and volume.^{151,160,181,217} Regrettably, since the data for the SOA mass and size distribution formed in the experimental setup used in this work was not available, no additional conclusions can be presented.

4.3.2.4.2. α -acyloxyhydroperoxy aldehydes

Formation of the α -acyloxyhydroperoxy aldehydes was investigated as described in Section 4.3.2.2. Similar to the experiments under dry conditions, it was concluded that no α -acyloxyhydroperoxy aldehydes were produced when α -pinene ozonolysis under humid conditions was performed. These results are in good agreement with the absence of the significant quantities of α -acyloxyhydroperoxy aldehydes in cyclohexene SOA samples, produced under humid conditions, as described in Section 4.3.1.4.2.

4.3.2.4.3. Other high-molecular weight SOA components

No additional HMW compounds were detected in the α -pinene SOA samples generated under humid conditions. Increase in the formation yields, by approx. a factor of 2 was observed, similar as for the LMW components, as discussed in Section 4.3.2.4. As already discussed in section 4.3.1.4.3, the increased RH impact on the SOA composition may be more pronounced, when the lower reactants concentrations are used, effectively increasing the relative water concentration, as compared to the precursor and ozone.¹⁸¹ These conclusions warrants further studies of the RH influence on SOA formation yields as well as on the formation yields of LMW and HMW components.

5. Summary and conclusions

The main goal of this work was to investigate the formation of the HMW components (including α -acyloxyhydroperoxy aldehydes), produced during the initial stages of SOA formation in the α -pinene/ozone system. In order to get additional insights into the SOA formation mechanism, analysis of a simpler, model precursor – cyclohexene – was also carried out.

The first step of this work was the development of the analytical method for the analysis of α -acyloxyhydroperoxy aldehydes. These compounds were proposed as one of the potential nucleation precursors of the α -pinene SOA. However, the presence of these compounds in the α -pinene SOA samples was never experimentally confirmed. The analysis of a series of α -acyloxyhydroperoxy aldehydes synthesized standards was performed with LC-ESI/MS/MS. The α -acyloxyhydroperoxy aldehydes were identified as their ammonia adducts for the first time. Fragmentation pathways of the several α -acyloxyhydroperoxy aldehydes were thoroughly investigated with tandem mass spectrometry and confirmed using isotopically labeled analogs. Acquired data was used to predict the tandem mass spectra of the α -acyloxyhydroperoxy aldehydes that could not be synthesized. LC/MS analysis was used to analyze the LMW α -pinene SOA components. These LMW compounds are currently regarded as the building blocks for the detected HMW SOA components.

The second step of this work was the construction of the flow-tube reactor for the SOA generation and sampling. In the flow – tube reactor, it was possible to produce SOA under precisely controlled conditions (RH, temperature, pressure as well as concentrations of the ozone and the precursor). Precursor concentration was monitored off-line with GC/FID. Adjustment of the reaction time was performed by selecting the flow-rate of the carrier gas and the position of the movable plunger, used to introduce the ozone into the reactor. A filter sampling assembly was built and then used for particles collection for the LC/MS analysis. Also, the box – model simulations were used to confirm the complete ozone consumption before reaching the filter cartridge, thereby minimizing the possibility for the filter artifacts formation.

The third step of this work was the analysis of the SOA samples, generated in the flow-tube reactor. SOA samples under both dry and humid conditions were prepared and their chemical composition was thoroughly investigated with the LC-ESI/MS/MS. Initially, the formation of the LMW carboxylic acids was investigated for both precursors. The experimental data was in excellent agreement with the previously published results, reporting the chemical composition of the freshly formed α -pinene SOA. After validation of the experimental setup and developed analytical method, the investigation of the HMW SOA components was carried out.

α -Acyloxyhydroperoxy aldehydes formation during gas-phase ozone-initiated oxidation of a model compound, cyclohexene, was investigated. For the cyclohexene SOA, standards for the majority of the investigated α -acyloxyhydroperoxy aldehydes were synthesized. Since the standards for the majority of the investigated α -acyloxyhydroperoxy aldehydes were available, the cyclohexene SOA samples collected from flow-reactor were compared with the standards using LC/MS/MS. Using the data obtained from the LC/MS analysis of the cyclohexene SOA samples the formation of the significant quantities of the α -acyloxyhydroperoxy aldehydes during cyclohexene ozonolysis was excluded. Afterwards, the formation of the α -acyloxyhydroperoxy aldehydes during α -pinene ozonolysis was investigated. Four α -acyloxyhydroperoxy aldehydes were previously proposed as the potential nucleation precursors, and standard for only one of these compounds was synthesized, due to limited availability of the corresponding substrates. The presence of the rest of α -acyloxyhydroperoxy aldehydes was investigated by predicting their fragmentation spectrum, using the data obtained during the first step of this investigation. Similarly as for the analysis of the cyclohexene SOA, the significant quantities of the α -acyloxyhydroperoxy aldehydes were not formed during α -pinene SOA formation. Since the significant quantities of α -acyloxyhydroperoxy aldehydes were not present in the SOA samples, it is unlikely that these compounds are important intermediates in the initial steps of the particles formation in the α -pinene/ozone system.

After confirming that the α -acyloxyhydroperoxy aldehydes most probably did not significantly impact the SOA formation during the initial steps of particles production, the formation of the remainder of HMW components was investigated. A number of HMW

compounds were produced during the initial stages of α -pinene SOA formation. The results from the HMW components analysis performed in this work indicated that the formation of ester is the most likely SOA nucleation mechanism, arguing against the gas-phase nucleation mechanism. Therefore, based on the results acquired in this study, direct participation of the SCI reaction products with the stable molecules, such as carboxylic acids and carbonyl compounds in the nucleation mechanism is unlikely. This is especially important for the revision of the α -pinene SOA self-nucleation mechanism, previously used in the number of modeling studies.

A number of previously unidentified HMW compounds were also detected. Data obtained for the model precursor was used to propose structures for those up-to-date unknown oligomers. This novel approach utilizing analysis of the deuterated analog was used to identify the HMW SOA components. Such approach appears to be very versatile, since it allows to exclude number of possible structures, based on the mass shift of the specific ion peak alone, as opposed to the most popular approach based only on tandem mass spectra interpretation. This allowed to assign structure for the two – previously unrecognized α -pinene HMW SOA components. These compounds were identified as aldol condensation products between carbonyl compounds and carbonyl-containing carboxylic acids.

The direct, experimental evidence were presented excluding the formation of the significant quantities of secondary ozonides in the α -pinene/ozone system. Results indicating the formation of secondary ozonides as the important α -pinene HMW SOA components were most likely misinterpreted in the previous investigations.

At the same time, the established formation mechanism of the previously unknown HMW α -pinene SOA components allowed proposing the growth mechanism of the freshly formed aerosol. The structures for these products were identified, based on the experimental data obtained from the SOA composition analysis, produced from the cyclohexene and cyclohexene-d10 ozonolysis.

The proposed growth mechanism of the freshly formed SOA includes reactive uptake of the carbonyl compounds, as opposed to the simple gas-particle phase partitioning. The direct, analytical evidence supporting these assumptions were presented for the first time.

Increased relative humidity enhances the SOA yield. However, the RH increase did not significantly impact the SOA chemical composition.

6. List of abbreviations

In this section, used abbreviations are listed in the alphabetical order.

ACN - acetonitrile

APCI - atmospheric pressure chemical ionization

BC – black carbon

BSOA – biogenic secondary organic aerosol

BVOC – biogenic volatile organic compound

CCN – cloud condensation nuclei

CE - capillary electrophoresis

CI - chemical ionization

CID – collision induced dissociation

CIMS - chemical ionization mass spectrometry

DMS - dimethyl sulfate

ECI - excited Criegee intermediate

EI – electron ionization

ESI – electrospray ionization

EIC – extracted ion current

FID – flame ionization detector

FTICRMS - Fourier transform ion cyclotron resonance mass spectrometry

GC - gas chromatography

GC/FID – gas chromatography with flame ionization detected

GC/MS - gas chromatography coupled to the mass spectrometry

GHG – greenhouse gas

HFC - hydrofluorocarbon

HMW – high molecular weight - used with respect to SOA fraction with the MW < 250

HR-MS – high resolution - mass spectrometry

ID - inner diameter

IMS - ion mobility spectrometer

IN – ice nuclei

LC - liquid chromatography/high performance liquid chromatography

LC/MS – liquid chromatography/high performance liquid chromatography coupled to the mass spectrometry

LC-ESI/MSⁿ - liquid chromatography coupled to the electrospray ionization tandem mass spectrometry

LIT – linear ion trap

LMW – low molecular weight - in this thesis used with respect to SOA fraction > 250

MALDI - matrix assisted laser desorption ionization

MS - mass spectrometry

MW - molecular weight

OA – organic aerosol

OC – organic carbon

PAH - polycyclic aromatic hydrocarbon

PIAMS - photoionization aerosol mass spectrometer

PM – particulate matter

PM₁₀ - particles having diameters 10 µm or less

PM_{2.5} – particles having diameters 2.5 µm or less

RH - relative humidity

SCI - stabilized Criegee intermediate

SOA – secondary organic aerosol

TDPBMS - thermal desorption particle beam mass spectrometry

TOF – time of flight (mass spectrometer)

UF – ultra fine

UFP – ultrafine particles

UHP – ultrahigh purity

VOC – volatile organic compound

Conferences, publications and internships abroad

Posters

Ranjit K Talukdar, Bartłomiej Witkowski, A. R. Ravishankara, and James B. Burkholder, "Henry's law coefficients and hydrolysis rate coefficients of atmospheric trace gases", 22nd International Symposium on Gas Kinetics, 18-22.06.2012, Boulder, CO.

Bartłomiej Witkowski, Tomasz Gierczak, "Analysis of α -acyloxyhydroperoxy aldehydes with electrospray ionization – tandem mass spectrometry (ESI-MSⁿ)", 22nd International Symposium on Gas Kinetics, 18-22.06.2012, Boulder, CO, USA

Ranjit K Talukdar, Bartłomiej Witkowski, A. R. Ravishankara, and James B. Burkholder, "Henry's law coefficients and hydrolysis rate coefficients of atmospheric trace gases" Cooperative Institute for Research in Environmental Sciences (CIRES) science rendezvous, 24.04.2012, Boulder, CO, USA.

Bartłomiej Witkowski, Tomasz Gierczak „Badanie załączków nukleacji wtórnych aerozoli organicznych (SOA)” Analityczne zastosowania chromatografii cieczowej, 15.10.10, Warszawa

Bartłomiej Witkowski, Tomasz Gierczak, Badanie załączków nukleacji w tworzeniu wtórnych aerozoli atmosferycznych metodą LC/MS/MS, ChemSession'10, 14-15.05.2010, Warszawa

Oral presentetions

Bartłomiej Witkowski, Tomasz Gierczak, "Analiza α -acylohydroperoksy aldehydów za pomocą chromatografii cieczowej połączonej z tandemową spektrometrią mas (LC-ESI/MSⁿ)" Analityczne zastosowania chromatografii cieczowej, 25-26.10.2012, Warszawa

Bartłomiej Witkowski and Tomasz Gierczak, „Study of the possible nucleating agents in the secondary organic aerosols (SOA) samples”, Joint Symposium of the International PhD Programs, 5–8,10,2012, Pułtusk

Bartłomiej Witkowski, Magdalena Biesaga, Tomasz Gierczak "Identyfikacja spoiw malarskich za pomocą technik chromatograficznych; GC/MS oraz HPLC/MS/MS" VIII Polska Konferencja Chemii Analitycznej, 4-9.07.2010, Kraków

Bartłomiej Witkowski, Tomasz Gierczak, "The LC/MS/MS analysis of the nucleation precursors in the formation of secondary organic aerosols (SOA)", The XXXIVth Symposium Chromatographic methods of investigating the organic compounds, 25-27.05. 2010, Szczyrk

Bartłomiej Witkowski, Magdalena Biesaga, Tomasz Gierczak, „Identyfikacja spoiw malarskich za pomocą technik chromatograficznych: GC/FID oraz LC/MS/MS”, Analiza chemiczna w ochronie zabytków, 10-11.12.2009, Warszawa

Publications in the peer-reviewed journals

Witkowski, B., M. Biesaga, and T. Gierczak, *Proteinaceous binders identification in the works of art using ion-pairing free reversed-phase liquid chromatography coupled with tandem mass spectrometry*. Analytical Methods, 2012. 4(5): p. 1221-1228.

Witkowski, B. and T. Gierczak, *Analysis of α -acyloxyhydroperoxy aldehydes with electrospray ionization–tandem mass spectrometry (ESI-MSⁿ)*. Journal of Mass Spectrometry, 2013. 48(1): p. 79-88.

Ewa Jabłonka-Gronowska, Bartłomiej Witkowski, Paweł Horeglad, Tomasz Gierczak, Karol Grela, *Testing the 1,1,3,3-tetramethyldisiloxane linker in olefin metathesis*, *Comptes Rendus Chimie*, Volume 16, Issue 6, June 2013, Pages 566-572

Internships abroad

Cooperative Institute for Research in Environmental Sciences (CIRES) University of Colorado, Boulder, CO, USA

Visiting research associate (08.12.2010 – 30.05.2011)

Visiting research associate (01.02.2012 – 31.07.2012)

Institute of Combustion Aerothermal Reactivity and Environment (ICARE), French National Centre for Scientific Research (CNRS), Orleans, France:

Visiting research associate (08.09.2013 – 08.10.2013)

References

- (1) Finlayson-Pitts, B. J.; Pitts Jr, J. N. *Chemistry of the Upper and Lower Atmosphere*; Academic Press: San Diego, 2000.
- (2) Hinds, W. C. *Aerosol Technology: Properties, Behavior, and Measurement of Airborne Particles*, Second edition ed.; Wiley-Interscience, 1999.
- (3) Seinfeld, J.; Pandis, S. *Atmospheric Chemistry and Physics: From Air Pollution to Climate Change*; John Wiley & Sons, 2006.
- (4) Valavanidis, A.; Fiotakis, K.; Vlachogianni, T. *Journal of Environmental Science and Health Part C-Environmental Carcinogenesis & Ecotoxicology Reviews* **2008**, *26*, 339.
- (5) Ruckerl, R.; Schneider, A.; Breitner, S.; Cyrus, J.; Peters, A. *Inhalation Toxicology* **2011**, *23*, 555.
- (6) Harrison, R. M.; Yin, J. X. *Science of the Total Environment* **2000**, *249*, 85.
- (7) Despres, V. R.; Huffman, J. A.; Burrows, S. M.; Hoose, C.; Safatov, A. S.; Buryak, G.; Frohlich-Nowoisky, J.; Elbert, W.; Andreae, M. O.; Poschl, U.; Jaenicke, R. *Tellus Series B-Chemical and Physical Meteorology* **2012**, *64*.
- (8) Heal, M. R.; Kumar, P.; Harrison, R. M. *Chemical Society Reviews* **2012**, *41*, 6606.
- (9) Kelly, F. J.; Fussell, J. C. *Atmospheric Environment* **2012**, *60*, 504.
- (10) Poschl, U. *Angewandte Chemie-International Edition* **2005**, *44*, 7520.
- (11) Tsigaridis, K.; Krol, M.; Dentener, F. J.; Balkanski, Y.; Lathière, J.; Metzger, S.; Hauglustaine, D. A.; Kanakidou, M. *Atmos. Chem. Phys.* **2006**, *6*, 5143.
- (12) Raes, F.; Van Dingenen, R.; Vignati, E.; Wilson, J.; Putaud, J. P.; Seinfeld, J. H.; Adams, P. *Atmospheric Environment* **2000**, *34*, 4215.
- (13) Ramanathan, V.; Crutzen, P. J.; Kiehl, J. T.; Rosenfeld, D. *Science* **2001**, *294*, 2119.
- (14) Ginoux, P.; Prospero, J. M.; Gill, T. E.; Hsu, N. C.; Zhao, M. *Reviews of Geophysics* **2012**, *50*.
- (15) Liousse, C.; Penner, J. E.; Chuang, C.; Walton, J. J.; Eddleman, H.; Cachier, H. *Journal of Geophysical Research: Atmospheres* **1996**, *101*, 19411.
- (16) Zender, C. S.; Miller, R. L. R. L.; Tegen, I. *Eos, Transactions American Geophysical Union* **2004**, *85*, 509.
- (17) Vignati, E.; Facchini, M. C.; Rinaldi, M.; Scannell, C.; Ceburnis, D.; Sciare, J.; Kanakidou, M.; Myriokefalitakis, S.; Dentener, F.; O'Dowd, C. D. *Atmospheric Environment* **2010**, *44*, 670.

- (18) Bingemer, H.; Klein, H.; Ebert, M.; Haunold, W.; Bundke, U.; Herrmann, T.; Kandler, K.; Müller-Ebert, D.; Weinbruch, S.; Judt, A.; Ardon-Dryer, K.; Levin, Z.; Curtius, J. *Atmos. Chem. Phys. Discuss.* **2011**, *11*, 2733.
- (19) Matthias-Maser, S.; Jaenicke, R. *Atmospheric Research* **1995**, *39*, 279.
- (20) Hallquist, M.; Wenger, J. C.; Baltensperger, U.; Rudich, Y.; Simpson, D.; Claeys, M.; Dommen, J.; Donahue, N. M.; George, C.; Goldstein, A. H.; Hamilton, J. F.; Herrmann, H.; Hoffmann, T.; Iinuma, Y.; Jang, M.; Jenkin, M. E.; Jimenez, J. L.; Kiendler-Scharr, A.; Maenhaut, W.; McFiggans, G.; Mentel, T. F.; Monod, A.; Prevot, A. S. H.; Seinfeld, J. H.; Surratt, J. D.; Szmigielski, R.; Wildt, J. *Atmospheric Chemistry and Physics* **2009**, *9*, 5155.
- (21) Atkinson, R.; Arey, J. *Atmospheric Environment* **2003**, *37*, S197.
- (22) Kanakidou, M.; Seinfeld, J. H.; Pandis, S. N.; Barnes, I.; Dentener, F. J.; Facchini, M. C.; Van Dingenen, R.; Ervens, B.; Nenes, A.; Nielsen, C. J.; Swietlicki, E.; Putaud, J. P.; Balkanski, Y.; Fuzzi, S.; Horth, J.; Moortgat, G. K.; Winterhalter, R.; Myhre, C. E. L.; Tsigaridis, K.; Vignati, E.; Stephanou, E. G.; Wilson, J. *Atmospheric Chemistry and Physics* **2005**, *5*, 1053.
- (23) Remer, L. A.; Kleidman, R. G.; Levy, R. C.; Kaufman, Y. J.; Tanre, D.; Mattoo, S.; Martins, J. V.; Ichoku, C.; Koren, I.; Yu, H. B.; Holben, B. N. *Journal of Geophysical Research-Atmospheres* **2008**, *113*.
- (24) Myhre, G. *Science* **2009**, *325*, 187.
- (25) Williams, J.; de Reus, M.; Krejci, R.; Fischer, H.; Strom, J. *Atmospheric Chemistry and Physics* **2002**, *2*, 133.
- (26) Matsuda, K.; Sase, H.; Muraio, N.; Fukazawa, T.; Khoomsu, K.; Chanonmuang, P.; Visaratana, T.; Khummongkol, P. *Atmospheric Environment* **2012**, *54*, 282.
- (27) Zhang, B.-Z.; Zhang, K.; Li, S.-M.; Wong, C. S.; Zeng, E. Y. *Environmental Science & Technology* **2012**, *46*, 7207.
- (28) Haywood, J.; Boucher, O. *Reviews of Geophysics* **2000**, *38*, 513.
- (29) Lohmann, U.; Feichter, J. *Atmospheric Chemistry and Physics* **2005**, *5*, 715.
- (30) Yu, H.; Kaufman, Y. J.; Chin, M.; Feingold, G.; Remer, L. A.; Anderson, T. L.; Balkanski, Y.; Bellouin, N.; Boucher, O.; Christopher, S.; DeCola, P.; Kahn, R.; Koch, D.; Loeb, N.; Reddy, M. S.; Schulz, M.; Takemura, T.; Zhou, M. *Atmospheric Chemistry and Physics* **2006**, *6*, 613.
- (31) Satheesh, S. K.; Moorthy, K. K. *Atmospheric Environment* **2005**, *39*, 2089.
- (32) Takemura, T.; Nakajima, T.; Dubovik, O.; Holben, B. N.; Kinne, S. *Journal of Climate* **2002**, *15*, 333.
- (33) Bauer, S. E.; Menon, S. *Journal of Geophysical Research: Atmospheres* **2012**, *117*, D01206.
- (34) Petters, M. D.; Kreidenweis, S. M. *Atmos. Chem. Phys.* **2007**, *7*, 1961.
- (35) Harrison, R. M. *Pollution - Causes, Effects and Control* (4th Edition); Royal Society of Chemistry.
- (36) Kampa, M.; Castanas, E. *Environmental Pollution* **2008**, *151*, 362.
- (37) MacNee, W.; Donaldson, K. *European Respiratory Journal* **2003**, *21*, 475.
- (38) Bernstein, J. A.; Alexis, N.; Barnes, C.; Bernstein, I. L.; Nel, A.; Peden, D.; Diaz-Sanchez, D.; Tarlo, S. M.; Williams, P. B. *Journal of Allergy and Clinical Immunology* **2004**, *114*, 1116.
- (39) Brook, R. D.; Rajagopalan, S.; Pope, C. A.; Brook, J. R.; Bhatnagar, A.; Diez-Roux, A. V.; Holguin, F.; Hong, Y. L.; Luepker, R. V.; Mittleman, M. A.; Peters, A.; Siscovick, D.; Smith, S. C.; Whitsel, L.; Kaufman, J. D.; Amer Heart Assoc Council, E.; Council Kidney Cardiovasc, D.; Council Nutr Phys Activity, M. *Circulation* **2010**, *121*, 2331.
- (40) Pope, C. A.; Ezzati, M.; Dockery, D. W. *New England Journal of Medicine* **2009**, *360*, 376.
- (41) Dockery, D. W.; Pope, C. A.; Xu, X.; Spengler, J. D.; Ware, J. H.; Fay, M. E.; Ferris, B. G.; Speizer, F. E. *New England Journal of Medicine* **1993**, *329*, 1753.
- (42) Laden, F.; Schwartz, J.; Speizer, F. E.; Dockery, D. W. *American Journal of Respiratory and Critical Care Medicine* **2006**, *173*, 667.

- (43) Pope, C. A.; Schwartz, J.; Ransom, M. R. *Archives of Environmental Health* **1992**, *47*, 211.
- (44) Kinney, P. L.; Ito, K.; Thurston, G. D. *Inhalation Toxicology* **1995**, *7*, 59.
- (45) Schwartz, J.; Dockery, D. W. *American Journal of Epidemiology* **1992**, *135*, 12.
- (46) Schwartz, J. *Environmental Research* **1991**, *56*, 204.
- (47) Schwartz, J.; Dockery, D. W. *American Review of Respiratory Disease* **1992**, *145*, 600.
- (48) Gauderman, W. J.; Avol, E.; Gilliland, F.; Vora, H.; Thomas, D.; Berhane, K.; McConnell, R.; Kuenzli, N.; Lurmann, F.; Rappaport, E.; Margolis, H.; Bates, D.; Peters, J. *New England Journal of Medicine* **2004**, *351*, 1057.
- (49) Xu, X. P.; Dockery, D. W.; Wang, L. H. *Archives of Environmental Health* **1991**, *46*, 198.
- (50) Pope, C. A. *Archives of Environmental Health* **1991**, *46*, 90.
- (51) DiazSanchez, D.; Tsien, A.; Fleming, J.; Saxon, A. *Journal of Immunology* **1997**, *158*, 2406.
- (52) DiazSanchez, D. *Allergy* **1997**, *52*, 52.
- (53) Diaz-Sanchez, D.; Proietti, L.; Polosa, R. *Current Allergy and Asthma Reports* **2003**, *3*, 146.
- (54) Pope, C. A.; Burnett, R. T.; Thun, M. J.; Calle, E. E.; Krewski, D.; Ito, K.; Thurston, G. D. *Jama-Journal of the American Medical Association* **2002**, *287*, 1132.
- (55) Ward, D. J.; Ayres, J. G. *Occupational and Environmental Medicine* **2004**, *61*.
- (56) Grahame, T. J.; Schlesinger, R. B. *Inhalation Toxicology* **2005**, *17*, 15.
- (57) Schlesinger, R. B. *Inhalation Toxicology* **2007**, *19*, 811.
- (58) Chen, L. C.; Lippmann, M. *Inhalation Toxicology* **2009**, *21*, 1.
- (59) Harrison, R. M.; Smith, D. J. T.; Kibble, A. J. *Occupational and Environmental Medicine* **2004**, *61*, 799.
- (60) Ziemann, P. J.; Atkinson, R. *Chemical Society Reviews* **2012**, *41*, 6582.
- (61) Atkinson, R.; Arey, J. *Chemical Reviews* **2003**, *103*, 4605.
- (62) Guenther, A.; Hewitt, C. N.; Erickson, D.; Fall, R.; Geron, C.; Graedel, T.; Harley, P.; Klinger, L.; Lerdau, M.; McKay, W. A.; Pierce, T.; Scholes, B.; Steinbrecher, R.; Tallamraju, R.; Taylor, J.; Zimmerman, P. J. *Geophys. Res.* **1995**, *100*, 8873.
- (63) Fuentes, J. D.; Lerdau, M.; Atkinson, R.; Baldocchi, D.; Bottenheim, J. W.; Ciccioli, P.; Lamb, B.; Geron, C.; Gu, L.; Guenther, A.; Sharkey, T. D.; Stockwell, W. *Bulletin of the American Meteorological Society* **2000**, *81*, 1537.
- (64) Tsigaridis, K.; Kanakidou, M. *Atmospheric Chemistry and Physics* **2003**, *3*, 1849.
- (65) Lack, D. A.; Tie, X. X.; Bofinger, N. D.; Wiegand, A. N.; Madronich, S. *Journal of Geophysical Research* **2004**, *109*, D03203.
- (66) Seinfeld, J. H.; Pankow, J. F. *Annual Review of Physical Chemistry* **2003**, *54*, 121.
- (67) Croteau, R.; Satterwhite, D. M.; Wheeler, C. J.; Felton, N. M. *Journal of Biological Chemistry* **1989**, *264*, 2075.
- (68) Chapman, S. *A theory of upper-atmospheric ozone*; Edward Stanford, 1930.
- (69) Finlaysonpitts, B. J.; Pitts, J. N. *Journal of the Air & Waste Management Association* **1993**, *43*, 1091.
- (70) United Nations Environment Programme, E. E. A. P. *Photochemical & Photobiological Sciences* **2012**, *11*, 13.
- (71) Norval, M.; Lucas, R. M.; Cullen, A. P.; de Gruijl, F. R.; Longstreth, J.; Takizawa, Y.; van der Leun, J. C. *Photochemical & Photobiological Sciences* **2011**, *10*, 199.
- (72) McKenzie, R. L.; Aucamp, P. J.; Bais, A. F.; Bjorn, L. O.; Ilyas, M.; Madronich, S. *Photochemical & Photobiological Sciences* **2011**, *10*, 182.
- (73) UNEP. http://ozone.unep.org/new_site/en/treaty_ratification_status.php, 2013.
- (74) UNEP. Montreal Protocol; http://ozone.unep.org/new_site/en/montreal_protocol.php, 1987.

(75) IPCC "IPCC/TEAP Special Report on Safeguarding the Ozone Layer and the Global Climate System: Issues Related to Hydrofluorocarbons and Perfluorocarbons

U.S. Government Review," Intergovernmental Panel on Climate Change, 2005.

(76) WMO "Scientific Assessment of ozone Depletion: 2010," World Meteorological Organization, 2010.

(77) WMO *Scientific Assessment of Ozone Depletion, 2006, Global Ozone Research and Monitoring Project - Report No. 37* Geneva, Switzerland, 2006, World Meteorological Organization.

(78) Blacet, F. E. *Industrial and Engineering Chemistry* **1952**, *44*, 1339.

(79) Fowler, D.; Cape, J. N.; Coyle, M.; Smith, R. I.; Hjellbrekke, A. G.; Simpson, D.; Derwent, R. G.; Johnson, C. E. *Environmental Pollution* **1999**, *100*, 43.

(80) Ashmore, M. R. *Plant, Cell & Environment* **2005**, *28*, 949.

(81) Bernacchi, C. J.; Leakey, A. D. B.; Kimball, B. A.; Ort, D. R. *Environmental Pollution* **2011**, *159*, 1464.

(82) Heagle, A. S. *Annual Review of Phytopathology* **1989**, *27*, 397.

(83) Wittig, V. E.; Ainsworth, E. A.; Naidu, S. L.; Karnosky, D. F.; Long, S. P. *Global Change Biology* **2009**, *15*, 396.

(84) Ebi, K. L.; McGregor, G. *Environmental Health Perspectives* **2008**, *116*, 1449.

(85) Mudway, I. S.; Kelly, F. J. *Molecular aspects of medicine* **2000**, *21*, 1.

(86) Criegee, R. *Angewandte Chemie-International Edition in English* **1975**, *14*, 745.

(87) Irfan, M.; Glasnov, T. N.; Kappe, C. O. *Organic Letters* **2011**, *13*, 984.

(88) Wolf, J. L.; Richters, S.; Pecher, J.; Zeuch, T. *Physical Chemistry Chemical Physics* **2011**, *13*, 10952.

(89) Ziemann, P. J. *The Journal of Physical Chemistry A* **2003**, *107*, 2048.

(90) Ziemann, P. J. *The Journal of Physical Chemistry A* **2002**, *106*, 4390.

(91) Tobias, H. J.; Ziemann, P. J. *The Journal of Physical Chemistry A* **2001**, *105*, 6129.

(92) Heaton, K. J.; Dreyfus, M. A.; Wang, S.; Johnston, M. V. *Environmental Science & Technology* **2007**, *41*, 6129.

(93) Kamens, R.; Jang, M.; Chien, C.-J.; Leach, K. *Environmental Science & Technology* **1999**, *33*, 1430.

(94) Atkinson, R.; Tuazon, E. C.; Aschmann, S. M. *Environmental Science & Technology* **1995**, *29*, 1860.

(95) Grosjean, D.; Grosjean, E.; Williams, E. L. *Environmental Science & Technology* **1994**, *28*, 186.

(96) EPA. Regulatory Impact Analysis for the Proposed Revisions to the National Ambient Air Quality

Standards for Particulate Matter; 2012, 2012; pp EPA.

(97) Grosjean, E.; Grosjean, D. *Environmental Science & Technology* **1997**, *31*, 2421.

(98) Khamaganov, V. G.; Hites, R. A. *The Journal of Physical Chemistry A* **2001**, *105*, 815.

(99) Munshi, H. B.; Rao, K.; Iyer, R. M. *Atmospheric Environment* **1989**, *23*, 1971.

(100) Nguyen, T. L.; Peeters, J.; Vereecken, L. *Physical Chemistry Chemical Physics* **2009**, *11*, 5643.

(101) J. A. Manion, R. E. H., R. D. Levin, D. R. Burgess Jr., V. L. Orkin, W. Tsang, W. S. McGivern, J.

W. Hudgens, V. D. Knyazev, D. B. Atkinson, E. Chai, A. M. Tereza, C.-Y. Lin, T. C. Allison, W. G. Mallard, F. Westley, J. T. Herron, R. F. Hampson, and D. H. Frizzell. NIST Chemical Kinetics Database. In *Standard Reference Database 17*; 7.0 ed.; National Institute of Standards and Technology, Gaithersburg, Maryland, 20899-8320, 2013.

- (102) Bonn, B.; Korhonen, H.; Petäjä, T.; Boy, M.; Kulmala, M. *Atmos. Chem. Phys. Discuss.* **2007**, *7*, 3901.
- (103) Ceulemans, K.; Compornolle, S.; Peeters, J.; Müller, J.-F. *Atmospheric Environment* **2010**, *44*, 5434.
- (104) Neeb, P.; Horie, O.; Moortgat, G. K. *The Journal of Physical Chemistry A* **1998**, *102*, 6778.
- (105) Atkinson, R.; Winer, A. M.; Pitts, J. N. *Atmospheric Environment* **1982**, *16*, 1017.
- (106) Baker, J.; Aschmann, S. M.; Arey, J.; Atkinson, R. *International Journal of Chemical Kinetics* **2001**, *34*, 73.
- (107) Witkowski, B.; Gierczak, T. *Journal of Mass Spectrometry* **2013**, *48*, 79.
- (108) Kukovincts, O. S.; Zvereva, T. I.; Kabalnova, N. N.; Kasradze, V. G.; Salimova, E. V.; Khalitova, L. R.; Abdullin, M. I.; Spirikhin, L. V. *Mendeleev Communications* **2009**, *19*, 106.
- (109) Jaworski, K.; Smith, L. L. *Journal of Organic Chemistry* **1988**, *53*, 545.
- (110) Tobias, H. J.; Docherty, K. S.; Beving, D. E.; Ziemann, P. J. *Environmental Science & Technology* **2000**, *34*, 2116.
- (111) Vibenholt, A.; Norgaard, A. W.; Clausen, P. A.; Wolkoff, P. *Chemosphere* **2009**, *76*, 572.
- (112) Docherty, K. S.; Kumboonlert, K.; Lee, I. J.; Ziemann, P. J. *Journal of Chromatography A* **2004**, *1029*, 205.
- (113) Murai, S.; Sonoda, N.; Tsutsumi, S. *Bulletin of the Chemical Society of Japan* **1964**, *37*, 1187.
- (114) Tobias, H. J.; Ziemann, P. J. *Environmental Science & Technology* **2000**, *34*, 2105.
- (115) Tobias, H. J.; Ziemann, P. J. *Analytical Chemistry* **1999**, *71*, 3428.
- (116) Pulfer, M. K.; Harrison, K.; Murphy, R. C. *Journal of the American Society for Mass Spectrometry* **2004**, *15*, 194.
- (117) Kamens, R. M.; Jaoui, M. *Environmental Science & Technology* **2001**, *35*, 1394.
- (118) Chew, A. A.; Atkinson, R. *Journal of Geophysical Research: Atmospheres* **1996**, *101*, 28649.
- (119) Paulson, S. E.; Sen, A. D.; Liu, P.; Fenske, J. D.; Fox, M. J. *Geophysical Research Letters* **1997**, *24*, 3193.
- (120) Ma, Y.; Russell, A. T.; Marston, G. *Physical Chemistry Chemical Physics* **2008**, *10*, 4294.
- (121) Hatakeyama, S.; Izumi, K.; Fukuyama, T.; Akimoto, H. *Journal of Geophysical Research* **1989**, *94*, 13013.
- (122) Winterhalter, R.; Van Dingenen, R.; Larsen, B. R.; Jensen, N. R.; Hjorth, J. *Atmospheric Chemistry and Physics* **2003**, *3*, 1.
- (123) Ma, Y.; Willcox, T. R.; Russell, A. T.; Marston, G. *Chemical Communications* **2007**, *0*, 1328.
- (124) Jenkin, M. E.; Shallcross, D. E.; Harvey, J. N. *Atmospheric Environment* **2000**, *34*, 2837.
- (125) Docherty, K. S.; Wu, W.; Lim, Y. B.; Ziemann, P. J. *Environmental Science & Technology* **2005**, *39*, 4049.
- (126) Peeters, J.; Vereecken, L.; Fantechi, G. *Physical Chemistry Chemical Physics* **2001**, *3*, 5489.
- (127) Hatakeyama, S.; Izumi, K.; Fukuyama, T.; Akimoto, H.; Washida, N. *Journal of Geophysical Research: Atmospheres* **1991**, *96*, 947.
- (128) Arey, J.; Atkinson, R.; Aschmann, S. M. *Journal of Geophysical Research: Atmospheres* **1990**, *95*, 18539.
- (129) Yu, J. Z.; Flagan, R. C.; Seinfeld, J. H. *Environmental Science & Technology* **1998**, *32*, 2357.
- (130) Koch, S.; Winterhalter, R.; Uherek, E.; Kolloff, A.; Neeb, P.; Moortgat, G. K. *Atmospheric Environment* **2000**, *34*, 4031.
- (131) Jaoui, M.; Kamens, R. M. *Journal of Geophysical Research: Atmospheres* **2001**, *106*, 12541.
- (132) Warscheid, B.; Hoffmann, T. *Atmospheric Environment* **2001**, *35*, 2927.
- (133) Hoppel, W.; Fitzgerald, J.; Frick, G.; Caffrey, P.; Pasternack, L.; Hegg, D.; Gao, S.; Leaitch, R.; Shantz, N.; Cantrell, C.; Albrechtinski, T.; Ambrusko, J.; Sullivan, W. *Journal of Geophysical Research: Atmospheres* **2001**, *106*, 27603.

- (134) Warscheid, B.; Hoffmann, T. *Rapid Communications in Mass Spectrometry* **2002**, *16*, 496.
- (135) Czoschke, N. M.; Jang, M.; Kamens, R. M. *Atmospheric Environment* **2003**, *37*, 4287.
- (136) Gao, S.; Keywood, M.; Ng, N. L.; Surratt, J.; Varutbangkul, V.; Bahreini, R.; Flagan, R. C.; Seinfeld, J. H. *The Journal of Physical Chemistry A* **2004**, *108*, 10147.
- (137) Gao, S.; Ng, N. L.; Keywood, M.; Varutbangkul, V.; Bahreini, R.; Nenes, A.; He, J.; Yoo, K. Y.; Beauchamp, J. L.; Hodyss, R. P.; Flagan, R. C.; Seinfeld, J. H. *Environmental Science & Technology* **2004**, *38*, 6582.
- (138) Iinuma, Y.; Boge, O.; Gnauk, T.; Herrmann, H. *Atmospheric Environment* **2004**, *38*, 761.
- (139) Tolocka, M. P.; Jang, M.; Ginter, J. M.; Cox, F. J.; Kamens, R. M.; Johnston, M. V. *Environmental Science & Technology* **2004**, *38*, 1428.
- (140) Czoschke, N. M.; Jang, M. *Atmospheric Environment* **2006**, *40*, 5629.
- (141) Reinhardt, A.; Emmenegger, C.; Gerrits, B.; Panse, C.; Dommen, J.; Baltensperger, U.; Zenobi, R.; Kalberer, M. *Analytical Chemistry* **2007**, *79*, 4074.
- (142) Muller, L.; Reinnig, M. C.; Warnke, J.; Hoffmann, T. *Atmospheric Chemistry and Physics* **2008**, *8*, 1423.
- (143) Camredon, M.; Hamilton, J. F.; Alam, M. S.; Wyche, K. P.; Carr, T.; White, I. R.; Monks, P. S.; Rickard, A. R.; Bloss, W. J. *Atmos. Chem. Phys.* **2010**, *10*, 2893.
- (144) Putman, A. L.; Offenberg, J. H.; Fisseha, R.; Kundu, S.; Rahn, T. A.; Mazzoleni, L. R. *Atmospheric Environment* **2012**, *46*, 164.
- (145) Hall, W. I. V.; Johnston, M. *Journal of the American Society for Mass Spectrometry* **2012**, *23*, 1097.
- (146) Yasmeen, F.; Vermeylen, R.; Maurin, N.; Perraudin, E.; Doussin, J.-F.; Claeys, M. *Environmental Chemistry* **2012**, *9*, 236.
- (147) Kristensen, K.; Enggrob, K. L.; King, S. M.; Worton, D. R.; Platt, S. M.; Mortensen, R.; Rosenoern, T.; Surratt, J. D.; Bilde, M.; Goldstein, A. H.; Glasius, M. *Atmos. Chem. Phys.* **2013**, *13*, 3763.
- (148) Zhao, J.; Ortega, J.; Chen, M.; McMurry, P. H.; Smith, J. N. *Atmos. Chem. Phys. Discuss.* **2013**, *13*, 9319.
- (149) Amin, H. S.; Hatfield, M. L.; Huff Hartz, K. E. *Atmospheric Environment* **2013**, *67*, 323.
- (150) Lee, S.; Kamens, R. M. *Atmospheric Environment* **2005**, *39*, 6822.
- (151) Venkatachari, P.; Hopke, P. K. *Journal of Environmental Monitoring* **2008**, *10*, 966.
- (152) Heaton, K. J.; Sleighter, R. L.; Hatcher, P. G.; Hall Iv, W. A.; Johnston, M. V. *Environmental Science & Technology* **2009**, *43*, 7797.
- (153) YOUNG, D. F.; MUNSON, B. R.; OKIISHI, T. H.; HUEBSCH, W. W. *A Brief Introduction to Fluid Mechanics*; John Wiley & Sons, 2011.
- (154) Duncianu, M.; Olariu, R. I.; Riffault, V.; Visez, N.; Tomas, A.; Coddeville, P. *The Journal of Physical Chemistry A* **2012**, *116*, 6169.
- (155) Tolocka, M. P.; Heaton, K. J.; Dreyfus, M. A.; Wang, S.; Zordan, C. A.; Saul, T. D.; Johnston, M. V. *Environmental Science & Technology* **2006**, *40*, 1843.
- (156) Jonsson, Å. M.; Hallquist, M.; Ljungström, E. *Environmental Science & Technology* **2005**, *40*, 188.
- (157) Bernard, F.; Fedioun, I.; Peyroux, F.; Quilgars, A.; Daele, V.; Mellouki, A. *Journal of Aerosol Science* **2012**, *43*, 14.
- (158) Atkinson, R. *Chemical Reviews* **1986**, *86*, 69.
- (159) Jenkin, M. E. *Atmospheric Chemistry and Physics* **2004**, *4*, 1741.
- (160) Jonsson, Å. M.; Hallquist, M.; Ljungström, E. *Environmental Science & Technology* **2008**, *42*, 5938.
- (161) Pratt, K. A.; Prather, K. A. *Mass Spectrometry Reviews* **2012**, *31*, 17.
- (162) Pratt, K. A.; Prather, K. A. *Mass Spectrometry Reviews* **2012**, *31*, 1.

- (163) Kotianova, P.; Matisova, E.; Puxbaum, H.; Lehotay, J. *Chemia Analityczna* **2004**, *49*, 833.
- (164) Yu, J.; Flagan, R. C.; Seinfeld, J. H. *Environmental Science & Technology* **1998**, *32*, 2357.
- (165) Yu, J. Z.; Cocker, D. R.; Griffin, R. J.; Flagan, R. C.; Seinfeld, J. H. *Journal of Atmospheric Chemistry* **1999**, *34*, 207.
- (166) Presto, A. A.; Huff Hartz, K. E.; Donahue, N. M. *Environmental Science & Technology* **2005**, *39*, 7036.
- (167) Goldstein, A. H.; Galbally, I. E. *Environmental Science & Technology* **2007**, *41*, 1514.
- (168) Stein, S. E. "Mass Spectra" in NIST Chemistry WebBook. In *NIST Chemistry WebBook*; Mallard, P. J. L. a. W. G., Ed.; National Institute of Standards and Technology: Gaithersburg MD, 20899, 2013.
- (169) Hall, W. A.; Johnston, M. V. *Aerosol Science and Technology* **2011**, *45*, 37.
- (170) Muller, L.; Reinnig, M. C.; Hayen, H.; Hoffmann, T. *Rapid Communications in Mass Spectrometry* **2009**, *23*, 971.
- (171) Muller, C.; Iinuma, Y.; Boge, O.; Herrmann, H. *Electrophoresis* **2007**, *28*, 1364.
- (172) Hoffmann, T.; Bandur, R.; Marggraf, U.; Linscheid, M. *Journal of Geophysical Research* **1998**, *103*, 25569.
- (173) Kostianinen, R.; Kauppila, T. J. *Journal of Chromatography A* **2009**, *1216*, 685.
- (174) Gao, Y.; Hall, W. A.; Johnston, M. V. *Environmental Science & Technology* **2010**, *44*, 7897.
- (175) Yasmeen, F.; Vermeylen, R.; Szmigielski, R.; Iinuma, Y.; Böge, O.; Herrmann, H.; Maenhaut, W.; Claeys, M. *Atmos. Chem. Phys.* **2010**, *10*, 9383.
- (176) Reinnig, M. C.; Muller, L.; Warnke, J.; Hoffmann, T. *Analytical and Bioanalytical Chemistry* **2008**, *391*, 171.
- (177) Claeys, M.; Iinuma, Y.; Szmigielski, R.; Surratt, J. D.; Blockhuys, F.; Van Alsenoy, C.; Böge, O.; Sierau, B.; Gómez-González, Y.; Vermeylen, R.; Van der Veken, P.; Shahgholi, M.; Chan, A. W. H.; Herrmann, H.; Seinfeld, J. H.; Maenhaut, W. *Environmental Science & Technology* **2009**, *43*, 6976.
- (178) Reinnig, M.-C.; Warnke, J.; Hoffmann, T. *Rapid Communications in Mass Spectrometry* **2009**, *23*, 1735.
- (179) Jang, M. S.; Czoschke, N. M.; Lee, S.; Kamens, R. M. *Science* **2002**, *298*, 814.
- (180) Wade, L. G. *Organic chemistry*, 6th ed.; Upper Saddle River, N.J. : Prentice Hall, 2005.
- (181) Bonn, B.; Schuster, G.; Moortgat, G. K. *The Journal of Physical Chemistry A* **2002**, *106*, 2869.
- (182) Viitanen, A.-K.; Saukko, E.; Virtanen, A.; Yli-Pirilä, P.; Smith, J. N.; Joutsensaari, J.; Mäkelä, J. M. *Environmental Science & Technology* **2010**, *44*, 8917.
- (183) Winkler, P. M.; Ortega, J.; Karl, T.; Cappellin, L.; Friedli, H. R.; Barsanti, K.; McMurry, P. H.; Smith, J. N. *Geophysical Research Letters* **2012**, *39*, L20815.
- (184) Pall. <http://www.pall.com/main/laboratory/product.page?id=20096>.
- (185) Sato, K. *Chemistry Letters* **2005**, *34*, 1584.
- (186) Pospelov, M. V.; Menyailo, A. T.; Bortyan, T. A.; Ustynyuk, Y. A.; Petrosya, V. S. *Zhurnal Organicheskoi Khimii* **1973**, *9*, 311.
- (187) Zelikman, E. S.; Yurev, Y. N.; Berezova, L. V.; Tsyskovs, V. K. *Zhurnal Organicheskoi Khimii* **1971**, *7*, 633.
- (188) Dussault, P. H.; Raible, J. M. *Organic Letters* **2000**, *2*, 3377.
- (189) Bailey, P. S. *Ozonation in Organic Chemistry. Vol. 1: Olefinic Compounds*; Academic Press, 1978; Vol. 39-1.
- (190) Rondeau, D.; Vogel, R.; Tabet, J.-C. *Journal of Mass Spectrometry* **2003**, *38*, 931.
- (191) MacMillan, D. K.; Murphy, R. C. *Journal of the American Society for Mass Spectrometry* **1995**, *6*, 1190.
- (192) Schalley, C. A.; Dieterle, M.; Schroder, D.; Schwarz, H.; Uggerud, E. *International Journal of Mass Spectrometry and Ion Processes* **1997**, *163*, 101.

- (193) Nilsson, J.; Carlberg, J.; Abrahamsson, P.; Hulthe, G.; Persson, B. A.; Karlberg, A. T. *Rapid Communications in Mass Spectrometry* **2008**, *22*, 3593.
- (194) Dreyfus, M. A.; Tolocka, M. P.; Dodds, S. M.; Dykins, J.; Johnston, M. V. *The Journal of Physical Chemistry A* **2005**, *109*, 6242.
- (195) Sigman, M. E.; Clark, C. D.; Painter, K.; Milton, C.; Simatos, E.; Frisch, J. L.; McCormick, M.; Bitter, J. L. *Rapid Communications in Mass Spectrometry* **2009**, *23*, 349.
- (196) Sigman, M. E.; Clark, C. D.; Caiano, T.; Mullen, R. *Rapid Communications in Mass Spectrometry* **2008**, *22*, 84.
- (197) Yin, H. Y.; Hachey, D. L.; Porter, N. A. *Journal of the American Society for Mass Spectrometry* **2001**, *12*, 449.
- (198) Yin, H.; Hachey, D. L.; Porter, N. A. *Rapid Communications in Mass Spectrometry* **2000**, *14*, 1248.
- (199) Sozzi, G.; Denhez, J.-P.; Audier, H. E.; Vulpius, T.; Hammerum, S. *Tetrahedron Letters* **1985**, *26*, 3407.
- (200) Dorigo, A. E.; McCarrick, M. A.; Loncharich, R. J.; Houk, K. N. *Journal of the American Chemical Society* **1990**, *112*, 7508.
- (201) Sample, S.; Djerassi, C. *Journal of the American Chemical Society* **1966**, *88*, 1937.
- (202) Sun, C.; Zhao, Y.-Y.; Curtis, J. M. *Rapid Communications in Mass Spectrometry* **2012**, *26*, 921.
- (203) Reynolds, J. C.; Last, D. J.; McGillen, M.; Nijs, A.; Horn, A. B.; Percival, C.; Carpenter, L. J.; Lewis, A. C. *Structural analysis of oligomeric molecules formed from the reaction products of oleic acid ozonolysis*, 2006; Vol. 40.
- (204) Treacy, J.; Curley, M.; Wenger, J.; Sidebottom, H. *Journal of the Chemical Society-Faraday Transactions* **1997**, *93*, 2877.
- (205) Greene, C. R.; Atkinson, R. *International Journal of Chemical Kinetics* **1992**, *24*, 803.
- (206) Nolting, F.; Behnke, W.; Zetzsch, C. *Journal of Atmospheric Chemistry* **1988**, *6*, 47.
- (207) Keywood, M. D.; Kroll, J. H.; Varutbangkul, V.; Bahreini, R.; Flagan, R. C.; Seinfeld, J. H. *Environmental Science & Technology* **2004**, *38*, 3343.
- (208) Alvarado, A.; Tuazon, E. C.; Aschmann, S. M.; Atkinson, R.; Arey, J. *Journal of Geophysical Research-Atmospheres* **1998**, *103*, 25541.
- (209) Kalberer, M.; Yu, J.; Cocker, D. R.; Flagan, R. C.; Seinfeld, J. H. *Environmental Science & Technology* **2000**, *34*, 4894.
- (210) Hamilton, J. F.; Lewis, A. C.; Reynolds, J. C.; Carpenter, L. J.; Lubben, A. *Atmospheric Chemistry and Physics* **2006**, *6*, 4973.
- (211) Nojgaard, J. K.; Norgaard, A. W.; Wolkoff, P. *Atmospheric Environment* **2007**, *41*, 8345.
- (212) Aschmann, S. M.; Tuazon, E. C.; Arey, J.; Atkinson, R. *Journal of Physical Chemistry A* **2003**, *107*, 2247.
- (213) Hatakeyama, S.; Tanonaka, T.; Weng, J.; Bandow, H.; Takagi, H.; Akimoto, H. *Environmental Science & Technology* **1985**, *19*, 935.
- (214) Thomas, M. C.; Mitchell, T. W.; Harman, D. G.; Deeley, J. M.; Murphy, R. C.; Blanksby, S. J. *Analytical Chemistry* **2007**, *79*, 5013.
- (215) Harrison, K. A.; Murphy, R. C. *Analytical Chemistry* **1996**, *68*, 3224.
- (216) Reynolds, J. C.; Last, D. J.; McGillen, M.; Nijs, A.; Horn, A. B.; Percival, C.; Carpenter, L. J.; Lewis, A. C. *Environmental Science & Technology* **2006**, *40*, 6674.
- (217) Jonsson, A. M.; Hallquist, M.; Ljungstrom, E. *Atmospheric Chemistry and Physics* **2008**, *8*, 6541.
- (218) Ma, Y.; Luciani, T.; Porter, R. A.; Russell, A. T.; Johnson, D.; Marston, G. *Physical Chemistry Chemical Physics* **2007**, *9*, 5084.

- (219) Wozniak, A. S.; Bauer, J. E.; Sleighter, R. L.; Dickhut, R. M.; Hatcher, P. G. *Atmospheric Chemistry and Physics* **2008**, *8*, 5099.
- (220) Liggio, J.; Li, S.-M. *Journal of Geophysical Research: Atmospheres* **2006**, *111*, D24303.